SOLVENTS IN MEMBRANE SYNTHESIS AND THEIR EFFECT ON NF/RO PERFORMANCE

FROM CONVENTIONAL ORGANIC SOLVENTS TO IONIC LIQUIDS

Hanne MARIËN

Supervisor:
Prof. Ivo F.J. Vankelecom

Members of the Examination Committee:
Prof. Wannes Keulemans, KU Leuven (Chairman)
Dr. Maria F. Jimenez Solomon, Unilever
Dr. Chris Dotremont, VITO
Prof. Guy Koeckelberghs, KU Leuven
Prof. Maarten Roeffaers, KU Leuven

Dissertation presented in partial fulfilment of the requirements for the degree of Doctor of Bioscience Engineering

September 2017

Doctoraatsproefschrift nr. 1451 aan de faculteit Bio-ingenieurswetenschappen van de KU Leuven

Uitgegeven in eigen beheer, Hanne Mariën, Dessel

Dankwoord

Voor ik mijn doctoraat definitief afrond, zou ik graag een aantal mensen bedanken die mij heel erg geholpen en gesteund hebben de voorbije vier jaar.

In de eerste plaats wil ik Ivo bedanken. Je hebt mij niet enkel de kans gegeven om aan een doctoraat te starten, je stond ook steeds klaar om te vergaderen, resultaten te bespreken en raad te geven. Dankzij je positieve en enthousiaste begeleiding en je blijvende geloof in mij en het project, heb ik dit onderzoek tot een goed einde kunnen brengen.

Daarnaast zou ik graag de leden van mijn doctoraatscommissie bedanken. Prof. Koeckelberghs, je was altijd bereid om te antwoorden op mijn chemische vragen gedurende mijn doctoraat. Je nuttige input heeft mijn inzicht in de chemie van de membranen sterk vergroot. Prof. Roeffaers, dr. Jimenez Solomon and dr. Dotremont, I really appreciate the time you took to read the PhD thesis so thoroughly. Thank you for your valuable questions and remarks during the preliminary defense. Bedankt, prof. Keulemans, om voorzitter van de commissie te willen zijn en om de verdedigingen in goede banen te leiden.

My time at COK would have never been so nice without all the great (ex-)membrane colleagues. Sanne, de enthousiaste en nauwgezette manier waarop jij je onderzoek deed en mij begeleid hebt tijdens mijn thesisjaar gaven mij zin om zelf ook aan een doctoraat te starten. Daarnaast was je ook gewoon een supertoffe collega, net zoals de andere leden van onze vrouwenbureau, Elke, Annelies en Lotte. Merci voor alle gezellige babbeltjes en voor de warmte (ook letterlijk ☺). Na jullie vertrek vreesde ik even om alleen achter te blijven op onze bureau, maar toen kwam er gelukkig Jason. De temperaturen lagen vanaf dan misschien wat lager, maar de gezellige babbeltjes waren er nog steeds. Merci! I would also like to thank Mehran for being such a nice office mate during the last months of my PhD. Met enkele collega's heb ik ook hele leuke tijden beleefd op conferenties. Samen met Cédric, Elke en Annelies naar OSN, met Rhea en Nick naar ICOM… Ik ben heel blij dat ik dit samen met jullie heb kunnen doen! Cédric en Rhea zou ik ook nog extra willen bedanken voor alle tijd die ze gestoken hebben in de TEM-, PLEPS- en ERD-metingen. And to all other (ex-)members of the membrane group, Maarten, Matthias, Maxime C & D, Jeroen, Lisendra, Abaynesh, Raymond, Peter, Yun, Azam, Nithya, Veysi, Stefaan, Ahmad, Ahmet, Waqas, Parimal, Daria, Remigio, Yanbo, … Thank you for the nice atmosphere at work, the dinners, BBQs and other activities. You were the best colleagues and I will miss you all.

Ik heb ook enkele thesisstudenten mogen begeleiden tijdens mijn doctoraat. Lotte, jouw harde en nauwgezette werk heeft heel veel bijgedragen aan mijn doctoraat! Julie en Ines, jullie interesse en ijver maakte het heel leuk om met jullie samen te werken. Ook al lag jullie thesis niet in lijn van mijn doctoraat, ik heb jullie met heel veel plezier mee begeleid.

Ik zou ook de rest van het COK willen bedanken voor de fijne sfeer op het werk. Birgit en de DDV collega's, merci voor de gezellige lunches. Ook Werner, Stef en Johan zou ik graag

bedanken voor hun hulp bij technische problemen. Bedankt Lieve, Inge, Birgit, Annelies en Ines voor alle administratieve hulp.

De voorbije vier jaar heb ik heel veel steun gekregen van mijn familie en schoonfamilie. Ook al was het hen misschien niet altijd even duidelijk wat ik hier allemaal aan het doen was, toch waren ze altijd geïnteresseerd en heel trots (papa: 'En, nog ontdekkingen gedaan?'). Danku mama, papa, Jonas en Yu Chi voor de gezellige dinsdagavondetentjes en de warme thuis. Danku oma om zo fier te zijn op mij. Marja, Johan, Katrijn, Hans, Jakob, Jasper en Delphine, bedankt voor de leuke maandagavondetentjes.

Lieve Bram, bedankt voor alles.

Hanne

Abstract

Membrane technology has grown significantly over the last decades and is used in a broad range of applications nowadays. Nanofiltration (NF) and reverse osmosis (RO) are applied for the separation of low molecular weight components (< 1000 Da) and salts from the feed stream. The main part of the commercial NF and RO membranes are either integrally skinned asymmetric (ISA) or interfacially polymerized thin film composite (TFC) membranes. Polyamide (PA) TFC membranes are the standard in aqueous NF and RO applications, thanks to their very thin, dense top layer, able to form hydrogen bonds with water. For solvent-resistant nanofiltration (SRNF) applications, mainly ISA membranes are applied currently, which are very simple and fast to prepare. Unfortunately, they often suffer from rather low solvent permeances, associated with their thicker selective layer compared to that of TFC membranes. Therefore, the application of TFC membranes in SRNF is currently intensively investigated.

The solvents used in the synthesis and post-treatment of (SR)NF and RO membranes have an impact on several aspects of the preparation process, like monomer and polymer solubility, monomer diffusion coefficients, solvent exchange rate and degree of swelling of the membrane. Therefore, they largely influence the chemical and morphological properties of the resulting membranes, and can thus significantly improve their performance. However, in interfacial polymerization, very similar solvents have always been applied to prepare the top layer, limiting the potential to obtain an optimized performance. Solvent post-treatments are often applied to improve this performance after synthesis, but the mechanism behind these treatments is still largely unclear. Therefore, in this PhD, the importance of the solvent type in interfacial polymerization and in post-synthesis solvent treatments was investigated. This resulted in important improvements in both the synthesis procedures and in membrane performance.

The first part of this thesis focused on the potential to use ionic liquids (ILs) as reaction medium in interfacial polymerization, by replacing either the standard hexane or aqueous phase by an IL. As the physicochemical properties of ILs differed largely from those of conventional solvents, their use affected top layer formation in several ways. The replacement of hexane by an IL led to multiple advantages in the synthesis process. Not only the concentration of the amine monomer used for top layer formation could be reduced drastically, also the addition of commonly used additives could be omitted. By recycling the IL for use in consecutive interfacial polymerization cycles, the mass intensity of the top layer formation process decreased with 64%, resulting in a 52% lower mass intensity compared to the conventional interfacial polymerization. Also the residual acyl chloride monomer in the IL after top layer formation could be recycled, as the IL protected it from hydrolysis by lowering the reactivity of dissolved water molecules. Since the top layers formed via the IL-based interfacial polymerization were thinner, smoother, more hydrophilic, and showed a higher

free volume size, they obtained a higher permeance and a significantly lower colloidal and organic fouling tendency.

In the second part of this research, post-synthesis solvent treatments of both TFC and ISA membranes were studied in detail to further enhance membrane performances. Solvent activation of TFC membranes is a frequently used technique to improve the RO and SRNF performance of this type of membranes. It generally results in a drastic increase in permeance, while no decrease in selectivity is observed. Despite the clear benefits of this solvent treatment, the mechanism behind it still has been unclear. In this work, the occurrence of PA oligomer leaching from the top layer during solvent activation was proven, and an attempt was made to further optimize the leaching process. Since a similar treatment could possibly have a comparable effect on other types of membranes than these TFC membranes, the influence of a solvent treatment on the morphology and performance of ISA polyimide (PI) membranes was also investigated. The membrane was first cross-linked chemically to enable the use of harsh organic solvents. As this type of membranes is totally composed of preformed, high molecular weight polymers, no oligomeric fragments could leach during the treatment, and therefore, no increase in permeance was observed here. Instead, the permeance drastically decreased and the retention increased after immersion in DMF, caused by densification of the membrane skin layer. The degree of densification was related to the polymer-solvent affinity, resulting in a varying degree of swelling and subsequent reorganization of the polymer chains. Besides the possibility to establish more energetically favorable interchain interactions during this reorganization, densification was also driven by extra cross-linking during immersion, due to a facilitated contact between the solvated, flexible polymer chains and partly unreacted cross-linker molecules. This simple treatment could transform ultrafiltration membranes into highly permeable membranes with selectivities in the (SR)NF range, showing an up to 400% higher solvent permeance compared to commercial SRNF membranes.

Samenvatting

Membraantechnologie kende de voorbije decennia een significante groei en wordt tegenwoordig gebruikt in een brede waaier van toepassingen. Nanofiltratie (NF) en *reverse osmosis* (RO) worden gebruikt voor het scheiden van componenten met een laag moleculair gewicht (< 1000 Da) en zouten van de voedingsstroom. Het overgrote deel van de commerciële NF en RO membranen zijn integrale asymmetrische (ISA) of interfaciaal gepolymeriseerde dunne-film-composiet (TFC)-membranen. Polyamide (PA) TFC-membranen zijn de standaard in waterige NF- en RO-toepassingen, dankzij hun zeer dunne, dense toplaag, in staat om waterstofbindingen te vormen met water. Voor solventresistente nanofiltratie (SRNF)-toepassingen worden op dit moment vooral ISA membranen gebruikt, die heel makkelijk en snel aangemaakt kunnen worden. Jammer genoeg hebben zij vaak lage solventpermeanties, geassocieerd met hun dikkere selectieve laag in vergelijking met die van TFC-membranen. Het gebruik van TFC-membranen in SRNF wordt daarom tegenwoordig intensief bestudeerd.

De solventen gebruikt in de synthese en nabehandeling van (SR)NF- en RO-membranen hebben een impact op verschillende aspecten van het bereidingsproces, zoals de monomeer- en polymeeroplosbaarheid, de diffusiecoëfficiënt van de monomeren, de snelheid van solventuitwisseling en de graad van zwelling van het membraan. Daardoor hebben ze een grote invloed op de chemische en morfologische eigenschappen van de resulterende membranen, en kunnen ze hun performantie dus significant verbeteren. In interfaciale polymerisatie werden tot nu toe echter steeds zeer gelijkaardige solventen gebruikt om de toplaag te vormen, wat het potentieel voor het bekomen van een optimale performantie verlaagt. Solventbehandelingen worden vaak toegepast om de performantie verder te verbeteren na de membraansynthese, maar het mechanisme achter deze behandelingen is voorlopig erg onduidelijk. Daarom werd in dit doctoraat het belang van het solventtype in interfaciale polymerisatie en in post-synthese solventbehandelingen onderzocht. Dit leidde tot belangrijke verbeteringen in zowel de syntheseprocedures als in de membraanperformantie.

In het eerste deel van dit doctoraat werd gefocust op het potentieel van ionische vloeistoffen (ILs) om gebruikt te worden als reactiemedium in interfaciale polymerisatie, door het vervangen van de standaard hexaan- of waterfase door een IL. Aangezien de fysicochemische eigenschappen van ILs sterk afweken van deze van conventionele solventen, beïnvloedde hun gebruik de toplaagvorming op verschillende vlakken. De vervanging van hexaan door een IL zorgde voor verscheidene voordelen in het syntheseproces. Niet enkel de concentratie van het aminemonomeer gebruikt voor toplaagvorming kon drastisch verlaagd worden, ook de toevoeging van algemeen gebruikte additieven werd overbodig. Door de IL te recycleren voor gebruik in achtereenvolgende interfaciale polymerisatiecyclussen daalde de massa-intensiteit van de toplaagvorming met 64%, wat resulteerde in een 52% lagere massa-intensiteit in vergelijking met de

conventionele interfaciale polymerisatie. Ook het overblijvende zuurchloridemonomeer in de IL na toplaagvorming kon gerecycleerd worden, omdat de IL het monomeer beschermde tegen hydrolyse door de reactiviteit van opgeloste watermoleculen te verlagen. Vermits toplagen gevormd via de IL-gebaseerde interfaciale polymerisatie dunner, vlakker en hydrofieler waren en grotere vrij-volume-elementen bevatten, vertoonden zij een hogere permeantie en een significant lagere gevoeligheid voor colloïdale en organische membraanvervuiling.

In het tweede deel van dit onderzoek werden post-synthese solventbehandelingen van zowel TFC- als ISA-membranen in detail bestudeerd om zo hun performantie verder te verbeteren. Solventactivatie van TFC-membranen is een frequent gebruikte techniek om de RO en SRNF-performantie van dit type van membranen te verbeteren. Het resulteert doorgaans in een drastische toename van de permeantie, terwijl geen afname in selectiviteit waargenomen wordt. Ondanks de duidelijke meerwaarde van deze behandeling was het mechanisme erachter nog steeds onduidelijk. In dit werk werd aangetoond dat PA-oligomeren vrijgezet worden uit de toplaag tijden solventactivatie, en werd getracht dit proces verder te optimaliseren. Vermits een soortgelijke behandeling een vergelijkbaar effect zou kunnen hebben op andere types van membranen, werd de invloed van een solventbehandeling op de morfologie en performantie van ISA polyimide (PI)-membranen ook onderzocht. Het membraan werd eerst chemisch vernet om het gebruik van agressieve organische solventen mogelijk te maken. Aangezien dit type van membranen volledig bestaat uit voorgevormde polymeren met een hoog moleculair gewicht, konden geen oligomere fragmenten vrijgezet worden tijdens de behandeling en werd in dit geval dan ook geen toename in permeantie waargenomen. In plaats daarvan daalde de permeantie drastisch, terwijl de retentie steeg na immersie in DMF, veroorzaakt door een densificatie van de selectieve laag van het membraan. De graad van densificatie hing samen met de polymeer-solventaffiniteit, die resulteerde in een variabele graad van zwelling en daaropvolgende reorganisatie van de polymeerketens. Naast het feit dat de polymeerketens onderling meer energetisch gunstige interacties konden aangaan tijdens de reorganisatie, werd de densificatie ook gedreven door extra vernetting tijdens de immersie. Dit was het gevolg van een verbeterd contact tussen de gesolvateerde, flexibele polymeerketens en de deels ongereageerde vernettingsmoleculen. Deze simpele behandeling kon ultrafiltratiemembranen omzetten in zeer permeabele membranen met selectiviteiten in het (SR)NF-gebied, die een maximum 400% hogere solventpermeantie vertoonden in vergelijking met commerciële SRNF-membranen.

List of abbreviations

ACN	acetonitrile
AFM	atomic force microscopy
ATR-IR	attenuated total reflectance infrared
BC	benzoyl chloride
$[C_2mim][EtSO_4]$	1-ethyl-3-methylimidazolium ethylsulfate
$[C_2mim][OTf]$	1-ethyl-3-methylimidazolium trifluoromethanesulfonate
$[C_4mim][Tf_2N]$	1-butyl-3-methylimidazolium bis(trifluoromethylsulfonyl)imide
$[C_4mpyr][Tf_2N]$	1-butyl-1-methylpyrrolidinium bis(trifluoromethylsulfonyl)imide
DLS	dynamic light scattering
DMF	N,N-dimethylformamide
DMSO	dimethylsulfoxide
DMSO-d	deuterated dimethylsulfoxide
EB	electron beam
ERD	elastic recoil detection
EtOH	ethanol
GPC	gel permeation chromatography
HDA	1,6-hexanediamine
H-NMR	proton nuclear magnetic resonance
IL	ionic liquid
IPA	isopropanol
IPC	isophthaloyl chloride
ISA	integrally skinned asymmetric
MF	microfiltration
MO	methyl orange
MPD	*meta*-phenylenediamine
MW	molecular weight
MWCO	molecular weight cut-off
NEPOMUC	neutron-induced positron source Munich
NF	nanofiltration
NMP	N-methylpyrrolidone
OPD	*ortho*-phenylenediamine
o-Ps	*ortho*-positronium
PA	polyamide
PALS	positron annihilation lifetime spectroscopy
PEG	poly(ethylene glycol)
PI	polyimide
PIP	piperazine
PLEPS	pulsed low energy positron system
PPD	*para*-phenylenediamine

PS	polystyrene
PSf	polysulfone
PVP	polyvinylpyrrolidone
RB	rose Bengal
RMS	root mean square
RO	reverse osmosis
SB	Sudan black
SDS	sodium dodecyl sulfate
SEM	scanning electron microscopy
SRNF	solvent-resistant nanofiltration
TEA	triethylamine
TEM	transmission electron microscopy
TFC	thin film composite
TMC	trimesoyl chloride
TPC	terephthaloyl chloride
THF	tetrahydrofuran
UF	ultrafiltration
UV	ultraviolet
UV-vis	ultraviolet-visible
XPS	X-ray photoelectron spectroscopy

List of symbols

A	membrane area
a	hydrodynamic radius
c_f	solute concentration in feed
c_p	solute concentration in permeate
D	diffusion coefficient
k_B	Boltzmann constant
m_f	final dry mass membrane
m_i, m_m	initial dry mass membrane
m_{m+s}	mass solvent impregnated membrane
m_{m+w}	mass water impregnated membrane
M_p	peak molecular weight
P_{ow}	octanol-water partition coefficient
R	ideal gas constant
δ_D	dispersive interactions
δ_H	hydrogen bonding interactions
ΔH_{vap}	enthalpy of vaporization
ΔP	pressure gradient
δ_P	polar interactions
$\Delta_{s\text{-}p}$	Hansen solubility parameter distance between solvent and polymer
η	viscosity
ρ	density
σ	interfacial tension

Table of contents

CHAPTER 1

Introduction and scope of the thesis

Part 1.3 was largely based on Ivo F.J. Vankelecom, Hanne Mariën in Nanofiltration: Principles and Applications, 2nd edition (*eds. Andrea Schäfer, Tone Fane*), 2018. Copyright (2018) Elsevier. This book chapter was an update, fully performed by Hanne Mariën, of a similar book chapter dating from 2004.

1.1 Membrane technology

Membrane technology is a term which includes the separation of components by the use of a semipermeable barrier, the membrane. Since some components can pass the membrane, while others cannot, each of them is enriched at one side of the membrane. This is represented in Figure 1.1. The part of the feed solution which passes the membrane, is called the permeate, while the retained stream is called the retentate. Whether or not a component permeates, depends on several properties of both the component and the membrane.[1,2]

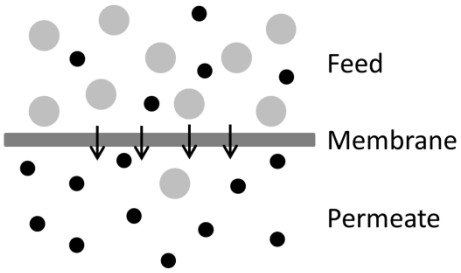

Figure 1.1: Schematic representation of a membrane separation process.

Separation processes are an important aspect in many types of industries. In the chemical and pharmaceutical industry, even 40-70% of the capital and operating costs are related to separation processes.[3] This demonstrates the importance of choosing the most efficient technology for every application. Besides membrane technology, other methods, like distillation, crystallization, extraction and adsorption, can also be applied for the separation of mixtures.[4] However, in many cases, membrane technology holds clear advantages. It can be applied as a continuous process, generally showing a low energy use and mild separation conditions. Moreover, membrane properties can easily be adapted, it is an easy technique to combine with other separation processes and to scale up, and no extra waste streams are created.[1]

1.1.1 Classification

Different membrane properties can be used for classifying the huge amount of existing membranes. The first property is the type of material used to form the membrane. This can either be organic or an inorganic in nature. Organic membranes, which are mostly polymeric, form the most important membrane class. Inorganic membranes can be metal-, ceramic, glass- or zeolite-based. Although they are generally more stable than polymeric membranes, both chemically, thermally and mechanically, they also possess some disadvantages. Compared to polymeric membranes, inorganic membranes are more brittle and more expensive, they are more difficult to process and their pore size can be tuned less easily. Therefore, their application range is more narrow.[1,5,6] In this thesis, polymeric membranes will be applied.

Membranes can also be classified based on their morphology. A distinction can be made between porous and dense membranes (Figure 1.2), in which the porosity determines the size of the components which are retained. Moreover, the porosity can be either homogeneous or heterogeneous throughout the membrane cross-section. The former ones are called symmetric membranes, and commonly have a thickness between 10 and 200 µm. Their selectivity is determined by the total membrane cross-section. Asymmetric membranes, on the other hand, consist of a thin, selective layer of 0.1 - 0.5 µm on top of a more porous support layer with a thickness of 50 – 150 µm (Figure 1.2). In this case, the separation performance is only determined by the selective layer of the membrane.[1] Asymmetric membranes are generally more efficient, since the thickness of the selective layer determines the rate of transport through the membrane.[7] In integrally skinned asymmetric (ISA) membranes, the support and top layer are prepared in one step, while in thin film composite (TFC) membranes, both layers consist of a different material and are prepared separately.[2] The formation and properties of TFC membranes, used in this thesis, are discussed in 1.3 and 1.4.

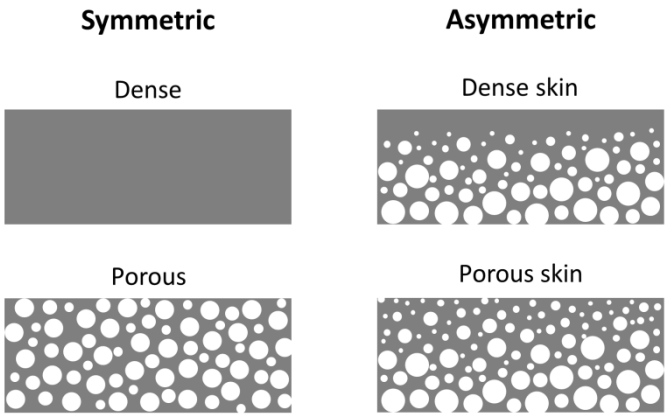

Figure 1.2: Schematic representation of the different membrane morphologies.

The last classification is based on the driving force causing transport through the membrane. This driving force is the gradient in electrochemical potential of the permeating component over the membrane, and can be either a concentration, pressure, temperature or electric potential difference. Only when one component permeates, a linear relationship exists between the transport rate of the component and the driving force. In other cases, coupling of component fluxes and different driving forces can occur.[1,4] Since pressure-driven membrane processes are applied in this thesis, they are further discussed in 1.2.

1.1.2 Performance

Membrane performance is quantified primarily by the determination of two parameters, flux (or permeance) and retention. The flux is a measure for the rate at which the filtration process proceeds, denoted by the volume of feed solution that permeates through a certain membrane area at a certain filtration time. For deriving the permeance, the flux is divided by the applied pressure. The retention is a measure for the membrane selectivity. It is

represented as the fraction of the total concentration of a component in the feed solution, retained by the membrane.[1]

Besides these directly measurable parameters, the chemical, thermal and mechanical stability of the membrane also largely influence its long-term performance. Moreover, membrane performance can be negatively affected during filtration by two phenomena, fouling and concentration polarization. Fouling is a general term for reversible and irreversible pollution of the membrane, caused by either the formation of a gel or cake layer on the membrane surface, or by pore blocking. It occurs due to e.g. precipitation of insoluble inorganic substances, adsorption of organic components or accumulation of biological substances, and results in a continuously decreasing permeance. A fouled membrane can be regenerated by backflushing or chemical cleaning.[1,8,9] Concentration polarization is related to the increasing concentration of retained components in the feed solution close to the membrane, which increases the osmotic pressure difference between the feed and permeate side. After an initial decrease in permeance, the system will reach a steady state. Concentration polarization is reversible and can be limited, e.g. by adequate stirring of the feed solution and by using spacers.[1,8]

1.2 Pressure-driven membrane processes

1.2.1 Classification

Pressure-driven membrane processes are divided into four categories, microfiltration (MF), ultrafiltration (UF), nanofiltration (NF) and reverse osmosis (RO), based on the porosity of their selective layer, and thus the size of the components that are retained. Going from MF to RO, the osmotic pressure of the feed and the density of the membrane increases, resulting in a higher necessary applied pressure and a lower permeance. Typical values are shown in Table 1.1.

Table 1.1: Classification of pressure-based membrane processes.[1,2,9]

	MF	UF	NF	RO
Pore size (nm)	50 - 10 000	1 - 100	< 2	No discrete pores
Applied pressure (bar)	0.1 - 2.0	1.0 - 5.0	5.0 - 20	10 - 100
Permeance (L m^{-2} h^{-1} bar^{-1})	> 50	10 - 50	1.4 - 20	0.05 - 1.4
Retained components	Particles Clays Bacteria	Macromolecules MW 10^4 - 10^6 Da Viruses	Small molecules MW 200 - 1000 Da Multivalent ions	Small molecules MW 100 – 1000 Da Monovalent ions

1.2.2 Transport mechanism

Two mechanisms are generally applied to describe molecular transport in pressure-driven membrane processes: pore flow and solution-diffusion (Figure 1.3). According to the pore flow model, the pressure gradient causes a convective flow through permanent,

interconnected pores. Separation occurs since some components are excluded from the pores, while others can pass. Solution-diffusion takes place when no permanent pores are present in the polymer matrix. In this case, molecules are sorbed into the membrane, and subsequently diffuse through transient free volume elements, formed by thermal motion of the polymer chains. Membrane selectivity originates from differences in solution thermodynamics and diffusion rate of different components.[2,10]

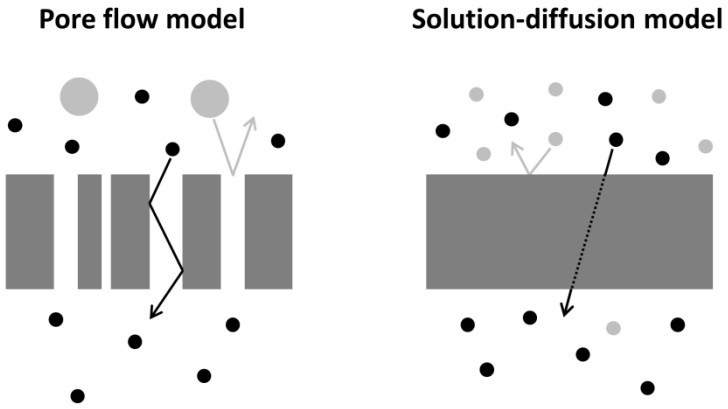

Figure 1.3: Mechanisms used to describe molecular transport through membranes.

The transition from transient to permanent pores is situated in a pore diameter range of 0.5 - 1.0 nm. Transport through MF and UF membranes, all having pores larger than 1.0 nm (Table 1.1), can thus be fully described by the pore flow model. The solution-diffusion model, on the other hand, is used to explain the flow through RO and dense NF membranes, since transport occurs through transient pores having a diameter of less than 0.5 nm (Table 1.1). However, flow through membranes with pores diameters of 0.5 – 1.5 nm, like more loose NF membranes, cannot adequately be described by a single mechanism.[2]

1.2.3 Applications

RO membranes are applied for desalination of seawater and brackish water, containing a salt concentration of 0.2 – 5.0 % (w w^{-1}). To meet the target NaCl concentration for potable water applications (< 500 ppm), a minimum of 99.3% NaCl retention is required in a single-stage seawater desalination unit. For the desalination of brackish water, a NaCl retention of 95-98% is often sufficient. However, membranes with lower selectivity can also be used in multi-stage processes. Besides a high selectivity, an appropriate water flux is also crucial. Water fluxes of more than 40 L m^{-2} h^{-1} are currently obtained in seawater desalination.[2] Nowadays, RO represents 65% of the total worldwide desalination capacity,[11] showing a two to eight times lower specific energy consumption than distillation technologies.[12]

NF membranes are also described as loose RO membranes, due to their moderate salt retention and significantly higher flux. Although NF membranes were initially merely used for aqueous purposes, their use has more recently been extended towards organic solvent-based applications. Solvent-resistant nanofiltration (SRNF) membranes can be applied as

solvent recovery or exchange step, as purification or solute enrichment step in different industries, e.g. in the pharmaceutical, (petro)chemical or food industry. [13,14] The combination of these membrane-based separation steps with other separation technologies has the potential to significantly improve the green character and yield of several industrial processes.[15]

UF membranes have applications in the dairy, pharmaceutical, food and beverage and water treatment industry, e.g. for the purification of proteins, the concentration of enzymes or the removal of oil from wastewater. Also MF membranes are applied in these industries, where they serve e.g. as filter to clarify wine or to remove large colloids and particulates from wastewater.[16]

1.3 Preparation of thin film composite membranes

TFC membranes are a specific type of asymmetric membranes, in which the dense top layer and the porous support are prepared separately. Therefore, the synthesis processes of both layers can be optimized independently, resulting in a high-performance NF or RO membrane. Due to their superior properties and performance compared to ISA membranes, TFC membranes are the general membrane type for RO and NF nowadays.[17] The support is made via phase inversion and gives mechanical strength to the membrane. It commonly has UF or MF properties and does not provide any selectivity or resistance against flow in NF or RO applications. The support is often further reinforced by a non-woven fabric, providing easy handling. The top layer, commonly made via interfacial polymerization, is the selective layer. Due to its extremely low thickness (10-150 nm), it cannot be used on its own and thus needs to be supported.[18]

1.3.1 Phase inversion

In phase inversion, ISA membranes are formed via the controlled transformation of a liquid polymer film into a solid membrane.[19] The method was developed in the 1960s by Loeb and Sourirajan to make RO membranes.[20] Besides such dense membranes, also porous asymmetric membranes can be formed via phase inversion. They can be used as UF or MF membrane, or as support for TFC membranes.

During phase inversion, a thermodynamically stable polymer film undergoes demixing, separating the homogeneous film into a polymer-rich and a polymer-lean phase.[21,22] This can be induced by immersion in a non-solvent bath ('immersion precipitation'), by evaporating the volatile solvent from a polymer that was dissolved in a solvent/non-solvent mixture ('controlled evaporation'), by lowering the temperature ('thermal precipitation'), or by placing the cast film in a vapor phase that consists of a non-solvent saturated with a solvent ('precipitation from vapor phase').[1,14] Immersion precipitation is the most intensively investigated and most frequently used technique, due to the broad range of membrane morphologies which can be obtained.[23]

Both thermodynamic and kinetic aspects of the phase inversion process determine the final membrane morphology. The thermodynamics are related to the type of demixing. In binodal demixing, the most common demixing type, polymer-lean nuclei are formed in a polymer-rich phase. These nuclei are transformed, via the nucleation and growth mechanism, into the membrane pores, while the polymer-rich phase ultimately forms the membrane matrix.[1,24] The kinetics determine the speed of the demixing process. In immediate demixing, nuclei are formed close to the film surface immediately after contact with the non-solvent, and subsequently grow towards the bottom side of the film. This results in a porous membrane morphology. When demixing is delayed, more solvent can evaporate before solidification, generally resulting in more dense membranes.[4,21,25]

The thermodynamic and kinetic aspects of phase inversion are largely influenced by the synthesis conditions.[23] Polymer, solvent and non-solvent type and concentration have to be chosen properly to obtain a system in which the polymer is highly soluble in the solvent but insoluble in the non-solvent, while solvent and non-solvent have to be at least partially miscible to induce solvent exchange during phase inversion.[19,26–32] The most common polymer types used to prepare membranes via phase inversion, are polysulfone (PSf), polyethersulfone, polyacrylonitrile, cellulosics, poly(vinylidene fluoride), polyimide (PI) and polyamide (PA).[23] Moreover, inorganic[33–36] or organic additives[37–41] can be added to the polymer solution or the non-solvent bath (also called coagulation bath), an evaporation step can be inserted between film formation and phase inversion,[26,28–33,42,43] the temperature of the coagulation bath be altered,[31,44] and a post-synthesis treatment (e.g. annealing or drying) can be applied,[29,44–47] all determining the final membrane morphology.

1.3.2 Cross-linking

A specific type of post-treatment of membranes prepared via phase inversion, is cross-linking. This is mainly applied to improve the chemical stability of the membrane, which is often necessary for SRNF applications.[13] Possible methods are thermal, chemical, ultraviolet (UV) or electron beam (EB) cross-linking.[48–51]

In this thesis, cross-linked PI is used as support polymer in the preparation of TFC SRNF membranes. PI is a very suitable polymer for this application due to its resistance to several organic solvents, and its mechanical and thermal stability. Moreover, by cross-linking PI, it becomes stable towards all organic solvents and can thus be used in any solvent stream.[52] Chemical cross-linking of PI occurs via reaction with a diamine or diol. The cross-linking reaction with a diamine is presented in Figure 1.4. By attacking a carbonyl group of the PI chain, the diamine breaks up the imide bond and creates an intermolecular amide bond. After reaction at both ends of the diamine, a cross-link between two PI chains is formed.[53–55]

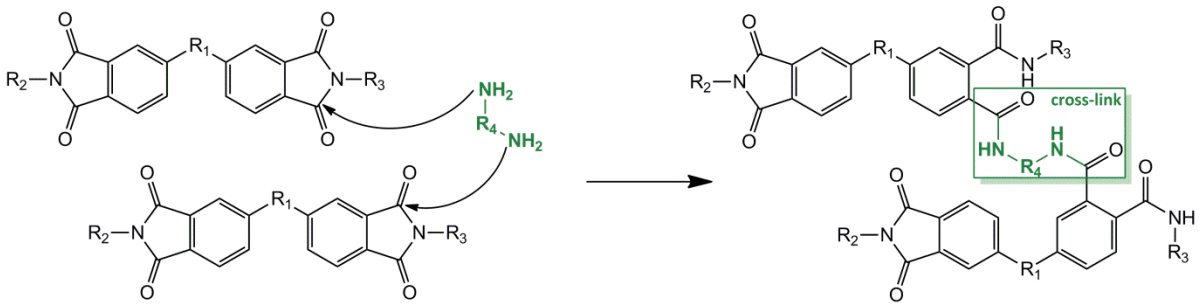

Figure 1.4: Reaction scheme of the cross-linking of PI with a diamine.

Cross-linking is mostly performed in an alcoholic solution, which is said to swell the PI matrix, resulting in a better accessibility for the cross-linker molecules.[49,53–57] Therefore, besides the concentration and reactivity of the cross-linker, also its size and the free volume in the membrane influence the obtained cross-linking degree.[53] A simplified method was presented later on, which combines phase inversion and cross-linking via the addition of the cross-linker in the coagulation bath. This both reduces the necessary synthesis steps and the need for organic solvents, since no swelling medium was necessary due to the immediate contact of the cross-linker with the entire polymer film before solidification.[58,59]

1.3.3 Interfacial polymerization

The development of the interfacial polymerization method to prepare TFC membranes by Cadotte in the 1970s led to a major breakthrough and is nowadays the most important technique for the preparation of TFC RO and NF membranes.[60,61] In this synthesis method, a polymer film is formed via a reaction between two monomers at the interface of two immiscible solvents (Figure 1.5). A porous support is first impregnated with a (mostly aqueous) solution containing the first monomer. The excess of solution is removed and the saturated support is brought into contact with an organic solution containing the second monomer. At the interface between the two immiscible solvents, the monomers react to form a dense film on top of the porous support. Since the formation of this top layer inhibits further contact between the two monomers, the reaction is called ‘self-terminating’ and the formed film is typically very thin, ranging from a few tens to a few hundreds of nanometers.[14]

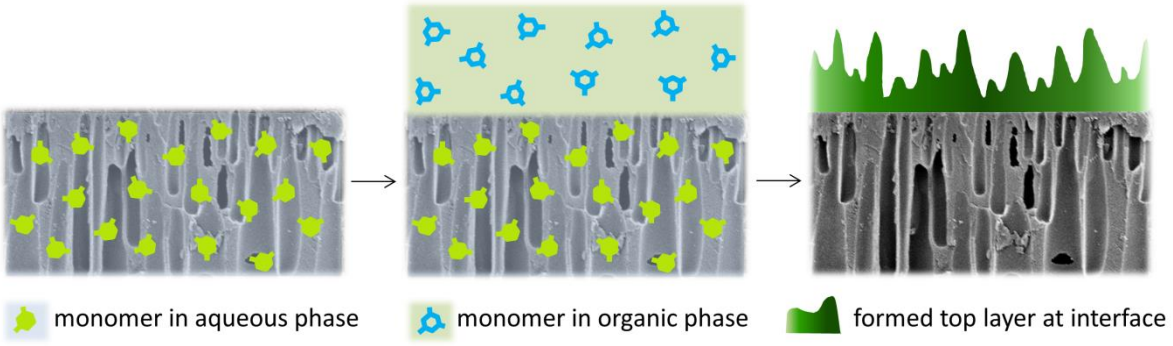

Figure 1.5: Schematic representation of the interfacial polymerization process.

Various types of polymers can be formed as a top layer via the interfacial polymerization technique, like PA,[17,62] PA-urethane,[63] PA-urea,[64] polyester,[65–69] polyamine[70] and polysulfonamide[71]. By far the most widespread type of top layer for (SR)NF and RO applications is PA, formed via the reaction between an amine and an acyl chloride. In this case, the support is impregnated with an aqueous amine solution, and subsequently brought into contact with an acyl chloride dissolved in an apolar organic solvent, commonly hexane or isopar. The film is assumed to be formed in the organic phase due to the very low solubility of the acyl chloride in the aqueous phase, and gradually grows away from the aqueous phase. This results in a thin, dense and highly cross-linked PA top layer, being able to form hydrogen bonds. These properties result in both a high salt retention and water flux and make the PA TFC membrane very suitable for aqueous NF and RO applications.[17,18]

Recently, a more efficient, time and material saving approach to prepare TFC membranes was developed by adding the amine monomer for the interfacial polymerization to the coagulation bath, making it possible to perform phase inversion and impregnation of the support with the amine monomer at the same time.[72] Moreover, a cross-linker for the support could also be added to the coagulation bath, converting a three-step synthesis (phase inversion, cross-linking and impregnation) to a one-step process.[73]

The composition and morphology of the membrane top layer depend on different parameters, like the morphological and chemical properties of the support, the type of solvents used (determining e.g. their interfacial tension and the partition coefficient and diffusion rate of the monomers), the concentration and reactivity of the reactants, the use of additives, and the presence of by-products or competitive side-reactions.[74] The most important parameters for this thesis are discussed below.

Supports

The support provides the mechanical stability of the composite membrane. For aqueous NF and RO, PSf and polyethersulfone UF membranes are frequently used supports.[74] Since these polymers are sensitive to certain organic solvents, their potential for SRNF applications is limited. Polymers with a higher solvent stability are PI, polyacrylonitrile, poly (ether ether ketone) and poly(vinylidene fluoride), which can be cross-linked if required.[32,56,75]

Support morphology (pore size, porosity) and chemical properties (hydrophilicity, reactivity with the monomers) have an influence on the interfacial polymerization process and the characteristics of the resulting top layer. Support hydrophilicity can be increased by adding additional hydrophilic polymers to the casting solution. The addition of hydrophilic poly(ethylene glycol) (PEG) and polyvinylpyrrolidone (PVP) to a PSf casting solution has shown to lower the water permeability of the composite PA membrane. It is assumed that the amine monomer, added to the support before interfacial polymerization, interacts with PEG and PVP through hydrogen bonding, limiting its eruption into the organic phase and causing the PA to be formed partly in the pores of the support.[76]

The non-uniform transport of the amine monomer from the aqueous to the organic phase, which only occurs at the surface pores of the support, is also expected to be one of the determining factors for the typical ridge-and-valley structure of aromatic PA membranes (Figure 1.6), as the application of a support-free interfacial polymerization causes the surface of the PA film to be considerably more smooth.[77] This was confirmed by the fixation of a nanostrand layer on the support before interfacial polymerization, which also promotes homogeneous transport of the amine monomer and results in more smooth PA films. However, the surface roughness varied with varying MPD concentration, indicating that also other factors influence the observed surface morphology. By removing the nanostrand layer after top layer formation via acid dissolution and transferring the free-floating PA film to a polymeric or alumina support, a TFC membrane with a two orders of magnitude higher acetonitrile permeance compared to commercially available membranes was obtained.[78]

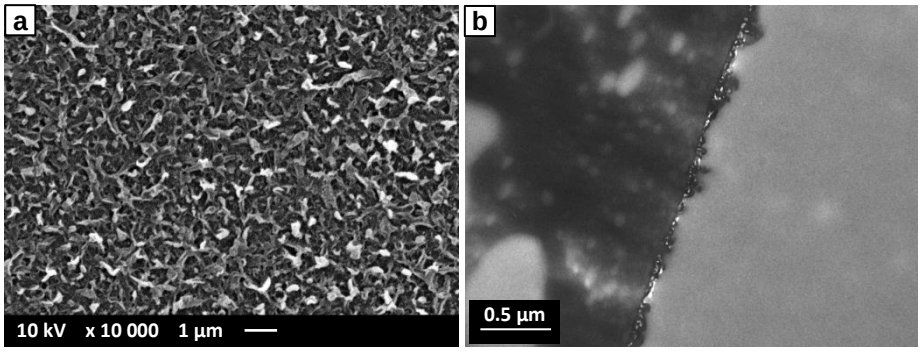

Figure 1.6: (a) Surface SEM and (b) cross-section TEM image of the typical ridge-and-valley morphology of an aromatic PA top layer formed on a porous support.

In SRNF, support hydrophilicity not only affects top layer formation, but also influences the solvent flux during filtration directly. This is related to the affinity between the solvent and the support, as PA membranes show a higher tetrahydrofuran flux when formed on a hydrophilic cross-linked PI support than on a hydrophobic poly(ether ether ketone) support, while the opposite trend is observed for the flux of hydrophobic toluene.[79]

Monomers

Several amines and acyl chlorides are reported for the formation of a PA top layer. In general, PA films made with aromatic diamines show better retentions, but lower fluxes than those with aliphatic diamines.[80] Therefore, aromatic diamines are commonly used in the synthesis of RO membranes, while aliphatic diamines are applied for the preparation of more loose NF membranes. Typical amines are *meta*- and *para*-phenylenediamine (MPD and PPD [81]) and piperazine (PIP). The mutual position of the amines strongly affects membrane performance. Reactions of *ortho*-phenylenediamine (OPD), MPD or PPD with isophthaloyl or terephthaloyl chloride (IPC or TPC) resulted in the best retentions and highest fluxes when the diamines and the diacyl chlorides were located at the same position on the aromatic ring.[82] Reaction of trimesoyl chloride (TMC) with MPD, as presented in Figure 1.7, gives the best membrane performance and is the commonly used combination nowadays in the

synthesis of RO membranes. TMC has a triple functionality and can thus form cross-linked polymer chains. The unreacted acyl chloride groups are hydrolyzed to carboxylic acid groups, causing the top layer to be charged at neutral pH.

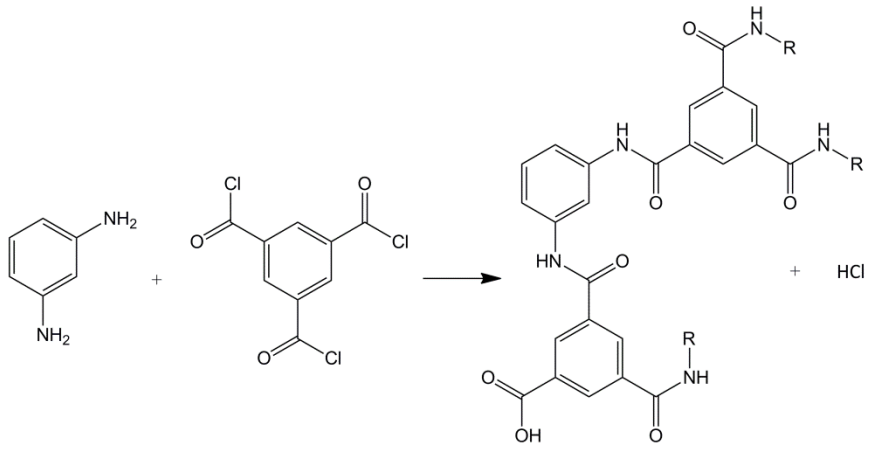

Figure 1.7: Reaction of MPD and TMC to form PA. Carboxylic acid groups result from hydrolysis of unreacted acyl chloride groups. HCl is formed as by-product.

Variations on the commonly used monomers are proposed for different purposes. An improved water permeance is obtained by using more hydrophilic or cycloaliphatic monomers or by altering top layer charge.[83–89] Recently, the use of contorted monomers to create a top layer with enhanced microporosity and higher interconnectivity of the intermolecular network voids was proposed. Via a reaction of TMC with contorted aromatic phenols, a polyarylate (aromatic polyester) top layer with a thickness down to 20 nm was formed. The membrane showed solvent permeances for SRNF purposes up to two orders of magnitude higher than conventional TFC membranes.[90] A drawback of aromatic PA composite membranes, their high fouling tendency, is attributed to the high surface roughness, surface charge and hydrophilicity of the PA layer. Although fouling is mainly limited by surface modification via grafting,[91–94] some alternative amine and acyl chloride monomers are reported to improve the fouling resistance of the PA top layer.[64,95,96] Another limitation of aromatic PA composite membranes is their sensitivity for chlorine, a common disinfectant in water treatment. It is assumed to be caused by the presence of N-H bonds in the PA top layer, which are chlorinated to form N-Cl. This causes the hydrogen bonds between the PA chains to be destructed. In fully aromatic PA, an Orton rearrangement can take place, in which the chlorine group is irreversibly transferred from the amide bond to the aromatic ring.[97] By using secondary amines, no hydrogen is present in the formed amide bond, making the membrane more resistant to chlorine.[98] Moreover, the chlorine tolerance could be improved by using aromatic diamines having their amine groups in ortho position,[99] or by adding other groups, like chlorine, methyl or fluorine-containing groups in ortho position to the amine group. This causes sterical hindrance for chlorine attack and influences the basicity of the nitrogen atom of the amide bond.[89,100,101]

Solvents

In conventional PA formation via interfacial polymerization, the solvent for the amine monomer is water, while the acyl chloride monomer is dissolved in an apolar organic solvent, mostly hexane. Due to the very low solubility of the acyl chloride in water, the PA film is assumed to be formed in the organic phase.[102,103] The ratio of the two monomers in the reaction zone determines the degree of cross-linking of the formed film, and is influenced by their transport rate across the interface as well as their solubility and diffusion rate in the organic phase.

Other organic solvents reported in literature are heptane, dodecane, cyclohexane, benzene, 1,2-dichloroethane and isopar.[63,104–107] While the diffusivity of the amine monomer in the organic phase is determined by the organic solvent viscosity, the amine solubility seems to be related to the organic solvent surface tension.[63,104] Moreover, the interfacial tension between the aqueous and the organic phase influences the transport rate of the amine across the interface. Also the solubility of the formed PA film in the organic solvent is important, since it determines the speed of precipitation of the film. Fast precipitation inhibits further reaction and may result in a lower molecular weight of the PA.[105,108]

Furthermore, the organic solvent temperature has been altered to optimize the membrane performance. Although only the temperature of the organic solution itself was controlled, the temperature of the whole system is expected to be altered after pouring this heated or cooled organic solution on the impregnated support. When using isopar, an increase in temperature from 10 to 50°C resulted in a remarkable improvement in water flux, together with only a slight decrease in salt retention.[63,104] Recently, the application of sub-zero temperatures of the TMC/heptane solution resulted in a 9 times increase in water permeance, while the salt retention only decreased 4%.[107]

Additives

Different types of additives are used in the aqueous or the organic phase to improve membrane performance. Surfactants can be added to facilitate the impregnation of the support with the aqueous amine solution and to lower the water-organic interfacial tension, which promotes the transport of the amine monomers towards the organic phase.[109,110] This mostly results in an increase in water flux of the composite membrane.

Because hydrogen chloride (HCl) is formed during PA formation, acid acceptors (e.g. sodium hydroxide) can be added to the aqueous phase to prevent the amine monomers from being protonated by HCl and lose reactivity.[80,110] However, a negative effect on the membrane performance was observed in some cases, which might be caused be the hydrolysis of the acyl chloride by the hydroxyl ions of the acid acceptor.[110,111] Some acid acceptors, like triethylamine (TEA), can also act as a catalyst for the reaction between the amine and the acyl chloride monomer. Because TEA is more nucleophilic than the amine monomer, it reacts

with the carbonyl group of the acyl chloride, creating an intermediate which is more reactive towards the amine monomer than the original acyl chloride.[110]

Other additives, like small alcohols and polar aprotic solvents, create a more diffuse interface.[63,105,112–118] This generally results in an improved flux of the composite membrane due to the formation of a thinner top layer.[112,113]

1.3.4 Post-treatments

To improve membrane selectivity by completing the cross-linking of the top layer and to remove residual organic solvent, a curing step at elevated temperature can be applied. By increasing the curing temperature or time, degree of crosslinking and membrane density is increased. However, too high temperatures can damage the membrane, which results in a decrease in selectivity. Conventional curing temperatures lie in the range of 40 to 120°C.[104]

Another post-treatment of TFC PA membranes is their immersion in or filtration with an activating solvent. By applying a mild solvent treatment with ethanol or isopropanol, an improvement in water permeance, together with a constant selectivity of commercial TFC RO membranes was observed.[119,120] The replacement of the general poly(ether)sulfone support of RO membranes by a solvent-stable, cross-linked PI support, enabled the use of more harsh activating solvents. A 10 min filtration with dimethylformamide (DMF) as activating solvent caused the methanol, DMF and acetone permeance to increase with a factor 3, 5 and 2, respectively, while a flux was initiated for toluene, ethyl acetate and tetrahydrofuran. Moreover, in many cases, the retention even increased.[57] By increasing the immersion time from 12 to 24 h, the increase in ethanol permeance improved from a factor 5.5 to 16, or from a factor 3.5 to 5.5 with DMF or dimethylsulfoxide (DMSO) as activating solvent, respectively.[73] Although the mechanism of solvent activation is still unclear, it is hypothesized that the activating solvent acts as a swelling agent for the PA top layer. During swelling, low molecular weight PA fragments would dissolve and leach out of the top layer. This would create additional free volume, which was first blocked by the PA oligomers. The increase in retention which is often observed, is explained by the occurrence of annealing during the activation process, which leads to the removal of imperfections and defects in the top layer.[57,119]

To selectively improve the permeance of TFC PA membranes for SRNF applications with apolar solvents, the polarity of the top layer surface can be reduced via end-capping. This includes the reaction of unreacted acyl chloride groups at the surface after interfacial polymerization with apolar components containing an amine group. By end-capping the acyl chlorides with a fluoroalkylamine, a 5 times higher toluene flux was obtained.[121] Also the blending of apolar polymers, like poly(dimethylsiloxane), in the PA top layer by adding the polymer to the organic acyl chloride solution was proposed to reduce top layer polarity and improve the apolar solvent permeance.[122,123]

1.4 Characterization of the interfacial polymerization mechanism and top layer properties

1.4.1 In-situ techniques

Interfacial polymerization is a complicated process at molecular level since several phenomena, including mass and heat transfer of several compounds, and chemical reaction occur simultaneously. Moreover, top layer formation typically occurs in a sub-second time frame in presence of multiple additives. To look into the formation of the interfacial film, some in-situ techniques have been applied. Table 1.2 summarizes the studied parameters and the main conclusions. Although these techniques provide qualitative information on the progress of the reaction, the measurements are difficult to be interpreted quantitatively, and the extremely short time frame of the interfacial polymerization process remains an obstacle for accurate in-situ observation of film formation.

Table 1.2: In-situ techniques used for studying the interfacial polymerization mechanism.

Applied method	In-situ parameter studied	Main conclusions
Light reflection[124]	Film growth	< 0.02 wt.% TMC: reaction controlled by diffusion of TMC
Pendant drop tensiometry[124]	Film growth	Reaction between MPD and TMC initiated within 1 s and completed within 20 s
Diffuse reflectance spectroscopy[103]	PA thickness	50 % of the PA thickness is produced in < 2 s
Microfluidic device with optical microscope[125]	Rate and location of film formation	Amine monomer type determines the reaction kinetics and the location of reaction zone
Optical contact angle device[102]	Location of film formation	Film grows towards organic phase (polyester instead of PA)

1.4.2 Simulations

To overcome this obstacle, several models were developed to simulate the interfacial polymerization process. The analytical model presented by Freger predicted the occurrence of three kinetic regimes in interfacial PA formation. During incipient film formation, a loose polymer film is formed in a narrow region, of which the core further densifies. This regime is followed by a slowdown of film growth and ends with the diffusion-limited growth of the top layer, in which further growth is determined by the diffusion rate of the monomers through the dense film.[126] Later, a simulation by Nadler *et al*. applied a modified cluster-cluster aggregation model to describe the polymerization process. This simulation confirmed the non-uniformity of the top layer, having a dense core with looser ends and an inhomogeneous charge distribution.[127] A further optimization of the simulation by Oizerovich-Honig *et al*. showed a total film formation within 1 ms. It also confirmed the rough surface morphology of aromatic PA, having a non-uniform distribution of surface pore sizes. This might be explained by the initial formation of small clusters of different sizes, which subsequently agglomerate into the initial film. Also larger clusters, growing in the

organic phase in close vicinity to the forming film, can later on aggregate with the film and cause the surface to be even more rough.[128]

1.4.3 Post-synthesis characterizations

To describe the morphological and chemical properties of interfacially polymerized PA top layers, some advanced post-synthesis characterizations were performed. Freger *et al*. used a combination of atomic force microscopy (AFM) and transmission electron microscopy (TEM) with selective staining to distinguish differently charged domains. This suggested the PA top layer to have sandwich-like structure, with a high density core and looser, appositely charged ends at both sides. While the upper surface of the top layer was negatively charged, a small positive charge was observed at the support side of the top layer.[129] This morphology was however contradicted by Pacheco *et al.*, who characterized both the cross-section and projected area of isolated PA films with TEM by dissolving the support after interfacial polymerization. These measurements suggested the presence of a dense, nodular PA layer at the bottom of the film, having a relatively smooth interface with the support, with a more loose and rough PA layer on top of it.[130]

Due to the complex density profile of the PA top layer, which is assumed to consist of both permanent cavities and transient holes (Figure 1.8),[131] advanced characterization techniques are necessary to determine the top layer pore size and distribution. Currently, positron annihilation lifetime spectroscopy (PALS) is the only technique to probe the size of the transient free volume elements. PALS analysis on commercial PA NF and RO membranes showed the free volume radius to be in the range of 0.2 – 0.6 nm.[131] Moreover, the size of these network holes correlated strongly with the retention of uncharged solutes.[132,133] To gain more insight in the size and shape of the permanent pores, Pacheco *et al*. visualized the internal PA morphology in 3D via TEM tomography. These measurements proved the presence of those permanent cavities, which were enclosed by thin sections of PA, as presented in Figure 1.8. Most of these voids originated close to the back surface of the top layer, and many of them extended towards the front surface, where they gave shape to the ridges of the ridge-and-valley morphology. Some of the voids were open towards the bottom surface of the top layer, while others were fully encapsulated by PA.[134]

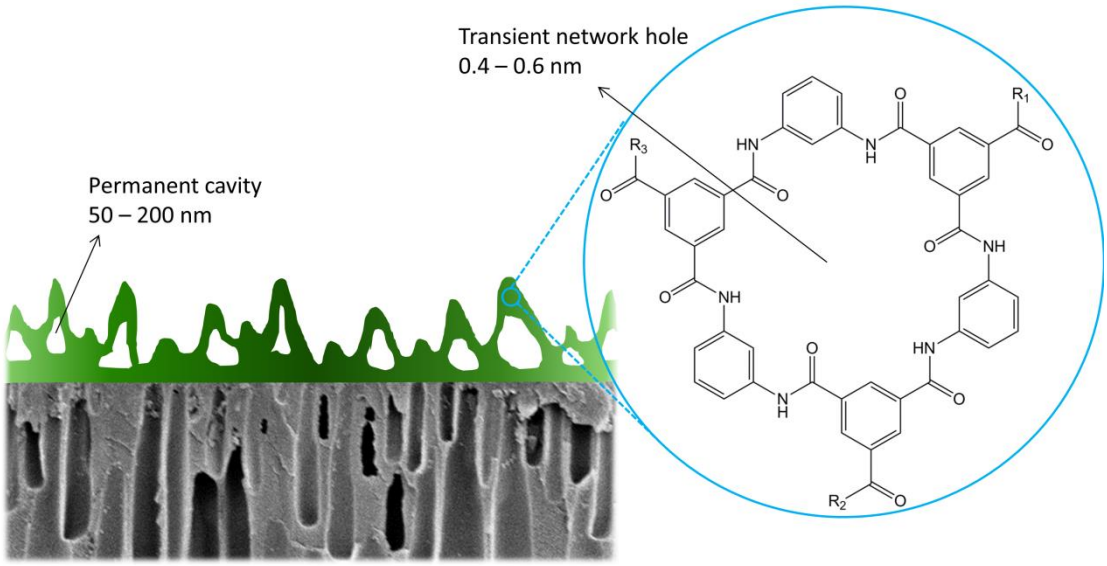

Figure 1.8: Schematic representation of the different hole types in an aromatic PA top layer (adapted from [131]).

1.5 Ionic liquids

Although the discovery of ionic liquids (ILs) dates back to the 1910s, interest in this type of solvents increased mainly during the last two decades.[135] Nowadays, several large-scale industrial applications exist, in which ILs serve as reaction medium for organic or biochemical reactions. They often show benefits compared to conventional organic solvents, like a better control of product distribution, a higher reaction rate or an improved product recovery.[136,137]

1.5.1 Properties

ILs are a very broad group of salts which are liquid at ambient temperatures. Their low melting point results from the combination of bulky, asymmetrical cations and small anions, which tend to have a bad packing and a lower lattice energy.[138] Most cations are based on imidazolium, pyrridinium, pyrrolidinium, ammonium or phosphonium, usually completely substituted. Anions are commonly weakly basic inorganic or organic compounds with a diffuse negative charge.[139]

Besides the melting point, many other IL properties, like their liquid range, viscosity and miscibility with other solvents, are determined by the composition of both cation and anion. Thanks to the possibility to obtain the desired solvent properties for a certain application by choosing an appropriate cation-anion combination, ILs are often called designer solvents.[139] The miscibility of ILs and water is mainly influenced by the nature of the anion and, more specifically, by its ability to form hydrogen bonds with water.[140] IL viscosity, however, is affected by both anion and cation type, and by the length of the alkyl substituents on the cation. An increase in alkyl chain length causes the viscosity to increase significantly.[141] The polarity of ILs is difficult to determine, since their dielectric constant cannot be measured

directly. Although it was first assumed that ILs have a high polarity due to their positive and negative charges, studies indicate the polarity to be rather moderate and comparable to that of lower alcohols.[142] Also the toxicity of ILs has been questioned and is not fully elucidated yet. ILs are often described as green solvents due to their non-volatility, thermal stability and non-flammability. However, they also appear to be fairly toxic and sometimes non-digestible.[143] An important parameter in IL toxicity is the alkyl chain length on the cation. Longer alkyl chains generate more toxic ILs, which is related to their higher molecular similarity with e.g. lipids in cell membranes, resulting in a faster uptake into cells and possible inhibition of certain enzymes.[144]

1.5.2 Synthesis

Different synthesis methods for ILs exist. In the most common method, a positive charge on the cation is first created via quaternization under stirring and heating, with an alkylhalide as alkylating agent. The formation of a dialkylimidazolium cation via quaternization is shown in Figure 1.9. Alkylchlorides, -bromides or -iodides all can be applied, with chlorides being the least reactive. The reactivity of the alkylhalide also decreases with increasing alkyl chain length.[145]

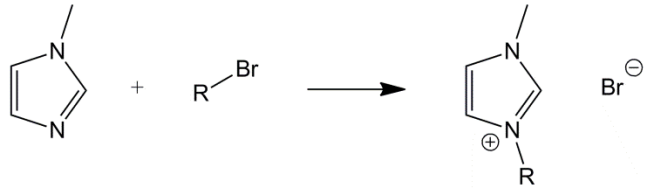

Figure 1.9: Reaction scheme of the quaternization of methylimidazole using an alkylhalide.

In the next step, the cationic reaction product from Figure 1.9 can be combined with the desired anion via metathesis. In the synthesis of water-immiscible ILs, the free acid, metal or ammonium salt of the anion is applied. Figure 1.10 shows the metathesis reaction of an alkyl-methylimidazolium bromide with a metal salt of bis(trifluoromethylsulfonyl)imide, which is performed in aqueous solution. Remaining traces of the formed IL in the aqueous solution can be extracted with dichloromethane. When the free acid of the anion is used, a hydrogen halide is formed, which can be easily removed by washing with water.[139]

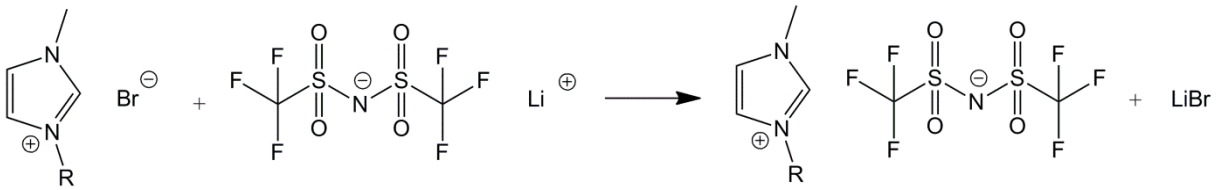

Figure 1.10: Reaction scheme of the metathesis of an alkyl-methylimidazolium bromide with the metal salt of bis(trifluoromethylsulfonyl)imide.

In the synthesis of water-miscible ILs, the same metathesis procedure is generally applied. However, more care should be taken for separating the resulting IL from the by-products.

Sometimes, the silver salt of the desired anion is applied, which results in water-insoluble silver halides as a by-product. This route is, however, more expensive.[139]

A disadvantage of IL synthesis using halides, is the contamination of the reaction product with traces of halides, which can significantly change the chemical and physical properties of the formed IL.[146] Therefore, different strategies for halide-free IL synthesis were also developed.[139]

1.5.3 Applications

ILs are applied as reaction medium in a wide range of organic and biochemical reactions. In the synthesis of polymers, the use of ILs was already reported in polycondensations and in radical and ionic polyadditions. In polycondensation reactions, ILs have shown to possess catalytic properties, as relatively high molecular weight PA could be formed via the reaction of a dicarboxylic acid with a diamine, without the addition of any other catalyst.[147,148] In the radical polymerization of methyl methacrylate, the use of an IL caused the propagation rate to increase and the termination rate to decrease significantly, resulting in a higher molecular weight polymer.[149–151]

Besides these single-phase reactions, ILs are also used as reaction medium in biphasic polymerizations. The formation of polyurea and PA films at the interface between hexane and an IL was described, as well as the synthesis of polyaniline nanoparticles at the interface between water and an IL.[152,153]

In membrane synthesis, ILs were already applied as solvent in cellulose, cellulose acetate and polybenzimidazole solutions, which were then transformed into a membrane via phase inversion. The IL improved the solubility of the polymers and altered the pore morphology of the resulting membrane by acting on the phase inversion process. Moreover, the IL could easily be recovered from the coagulation bath by evaporating water.[154–158] In top layer formation via interfacial polymerization, the use of ILs as low concentration additives, which acted as surfactants or phase transfer catalysts, was reported.[159]

1.6 Thesis objectives and outline

The main part of the commercial NF and RO membranes are either integrally skinned asymmetric or interfacially polymerized TFC membranes. PA TFC membranes are the standard in aqueous NF and RO applications, due to their very thin, dense top layer, able to form hydrogen bonds with water. Nevertheless, efforts are still made to improve their performance and to tackle certain shortcomings, like their high fouling tendency and low chlorine resistance. For SRNF applications, mainly integrally skinned asymmetric membranes are applied nowadays, which are very simple and fast to prepare. They, however, still suffer from rather low solvent permeances, associated with their thicker selective layer compared

to that of TFC membranes. Therefore, the application of TFC membranes in SRNF is currently intensively investigated.

The importance of the type of solvents used in the synthesis and post-treatment of (SR)NF and RO membranes cannot be underestimated. Since they have an impact on several aspects of the membrane preparation process, like monomer and polymer solubility, monomer diffusion coefficients, solvent exchange rate and degree of swelling of the membrane, they drastically influence the final chemical and morphological properties of the membrane. In this PhD, the importance of the solvent type, either in membrane preparation via interfacial polymerization (part 1) or in post-synthesis solvent treatments (part 2) is studied, as illustrated in Figure 1.11.

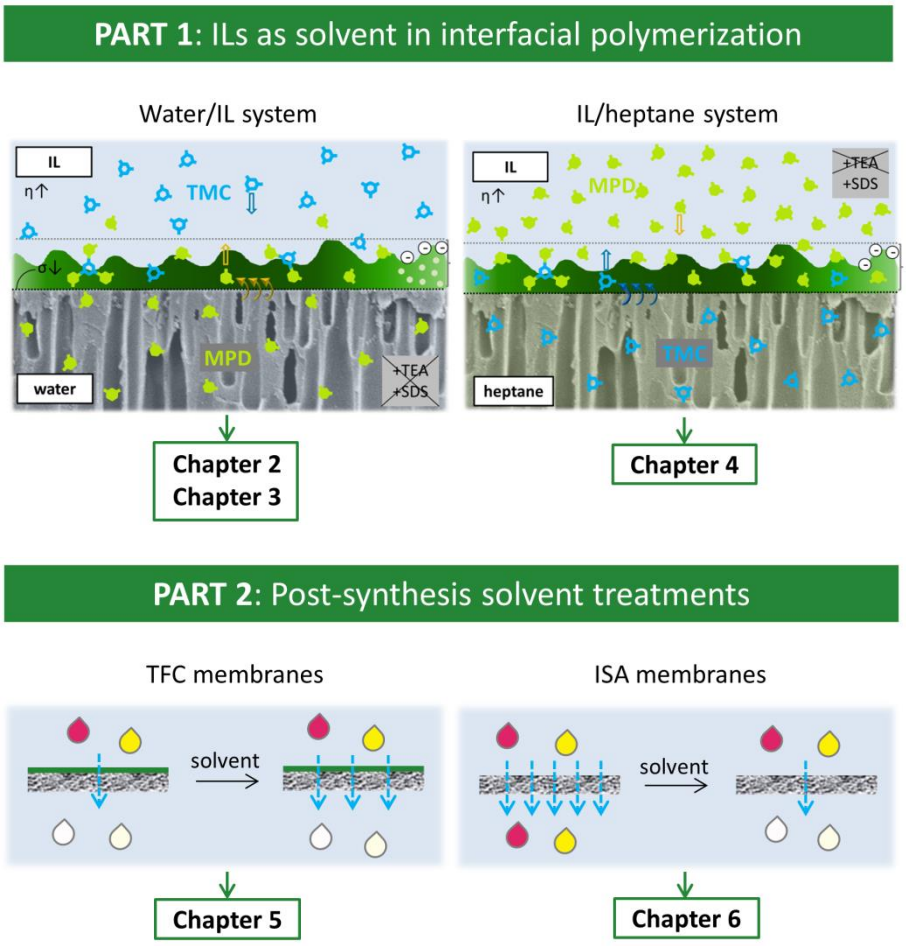

Figure 1.11: Schematic representation of the content of this dissertation.

The first part of this dissertation focuses on the potential to use ILs as reaction medium in interfacial polymerization. The solvents used in interfacial polymerization have a significant impact on the film formation process and on the top layer properties. However, until now, an aqueous phase was always applied for the amine monomer, while all tested water-immiscible organic solvents showed very similar properties to the originally used hexane phase. The use of ILs as solvent already showed to affect the polymerization rate and obtained molecular weight in single-phase polymerizations. As the physicochemical

properties of ILs differ largely from those of conventional solvents, a large effect on top layer formation was assumed by using ILs in interfacial polymerization. This was expected to result in a top layer with beneficial properties, affecting both the general RO performance and the fouling resistance of TFC PA membranes in a positive way. In addition, it would result in a more sustainable membrane preparation process. In **Chapter 2**, the conventional hexane phase was replaced by an IL (Figure 1.11). This top layer synthesis process was further optimized in **Chapter 3** through analysis of the effect of the reaction time, rinsing time and water content in the IL and through the development of methods for post-synthesis membrane drying and for recycling the IL for use in consecutive interfacial polymerization cycles. In **Chapter 4**, an IL was applied as replacement for the conventional aqueous phase (Figure 1.11).

In the second part of the dissertation, post-synthesis solvent treatments are studied in detail to further enhance membrane performances (Figure 1.11). Solvent activation of TFC membranes is a frequently used technique to improve the RO and SRNF performance of this type of membranes. It generally results in a drastic increase in permeance, while no decrease in selectivity is observed. Despite the clear benefits of this solvent treatment, the mechanism behind it is still unclear. This makes it difficult to further optimize the process. Therefore, solvent activation of TFC membranes is investigated fundamentally in **Chapter 5**, in an attempt to elucidate the mechanism and optimize the activation process. It was realized that a similar solvent treatment could possibly have a comparable effect on other types of membranes than these TFC membranes. Therefore, the influence of a solvent treatment on the morphology and performance of ISA membranes is studied in **Chapter 6**, in order to improve their SRNF performance.

CHAPTER 2

Preparation of high-performance thin film composite membranes using ionic liquids as the organic reaction medium

Fundamental study

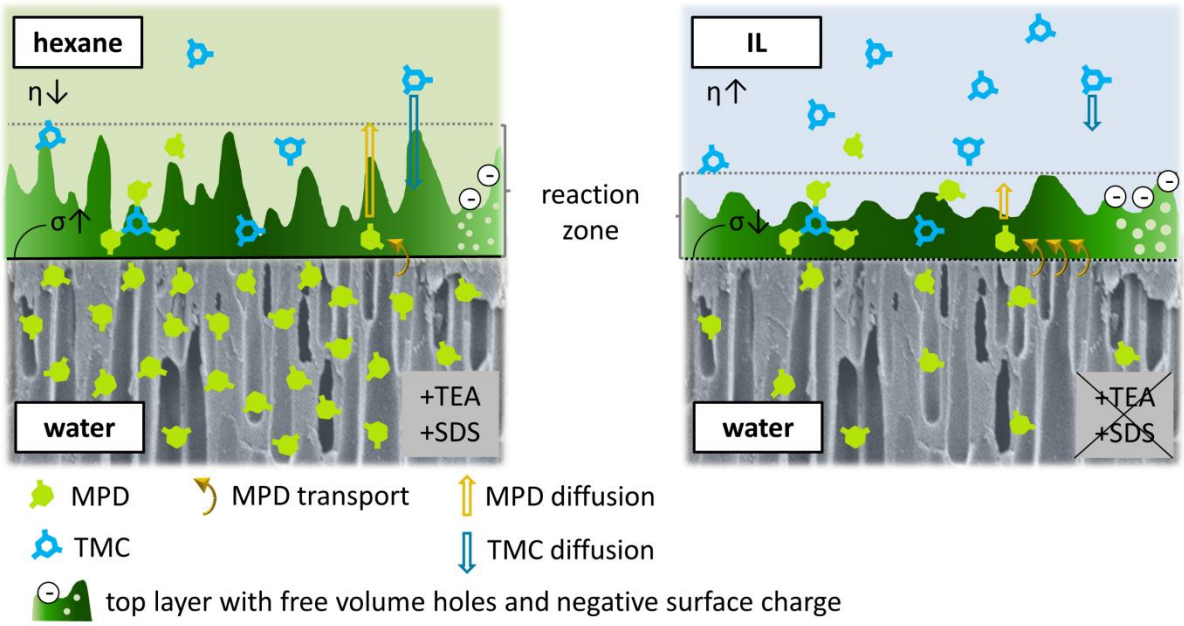

Abstract

A novel form of interfacial polymerization to synthesize thin film composite membranes was developed, simultaneously realizing a more sustainable membrane preparation and an improved nanofiltration performance. By introducing an ionic liquid as organic reaction phase, having extremely different physico-chemical properties than commonly used organic solvents, top layer formation was influenced in several beneficial ways. Besides eliminating hazardous solvents in the preparation, the optimal concentration of *meta*-phenylenediamine, the most toxic of both monomers, could be reduced 20-fold. Also the common use of surfactants and catalysts became redundant. Moreover, a much thinner top layer with a higher free volume diameter and thus a high ethanol permeance of 0.61 L m^{-2} h^{-1} bar^{-1} (99% Rose Bengal (RB, 1017 Da) retention) was formed without the use of any additive. This EtOH permeance is 550% and 160% higher than that for the conventional interfacial polymerization (without and with additives, respectively). In reverse osmosis, high NaCl retentions of 97% could be obtained, together with a high water permeance of 1.09 L m^{-2} h^{-1} bar^{-1}. This might be caused by the improved surface hydrophilicity and charge. Finally, the remarkable decrease in surface roughness of the top layer significantly reduced the membrane's fouling tendency.

2.1 Introduction

Nanofiltration (NF) and reverse osmosis (RO) are pressure-driven membrane processes in which low molecular weight components can be retained on a molecular level.[13,14,62,74] Many large-scale aqueous applications exist, e.g. in saltwater desalination and wastewater treatment.[160] Nowadays, RO represents 65% of the total worldwide desalination capacity,[11] showing a two to eight times lower specific energy consumption than distillation technologies.[12] Solvent resistant NF (SRNF) has been emerging more recently as a potential energy-saving replacement for distillation and a waste-free alternative for extractions and chromatographic separations in (petro)chemical, pharmaceutical and food industry.[13,14]

Thin film composite (TFC) membranes, consisting of a very thin, mostly polyamide (PA) selective layer on top of a porous support,[61] are a widespread membrane type in RO and aqueous NF, and are now also being explored for use in SRNF. The porous support, made via phase inversion, typically consists of poly(ether)sulfone for aqueous applications.[74] The PA film is prepared via interfacial polymerization,[61] by impregnating the support with an aqueous amine solution and subsequently bringing its surface into contact with an immiscible organic (typically hexane) acyl chloride solution. Common monomers are *meta*-phenylenediamine (MPD) or piperazine and trimesoyl chloride (TMC).[109,161] Near the water-hexane interface, both monomers react to form a PA film with a thickness of a few tens of nanometers.[74] The reaction zone for top layer formation is assumed to be located in the organic phase under standard conditions, due to the very low solubility of TMC in water.[102,103] The very thin, dense and highly cross-linked top layer, capable of forming hydrogen bonds with aqueous feeds, causes the membrane to be highly selective while still maintaining a high water permeance. Sustainability of large-scale applications could, however, still be considerably improved by further enhancing the PA TFC membrane permeance and by reducing its fouling behavior. Earlier research demonstrated that a three times increase in permeance can reduce the energy consumption of brackish water RO by 46%.[162] Factors affecting fouling in NF and RO are membrane surface charge, hydrophobicity and roughness.[163,164] In interfacially polymerized PA membranes, the so-called 'ridge-and-valley' structures at the membrane surface can sometimes be very pronounced and are considered to be an important factor in membrane fouling.[164,165]

Owing to their unique characteristics, potential applications of ionic liquids (ILs) are extensively investigated nowadays, e.g. in (bio)catalysis,[166,167] polymer formation,[15,168] gas separations,[169,170] and in energy-related applications.[171] In the field of membrane preparation, ILs have already been used as casting solvent to prepare membranes via phase inversion[154–158] and as low concentration additives in interfacial polymerization.[159]

In this work, a novel form of interfacial polymerization to form TFC membranes is presented by introducing ILs as the organic reaction phase. The use of ILs as water-immiscible solvent in membrane formation via interfacial polymerization has never been described before. As top layer formation is assumed to take place in the organic phase, the organic solvent

properties have a major influence on the properties of the selective layer. Replacement of the conventional hexane phase by other organic solvents has been reported,[63,104,105,172] but due to the large similarity in physico-chemical properties, only a small impact on the actual top layer formation was observed. This impact is expected to be much higher when using ILs, since their properties (e.g. interfacial tension, viscosity, solubility of organic compounds) are extremely different and tunable for specific aims.[138,142]

Therefore, besides the elimination of neurotoxic hexane, this water/IL interfacial polymerization system is expected to show several additional benefits during membrane preparation in terms of sustainability and performance, explicitly resulting from the specific IL properties. Firstly, the typically low water-IL interfacial tensions,[173] caused by the surfactant properties of some water-immiscible ILs, might eliminate the need for adding surfactants, commonly used in interfacial polymerization to improve the transport of the amine monomer across the interface.[72,110,174–176] Furthermore, this high interfacial transport rate might also reduce the aqueous amine concentration needed to obtain a sufficient concentration in the reaction zone in the IL phase, especially because organic compounds generally show a high solubility in ILs. Due to the high viscosity of ILs, the diffusion rate of the amine monomer in the reaction zone is expected to become more rate limiting, thus lowering its diffusion pathway before reacting with the acyl chloride. This would likely cause the top layer to be thinner as well as smoother, which potentially improves the membrane's permeance and lowers its fouling tendency.

2.2 Experimental

2.2.1 Materials

Polysulfone (PSf, Udel® P-1700) and polyimide (PI, Matrimid® 9725) were purchased from Solvay and Huntsman, respectively. The non-woven polypropylene/polyethylene fabric Novatexx 2471 was kindly provided by Freudenberg (Germany). Hexanediamine (HDA, 99.5%, Acros), *meta*-phenylenediamine (MPD, 99+%, Acros), triethylamine (TEA, 99+%, Sigma-Aldrich), sodium dodecyl sulfate (SDS, 99%, Acros) and trimesoyl chloride (TMC, 98%, Acros) were used for membrane synthesis. N-methylpyrrolidone (NMP, 99%, Acros), tetrahydrofuran (THF, 99.9+%, Sigma-Aldrich), hexane (99+%, Chem-Lab), acetonitrile (ACN, 99.99%, Fisher), dimethylformamide (DMF, 99+%, Acros) and ethanol (EtOH, 99.99%, Fisher) were used as received. 1-Butyl-3-methylimidazolium bis(trifluoromethylsulfonyl)imide ($[C_4mim][Tf_2N]$, 99+%, Iolitec) and 1-butyl-1-methylpyrrolidinium bis (trifluoromethylsulfonyl)imide ($[C_4mpyr][Tf_2N]$, 99+%, Iolitec) were used after drying for 16 h at 80 °C under vacuum. Rose Bengal (RB, 1017 Da, Sigma Aldrich, Figure S2.1 in the appendix A), Sudan black B (SB, 457 Da, Fluka, Figure S2.1 in appendix A) and sodium chloride (NaCl, 99.8%, VWR) were applied as test solute. Colloidal silica (LUDOX TM-50, Sigma-Aldrich) and meat peptone (enzymatic digest, Sigma-Aldrich) were used as model fouling agents.

2.2.2 Membrane synthesis

Supports were synthesized via phase inversion. PSf and PI powders were first dried overnight in an oven at 100 °C. Homogeneous polymer solutions were prepared by stirring mixtures of PSf (18% (w w^{-1})) in NMP and PI (14% (w w^{-1})) in NMP/THF (3/1). They were left untouched overnight to remove air bubbles created during the stirring. The polymer solution was cast at a constant speed (4.4 x 10^{-2} m s^{-1}) and with a wet thickness of 200 µm using an automatic casting device (Braive Instruments, Belgium) on a non-woven impregnated with NMP. Then, the film was immersed in a coagulation bath. For PI films, 30 s evaporation was inserted between the casting and the immersion to allow THF evaporation from the film surface. The coagulation bath consisted of MPD (0.1-2.0% (w v^{-1})) in Milli-Q water to simultaneously perform phase inversion and impregnation of the support with MPD.[72] In specified cases, TEA (2.0 or 0.5% (w v^{-1})) and SDS (0.1% (w v^{-1})) were also added as typical interfacial polymerization additives. For PI supports, HDA (0.5% (w v^{-1})) was added to the coagulation bath to also simultaneously cross-link the support. After 5 min, the support was removed from the bath to perform the interfacial polymerization.

First, excess aqueous solution was removed from the impregnated support surface using a rubbery wiper. A solution of TMC (0.01-1.5% (w v^{-1})) in hexane, $[C_4mim][Tf_2N]$ or $[C_4mpyr][Tf_2N]$ was subsequently poured gently on the support. After 60 s, the solution was drained off and the membrane was rinsed to remove unreacted TMC. The rinsing solvent was hexane or ACN when the interfacial polymerization was performed with a TMC solution in hexane or in IL respectively. After 1 min, the membrane was put in a water bath to remove unreacted MPD. Finally, the TFC membrane was stored in distilled water until further use.

2.2.3 Membrane performance

A high throughput filtration module which allows to run 16 simultaneous dead-end filtrations under exactly the same operating conditions was used to test the membrane performance.[177] The active area of each membrane coupon was 1.77 x 10^{-4} m². To minimize concentration polarization, the feed was stirred at 400 rpm. The membrane performance was evaluated with a RB or SB (both 35 µM) solution in EtOH and a NaCl (1 g L^{-1}) solution in Milli-Q water. Four coupons per membrane were tested simultaneously and the performance was averaged.

The permeance (L m^{-2} h^{-1} bar^{-1}) was calculated using Equation 2.1, with V (L) the permeate volume, A (m²) the membrane area, t (h) the filtration time and ΔP (bar) the applied pressure:

$$Permeance = \frac{V}{A \times t \times \Delta P} \qquad (2.1)$$

The retention (%) was calculated using Equation 2.2, with c_f and c_p the solute concentration in feed and permeate respectively:

$$Retention = \frac{c_f - c_p}{c_f} \times 100 \quad (2.2)$$

RB and SB concentrations in EtOH were determined with a UV-Vis spectrophotometer (UV-1650 PC, Shimadzu) at 550 and 601.4 nm respectively. The conductivity of NaCl solutions in water was measured with a Consort C3010 multi-parameter analyzer.

Fouling experiments were performed using a cross-flow filtration module, allowing to run 4 simultaneous filtrations under exactly the same operating conditions. The pump frequency was set at 48 Hz and the feed temperature was held constant at 25-26°C. The active area of each coupon was 1.10 x 10^{-3} m². Aqueous colloidal silica (200 mg L^{-1}) and meat peptone (15 mg L^{-1}) solutions were applied as fouling agent to evaluate the decrease in membrane permeance, using Equation 2.1. The size and polydispersity of the silica colloids in the feed solution were determined using dynamic light scattering (DLS), measuring back-scattering at a scattering angle of 165° with a Nanoplus 3 equipment (Particulate Systems) .

First, the pure water permeance was determined at 20 bar, after a 16 h equilibration at the same pressure. Then, the feed was replaced and a fouling experiment was performed for 25-28 h at 20 bar. To investigate the permeance recovery after the fouling test, the membrane was rinsed with pure water for 1h without pressure. Then the pressure was increased again to 20 bar, and the membrane was equilibrated for 1h before determining the pure water permeance again. Two coupons per membrane were tested simultaneously and the performance was averaged.

2.2.4 Membrane characterization

The morphology of the top layer surface was analyzed with scanning electron microscopy (SEM), using a JEOL JSM-6010LV SEM. Before the measurement, a conductive gold/palladium layer was deposited on the samples with a JEOL JFC-1300 auto fine coater.

To analyze top layer cross-sections at high resolution, transmission electron microscopy (TEM) was applied. Unstained membrane samples were embedded in an araldite resin (Polyscience) and cut into ultrathin (70 nm) cross-sections with a Reichert Ultracut E microtome. Images were taken with a Zeiss EM900 TEM. The thickness was determined on the TEM images at 17 positions at regular distance intervals and was averaged.

The roughness of the top layer surface was analyzed with atomic force microscopy (AFM) at ambient conditions using an Agilent 5500 AFM in tapping mode with NCSHR probes from NanoAndMore GmbH. The cantilever was made out of Si with a spring constant of 40-50 Nm^{-1} and a nominal tip apex radius of < 5 nm. The samples were measured over an area of 25 µm² and analyzed with the WSxM software.[178] The reported RMS roughness is the average of at least two different locations of 4 µm² on the same sample.

Top layer free volume diameters were determined using the pulsed low energy positron system (PLEPS) at the neutron-induced positron source Munich (NEPOMUC). The

measurements were performed at ambient temperature (30°C) with an implantation energy of 1.0 keV. The pick-off lifetime of the o-positronium, which can be extracted from the measured spectra, was correlated to the free volume size using the Tao-Eldup model.[179,180]

Attenuated total reflectance infra-red (ATR-IR) spectroscopy was used to determine the chemical composition of the membrane surface after drying, taking 64 scans at a resolution of 4 cm^{-1} with a Varian 620 FT-IR imaging microscope with a germanium crystal.

Elastic recoil detection (ERD) was applied to estimate the cross-linking degree of the PA top layer. The membrane was irradiated with a 170 MeV $^{127}I^{12+}$ beam, having an incident angle of 10° with respect to the membrane surface, and a scattering angle for recoil ions of 38°. The recoil ions were analysed with a $\Delta E–E_{res}$ detector telescope, having a solid angle of detection of 3.5 msr.[181]

Zeta potential measurements were used to analyze differences in surface charge of the top layer. The measurements were performed using a SurPASS Electrokinetic Analyzer (Anton Paar) by placing two identical membrane coupons in an adjustable-gap measuring cell with a channel height of 95 ± 5 µm. The background solution was 0.001 M KCl and the pH was adjusted using HCl (0.1 M) and NaOH (0.1 M), in a range from 3 to 8. The solution was pumped through the cell and the electrokinetic behavior was measured under inert N_2 atmosphere. A pair of Ag/AgCl electrodes monitored the streaming current. Data were analyzed with Visiolab.

To analyze membrane hydrophilicity, contact angle measurements were performed using a Krüss DSA 10-Mk2 drop shape analyzer. Droplets of 2 µl were applied and the values of 10 droplets on each sample were averaged.

2.2.5 MPD mass transfer

To characterize the differences in transport rate of MPD from the aqueous to the organic phase when replacing hexane by $[C_4mim][Tf_2N]$, an aqueous solution of MPD (2.0% (w v^{-1})) was brought into contact with pure hexane or $[C_4mim][Tf_2N]$. 0.1 ml samples of the aqueous solution were taken at a distance of 1 cm from the interface after different contact times between 0 and 35 min (see Figure S2.2 in appendix A for experimental setup). The MPD concentration of the samples was determined with a UV-Vis spectrophotometer (UV-1650 PC, Shimadzu) at 289 nm after diluting them 200 times to obtain a linear relationship between absorbance and MPD concentration. Every experiment was performed three times and the values were averaged. The aqueous MPD solutions were kept in the dark during the whole experiment to prevent oxidation of MPD.

2.2.6 MPD solubility in the organic phase

The solubility of MPD in hexane was determined by dissolving 0.05% (w v^{-1}) in hexane and gradually increasing the MPD concentration with steps of 0.01% (w v^{-1}). Steps of 0.03%

(w v^{-1}) were used to analyze its solubility in [C_4mim][Tf_2N]. The emergence of white flakes from a certain concentration onward indicated that the solubility limit was exceeded.

2.3 Results and discussion

When using an IL as organic phase in interfacial polymerization, it has to be water immiscible to create a biphasic system. This parameter mainly depends on the nature of the anion, although the cation also influences the hydrophobicity.[138,140] Possible anions are hexafluorophosphate, some less polar borates and fluoralkylsulfonyl anions.[138,140] Since the first one can decompose in the presence of water to form hazardous hydrogen fluoride, and the second group is less available, a common anion from the third group, [Tf_2N], was chosen. Its fluor groups are bound to carbon, which makes it inert to hydrolysis.[138] It was combined in the IL with a very common imidazolium cation, [C_4mim]. No pollution of the aqueous phase with IL is expected when using [C_4mim][Tf_2N] due to its extremely low solubility in water (1.70 10^{-2} mol L^{-1} at equilibrium, after agitating vigorously and waiting for 48 h).[182] So after 1 min of interfacial polymerization without any stirring, the dissolution of [C_4mim][Tf_2N] in water will be negligible.

The traditional water/hexane interfacial polymerization method will be referred to below as the 'conventional system'. The system with [C_4mim][Tf_2N] as organic phase will be called the 'water/IL system'. All TFC membranes were made on a polysulfone (PSf) support, unless specified otherwise.

The properties of hexane and [C_4mim][Tf_2N] with a possible impact on the interfacial polymerization process are summarized in Table 2.1, with η the dynamic viscosity, ρ the density and σ the interfacial tension.

Table 2.1: Properties of hexane and [C_4mim][Tf_2N] at 20 °C.

	η (mPa s)	ρ (g cm^{-3})	MPD solubility (% w v^{-1})	$\sigma_{water\text{-}organic}$ (mN m^{-1})
Hexane	0.31 [183]	0.66 [183]	0.07-0.1	50.80 [184]
[C_4mim][Tf_2N]	63.05 [185]	1.44 [186]	> 1.0 [a]	13.69 [173]

[a] 1.0% (w v^{-1}) MPD still dissolved well in [C_4mim][Tf_2N]; no higher concentrations were tested.

2.3.1 Influence of synthesis conditions

Determination of the monomer concentration range

In the conventional system, the very low solubility of TMC in the aqueous phase causes the interfacial polymerization to mainly occur in the organic phase.[102,103] The organic solvent properties thus have the potential to drastically influence top layer formation. When an IL is applied instead of hexane, the properties of this phase change drastically in terms of viscosity, density, solubility of the monomers, etc., which will impact the optimal monomer concentrations for forming a highly cross-linked film. To determine a useful concentration

range, preliminary experiments were performed in the absence of a support. Solutions of various MPD concentrations in water were therefore brought into contact with solutions of various TMC concentrations in $[C_4mim][Tf_2N]$ in small glass bottles. PA formation was determined visually by the presence of a white layer (Figure S2.3 in appendix A), while the formation of a cross-linked film was determined qualitatively by the possibility of simply removing the film from the bottle with a pincette.

In the conventional system, concentrations of 2.0% (w v^{-1}) MPD in water and 0.1% (w v^{-1}) TMC in hexane are commonly considered optimal for obtaining highly cross-linked, useful top layers. Table 2.2 shows that no or very little polymer formation occurred (--) in the water/IL system using these concentrations. With increasing TMC concentrations, polymerization occurred fast, but the polymer was not cross-linked sufficiently (-). Only the combination of a high TMC concentration and a low MPD concentration visually resulted in a well cross-linked PA film (+).

Table 2.2: Determination of PA formation for various concentrations of MPD in water and TMC in $[C_4mim][Tf_2N]$.[a]

C_{MPD} (% w v^{-1}) → C_{TMC} (% w v^{-1}) ↓	0.1	0.2	0.3	0.4	0.5	1.0	2.0
0.10					--	--	--
0.25					-	-	-
0.50	+	+-	-	-	-	-	-
1.00	+	+	+	+-	+-	-	-

[a] '--' represents no or very little PA formation, '-' a non-cross-linked film, '+-' a partly cross-linked film and '+' a well cross-linked film. These conclusions were based on mere visual observations. The concentrations in the black box were not tested.

These results show that the influence of the TMC concentration should be investigated at lower MPD concentrations than usual, while a higher TMC concentration should be used for the study of the MPD concentration. To better visualize the difference in selectivity of membranes without and with a partly or highly cross-linked top layer, RB, a high-molecular weight test solute, was first used. A selection of the best membranes was made later on for determining their RO performance with NaCl as test solute.

Effect of TMC concentration

Based on above observations, the TMC concentration was varied at 0.2% (w v^{-1}) MPD. As shown in Figure 2.1, high-performance membranes for SRNF applications were formed in the conventional system with TMC concentrations down to 0.1% (w v^{-1}) in hexane. Further lowering the TMC concentration caused a strong decrease in RB retention. In contrast, for the IL system, an acceptable retention could only be obtained at TMC concentrations in $[C_4mim][Tf_2N]$ of 0.5% (w v^{-1}) or more.

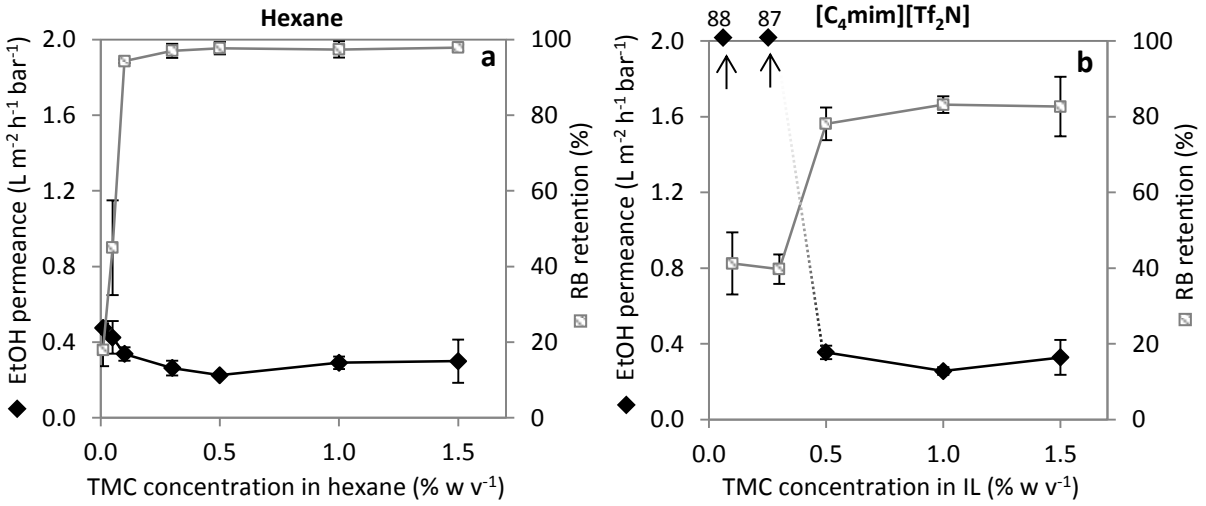

Figure 2.1: EtOH permeance and RB retention of TFC membranes synthesized with different TMC concentrations in (a) hexane and (b) [C_4mim][Tf_2N] and a 0.2% (w v^{-1}) MPD concentration in water.

This can be explained by the large viscosity difference of hexane and [C_4mim][Tf_2N] (Table 2.1), determining the diffusion rate of TMC to the reaction zone in the organic phase. For solvents like hexane, the solute diffusion coefficient D can be calculated using the Stokes-Einstein equation (Equation 2.3), with k_B the Boltzmann constant, T the absolute temperature, η the dynamic viscosity of the solvent and a the hydrodynamic radius of the solute:[187]

$$D = \frac{k_B T}{6\pi\eta a} \qquad (2.3)$$

For highly viscous media like ILs, a different relation was derived, as shown in Equation 2.4:[187]

$$D = \frac{k_B T}{4\pi\eta a} \qquad (2.4)$$

Assuming the hydrodynamic radius of the solute to be similar in both solvents, the ratio of the diffusion coefficients in hexane and [C_4mim][Tf_2N] becomes (Equation 2.5):

$$\frac{D_{hex}}{D_{IL}} = \frac{2\times\eta_{IL}}{3\times\eta_{hex}} = 136 \qquad (2.5)$$

indicating that the solute diffusion rate in [C_4mim][Tf_2N] is more than 2 orders of magnitude lower than in hexane.

Although in early research on interfacial polymerization, the reaction was assumed to take place immediately after the rate-limiting transport of MPD across the interface,[108] more recent models showed the importance of the monomer diffusion rate in the organic phase.[126,127] It is assumed that, at conventional TMC concentrations, the amount of TMC close enough to the interface to instantaneously react with MPD is too low for complete film formation. In this situation, diffusion of TMC from the bulk organic phase towards the reaction zone would be necessary, and the organic solvent viscosity would indeed be an

important factor influencing the diffusion rate and thus the necessary TMC concentration. Therefore, the fraction of the interface area covered with TMC molecules when using the conventional 0.1% (w v^{-1}) TMC was calculated theoretically. Based on the diameters of an MPD and a TMC molecule (0.7 and 0.9 nm respectively), it was assumed that MPD can instantaneously collide and react with TMC molecules which are localized in the region from 0 to 1.6 nm from the interface (Figure 2.2). Therefore, the TMC molecules in this zone were considered to immediately react without diffusion. From the calculations in Table S2.1 in appendix A, it is concluded that the TMC molecules in this zone all together occupy only 0.23% of the total interfacial area. This means that, when they all react with three different MPD molecules (Figure 2.2), the total fraction of the interfacial area covered with these small oligomers is still lower than 1%. Although some simplifications and assumptions were made in these calculations, it is clear that no dense PA film is formed without any diffusion of TMC from the bulk towards the interface. Moreover, also MPD molecules will have the chance to diffuse more upwards in the organic phase. Due to the very low initial coverage of the interfacial area with oligomers, this diffusion will only slightly be hindered by these oligomers, and the diffusion coefficients of the monomers in the pure organic solvent will thus likely be an important factor in the interfacial polymerization reaction.

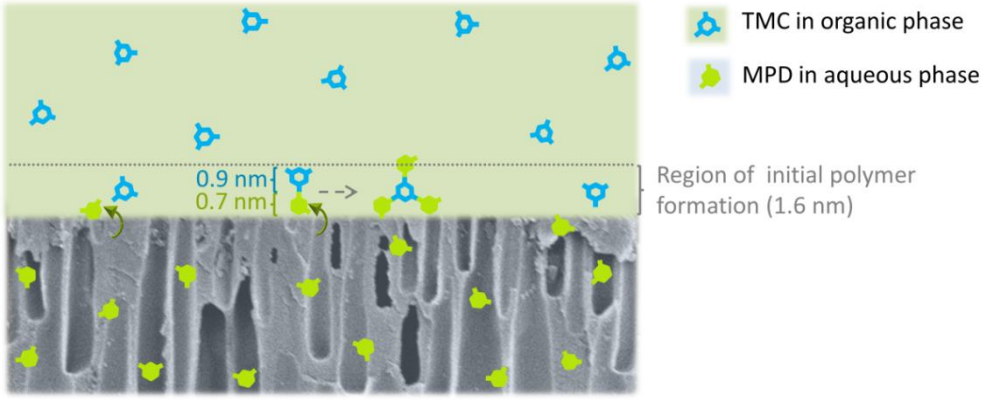

Figure 2.2: Schematic representation of the region used for calculating the interfacial surface coverage by TMC and by the initially formed oligomers.

Due to the high viscosity of the IL, less TMC molecules in the IL thus diffuse into the reaction zone during the short interfacial polymerization time, explaining the need for higher TMC concentrations. Since the EtOH permeance in the conventional system (Figure 2.1a) remained low below 0.1% (w v^{-1}) TMC, a top layer was probably still formed, but the TMC/MPD ratio was too low to achieve a reasonable cross-linking. However, in the water/IL system (Figure 2.1b), the very high EtOH permeance below 0.5% (w v^{-1}) TMC indicates the absence of a top layer.

Additional evidence for this TMC concentration dependent top layer formation in the water/IL system was provided by ATR-IR spectroscopy (Figure 2.3). When using 0.3% TMC in [C_4mim][Tf_2N], only support related peaks were observed. However, three amide peaks

appeared (at 1660, 1608 and 1545 cm^{-1}) when applying 0.5% or 1.0% TMC, confirming the trend in performance.

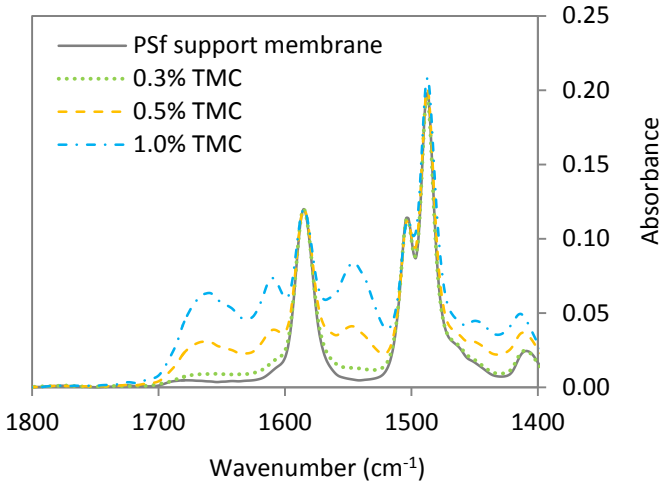

Figure 2.3: ATR-IR spectra of TFC membranes synthesized according to the water/IL system with different TMC concentrations and a constant MPD concentration of 0.2% (w v^{-1}).

Effect of MPD concentration

Based on the preliminary film formation tests, the MPD concentration was varied at 1.0% (w v^{-1}) TMC. Whereas high-performance membranes were formed at every MPD concentration tested in the conventional system, a very low MPD concentration of 0.1% (w v^{-1}) was needed in the water/IL system to form a good top layer (RB retention > 90%) (Figure 2.4). This is in line with the film formation results in Table 2.2.

The MPD concentration in the organic reaction zone is influenced by the transport rate of MPD across the interface and the solubility of MPD in the organic phase. An enhanced transport rate of dissolved species occurs between two phases with low interfacial tension, attributed to the higher partial miscibility of both solvents.[188] The use of a co-solvent to enhance the miscibility between two phases is a frequently used technique to facilitate interfacial MPD transport in interfacial polymerization to improve top layer formation.[105,112,114,115]

In the conventional system, a high interfacial tension (Table 2.1) and thus a limited transport rate of MPD across the interface may indicate the need for high aqueous MPD concentrations to obtain a sufficient amount of MPD in the organic reaction zone. However, increasing the MPD concentration did not enhance the RB retention. Probably, the MPD transport is limited by the very low MPD solubility in hexane (Table 2.1). The at least ten times higher MPD solubility in $[C_4mim][Tf_2N]$ and almost four times lower interfacial tension (Table 2.1) created an improved MPD transport in the water/IL system. Therefore, a too high MPD concentration for good cross-linking was present in the reaction zone at high aqueous MPD concentrations.

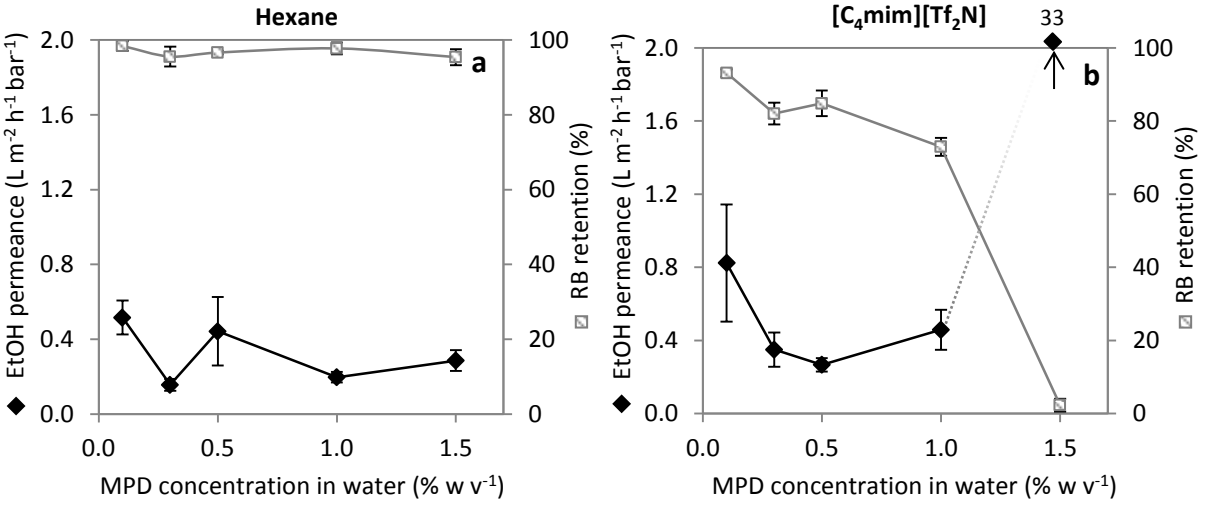

Figure 2.4: EtOH permeance and RB retention of TFC membranes synthesized with different MPD concentrations in water and a 1.0% (w v^{-1}) TMC concentration in (a) hexane or (b) [C_4mim][Tf_2N].

The differences in transport of MPD across the interface in the conventional and the water/IL system were confirmed by an MPD transport test. Figure 2.5 represents the MPD concentration decrease in the aqueous phase at 1 cm distance from the interface after bringing the aqueous MPD solution into contact with pure hexane or [C_4mim][Tf_2N]. In the case of hexane, the MPD concentration decrease was very small and ceased at longer contact times due to the low MPD solubility in hexane. However, an improved transport of MPD to [C_4mim][Tf_2N] was observed, which continued during the whole experiment. After 35 min, the MPD concentration decrease in the aqueous phase was almost 7.5 times higher when using [C_4mim][Tf_2N] instead of hexane (15.0% compared to 2.1%).

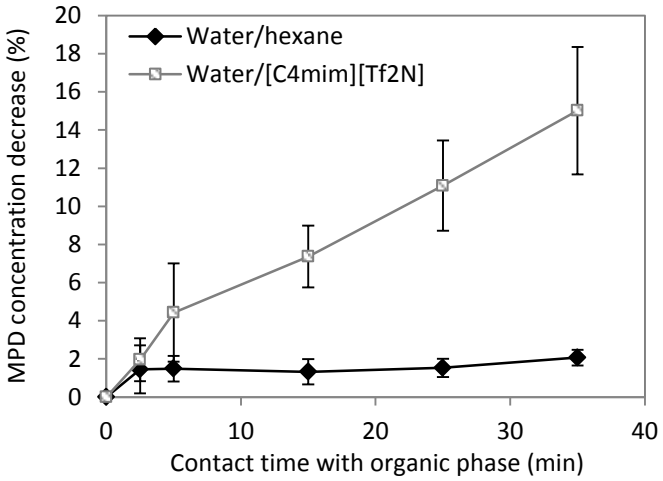

Figure 2.5: MPD concentration decrease in the aqueous phase (relative to the starting concentration of 2.0% (w v^{-1})) at 1 cm from the interface, after bringing the (unstirred) aqueous MPD solution into contact with a pure organic phase for different times.

The filtration results of the TFC membranes synthesized via the water/IL system were further supported by ATR-IR (Figure 2.6). When applying 0.1% MPD, amide peaks were present in the spectrum as expected, but with 1.0 and 1.5% MPD, these peaks became extremely

intense. This indicated the formation of a very thick top layer, which is in contrast with the lower RB retentions. SEM and TEM images of the TFC membrane surface made with 1.5% MPD (Figure 2.7) indeed showed the presence of a very thick but inhomogeneous, crust-like PA structure, being very different from a top layer with high selectivity (Figure S2.5c in appendix A and Figure 2.9c). This explains both the very large amide peaks (resulting from spots covered with a PA layer) and the very low RB retention of the membrane (due to the uncovered zones).

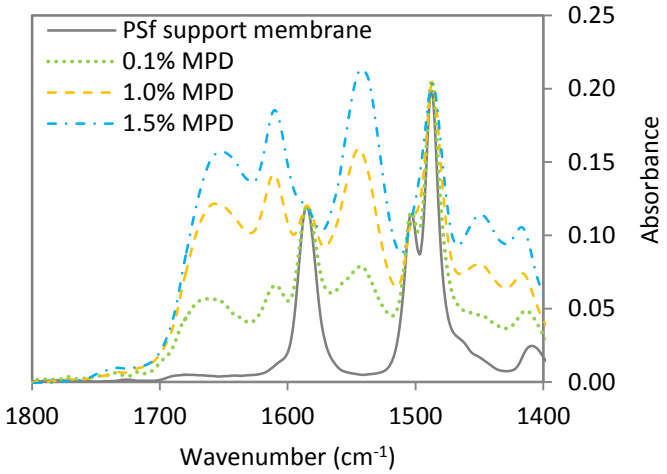

Figure 2.6: ATR-IR spectra of TFC membranes synthesized according to the water/IL system with different MPD concentrations and a constant TMC concentration of 1.0% (w v^{-1}).

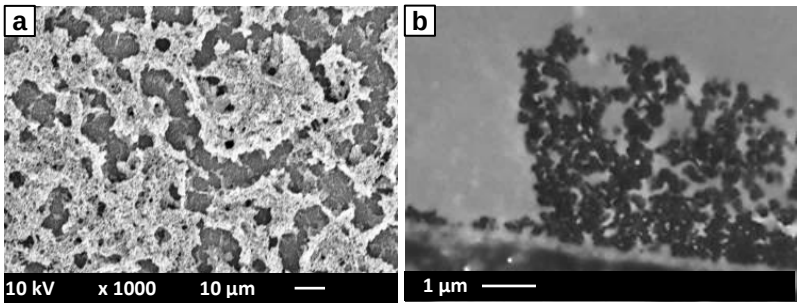

Figure 2.7: (a) Surface SEM and (b) cross-section TEM images of the top layer of a TFC membrane synthesized according to the water/IL system with monomer concentrations of 1.5% (w v^{-1}) MPD and 1.0% (w v^{-1}) TMC.

Use of additives

In traditional interfacial polymerization, additives are often used to enhance top layer formation. Typical additives are a surfactant, like sodium dodecyl sulfate (SDS), and an acylation catalyst/proton acceptor, like triethylamine (TEA), both added to the aqueous phase.[72,110,172,175,176] Figure 2.8a shows that using additives in the conventional system resulted in a four times increase in permeance. This is caused by a polymerization rate increase, said to result in the formation of a thinner top layer,[126] having a more open top layer morphology.[72] A small improvement in permeance was already obtained using only SDS, lowering the water-hexane interfacial tension and facilitating MPD transport to the

organic phase.[109] When only TEA was added, no permeance increase was observed. The slow transport of MPD to the organic phase possibly limited the potential reaction rate increase realized by the catalyst, or the interfacial transport of TEA itself towards the reaction zone was also too slow. However, when adding both SDS and TEA, the transport of MPD (and TEA) as well as the reaction between MPD and TMC was enhanced and a maximal increase in polymerization rate was achieved, similar to earlier observations.[110]

In the water/IL system, monomer concentrations of 0.1% (w v^{-1}) MPD and 0.5% (w v^{-1}) TMC were used. Besides the conventional 2.0% (w v^{-1}) TEA, a concentration of 0.5% (w v^{-1}) was also tested because the interfacial transport of TEA is possibly facilitated, as is the case for the MPD transport. A too high TEA concentration may then negatively influence the polymerization. In the water/IL system, the membrane performance could not be improved by adding SDS (Figure 2.8b). Probably, the MPD transport across the interface was already fast (Figure 2.5) because of the low water-IL interfacial tension and the high MPD solubility in [C_4mim][Tf_2N] (Table 2.1). Several authors have mentioned the capability of ILs to orient their hydrophilic part to the aqueous side and their hydrophobic part to the IL, making them act like a surfactant.[189–191] This makes it unnecessary to use SDS here. Also TEA is not useful for enhancing the membrane performance (Figure 2.8b). Two effects of the addition of TEA might be influenced by the replacement of hexane by an IL. The first one is the effect of the catalytic activity of TEA on the polymerization rate. The high IL viscosity (Table 2.1) slows down the diffusion of the monomers in the reaction zone (as calculated above using the Stokes-Einstein equation), which probably causes the polymerization to be highly diffusion limited. In such conditions, a catalyst is not effective. On the other hand, TEA also acts as a proton acceptor, neutralizing HCl, formed as by-product during interfacial polymerization. Due to the solubility of TEA in the hexane phase (log P_{ow} = 1.45 [192]), it can neutralize HCl immediately after its formation in the organic reaction zone. When no TEA is added, MPD in the reaction zone might be protonated by HCl and become unreactive. In this case, new MPD needs to be supplied from the aqueous phase. Since the interfacial transport of MPD is promoted in the water/IL system (Figure 2.5), a faster supply of fresh MPD might result in a lower need for TEA to prevent MPD protonation.

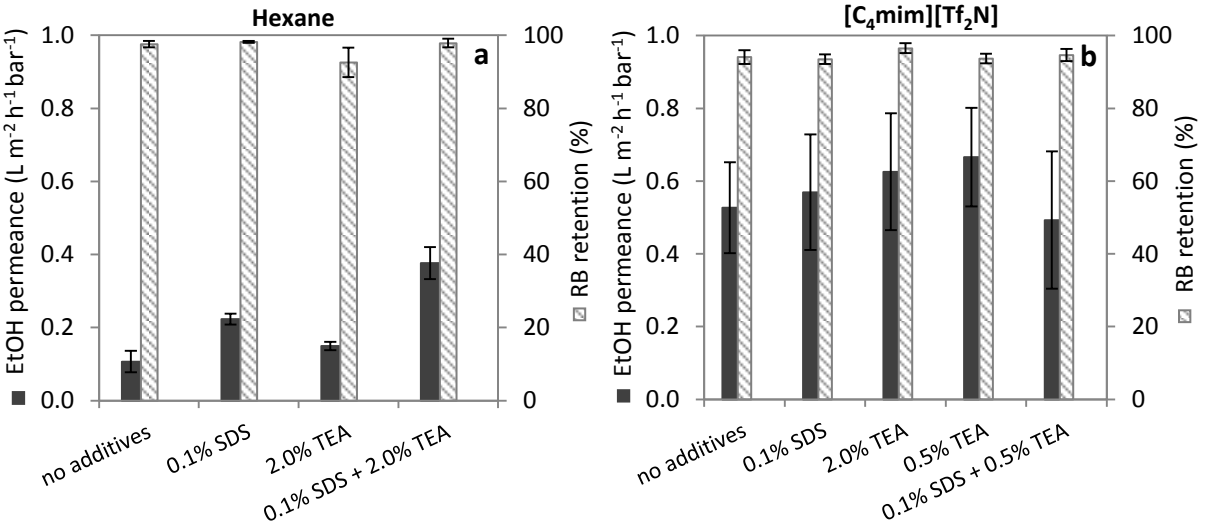

Figure 2.8: Influence of the variation of the additives SDS and TEA in the aqueous phase on EtOH permeance and RB retention of TFC membranes synthesized (a) according to the conventional system with 2.0% (w v^{-1}) MPD and 0.1% (w v^{-1}) TMC and (b) according to the water/IL system with 0.1% (w v^{-1}) MPD and 0.5% (w v^{-1}) TMC.

To support the performance results, SEM images of a top layer made without and with adding SDS and TEA were taken for both systems (Figure 2.9). For comparison, a SEM image of a pristine PSf support surface is shown in Figure S2.4 in appendix A. In the conventional system, the surface morphology changed from a rather 'grainy' structure to the typical 'ridge-and-valley' structure by adding SDS and TEA (Figure 2.9a and b). This latter seems to be more open, as explained before, which likely caused the increase in permeance. In the water/IL system, corresponding to the filtration results, no clear change in surface morphology was observed (Figure 2.9c and d). It is, however, very clear that the morphology of the top layer is largely influenced by the organic phase (compare a and c; b and d). The use of an IL results in the formation of a 'clustered nodular' structure.

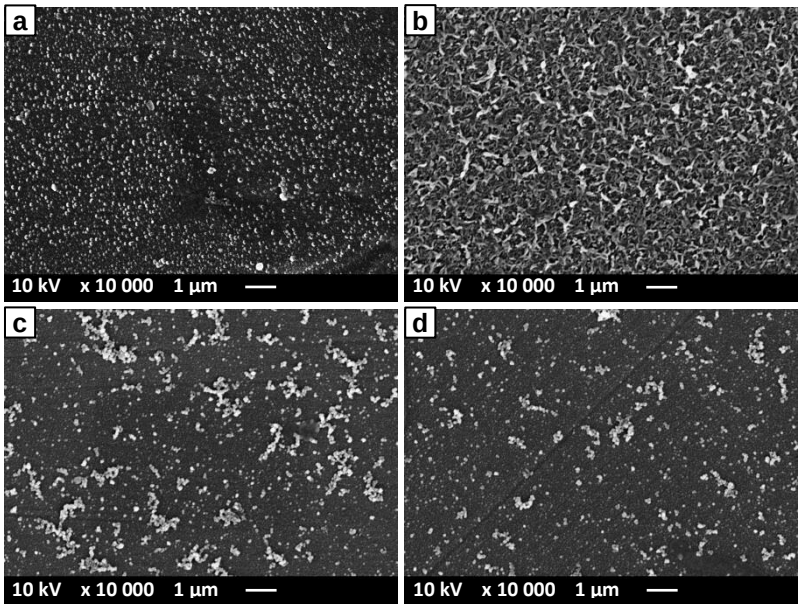

Figure 2.9: SEM images of the surface of TFC membranes synthesized according to the conventional system with monomer concentrations of 2.0% (w v^{-1}) MPD and 0.1% (w v^{-1}) TMC, (a) without and (b) with SDS and TEA, and according to the water/IL system with 0.1% (w v^{-1}) MPD and 0.5% (w v^{-1}) TMC, (c) without and (d) with SDS and TEA.

A clear difference in permeance in favor of the water/IL system can be derived from Figure 2.8a and b. Variations in top layer morphology and chemical composition, potentially causing this difference in performance, are thoroughly discussed in 2.3.2.

Effect of support type

To create TFC membranes with a broad application range, going from RO and aqueous NF to SRNF, the less stable PSf support was replaced by a solvent-resistant cross-linked PI support. The filtration results of TFC membranes made with 0.1% (w v^{-1}) MPD in water and 0.5% (w v^{-1}) TMC in [C_4mim][Tf_2N] indicated that, although the change in EtOH permeance was not significant when replacing PSf by cross-linked PI (from 0.53 ± 0.13 to 0.61 ± 0.07 L m^{-2} h^{-1} bar^{-1}), a clear increase in RB retention from 94.1 ± 1.9 to 99.1 ± 0.2% occurred. Also for SB, a lower molecular weight (457 Da), uncharged solute, a high retention of 96.2 ± 1.4% was obtained when using a TFC membrane on a cross-linked PI support.

Differences in performance could be caused by changes in top layer structure due to the use of a more hydrophilic support like cross-linked PI.[76,79] Based on a model proposed by Ghosh *et al.*,[76] MPD has better interactions with more hydrophilic supports, which limits the violence of the MPD eruption from the support pores and creates smaller PA nuclei. SEM and AFM images (Figure 2.10) show that the nodular PA structures might have been somewhat smaller in the case of a cross-linked PI support. However, due to the very small difference, no clear conclusions about the exact mechanism can be drawn.

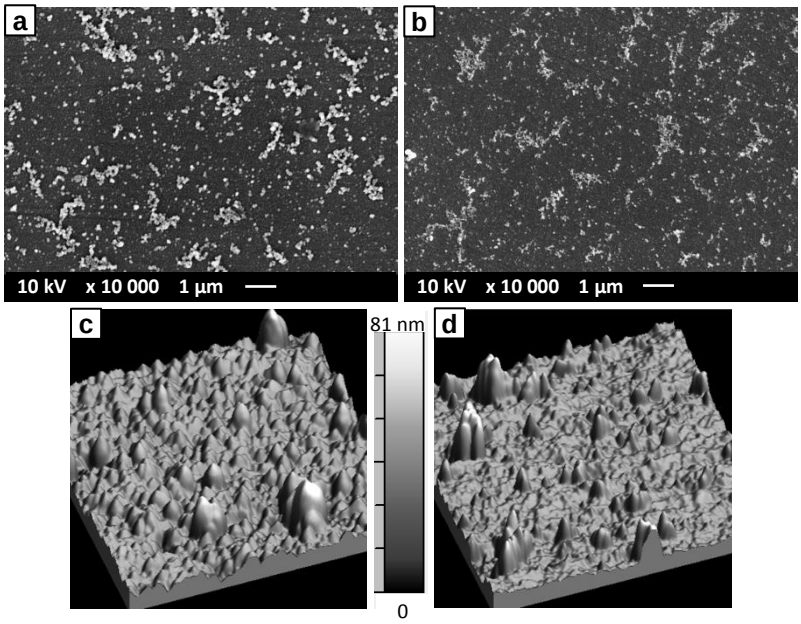

Figure 2.10: SEM and AFM images of the surface of TFC membranes synthesized according to the water/IL system on (a, c) a PSf and (b, d) a cross-linked PI support, with monomer concentrations of 0.1% (w v^{-1}) MPD and 0.5% (w v^{-1}) TMC.

2.3.2 Further top layer characterization

To gain a more fundamental insight in the differences in morphology and chemical structure of the top layer by replacing hexane by [C_4mim][Tf_2N], several characterizations were executed on the best performing membranes of both systems (i.e. PA on PSf via the conventional system with addition of SDS and TEA, and PA on cross-linked PI via the water/IL system without the use of additives). A conventional PA on PSf membrane without additives was also included in the investigations, since the lower surface roughness of this membrane compared to the one with additives (compare Figure 2.9a and b and the RMS roughness in Table 2.3) results in a more reliable chemical surface analysis, and might thus be a better choice for comparison with the membrane made via the water/IL system.

Table 2.3 gives an overview of the morphological and chemical properties of the selected membranes, together with their performance using either a RB/EtOH or a NaCl/water feed solution. Compared to the conventional PA membrane prepared without additives (M1), the membrane made via the water/IL system (M3) showed a remarkably higher EtOH (x 550%) and water permeance (x 350%), while the RB and NaCl retentions were very similar. These differences were caused by a combination of morphological and chemical alterations of the top layer.

Concerning morphology, both the significantly reduced thickness and the higher free volume diameter of the top layer made via the water/IL system (Table 2.3) support its higher permeance. The reduced thickness is expected to be caused by the high IL viscosity (Table 2.1), lowering the diffusivity of MPD in the reaction zone, as described by the Stokes-Einstein equation (Equation 2.3 and 2.4). This might have reduced the thickness of the reaction zone. Nadler *et al*. simulated the interfacial polymerization process using a model of diffusion-

limited cluster aggregation, in which a more diffusion-limited regime creates lower density structures.[127] This can be an explanation for the higher free volume diameter of the top layer prepared via the water/IL system. The value is, however, still situated in the standard free volume diameter range for RO and NF membranes,[131] and therefore, no decrease in retention was observed. Chemical differences between membranes M1 and M3 are situated in the surface charge and hydrophilicity of the top layer (Table 2.3). The membrane made via the water/IL system shows both a higher surface hydrophilicity and a more negative surface charge, probably resulting from a higher concentration of hydrolyzed unreacted acyl chloride groups at the surface. However, the average cross-linking degree over the upper 0-22 nm, derived from the average O/N ratio in this region, is very similar (Table 2.3). The higher surface charge and hydrophilicity probably also positively influence the (water) permeance. When comparing the conventional membrane prepared with additives (M2) with the water/IL-prepared membrane (M3), the differences in top layer properties are generally less clear. This might be due to the smaller difference in performance between these membranes, and by the lower reliability of some characterizations on membrane M2 due to its high surface roughness.

Table 2.3: Overview of the performance and the morphological and chemical properties of three selected membranes made via the conventional and the water/IL system.

Membrane	M1	M2	M3
System	Conventional	Conventional	Water/IL
Support	PSf	PSf	Cross-linked PI
SDS + TEA	No	Yes	No
EtOH permeance ($L\ m^{-2}\ h^{-1}\ bar^{-1}$)	0.11 ± 0.03	0.38 ± 0.04	0.61 ± 0.07
RB retention (%)	97.6 ± 0.9	97.9 ± 1.2	99.1 ± 0.2
Water permeance ($L\ m^{-2}\ h^{-1}\ bar^{-1}$)	0.31 ± 0.10	1.23 ± 0.29	1.09 ± 0.11
NaCl retention (%)	96.7 ± 1.9	95.5 ± 2.9	96.8 ± 0.9
Surface morphology [a]	Grainy	Ridge-and-valley	Nodular
Thickness (nm) [b]	43 ± 7	60 ± 32	25 ± 6 [c]
RMS roughness (nm) [d]	18 ± 1	30 ± 9	13 ± 1
Free volume diameter (nm) [e]	0.516	0.506	0.594
Degree of cross-linking (O/N ratio)[f]	Equal (1.77)	-	Equal (1.73)
Charge at pH 7.2 (zeta potential (mV)) [g]	Less negative (-66.2)	Less negative (-67.5)	More negative (-75.9)
Hydrophilicity (contact angle(°))	Less hydrophilic (49.2 ± 5.1)	More hydrophilic (35.8 ± 7.3)	More hydrophilic (39.3 ± 3.2)

[a] Based on the surface SEM images in Figure 2.9.

[b] Calculated from the cross-section TEM images in Figure S2.5 in appendix A.

[c] Top layer formed on a PSf support instead of a cross-linked PI support.

[d] Calculated from the surface AFM images in Figure S2.6 in appendix A.

[e] Determined via PLEPS measurements (Figure S2.7 in appendix A).

[f] Determined via ERD, average of upper 0-22 nm region (Figure S2.8 in appendix A).

[g] Determined via zeta potential measurements (Figure S2.9 in appendix A).

Since SEM indicated that the surface morphology of the best-performing membranes (M2 and M3) was very different (Figure 2.9), alterations in surface roughness were also investigated. Table 2.3 shows that the surface roughness decreased significantly by switching from the conventional (with additives) to the water/IL system, which might be an important advantage in terms of fouling, one of the major drawbacks in membrane technology in general.[164,165,193–195] Differences in fouling tendency between membranes prepared via the two systems are discussed in 2.3.3.

Figure 2.11 summarizes the effects of the properties of hexane and $[C_4mim][Tf_2N]$ on the top layer formation. As the high viscosity of $[C_4mim][Tf_2N]$ slows down the diffusion of TMC to the reaction zone, a higher TMC concentration was required in the water/IL system for the formation of a highly cross-linked top layer. However, the MPD concentration in the aqueous phase could be decreased drastically, as MPD transport to $[C_4mim][Tf_2N]$ was facilitated by its high solubility in the IL and the low water-IL interfacial tension. In addition, the low diffusion rate of MPD in the IL caused the top layer to have larger free volume elements and a remarkably lower thickness, while its morphology changed from a typical 'ridge-and-valley' structure to a less rough, 'clustered nodular' structure by replacing hexane by $[C_4mim][Tf_2N]$. Moreover, the use of the IL resulted in a higher surface hydrophilicity and charge. Finally, in contrast to the conventional system, high performance membranes in the water/IL system were achieved without using SDS and TEA.

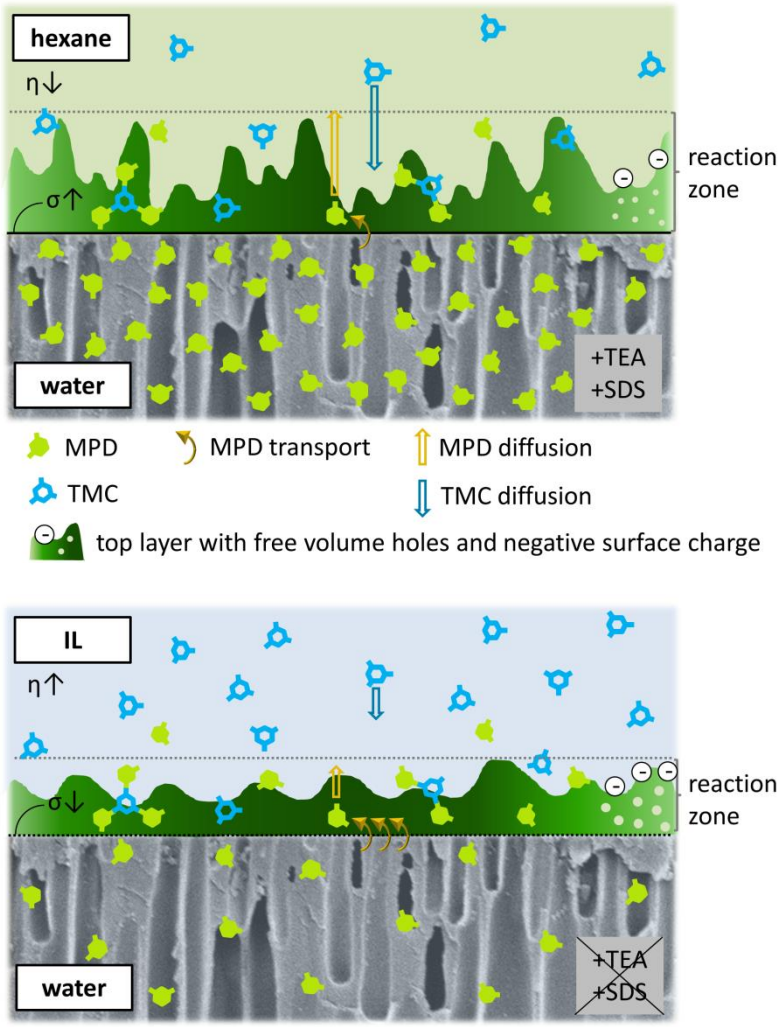

Figure 2.11: Representation of the effects of the properties of the non-aqueous phase on the interfacial polymerization process in the conventional and the water/IL system.

2.3.3 RO performance and fouling tendency

Table 2.3 shows the excellent RO performance of the membrane made via the water/[C_4mim][Tf_2N] system on a cross-linked PI support (M3). Another type of IL, [C_4mpyr][Tf_2N], was also tested as non-aqueous phase in interfacial polymerization. This membrane showed a somewhat higher water permeance (1.28 ± 0.07 for [C_4mpyr][Tf_2N] versus 1.09 ± 0.11 L m^{-2} h^{-1} bar^{-1} for [C_4mim][Tf_2N]) and lower NaCl retention (92.8 ± 1.8 for [C_4mpyr][Tf_2N] versus 96.8 ± 0.9 % for [C_4mim][Tf_2N]). This could be ascribed to the higher viscosity of the IL (76 mPa s[196] versus 51 mPa s[185] at 25 °C), rendering the monomer and cluster aggregation during interfacial polymerization even more diffusion limited, resulting in the formation of a less dense top layer. A high-performance membrane was, however, still obtained, confirming the versatility of the water/IL system.

In industrial water treatment, other components than NaCl are also present in the feed stream. Silica is a component which can be found in all types of surface waters and which can, mainly in its colloidal form, cause severe membrane fouling, resulting in a strong flux

decline.[197] The surface morphology and roughness of the top layer are described as one of the important factors influencing colloidal fouling.[64,164,165] To investigate the potentially lower colloidal fouling tendency of the water/IL-prepared membranes, silica particles with a colloidal diameter of 37.8 ± 0.6 nm and a polydispersity index of 0.141 ± 0.026 were used as fouling agent. Figure 2.12 indicates that the membrane prepared via the water/IL system (M3 in Table 2.3) indeed has a remarkably lower colloidal fouling tendency compared to the membrane prepared via the conventional system (M2 in Table 2.3), as the relative decline in permeance after 28h filtration was significantly lower (3% versus 16%). After applying a simple, rather mild rinsing step with water, the permeance increased again to 98% of the initial value for M3, and to 93% for M2.

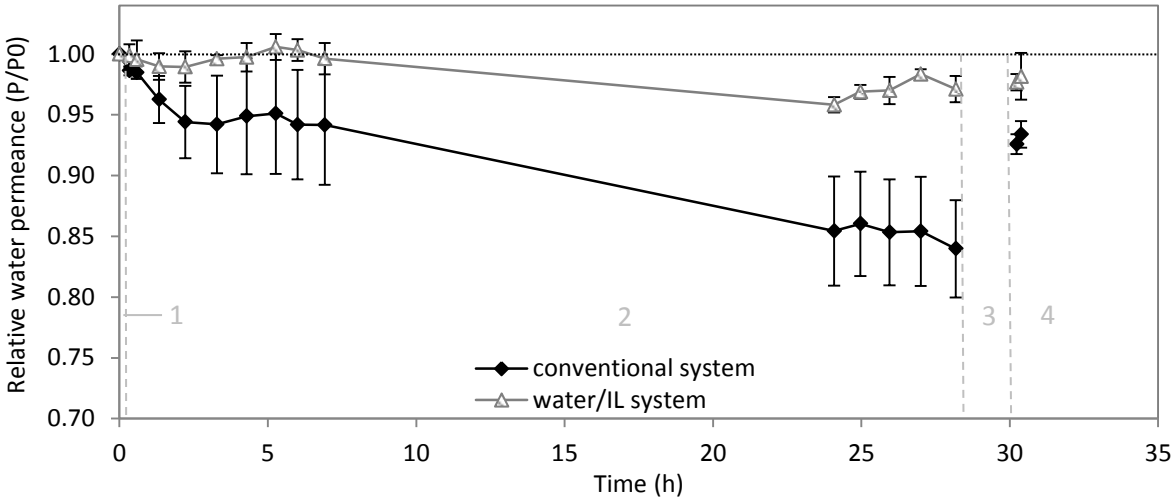

Figure 2.12: Relative water permeance of membranes prepared according to the conventional and the water/IL system, using a feed solution of 200 mg L^{-1} colloidal silica in water. Region (1) represents the measurement of the initial pure water permeance, (2) the fouling experiment, (3) the rinsing step with water, and (4) the determination of the pure water permeance after rinsing.

Another common type of fouling of RO membranes, is organic fouling. While the rough ridge-and-valley morphology of PA membranes is assumed to be the primary cause of colloidal fouling,[164,165,193] hydrophilicity and charge also contribute to organic and biofouling. A more hydrophilic surface generally results in a lower fouling tendency due to the reduced interaction between the organic or biofoulant and the membrane.[198–201] Biofouling is also counteracted by negatively charged membrane surfaces, as most bacterial surfaces have a negative charge as well.[200] However, when inorganic ions, like Ca^{2+}, are present in the feed, adsorption of natural organic matter on the membrane surface is promoted since the ions can form bridges between the negatively charged membrane and the organic foulant.[202]

Figure 2.13 presents the relative water permeance during filtration with meat peptone as model organic foulant. This fouling agent was chosen because it contains many components present in natural organic matter, i.e. proteins, polysaccharides, amino acids and fatty acids. Using this meat peptone feed solution, the decline in permeance of the water/IL-prepared

membrane (M3) after 25 h filtration was somewhat higher (8%) than with colloidal silica as fouling agent. Potentially, membrane-foulant interactions play a more significant role here, next to surface roughness. However, this result is still very good, and again better than for the membrane prepared via the conventional system (M2), which shows a 20% decline in permeance. After the same mild rinsing step with water, the water permeance increased again to 100 or 90% of the initial value for M3 and M2, respectively.

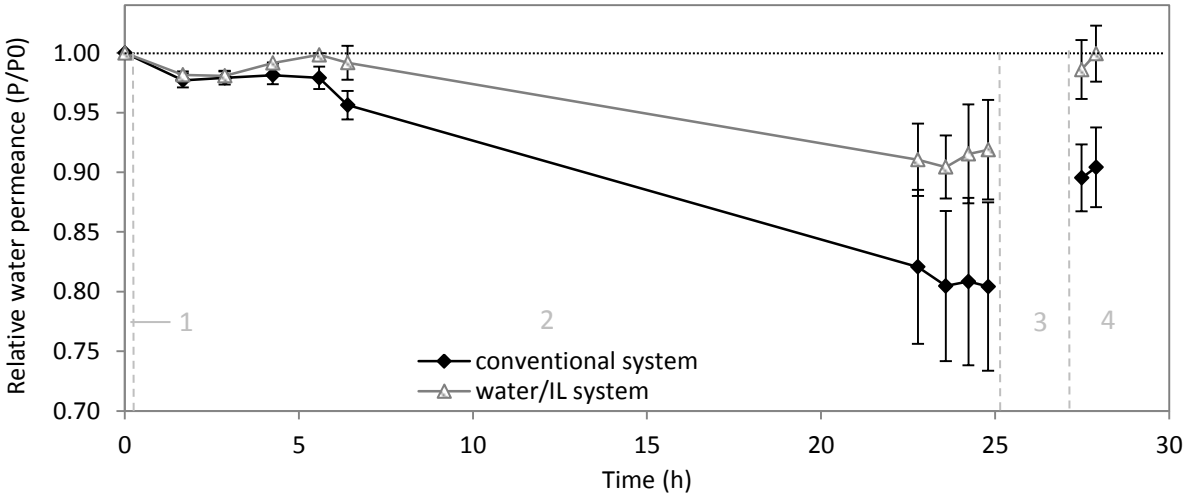

Figure 2.13: Relative water permeance of membranes prepared according to the conventional and the water/IL system, using a feed solution of 15 mg L^{-1} meat peptone in water. Region (1) represents the measurement of the initial pure water permeance, (2) the fouling experiment, (3) the rinsing step with water, and (4) the determination of the pure water permeance after rinsing.

2.4 Conclusions

A new, green method for the synthesis of TFC membranes via interfacial polymerization has been presented, in which the hazardous and volatile hexane phase is substituted by a water-immiscible IL.

The viscosity of the organic solvent played a crucial role by determining the diffusion rate of both monomers to and in the reaction zone. The high viscosity of [C_4mim][Tf_2N] induced the need for higher TMC concentrations. Moreover, the reaction zone became more restricted due to the slow diffusion of MPD, creating a remarkably thinner and smoother selective layer. Besides, the highly diffusion-limited regime during the interfacial polymerization was expected to be the reason for the higher average free volume diameter in the top layer of the water/IL-based membranes. Although the membranes showed a similar average degree of cross-linking, the top layer surface in the water/IL system was significantly more negatively charged and more hydrophilic. A second important parameter during membrane preparation was the MPD solubility in the organic phase, which determined, together with the water-organic interfacial tension, the rate and extent of the interfacial MPD transport. The high MPD solubility in the IL and the low water-IL interfacial tension induced an improved MPD transport, which drastically reduced the aqueous MPD concentration from

the conventional 2.0 to 0.1% (w v^{-1}). The surfactant properties of the IL also eliminated use of SDS, while a high performance was obtained without the addition of TEA as base/catalyst.

Besides the important advantages of the water/IL system in terms of sustainability (i.e. the 20 times reduction in MPD concentration and the elimination of commonly used neurotoxic hexane and additives like SDS and TEA), the membrane performance was also improved. A high EtOH permeance of 0.61 L m^{-2} h^{-1} bar^{-1} (99.1% RB retention) was obtained, which is 560% and 160% higher than the EtOH permeance for the conventional system (without and with the addition of SDS and TEA respectively). Even for RO, excellent membranes could be obtained at lab-scale, showing a NaCl retention up to 96.8%. Compared to those prepared via the conventional system without or with additives, the membranes synthesized according to the water/IL system showed a 350% higher or equal water permeance, respectively, with comparable selectivity. Moreover, due to their decreased surface roughness, these membranes were significantly more resistant to fouling, using colloidal silica (with a colloidal diameter of 38 mm) and meat peptone as fouling agent.

2.5 Acknowledgements

We are grateful for the financial support from KU Leuven (OT (11/061) funding), the Belgian Federal Government (I.A.P. – P.A.I. grant (IAP 7/05 FS2)) and the Flemish Government (long term Methusalem (CASAS) funding). We also wish to thank A. Vandoren and J. Billen from the Laboratory for Entomology of KU Leuven for chemicals and procedures for TEM, A. Volodin from the Laboratory of Solid-State Physics and Magnetism of KU Leuven for the AFM measurements, and M. d'Halluin from the Centre of Surface Chemistry and Catalysis of KU Leuven for the DLS analysis. We would also like to thank A. Szymczyk from the Institut des Sciences Chimiques of the university of Rennes for performing the zeta potential measurements, the Heinz Maier-Leibnitz Zentrum for the PLEPS measurements and T. Koschine and R. Verbeke from the Centre of Surface Chemistry and Catalysis of KU Leuven for the evaluation of the PLEPS results. We are thankful to A. Bergmaier from Institut für Angewandte Physik und Messtechnik of Universität der Bundeswehr München and R. Verbeke from the Centre of Surface Chemistry and Catalysis of KU Leuven for performing ERD measurements and analyzing the results.

CHAPTER 3

Preparation of high-performance thin film composite membranes using ionic liquids as the organic reaction medium

Optimization

Based on Hanne Mariën, Ivo F.J. Vankelecom, *submitted*.

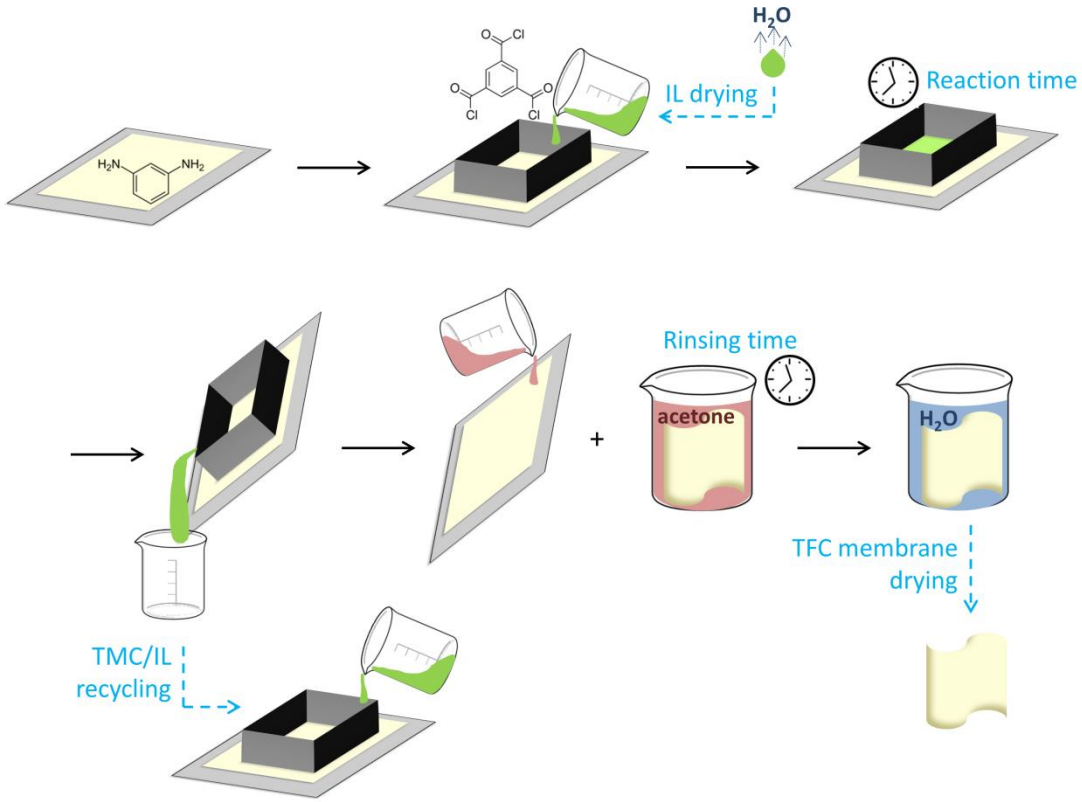

Abstract

A new form of interfacial polymerization to form thin film composite (TFC) membranes, in which ionic liquids (ILs) were introduced as the organic reaction phase, was developed in our previous work. The use of this water/IL system realized a more sustainable membrane preparation and an improved RO/NF performance. Different steps in the synthesis were now analyzed to further improve the time and cost efficiency, as well as the environmental impact of the preparation process and to maximize the resulting membrane performance. Time efficiency was improved by shortening the interfacial polymerization time to 10 s, while the waste generation was drastically lowered by recycling the IL for subsequent interfacial polymerization cycles. This resulted in a 64% decrease in mass intensity of the top layer formation process, while a 52% lower mass intensity compared to the conventional system was obtained. Moreover, residual trimesoyl chloride (TMC) monomers present in the IL could also be recycled, since the IL protected TMC from being hydrolyzed, even at very high water contents in the IL (> 1000 ppm). Successful introduction of the recycling step, together with the possibility to dry the formed membrane sheets without loss of performance by conditioning with glycerol, clearly demonstrated the upscaling potential of the new preparation method. Finally, the rinsing time after interfacial polymerization was optimized to further improve the performance and to avoid the presence of residual synthesis solvents or monomers during the filtration.

3.1 Introduction

Nanofiltration (NF) and reverse osmosis (RO) are pressure-driven membrane processes in which low molecular weight components can be retained on a molecular level.[13,14,62,74] Many large-scale aqueous applications exist, e.g. in saltwater desalination and wastewater treatment.[160] Nowadays, RO represents 65% of the total worldwide desalination capacity,[11] showing a two to eight times lower specific energy consumption than distillation technologies.[12]

Thin film composite (TFC) membranes, consisting of a very thin, mostly polyamide (PA), selective layer on top of a porous support,[61] are a widespread membrane type in RO and aqueous NF. The porous support, made via phase inversion, typically consists of poly(ether)sulfone for aqueous applications.[74] The PA film is prepared via interfacial polymerization,[61] realized by impregnating the support with an aqueous amine solution and subsequently bringing its surface into contact with an immiscible organic (typically hexane or isopar) acyl chloride solution. Common monomers are *meta*-phenylenediamine (MPD) or piperazine and trimesoyl chloride (TMC).[109,161] Near the water-organic interface, both monomers react to form a PA film with a thickness of a few tens of nanometers.[74] The reaction zone for top layer formation is assumed to be located in the organic phase under standard conditions, due to the very low solubility of TMC in water.[102,103] The very thin, dense and highly cross-linked top layer, capable of forming hydrogen bonds with aqueous feeds, causes the membrane to be highly selective, while still maintaining a high water permeance.[178]

In Chapter 2, a novel form of interfacial polymerization to form TFC membranes was presented by introducing ionic liquids (ILs) as the organic reaction phase.[203] The fundamental study clearly demonstrated the importance of the physicochemical properties of the non-aqueous phase on the top layer formation process. Since top layer formation is assumed to take place in the organic phase, transport of monomers and additives towards this phase, as well as their diffusion inside the organic phase and the polymerization reaction itself, are affected by the properties of the organic phase. The most important beneficial properties of the IL applied, 1-butyl-3-methylimidazolium bis(trifluoromethylsulfonyl)imide ($[C_4mim][Tf_2N]$), proved to be its high viscosity, its low interfacial tension with water, its surfactant properties and its high solubility for MPD, all being extremely different from commonly used hexane or isopar. It offered this novel interfacial polymerization system several important advantages. By replacing hexane by $[C_4mim][Tf_2N]$, the optimal MPD concentration in the aqueous phase could be reduced 20 times and the addition of sodium dodecyl sulfate and triethylamine, as surfactant and base/catalyst respectively, became redundant. Moreover, the top layer was significantly thinner, more open and more hydrophilic, resulting in a higher water permeance. Finally, the lower roughness of the top layer prepared via the water/IL system offered the membrane a clearly lower fouling tendency.

In this work, the novel water/IL system was further optimized in terms of membrane performance and of efficiency and waste reduction of the preparation process. Therefore, five different steps in the synthesis process were studied, as shown in more detail in Figure 3.1. In the first step, the effect of the IL drying method and the water content of the IL were investigated. Further, the optimal interfacial polymerization time and the minimal rinsing time for complete removal of the organic solution were determined. Finally, a method was developed to dry the resulting TFC membranes without loss of performance and to recycle the TMC/IL solution for subsequent interfacial polymerization cycles.

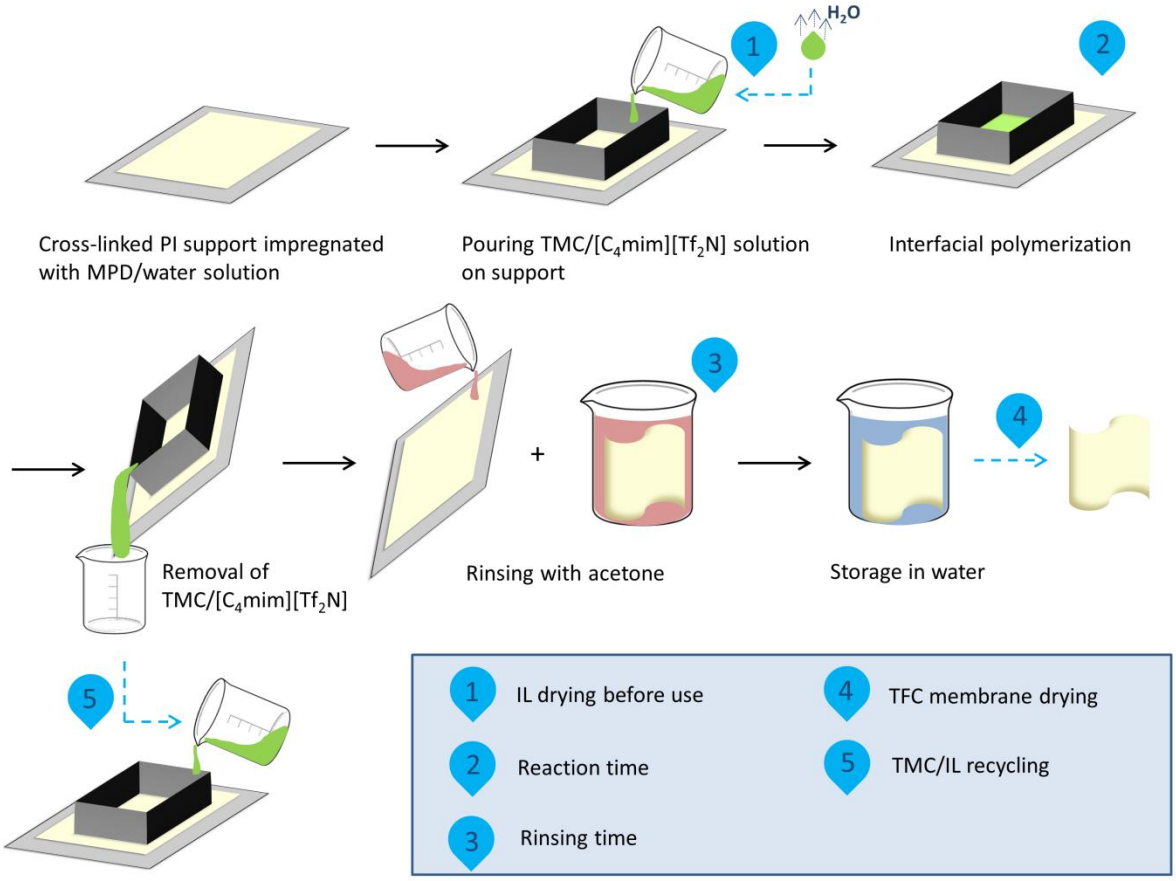

Figure 3.1: Schematic overview of the different steps in the interfacial polymerization process using the water/IL system. The numbers represent the steps which were further investigated in this work.

3.2 Experimental

3.2.1 Materials

Polyimide (PI, Matrimid® 9725) was purchased from Huntsman (Switzerland). The non-woven polypropylene/polyethylene fabric Novatexx 2471 was kindly provided by Freudenberg (Germany). Hexanediamine (HDA, 99.5%, Acros), *meta*-phenylenediamine (MPD, 99+%, Acros) and trimesoyl chloride (TMC, 98%, Acros) were used for membrane synthesis. N-methylpyrrolidone (NMP, 99%, Acros), tetrahydrofuran (THF, 99.9+%, Sigma-Aldrich), hexane (99+%, Chem-Lab), acetone (technical, VWR) and ethanol (EtOH, 99.99%,

Fisher) were used as received. 1-Butyl-3-methylimidazolium bis(trifluoromethylsulfonyl)imide ([C_4mim][Tf_2N], 99+%, Iolitec) was used after drying for 16 h at 80 °C under vacuum, or after drying with molecular sieve (3A, 8 to 12 mesh, Acros) for 96 h at room temperature. Sodium chloride (NaCl, 99.8%, VWR) was applied as test solute in Milli-Q water.

3.2.2 Membrane synthesis

Supports were synthesized via phase inversion.[19] PI powder was first dried overnight in an oven at 100 °C. A homogeneous polymer solution was prepared by stirring a mixture of PI (14% (w w^{-1})) in NMP/THF (3/1). It was left untouched overnight to remove air bubbles created during the stirring. The polymer solution was cast at a constant speed (4.4 x 10^{-2} m s^{-1}) and with a wet thickness of 200 µm using an automatic casting device (Braive Instruments, Belgium) on a non-woven impregnated with NMP. Then, the film was immersed in a coagulation bath. 30 s evaporation was inserted between the casting and the immersion to allow THF evaporation from the film surface. The coagulation bath consisted of HDA (0.5% (w v^{-1})) and MPD (0.1% (w v^{-1})) in Milli-Q water to simultaneously perform phase inversion, cross-linking and impregnation of the support with MPD.[73] After 5 min, the support was removed from the bath to perform the interfacial polymerization.

First, excess aqueous solution was removed from the impregnated support surface using a rubbery wiper. A solution of TMC (0.5% (w v^{-1})) in [C_4mim][Tf_2N] was subsequently poured gently on the support. After 60 s (unless specified otherwise), the solution was drained off and in specified cases, a pressurized air flow was applied to further remove the TMC/IL solution from the membrane surface. The membrane was then rinsed with acetone to remove the last traces of unreacted TMC and IL. Afterwards, the membrane was placed in a water bath to remove unreacted MPD. Finally, the TFC membrane was stored in distilled water until further use. In specified cases, the membrane was dried before filtration. As conditioning step before drying, a solvent exchange with EtOH as well as the impregnation with PEG400/EtOH, PEG400/water, PEG200/water or glycerol/water (3/2 v v^{-1}) was applied.

3.2.3 Membrane performance

See 2.2.3.

3.2.4 Membrane characterization

See 2.2.4 for SEM protocol.

An elemental analysis was performed with elemental recoil detection (ERD) to determine the presence of traces of IL on or in the membrane after interfacial polymerization. See 2.2.4 for ERD protocol.

3.2.5 Other measurements

The transport of HCl, formed during interfacial polymerization, from the organic to the aqueous phase was analyzed by measuring the pH of the aqueous phase before and after the formation of a free-floating PA film. Potential evaporation of TMC during drying a TMC/IL solution under vacuum was determined by repeatedly adding a fresh amount of water to a dried and non-dried solution and measuring the pH of the consecutive aqueous phases, after vigorously stirring the biphasic solution for one hour and letting the phases separate. Mixing the TMC/IL solution with water causes the TMC to hydrolyze and form HCl, which is transported to the aqueous phase. The pH measurements were performed with a VWR pH 1100L meter.

The water content of the IL was determined using a Mettler Toledo C30S coulometric Karl Fisher titrator. 0.3 – 0.7 g of IL was injected, depending on the expected water content.

3.2.6 Mass and solvent intensity

The mass and solvent intensities of the top layer formation process were calculated for the conventional water/hexane interfacial polymerization and for the water/IL system according to Equation 3.1 and 3.2:[204]

$$Mass\ intensity = \frac{mass\ of\ all\ materials\ used\ excluding\ water\ (kg)}{mass\ of\ product\ (kg)} \quad (3.1)$$

$$Solvent\ intensity = \frac{mass\ of\ all\ solvents\ used\ excluding\ water\ (kg)}{mass\ of\ product\ (kg)} \quad (3.2)$$

3.3 Results and discussion

The five different steps in the top layer synthesis via the water/IL system, shown in Figure 3.1, were investigated separately to improve the time and cost efficiency, as well as the environmental impact of the preparation process.

3.3.1 Ionic liquid drying

Since all ILs are hygroscopic to some extent, even hydrophobic, water-immiscible ones like [C_4mim][Tf_2N],[182] traces of water can be present in the IL during dissolution of TMC and subsequent interfacial polymerization. Because TMC can be hydrolyzed under influence of water and lose its reactivity, the water content of the IL (step 1 in Figure 3.1) is a factor which potentially influences top layer quality by affecting the degree of crosslinking and hydrophilic character. The most common method to dry ILs is moderate heating under vacuum, which was also applied in Chapter 2. Another possibility is the use of molecular sieves. A possible drawback of the latter is the slow diffusion of the water molecules towards the molecular sieve due to the high viscosity of some ILs. This can be overcome by adding a

volatile solvent to the IL, which can be easily evaporated afterwards.[139] The efficiency of the different IL drying methods as well as the effect of the water content of the IL on final membrane performance were studied.

To investigate the effect of the water content in the IL on top layer formation, the dried IL was exposed to air for different times. IL samples with a varying water content were thus obtained and used for dissolution of TMC and subsequent interfacial polymerization. Figure 3.2 shows the performance of TFC membranes synthesized with TMC/[C_4mim][Tf_2N] solutions containing different concentrations of water. An increasing amount of water in the IL was expected to reduce the cross-linking degree of the top layer due to TMC hydrolysis, which would result in a decreasing NaCl retention. For comparison, a water content of 1000 ppm corresponds to a number of water molecules being equal to the total number of acyl chloride groups of the TMC molecules in the solution, meaning that theoretically, all TMC molecules could be hydrolyzed totally and lose their reactivity towards polymerization. Surprisingly, no decrease in NaCl retention was observed, even at very high water concentrations of 1200 ppm. This shows the absence of TMC hydrolysis in the IL. The lack of reactivity of water in some ILs has been described before, although the exact mechanism is still unclear. It is assumed to be caused by the molecular dispersion of water in the IL and the strong water-IL interactions.[205] Solutes sensitive towards hydrolysis have shown to be stable for several hours when dissolved in [C_4mim][Tf_2N], the IL used in this work, containing 1500 ppm water.[206] This is a great advantage for the reuse of residual TMC during the recycling of the TMC/IL solution, as discussed further.

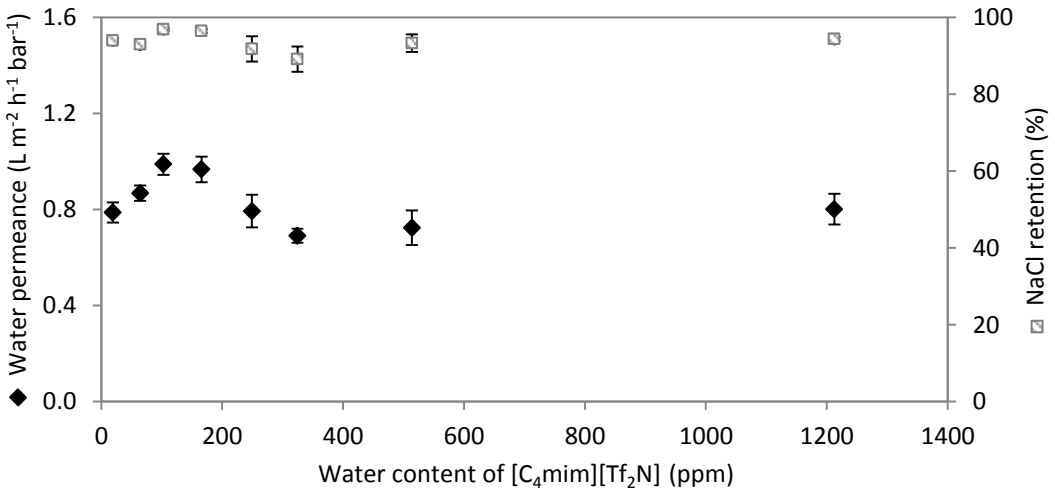

Figure 3.2: Influence of the water content in [C_4mim][Tf_2N] on the water permeance and NaCl retention of TFC membranes synthesized according to the water/IL system.

Although the NaCl retention is not negatively influenced by the high water content in the IL, it is still important to dry the IL before use. On the one hand, IL properties like viscosity and surface tension, which are aimed to be held constant, can vary significantly with increasing water content.[207,208] On the other hand, a high concentration of water in the IL can eventually cause the TMC molecules to hydrolyze when the contact is very long (e.g. several

days[206]), which is the case when the TMC/IL solution is recycled over long time periods, as discussed further.

Besides heating under vacuum, the use of molecular sieve 3A was investigated as a more convenient and less energy-intensive method for drying [C_4mim][Tf_2N]. Most ILs are diluted with a volatile organic solvent before exposure to sorbents to reduce the viscosity and thus increase the diffusion rate of water towards the sorbent.[139] Since the organic solvent must be evaporated afterwards, it would make this drying method less efficient again. However, due to the moderate viscosity of [C_4mim][Tf_2N], the addition of an extra solvent was unnecessary and the water content could be reduced from 528 to 66 ppm easily upon 96 h contact with molecular sieve 3A. The resulting membrane performance was very similar to the ones in Figure 3.2.

3.3.2 Reaction time

After pouring the TMC/IL solution on the impregnated support, interfacial polymerization is taking place. In our previous work, a reaction time of 60 s was applied. However, a shorter reaction time would be beneficial to obtain a highly productive process. Since polyamide formation proceeds very fast,[108] the top layer in the conventional system is assumed to be formed completely within a time frame of a few seconds. A lab-scale reaction time of 15 s was applied earlier in the conventional interfacial polymerization and resulted in a high-performance polyamide top layer.[110] In the water/IL system, not only the polymerization reaction itself is very fast, also the interfacial transport of MPD towards the reaction zone is accelerated.[203] On the other hand, the high viscosity of the IL limits the diffusion rate of the monomers towards each other, which might slow down the polymerization process. Therefore, the possibility to use a very short reaction time in the water/IL system was investigated (step 2 in Figure 3.1).

Figure 3.3 shows that lowering the interfacial polymerization time from 60 to 10 s in the water/IL system did not change the NaCl retention nor the water permeance significantly. Due to the practical limitations of lab-scale membrane preparations, reaction times lower than 10 s could not be applied accurately.

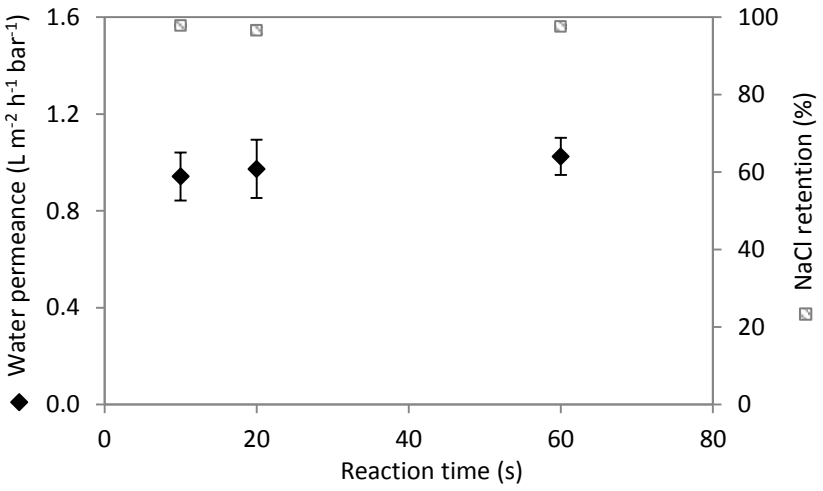

Figure 3.3: Influence of the interfacial polymerization time on the water permeance and NaCl retention of TFC membranes synthesized according to the water/IL system.

The SEM images in Figure 3.4 indicate that the morphology of the top layer surface did not change significantly by lowering the reaction time. Since the immediate formation of a dense PA film limits further diffusion of MPD in the organic phase, a drastic slowdown of the reaction was observed in earlier research,[126] the so-called 'self-termination' of the interfacial polymerization. This diffusion limitation prevents further growth of the top layer at the surface, as supported by the SEM images.

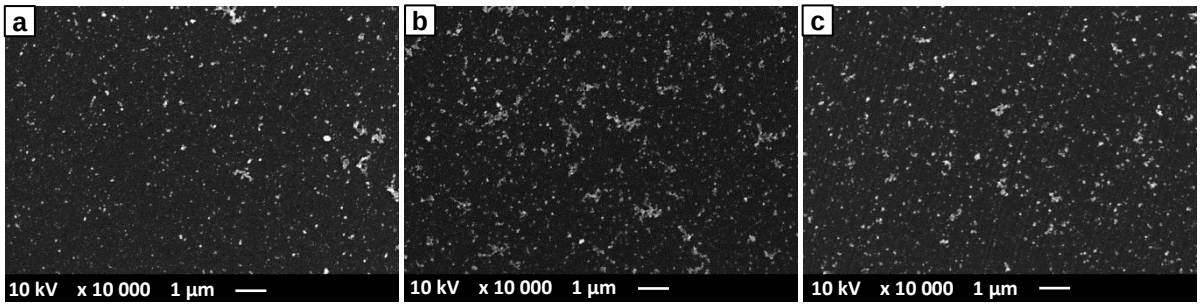

Figure 3.4: Surface SEM images of TFC membranes synthesized according to the water/IL system, using an interfacial polymerization time of (a) 10 s, (b) 20 s and (c) 60 s.

Due to the improved MPD transport across the interface towards the reaction zone in the water/IL system, as explained in Chapter 2,[203] a quicker initiation of the reaction could lead to an even faster top layer formation in this system compared to the conventional interfacial polymerization. The slower diffusion of the monomers in the highly viscous reaction zone in the water/IL system, on the other hand, could lead to a more diffusion-limited interfacial polymerization and could thus slow down the top layer formation. Oizerovich-Honig *et al*. reported an average monomer diffusion coefficient of 10^{-5} cm s^{-1} in the conventional interfacial polymerization, leading in their model to the growth of a film within 1 ms. After this time, the extent of film growth was greatly reduced.[128] Due to the 136 times lower monomer diffusion rate in the IL (Equation 2.5 in Chapter 2), but also the 58% thinner reaction zone (derived from the differences in top layer thickness in Table 2.3 in Chapter 2)

and the improved MPD transport, the top layer is still expected to be formed within 1 s in the water/IL system. This is however difficult to prove and beyond the scope of this work.

3.3.3 Rinsing time

Since residual solvents or reagents in or on the membrane can contaminate the feed or permeate during filtration, their presence is undesired. The high viscosity of $[C_4mim][Tf_2N]$ (63.05 mPa.s at 20°C[185]) causes the TMC/IL solution to be removed less easily from the membrane surface after top layer formation. Therefore, the rinsing time with acetone for complete removal of the TMC/IL solution was investigated (step 3 in Figure 3.1).

Figure 3.5 shows that increasing the rinsing time from 10 s to 60 min caused the membrane permeance to increase from 0.76 to 1.01 L m^{-2} h^{-1} bar^{-1}, while the selectivity was unchanged. No further improvements were observed for longer rinsing times. It was expected that after short rinsing, traces of IL would still be present on the membrane surface or in the top layer. This was confirmed by ERD measurements, detecting the presence of F in the membrane after 10 s rinsing (Figure S3.1 in appendix B). Since the IL consists of rather large, water-immiscible molecules, they cannot be further removed adequately during the aqueous filtration. Therefore, the IL can form a layer on the surface or partly block the free volume in the top layer, creating an extra resistance barrier for water permeation. The almost invisible nodular structure of the top layer surface after 10 s rinsing (Figure 3.6a) suggested that the membrane was indeed covered with a layer of IL. As shown in Figure 3.6b and c, the membrane surface morphology became more clearly visible after longer rinsing times. From 10 min onwards, no F could be detected on the membrane anymore via ERD analysis (Figure S3.1 in appendix B). A higher rinsing time of 60 min was, however, further used, since this resulted in the best membrane performance and the most clearly visible top layer morphology. In industrial membrane synthesis, more efficient large-scale rinsing methods will probably enable the use of shorter rinsing times.

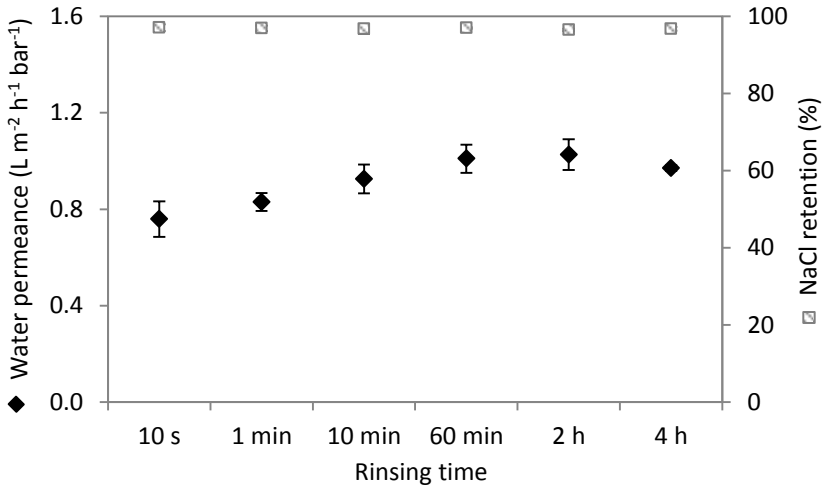

Figure 3.5: Influence of the rinsing time with acetone on the water permeance and NaCl retention of TFC membranes synthesized according to the water/IL system.

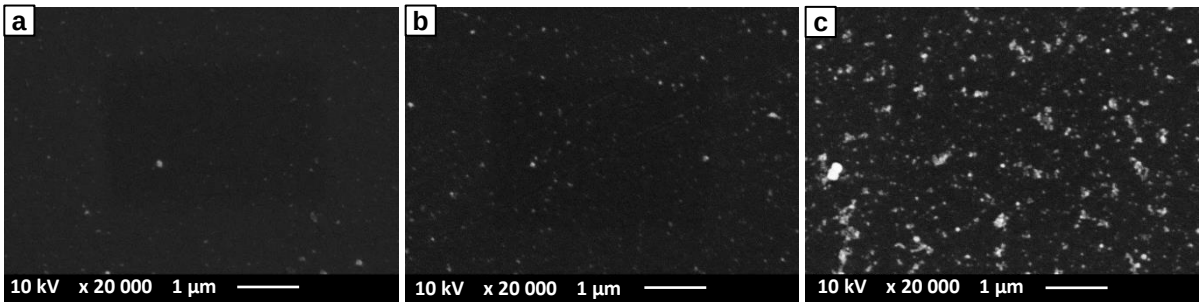

Figure 3.6: Surface SEM images of TFC membranes synthesized according to the water/IL system, followed by rinsing with acetone for (a) 10 s, (b) 10 min and (c) 60 min.

3.3.4 TFC membrane drying

To make RO membranes suitable for industrial use, they should retain a stable performance after the drying process used for module preparation.[209] When air-drying an unconditioned membrane, the pores of the support collapse, strongly lowering the permeance. Both the exchange of the water inside the membrane by solvents with a lower surface tension, as the impregnation of the membrane with pore preserving agents have been applied earlier as conditioning steps to overcome pore collapse.[47,209] Therefore, the possibility of drying the TFC membrane prepared via the water/IL system without loss in performance, after applying different conditioning treatments, was studied (step 4 in Figure 3.1).

Effect on support

First, a cross-linked PI support without a top layer was prepared to investigate the effect of different conditioning treatments on the support performance. As derived from Figure 3.7a, a non-dried support showed a very high water permeance of around 500 L m^{-2} h^{-1} bar^{-1} and no retention for NaCl. When the support was dried at room temperature or at 50°C, a dramatic decrease in permeance took place to values lower than those of TFC membranes, indicating the occurrence of severe pore collapse. Also the NaCl retention of the supports became moderately high.

Two different pore preserving steps were investigated. In the first one, the water present in the support was exchanged by EtOH, having a significantly lower surface tension than water (22.1 mN m^{-1} compared to 72.8 mN m^{-1}).[210] This might limit the collapse of the support pores during the drying step. However, after drying at 50°C, the support showed a very low water permeance of 0.12 L m^{-2} h^{-1} bar^{-1} together with a NaCl retention of 63%, being very similar to the performance of the dried supports in Figure 3.7a. Solvent exchange with EtOH thus clearly did not prevent the pores from collapsing.

Therefore, PEG 400, PEG 200 or glycerol were introduced in the support as pore preserving agents. Alcohols such as methanol, EtOH or isopropanol can be used as swelling agent for the support, making it easier for the pore preserving agent to reach all the pores. A comparison between EtOH and water as solvent when using PEG 400 (Figure 3.7b) indicated that EtOH did not show any advantages as swelling agent, as derived from the equal

performance of both supports after drying at 50°C. Therefore, cheaper water was further used as solvent. The use of PEG 400 (Figure 3.7b) did show beneficial effects as pore preserving agent, resulting in a strong increase in permeance and decrease in retention compared to the non-conditioned, dried support in Figure 3.7a. However, the permeance was still ten times lower than that of a non-dried support. Therefore, the size of the pore preserving agent was reduced by applying PEG 200 and glycerol in an attempt to enhance the PEG mobility to allow it to better reach even the smallest pores. Figure 3.7b clearly shows an increase in permeance, and thus a decrease in pore collapse, with a decreasing size of the pore preserving agent. When using glycerol, the performance of the dried support is very similar to that of a non-dried support. So, no influence on the performance of the resulting TFC membrane is expected from this glycerol-impregnated, dried support.

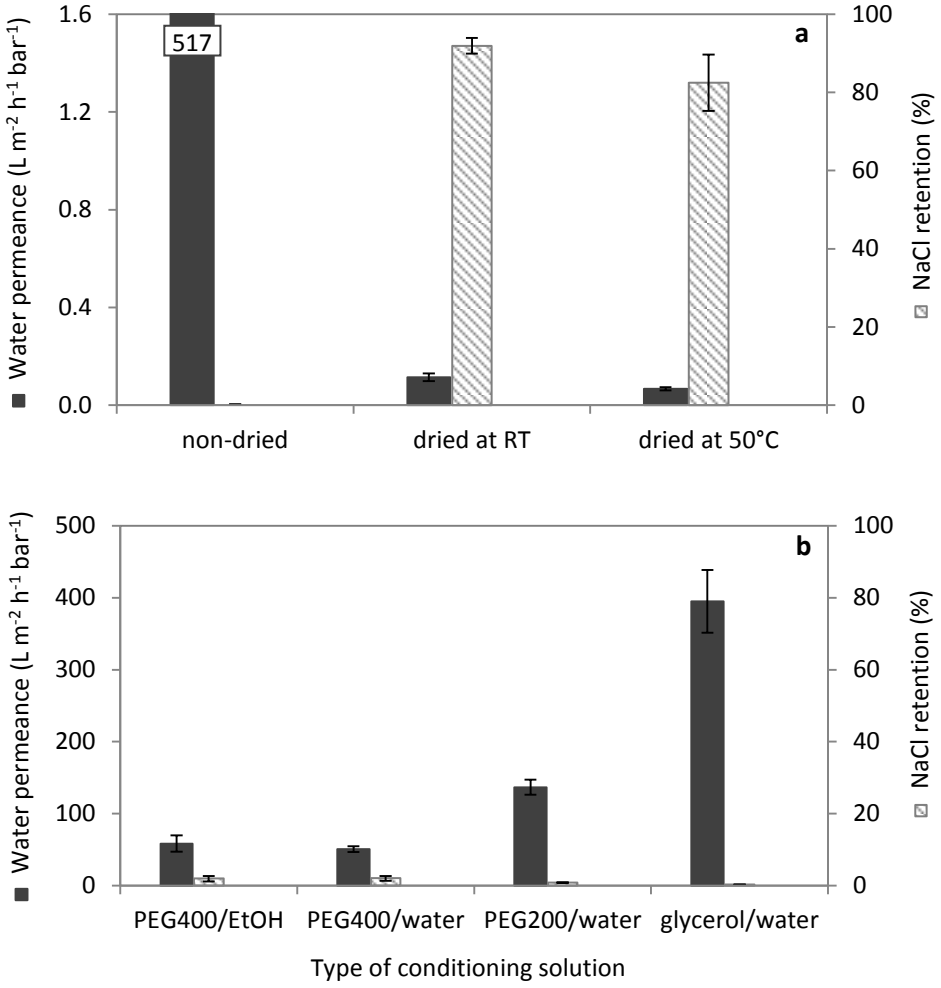

Figure 3.7: Influence of (a) membrane drying and (b) different conditioning steps before membrane drying at 50°C on the water permeance and NaCl retention of cross-linked polyimide supports.

Effect on TFC membrane

Since glycerol was the optimal pore preserving agent for the support, it was chosen to impregnate the TFC membrane with after interfacial polymerization. In Figure 3.8, a comparison is made between the performance of a non-dried, and a non-conditioned and conditioned, dried TFC membrane. As expected, a strong decrease in permeance occurred after drying a non-impregnated TFC membrane, both at room temperature and at 50°C drying. This pore collapse, however, seems to be somewhat less severe than that of the non-impregnated, dried supports, as derived from the higher permeance of the dried TFC membranes (Figure 3.8, 0.18 and 0.16 L m^{-2} h^{-1} bar^{-1}) compared to that of the dried supports (Figure 3.7a, 0.11 and 0.07 L m^{-2} h^{-1} bar^{-1}). Possibly, the presence of a top layer diminished the pore collapse of the support due to the partial intrusion of the top layer in the smallest support pores close to the surface of the support. Impregnation of the TFC membrane with a glycerol/water mixture proved to be an effective way to prevent pore collapse, based on the equal (after drying at room temperature) or only slightly lower water permeance (after drying the membrane at 50°C) compared to the non-dried TFC membrane.

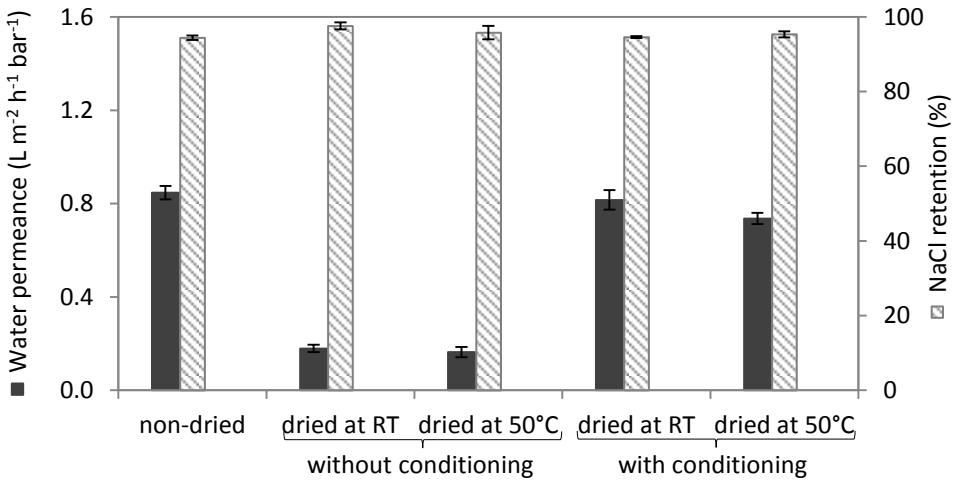

Figure 3.8: Influence of membrane drying and the impregnation with glycerol/water as conditioning step on the water permeance and NaCl retention of TFC membranes synthesized according to the water/IL system.

3.3.5 Ionic liquid recycling

To reduce the amount of waste and improve the cost-efficiency of the synthesis process, the possibility of recycling the IL for reuse in the next membrane batch preparation was investigated. This was achieved by applying a flow of pressurized air (6 bar) over the membrane surface after interfacial polymerization and directly collecting the TMC/IL solution, followed by washing the membrane with acetone to remove the last traces of solution from the surface.

Top layer resistance

The effect of blowing pressurized air over the PA top layer on the membrane performance is shown in Figure 3.9. The high NaCl retention, equal to the retention after conventional

rinsing of the membrane, proves that the thin PA film is fully resistant to the pressurized airflow. This was confirmed by SEM images, showing very similar surface morphologies of the top layer after the conventional rinsing step or after air blowing (Figure 3.10).

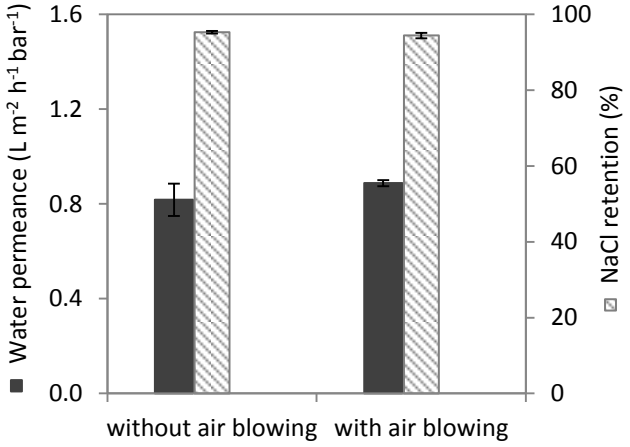

Figure 3.9: Influence of the way of TMC/IL removal from the membrane surface after interfacial polymerization on the water permeance and NaCl retention of TFC membranes synthesized according to the water/IL system.

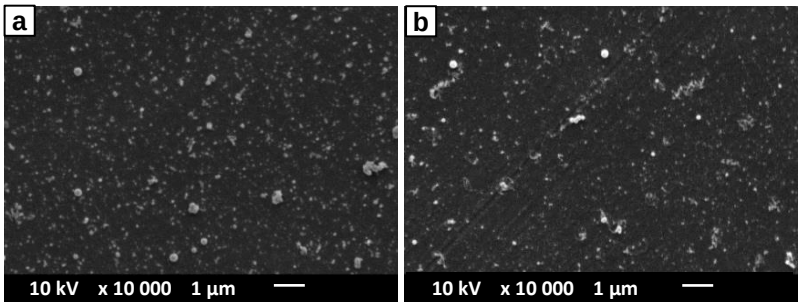

Figure 3.10: Surface SEM images of TFC membranes synthesized according to the water/IL system, (a) after the conventional rinsing step with acetone and (b) after air blowing, followed by rinsing with acetone.

IL purity after recycling

By air blowing the membrane surface after interfacial polymerization, 94-98% of the used TMC/IL solution could be recovered directly. The remaining traces of IL on the membrane surface were washed away with acetone. When a 100% recycling of the IL is desired, acetone can be distilled off easily.

To determine the need for purification steps or other treatments before reusing the collected TMC/IL solution in the second interfacial polymerization cycle, the presence of different species in the solution at the end of the first cycle was analyzed. Potential impurities would be water (taken up from the aqueous phase during interfacial polymerization), residual TMC, and HCl (formed during interfacial polymerization).

Water

After 1 min of interfacial polymerization, the water content of the IL solution increased from 34.9 to 690.7 ppm, indicating a significant uptake of water in the IL during top layer formation. Since the use of $[C_4mim][Tf_2N]$ as solvent has shown to dramatically reduce the reactivity of dissolved water molecules and protect TMC against hydrolysis, the uptake of water in the IL is not believed to affect the forming top layer. However, the water content should still be lowered again by vacuum drying to prevent the build-up of water in the solution during successive interfacial polymerization cycles (up to a saturation level of 20 000 ppm at 20°C [182]) and the eventual TMC hydrolysis after prolonged contact with dissolved water.

TMC

Although no TMC was lost by hydrolysis before or during interfacial polymerization, subsequent drying of the TMC/IL solution under vacuum might cause TMC to be removed by evaporation. At atmospheric pressure, TMC has a boiling point of 312°C and an enthalpy of vaporization of 55.32 kJ mol^{-1},[211] while IL drying is performed at 5 x 10^{-5} bar. To calculate the boiling point of TMC at this very low pressure, a derivative of the Clausius-Clapeyron relation (Equation 3.1) was used, in which T_1 and T_2 are the respective boiling points (K) at pressures P_1 and P_2 (bar), R is the ideal gas constant (8.314 J K^{-1} mol^{-1}) and ΔH_{vap} is the enthalpy of vaporization at P_2 (J mol^{-1}).

$$T_1 = \left(\frac{1}{T_2} - \frac{R \ln\frac{P_1}{P_2}}{\Delta H_{vap}}\right)^{-1} \qquad (3.1)$$

The calculated boiling point of pure TMC at 5 x 10^{-5} bar is 40°C, notably lower than the drying temperature of 80°C. In solution, however, interactions with the solvent can impede evaporation and increase the boiling point. To determine the degree of evaporation of TMC, a fresh TMC/IL solution was mixed with water, with and without a prior vacuum drying step. Water causes the residual TMC to hydrolyze to trimesic acid, forming HCl as a by-product. Since HCl prefers water as solvent (see further), the concentration of TMC in the IL can thus, via its hydrolysis to trimesic acid, be quantified by measuring the pH of the aqueous solution after phase separation. A series of washing steps with fresh water to obtain a complete hydrolysis of TMC indicated that 15% of the initial amount of TMC was removed during vacuum drying (See Table S3.1 in appendix B). The loss of TMC can be minimized by lowering the drying time or temperature, although a sufficiently low water content must still be achieved.

HCl

During interfacial polymerization, HCl is formed in the reaction zone. In the conventional system, it is assumed to be transported from the organic to the aqueous phase due to its insolubility in hexane. Upon contact with water, HCl ionizes completely, resulting in the

formation of H_3O^+ and Cl^-. This causes the aqueous HCl solubility to be very high. When replacing hexane by $[C_4mim][Tf_2N]$, the solubility of HCl in the organic phase might increase. However, as can be derived from the very low pK_a of $[Tf_2N]$ of 0.16,[212] the IL has a limited tendency to become protonated by HCl. The affinity of HCl will thus likely be higher for water than for the IL. This affinity difference is also applied in the synthesis of water-immiscible ILs, in which HCl, formed as a by-product during the metathesis reaction, is removed from the formed IL by washing it with water.[139] Therefore, HCl is, also in the water/IL system, expected to be transported towards the aqueous phase.

To confirm this statement, a PA film was formed via the conventional and the water/IL system in the absence of a support as described elsewhere,[203] and the pH of the aqueous MPD solution was measured before and after the interfacial polymerization. The results are shown in Table 3.1. In the conventional system, the starting pH of the solution is higher due to the much higher MPD concentration used in this system, which acts as a base. In both systems, the pH of the aqueous solution decreases drastically during interfacial polymerization. This is caused by both the removal of MPD from the aqueous phase to form the top layer and by the uptake of formed HCl. This already indicates that in both systems, HCl is transported from the organic reaction zone to the aqueous phase. MPD in the aqueous solution can act as a buffer by reacting with HCl to form $MPDH^+$ and Cl^-. Since the starting concentration of MPD in the water/IL system is much lower, this solution has a lower buffering capacity. A stronger decrease in pH is thus observed here. The MPD/$MPDH^+$ ratio before and after interfacial polymerization can be derived from the the pK_a of MPD for protonation of the first amine group (5.11). Protonation of the second amine group of MPD does not occur in this system due to the very low pKa (2.50). The HCl concentration in the aqueous phase after interfacial polymerization can then be calculated as the sum of the change in $[H_3O^+]$ and the change in $[MPDH^+]$. Earlier research proved that there is little transport of MPD from the aqueous phase to the reaction zone in the organic phase in the conventional system, while this transport is highly facilitated in the water/IL system.[203] Since the total amount of MPD incorporated in the PA top layer must be similar in both systems, a hypothetical concentration of 0.098% (w/v) MPD is assumed to react with TMC. Based on this assumption, the HCl concentration in the aqueous phase after interfacial polymerization is very similar for both systems, as derived from Table 3.1. This suggests that the transport of formed HCl from the organic reaction zone to the aqueous phase proceeds equally in both systems.

Table 3.1: pH change of the aqueous MPD solution during interfacial polymerization and the corresponding HCl concentration in this phase, both in the conventional and in the water/IL system.

		Conventional system 2.0% (w v^{-1}) MPD in water	Water/IL system 0.1% (w v^{-1}) MPD in $[C_4mim][Tf_2N]$
Before interfacial polymerization	pH	9.40	8.08
	$[H_3O^+]$ (M)	3.98×10^{-10}	8.32×10^{-9}
	$[MPDH^+]$ (M)	9.49×10^{-6}	9.90×10^{-6}
After interfacial polymerization	pH	8.78	5.69
	$[H_3O^+]$ (M) [a]	1.24×10^{-9}	1.64×10^{-6}
	$[MPDH^+]$ (M) [a]	3.76×10^{-5}	3.96×10^{-5}
	$\Delta[H_3O^+]$ (M)	8.43×10^{-10}	1.63×10^{-6}
	$\Delta[MPDH^+]$ (M)	2.81×10^{-5}	2.97×10^{-5}
	[HCl] (M)	**2.81×10^{-5}**	**3.13×10^{-5}**

[a] Assuming that 0.098% (w/v) MPD reacted with TMC to form the PA film in both systems.

Membrane synthesis with recycled IL

Since TMC is partly removed from the IL solution during the first interfacial polymerization cycle as well as during subsequent vacuum drying, additional TMC was added to reach the initial concentration of 0.5% (w v^{-1}). As derived from Figure 3.11, addition of 0.1% (w v^{-1}) TMC was sufficient to prepare high-performance RO membranes using a recycled TMC/IL solution. Higher TMC concentrations caused the NaCl retention to decrease slightly, since a too high TMC concentration results in a less optimal MPD/TMC concentration ratio in the reaction zone and thus a decreased cross-linking degree of the PA top layer.

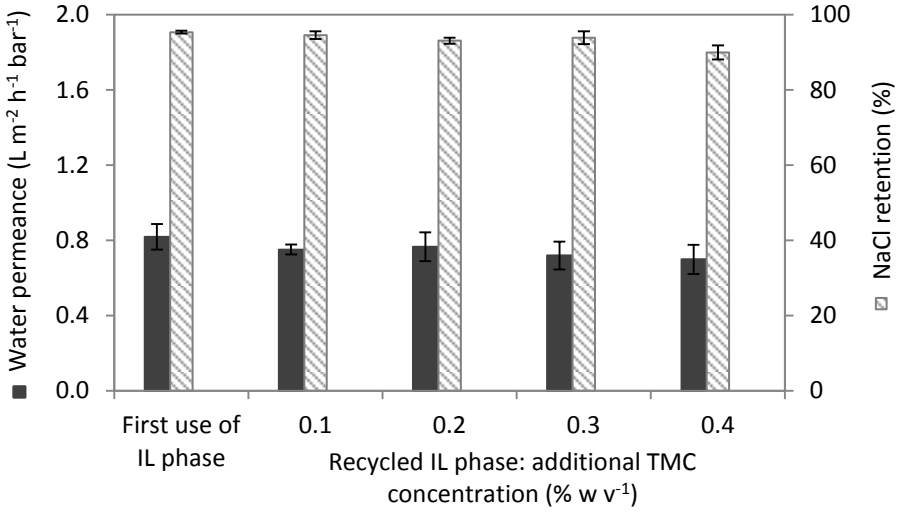

Figure 3.11: Water permeance and NaCl retention of TFC membranes synthesized according to the water/IL system, using fresh or recycled IL with different concentrations of TMC added.

3.3.6 Mass and solvent intensity

To support the 'green' aspect of the water/IL system in a quantitative manner, the mass and solvent intensity of the conventional and the water/IL system were compared, starting from a non-impregnated support (see Table S3.2 in appendix B for the calculations). For both systems, the direct recycling of the organic phase after interfacial polymerization, which can be reused after adjusting the TMC concentration to its initial value, was also considered. In the water/IL system, 94-98% of the organic phase could be recycled by pouring the solution off the membrane and further removing the residual solution by blowing pressurized air over the membrane surface. The remaining traces (2-6% of the original TMC/IL solution) were removed from the membrane surface by washing with acetone. Since in the conventional system, the residual solution could not be removed with pressurized air due to the high volatility of hexane, only 74% of hexane could be recycled in this system.

Without considering the recycling step, the mass intensity of the water/IL system was already significantly lower compared to the conventional system (Table 3.2). Besides the lower MPD concentration and the exclusion of TEA and SDS, the low mass intensity was achieved by minimizing the applied TMC/IL volume in interfacial polymerization by assuming spraying instead of pouring this phase on the support surface. Spraying is not possible in the conventional system due to the high volatility of hexane. When both the hexane and the IL phase were recycled, the difference in mass intensity between the two systems became even higher (Table 3.2), which clearly confirms the environmentally friendly character of the water/IL system. In all cases, the difference in solvent intensity between the two systems was smaller than the difference in mass intensity, since the lower MPD concentration and the exclusion of TEA and SDS in the water/IL system was not considered in the calculation of this metric.

Table 3.2: Mass and solvent intensities of the conventional and the water/IL-based interfacial polymerization, without and with recycling of the organic phase.

	Without recycling		With recycling	
	Conventional	Water/IL	Conventional	Water/IL
Mass intensity	15.3	11.6	8.7	4.2
Solvent intensity	12.1	11.4	5.4	4.1

3.4 Conclusions

The new type of interfacial polymerization to form TFC membranes, in which ILs were applied as organic reaction medium, as developed in Chapter 2,[203] was now further studied and the membrane preparation further optimized.

Different steps in the synthesis were analyzed to improve the time and cost efficiency of the preparation process and to maximize the resulting membrane performance. Interfacial

polymerization time was shortened to 10 s, while the waste generation, and thus the process cost and environmental footprint, was drastically lowered by recycling the IL for subsequent interfacial polymerization cycles. This resulted in a 64% decrease in mass intensity of the top layer formation process, while a 52% lower mass intensity compared to the conventional system was obtained. High-performance RO membranes were successfully formed using such recycled [C_4mim][Tf_2N] phase. Before reusing the IL in consecutive interfacial polymerization steps, water, taken up by the IL phase during top layer formation, was removed again by vacuum drying. HCl, formed as by-product during polymerization, was transported to the aqueous phase during the reaction and was thus not present in the phase to be recycled. Moreover, residual TMC monomers present in the IL phase could also be recycled, since the IL protected TMC from being hydrolyzed and becoming unreactive for top layer formation, even at very high water contents in the IL (> 1000 ppm). Only a small fraction of TMC was lost during the vacuum drying step to lower the water content in the IL. Successful introduction of the recycling step, together with the possibility to dry the formed membrane sheets without loss of performance by conditioning with glycerol, clearly demonstrated the upscaling potential of the new preparation method. Finally, the rinsing time after interfacial polymerization was optimized. Residual IL was present on the membrane surface at short rinsing times, creating an extra resistance barrier against water permeation and potentially leading to the presence of impurities in the feed. An increase in rinsing time could overcome these drawbacks.

3.5 Acknowledgements

We are grateful for the financial support from KU Leuven (OT (11/061) funding) and the Belgian Federal Government (I.A.P. – P.A.I. grant (IAP 7/05 FS2)). We also wish to thank S. Dewilde from the Department of Chemistry, Molecular Design and Synthesis of KU Leuven for supporting the Karl Fisher titrations, and A. Bergmaier from Institut für Angewandte Physik und Messtechnik of Universität der Bundeswehr München and R. Verbeke from the Centre of Surface Chemistry and Catalysis of KU Leuven for performing ERD measurements and analyzing the results.

CHAPTER 4

Preparation of high-performance thin film composite membranes by replacing the aqueous phase in interfacial polymerization by an ionic liquid

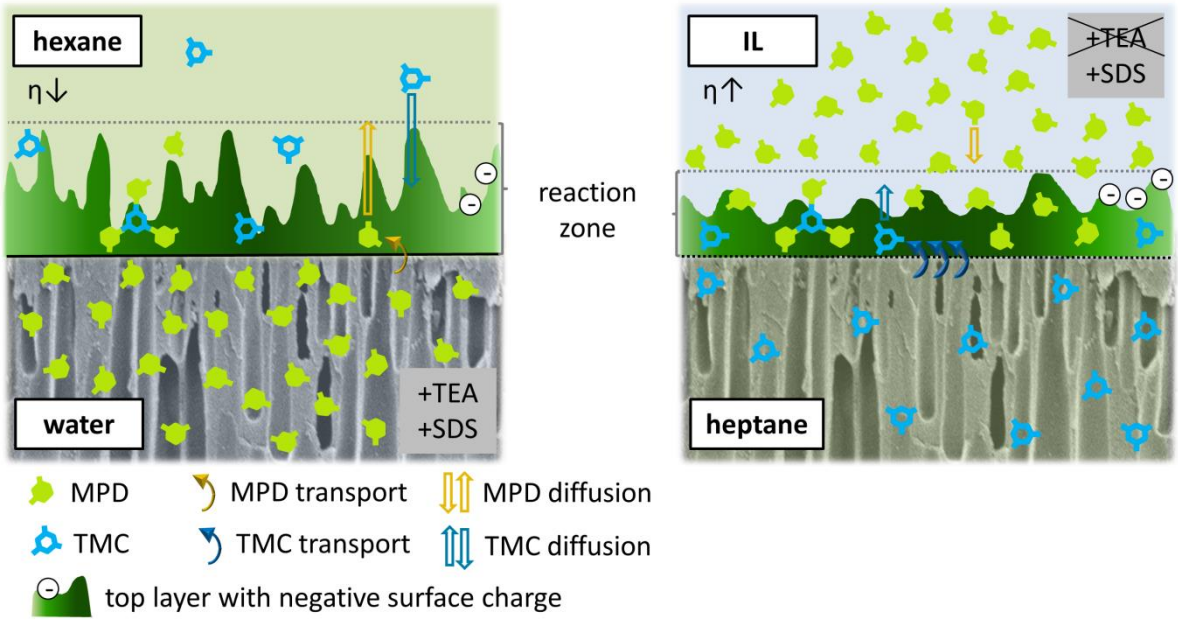

Abstract

A modified interfacial polymerization system was developed, in which the aqueous phase was replaced by an ionic liquid (IL). Due to the higher solubility of trimesoyl chloride in the IL phase compared to the conventional aqueous phase, the interfacial polymerization occurred inside the IL, and the orientation of the monomer phases needed to be reversed to form a homogeneous top layer. This resulted in reverse osmosis (RO) membranes with a drastically lower roughness than conventional polyamide (PA) top layers. Unexpectedly, the top layer surface did not contain free amine groups resulting from the supply of *meta*-phenylenediamine from the upper phase, and had a more negative charge than a conventional PA top layer. The NaCl retention was improved to 97.0 ± 0.6% by adding sodium dodecyl sulfate to the IL phase, while the water permeance was increased via the addition of co-solvents to the heptane or IL phase. Due to the large observed trade-off between selectivity and permeance here, no optimal membranes for RO applications could be obtained yet.

4.1 Introduction

Reverse osmosis (RO) is a pressure-driven membrane process in which monovalent salts are retained. Large-scale applications are mainly situated in the area of saltwater desalination to produce drinking water, process water and demineralized water.[213] Here, RO competes with other technologies, like distillation (e.g. multi-stage flash, multiple effect [12] or vapor compression distillation [214]). Due to its two to eight times lower specific energy consumption compared to these distillation technologies, RO has been a growing market.[12,214] It nowadays represents 65% of the total desalination capacity.[11]

Commonly used membranes for RO are thin film composite (TFC) polyamide (PA) membranes, in which the PA top layer is prepared via interfacial polymerization. In this method, a porous support is impregnated with an aqueous amine solution and subsequently being brought into contact with an immiscible (typically hexane) organic acyl chloride solution. Generally, *meta*-phenylenediamine (MPD) and trimesoyl chloride (TMC) are applied as aqueous and organic monomers respectively. Near the water-hexane interface, both monomers react to form a PA film with a thickness of a few tens of nanometers.[74] This dense, highly cross-linked top layer, capable of forming hydrogen bonds, results in both a high water permeance and a high NaCl retention and is therefore very suitable for RO applications.

In terms of membrane performance, sustainability of large-scale applications could still be considerably improved by reducing TFC membrane fouling behavior. It is stated that 80% of the problems in RO applications are associated with fouling.[215] Membrane-related factors affecting fouling in nanofiltration and RO are membrane surface charge, hydrophobicity and roughness.[163,164,216,217] In interfacially polymerized PA membranes, the so-called 'ridge-and-valley' structure at the membrane surface can sometimes be very pronounced and is considered to be an important factor in membrane fouling.[164,165] Also the negative charge of the membrane surface, caused by hydrolysis of excess, unreacted acyl chloride groups, might negatively influence the membrane fouling behavior. Many fouling agents are charged and can interact with charged membrane surfaces, either directly or via bridging with other ions, mainly Ca^{2+}, in the feed solution.[217,218]

In this chapter, a novel form of interfacial polymerization to form TFC membranes is presented, in which the aqueous monomer phase is replaced by an ionic liquid (IL). The successful formation of PA and polyurea films at an IL/hexane interface was already shown earlier, however, not for the formation of a membrane.[152] The authors suggested that, by replacing water by an IL and thus excluding water from the interfacial polymerization system, the side reaction of the acyl chloride monomer with water was prevented. This would explain the observed increase in molecular weight of the PA, formed via a reaction between hexanediamine or 1,4-diaminobutane and sebacoyl chloride.[152] In this work, exclusion of water might result in a higher degree of cross-linking of the top layer, potentially leading to a higher selectivity.

In the conventional interfacial polymerization, top layer formation is assumed to take place in the organic phase due to the very low solubility of TMC in water. Since aromatic acyl chlorides show a good solubility in different types of ILs,[219,220] the TMC solubility in the IL phase is expected to be drastically higher than in the conventional aqueous phase. This might cause the reaction zone to be shifted towards this IL phase. As the most homogeneous top layer is assumed to be formed when the reaction zone is located in the upper phase, a reversal of the orientation of the two monomer phases (Figure 4.1) can be essential. In this case, two positive effects on the membrane fouling tendency are expected. Firstly, interfacial polymerization in a highly viscous IL phase results, as can be concluded from Chapter 2, in a top layer with significantly lower surface roughness. Secondly, the supply of MPD instead of TMC from the top phase by reversing the orientation of the monomer phases is expected to result in free amine groups at the membrane surface instead of free carboxylic acid groups. Since they are uncharged at neutral pH, this would cause the top layer surface to have a lower charge. Both a lower surface roughness and a lower charge potentially reduce the membrane fouling tendency.

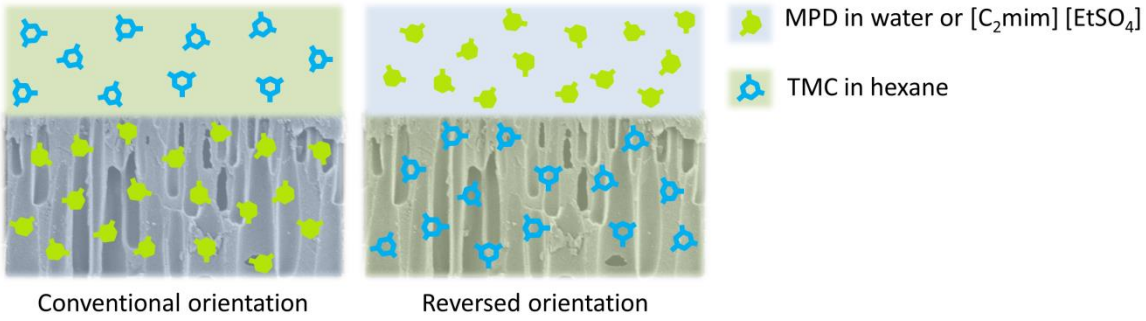

Figure 4.1: Schematic representation of the conventional and reversed orientation of the monomer phases in interfacial polymerization.

4.2 Experimental

4.2.1 Materials

Polysulfone (PSf, Udel® P-1700) and polyimide (PI, Matrimid® 9725) were purchased from Solvay and Huntsman, respectively. The non-woven polypropylene/polyethylene fabric Novatexx 2471 was kindly provided by Freudenberg (Germany). Hexanediamine (HDA, 99.5%, Acros), *meta*-phenylenediamine (MPD, 99+%, Acros), triethylamine (TEA, 99+%, Sigma-Aldrich), sodium dodecyl sulfate (SDS, 99%, Acros) and trimesoyl chloride (TMC, 98%, Acros) were used for membrane synthesis. N-methylpyrrolidone (NMP, 99%, Acros), tetrahydrofuran (THF, 99.9+%, Sigma-Aldrich), hexane (99+%, Chem-Lab), heptane (99+%, Acros), acetone (99.9+%, Sigma-Aldrich), ethyl acetate (99.5%, Acros) dimethylsulfoxide (DMSO, 99.5+%, Acros), dimethylformamide (DMF, 99+%, Acros), isopropanol (IPA, 99.96%, Fisher) and ethanol (EtOH, 99.99%, Fisher) were used as received. 1-Ethyl-3-methylimidazolium ethyl sulfate ([C_2mim][$EtSO_4$], 95+%, Sigma-Aldrich) and 1-ethyl-3-

methylimidazolium trifluoromethanesulfonate ([C_2mim][OTf], 99+%, Iolitec) were used after drying for 16 h at 40 °C under vacuum. Rose Bengal (RB, 1017 Da, Sigma Aldrich) and sodium chloride (NaCl, 99.8%, VWR) were applied as test solute.

4.2.2 Membrane synthesis

Supports were synthesized via phase inversion.[19] PSf and PI powders were first dried overnight in an oven at 100 °C. Homogeneous polymer solutions were prepared by stirring mixtures of PSf (18% (w w^{-1})) in NMP and PI (14% (w w^{-1})) in NMP/THF (3/1 (w w^{-1})). They were left untouched overnight to remove air bubbles created during the stirring. The polymer solution was cast at a constant speed (4.4 x 10^{-2} m s^{-1}) and with a wet thickness of 200 µm using an automatic casting device (Braive Instruments, Belgium) on a non-woven impregnated with NMP. Then, the film was immersed in a coagulation bath. For PI films, 30 s evaporation was inserted between the casting and the immersion to allow THF evaporation from the film surface.

When the top layer was formed via the conventional water/hexane interfacial polymerization, the procedure described in 2.2.2 was followed.

When top layer formation was performed via the IL/hexane-based interfacial polymerization, using the conventional orientation of the monomer phases (Figure 4.1), the coagulation bath consisted of distilled water. For PI supports, HDA (0.5% (w v^{-1})) was added to the coagulation bath to simultaneously cross-link the support.[73] After 5 min, the support was removed from the bath and washed with distilled water. Before impregnating it with the solution of MPD in [C_2mim][$EtSO_4$], the water inside the support was first exchanged with a [C_2mim][$EtSO_4$]/EtOH solution (1/3 (v v^{-1})) via immersion for 24 h. The support was dried overnight at room temperature to remove the EtOH, and subsequently impregnated with a solution of MPD (2% (w v^{-1})) in [C_2mim][$EtSO_4$] for 30 min. A solution of TMC (0.10-0.25% (w v^{-1})) in hexane was then poured gently on the support. After 60 s, the solution was drained off and the membrane was rinsed with hexane to remove unreacted TMC. After another 60 s, the membrane was put in a water bath to remove unreacted MPD. Finally, the TFC membrane was stored in distilled water until further use.

When using the reversed orientation of the monomer phases (Figure 4.1), either in the water/hexane- or the IL/hexane-based interfacial polymerization, the coagulation bath consisted of distilled water. For PI supports, HDA (0.5% (w v^{-1})) was added to the coagulation bath to simultaneously cross-link the support.[73] After 5 min, the support was removed from the bath and washed with distilled water. Before impregnating it with a solution of TMC in hexane or heptane, the support was first immersed in IPA for 16 h, and subsequently in hexane or heptane for 6 h, to fully exchange the water in the support with hexane or heptane. Then, the support was impregnated with a solution of TMC (0.10-0.25% (w v^{-1})) in hexane or heptane for 10 min. In specified cases, acetone (1.5-3.0% (w v^{-1})) was added to the solution. A solution of MPD (2% (w v^{-1})) in water, [C_2mim][$EtSO_4$] or [C_2mim][OTf] was

subsequently poured gently on the support. SDS (0.05-0.70% (w v^{-1})), TEA (2% (w v^{-1})), DMSO (2% (w v^{-1}), acetone (2% w v^{-1}) or ethyl acetate (2% (w v^{-1})) were added to the solution in specified cases. After 60 s, the solution was drained off and the membrane was rinsed with water to remove unreacted MPD. To remove the solution of TMC in hexane or heptane from the support, the membrane was immersed in acetone for 2 h, and subsequently in distilled water. Finally, the TFC membrane was stored in distilled water for further use.

4.2.3 Membrane performance

See 2.2.3.

4.2.4 Membrane characterization

See 2.2.4 for SEM, AFM and zeta potential procedure.

X-ray photoelectron spectroscopy (XPS) was used to determine the chemical states of the elements in the membrane top layer. The measurements were conducted using an ESCALAB 250 (Thermo Fisher Scientific Inc., Waltham, UK) with Al X-ray source and monochromator.

4.2.5 TMC mass transfer

To characterize the differences in transport rate of TMC from the heptane phase to the aqueous or the [C_2mim][$EtSO_4$] phase, a solution of TMC (0.3% (w v^{-1})) in heptane was brought into contact with distilled water or [C_2mim][$EtSO_4$]. 0.1 ml samples of the heptane solution were taken at a distance of 1 cm from the interface after different contact times between 0 and 45 min (see Figure S4.1 in appendix C for experimental setup). The TMC concentration of the samples was determined with a UV-Vis spectrophotometer (UV-1650 PC, Shimadzu) at 291.6 nm after diluting them 10 times to obtain a linear relationship between absorbance and TMC concentration. Every experiment was performed three times and the values were averaged.

4.3 Results and discussion

When replacing the aqueous phase in interfacial polymerization by an IL, it has to be immiscible with the applied organic phase (mostly hexane or isopar). An almost endless group of ILs meets this criterion. Therefore, a well-documented and commercially available cation, [C_2mim], was chosen and combined with [$EtSO_4$] as anion, which gives an IL with moderate viscosity (123.5 mPa s at 20°C,[221] compared to a viscosity of many common ILs in the range of 10-500 mPa s [222]). This is an important property, as the IL must be able to penetrate the support pores during impregnation of the support with this monomer phase.

The traditional water/hexane interfacial polymerization method will be referred to below as the ‘conventional system’. The system in which the aqueous phase was replaced by [C_2mim][$EtSO_4$] will be called the ‘IL/hexane system’.

4.3.1 Determination of the optimal monomer concentrations

The solvents used in interfacial polymerization determine the solubility of the monomers, their rate and extent of transport across the interface and their diffusion rate in both phases. Therefore, the monomer concentrations added to the phases to obtain an optimal MPD/TMC ratio in the reaction zone for the formation of a highly cross-linked PA network is different for every solvent system. In the conventional system, MPD and TMC concentrations of 2.0 and 0.1% (w v^{-1}) are generally applied. Table 4.1 shows the result of the visual observation of PA films, formed between hexane and [C_2mim][$EtSO_4$] without support, with varying monomer concentrations. Although the conventional 2.0% (w v^{-1}) MPD was useful, a TMC concentration somewhat higher than 0.1% (w v^{-1}) seemed to be necessary to form partly (+) or well-cross-linked films (++). To quantitatively determine the most optimal TMC concentration in this narrow range, membrane performance should be tested, as described further.

Table 4.1: Determination of PA formation for various concentrations of MPD in [C_2mim][$EtSO_4$] and TMC in hexane. [a]

C_{MPD} (% w v^{-1}) → C_{TMC} (% w v^{-1}) ↓	0.10	0.75	1.00	1.25	1.50	1.75	2.00
0.1	- -			-	+-	++	+-
0.2					-	+-	++
0.3						-	+
0.4							+
0.5							-
1.0	- -						- -

[a] "- -" represents no PA formation, "-" indicates a little PA formation, "+-" indicates a slightly cross-linked, "+" a partly crosslinked and "++" a well-cross-linked film. These conclusions were based on mere visual observations. The concentrations in the black box were not tested.

4.3.2 Position of the reaction zone

In the conventional interfacial polymerization with water and hexane as solvents for MPD and TMC respectively, top layer formation is assumed to occur in the organic phase under standard conditions due to the very low solubility of TMC in the aqueous phase. Since aromatic acyl chlorides show a good solubility in different types of ILs,[219,220] the solubility of TMC in [C_4mim][$EtSO_4$] in the IL/hexane system was expected to be higher than in the conventional aqueous phase. This might cause the reaction zone to shift from the hexane to the IL phase, which would lead to the undesired formation of a top layer inside the pores of the support, generally being more prone to defect creation. Therefore, the optimal orientation of the monomer phases to form a highly selective top layer was first investigated, both for the conventional system as for the IL/hexane system. A schematic representation of the two tested orientations is shown in Figure 4.1.

In the conventional interfacial polymerization system, the conventional orientation of the monomer phases was expected to result in the best membrane performance due to the

formation of the top layer in the hexane phase. This is confirmed in Figure 4.2. The lower RB retention and higher EtOH permeance of the membranes synthesized using the reversed orientation probably result from the formation of an inhomogeneous top layer, mainly located inside the support pores and not covering the whole support surface. Since SDS promotes the transport of MPD from the aqueous to the hexane phase, the negative effect of reversing the orientation of the monomer phases was even larger when this additive was used.

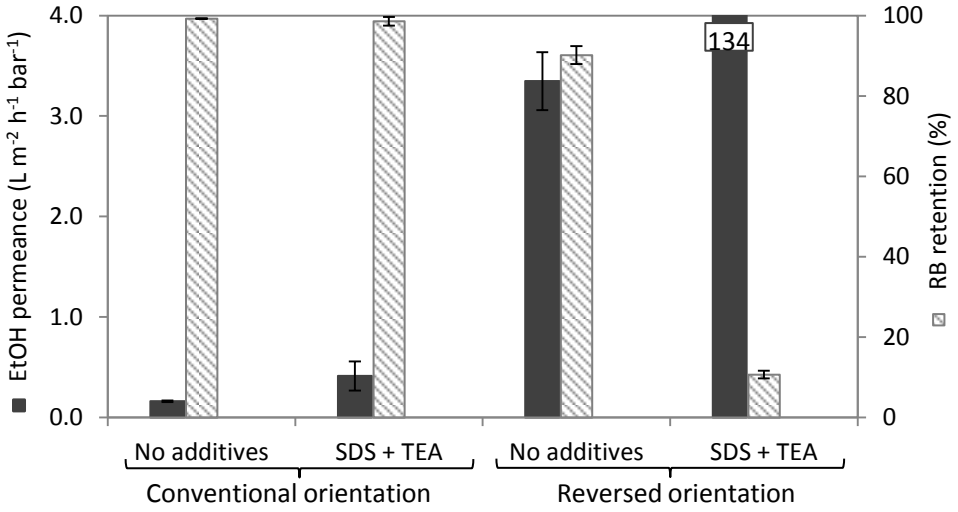

Figure 4.2: Influence of the orientation of the monomer phases on EtOH permeance and RB retention of TFC membranes synthesized according to the conventional system, with 2.0 % (w v^{-1}) MPD in water and 0.1 % (w v^{-1}) TMC in hexane, prepared on a PSf support, without or with SDS and TEA in the aqueous phase.

Although the PA top layer of TFC membranes for aqueous NF and RO applications is generally formed on a PSf support, both PSf and cross-linked PI were used as support polymers in the IL/hexane system. In our work about the use of an IL as organic reaction phase, a higher performance was indeed obtained when forming the PA top layer on a cross-linked PI support than on a PSf support (Chapter 2).[203] Moreover, the use of a cross-linked PI support causes the TFC membrane to be fully solvent resistant, broadening its application range from aqueous to organic solvent applications.

When applying the conventional orientation of the monomer phases in the IL/hexane system, the support, filled with water after phase inversion, was first immersed in a [C_2mim][$EtSO_4$]/EtOH (1/3 (v v^{-1})) mixture, after which the membrane was dried to remove the EtOH. The IL was mixed with EtOH to obtain a low viscosity solution which rapidly exchanges the water in the support. During subsequent membrane drying, the pores of the support might collapse, as observed previously in 3.3.4. The presence of the IL in the pores, however, was expected to prevent them from collapsing. Figure S4.2 in appendix C shows that this drying step indeed had an only small effect on the performance of both PSf and cross-linked PI supports, indicating that the pores were successfully preserved by the presence of the IL. The dried supports were thus useful for applying a top layer via interfacial polymerization.

On both types of supports, the TFC membrane showed the highest RB retention when the reversed orientation of the monomer phases was used, as shown in Figure 4.3, although the difference is rather small. Again, cross-linked PI supports resulted in TFC membranes with the highest performance and are therefore used from now on.

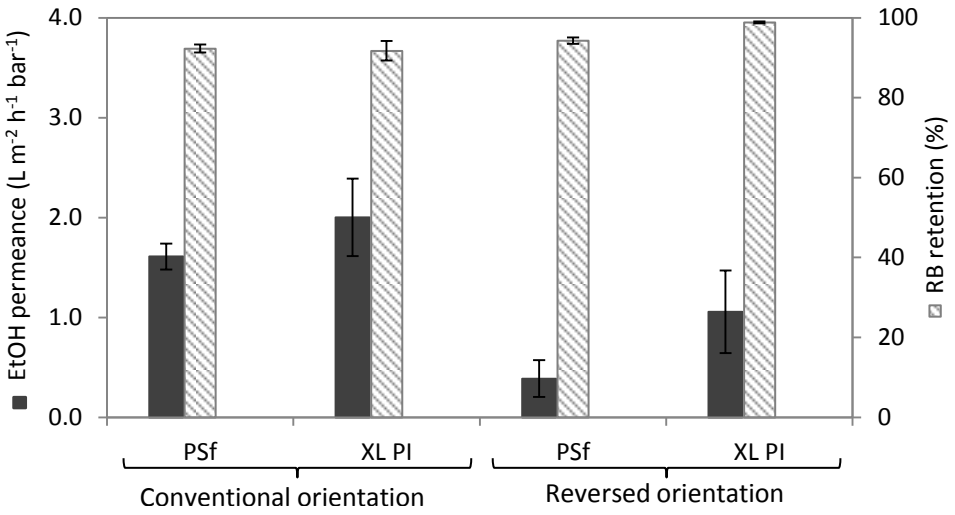

Figure 4.3: Influence of the orientation of the monomer phases on EtOH permeance and RB retention of TFC membranes synthesized according to the IL/hexane system, with 2.0 % (w v^{-1}) MPD in [C_2mim][$EtSO_4$] and 0.1 % (w v^{-1}) TMC in hexane, prepared on a PSf or a cross-linked (XL) PI support and without additives.

Because low-fouling RO membranes are aimed for, the membranes were further screened with NaCl as test solute. Figure 4.4 shows that the membranes prepared using the reversed orientation do have a drastically higher NaCl retention, indicating that the reaction zone in the IL/hexane system might indeed be shifted towards the IL phase. This orientation will therefore be further used in this work, and will be referred to as the 'reversed IL/hexane system'. Because the NaCl retention was still rather low, the TMC concentration was varied based on the film formation results in Table 4.1. This however did not influence membrane performance significantly (Figure 4.4). To make sure not to be on the border of the useful TMC concentration range, the middle concentration of 0.2% TMC was chosen for further use.

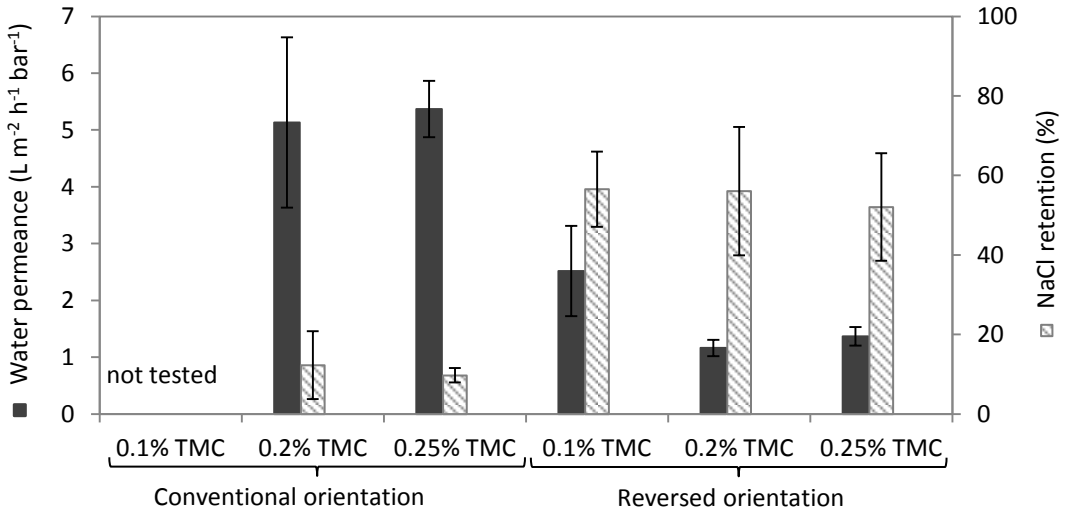

Figure 4.4: Influence of the orientation of the monomer phases on water permeance and NaCl retention of TFC membranes synthesized according to the IL/hexane system with 2.0% (w v^{-1}) MPD in [C_2mim][$EtSO_4$] and a varying TMC concentration in hexane, prepared on a cross-linked PI support and without additives.

A major problem of using hexane in the reversed orientation was its high volatility. This caused the support to dry very quickly after impregnation with the TMC solution in hexane, even before the interfacial polymerization was finished. Because this was expected to result in a non-optimal contact between the two monomer phases, hexane was replaced by less toxic and less volatile heptane. As these solvents are very similar, no difference in optimal monomer concentrations was expected, and the MPD and TMC concentrations were therefore not altered. As shown in Table 4.2, switching to heptane in the reversed orientation clearly resulted in a more selective top layer.

Table 4.2: Water permeance and NaCl retention of membranes synthesized according to the reversed IL/hexane and the reversed IL/heptane system.

	Reversed IL/hexane system	Reversed IL/heptane system
Water permeance (L m^{-2} h^{-1} bar^{-1})	1.16 (±0.14)	0.51 (±0.07)
NaCl retention (%)	56.1 (±16.1)	90.2 (±1.7)

To further confirm the possible shift of the reaction zone from the hexane (or heptane) to the IL phase, the difference in transport of TMC across the interface in the two systems was determined by a TMC transport test. The TMC concentration decrease in the heptane phase at 1 cm from the interface after the TMC solution was brought into contact with pure water or [C_2mim][$EtSO_4$], is shown in Figure 4.5. As expected, very little transport of TMC from heptane to water was observed due to its very low solubility in water. A substantial amount of TMC was, however, transported from heptane to the IL, which supports the hypothesis of a shift of the reaction zone towards this IL phase.

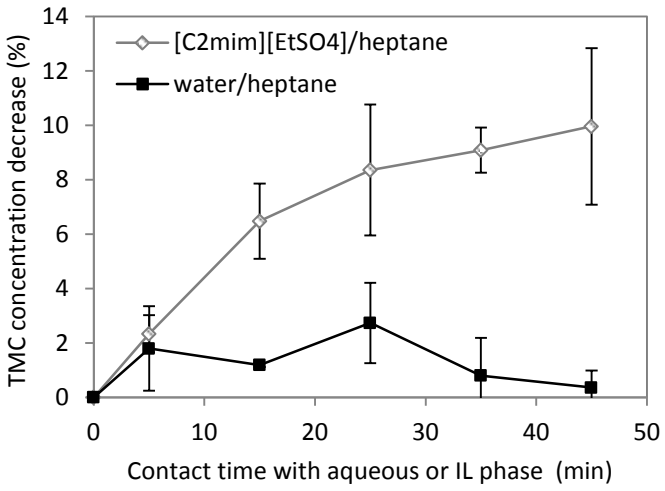

Figure 4.5: TMC concentration decrease in the heptane phase (relative to the starting concentration of 0.3% (w v^{-1})) at 1 cm from the interface after contacting the (unstirred) solution of TMC in heptane with pure water or [C_2mim][$EtSO_4$] for different times.

4.3.3 Further top layer characterization

If top layer formation takes place in the IL phase, the high viscosity of [C_2mim][$EtSO_4$] in the reversed IL/heptane system is expected to influence top layer morphology in a way similar to that in the water/IL system discussed in Chapter 2. In the water/IL system, the high IL viscosity slowed down the diffusion rate of the monomers, which was assumed to cause a narrowing of the reaction zone. This led to a decrease of the thickness, density and the roughness of the top layer. The SEM image in Figure 4.6a demonstrates the nodular morphology of the surface, similar to the membranes made via the water/IL system and in contrast to the ridge-and-valley structure of conventional PA membranes. AFM indicated the surface roughness to be 11 ± 1 nm (Figure 4.6b), which is also very similar to the membranes prepared via the water/IL system and significantly lower than the conventional PA membranes. This low surface roughness might be beneficial to reduce the fouling tendency of these membranes, as was already shown for the membranes made via the water/IL system.

Despite the very similar morphological properties of the membranes prepared via the water/IL and the reversed IL/heptane system, the latter shows a remarkably lower NaCl selectivity (90.2 ± 1.7% for the reversed IL/heptane- versus 96.8 ± 0.9 for the water/IL-prepared membranes). One possible reason is the presence of larger free volume elements in the top layer of the IL/heptane-based membranes. As discussed earlier, when simulating the interfacial polymerization process using a model of diffusion-limited cluster aggregation, a more diffusion-limited regime creates lower density structures.[127] A higher free volume size might thus result from the considerably higher viscosity of [C_2mim][$EtSO_4$] (123.5 mPa s at 20°C [221]), used in the IL/heptane system, compared to that of [C_4mim][Tf_2N] (63.1 mPa s at 20°C [185], used in the water/IL system. Besides the lower density, also the expected lower

surface charge using the reversed IL/heptane system might contribute to a lower salt retention, since both size and charge effects determine the retention of charged solutes.

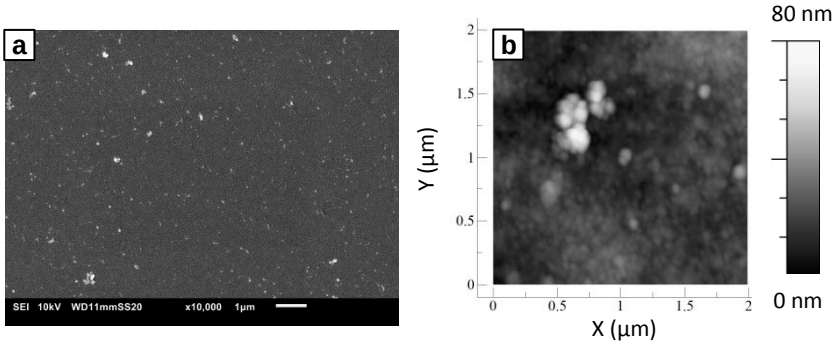

Figure 4.6: (a) Surface SEM and (b) surface AFM images of TFC membranes synthesized according to the reversed IL/heptane system, with monomer concentrations of 2.0% (w v^{-1}) MPD and 0.2% (w v^{-1}) TMC.

This surface charge is, next to the surface roughness, another parameter which might influence membrane fouling tendency.[217] In the conventional interfacial polymerization, the presence of TMC in the upper phase leads to the formation of a PA top layer with free acyl chloride groups at the surface, which hydrolyze and result in a negatively charged membrane surface. By using the reversed orientation of the monomer phases in the IL/heptane system, MPD is supplied from the top phase. This is expected to lead to a PA top layer with free amine groups at the surface, being uncharged at neutral pH. A lower charge generally leads to a lower fouling tendency, since many fouling agents have charged groups which can interact with the charged membrane surface, either directly or via bridging with other ions in the feed solution.[217,218]

To determine the presence of free amine groups at the top layer surface, XPS measurements of membranes made via the IL/heptane system with both the normal and reversed orientation of the monomer phases were performed. Unexpectedly, nitrogen was present in two chemical states when using the normal orientation (Figure 4.7a), while only one chemical state was observed when using the reversed orientation (Figure 4.7b). Since the top layer in the normal orientation was expected to be formed more into the pores of the support, and the X-ray penetrates the sample up to a depth of 10 nm, the chemical states in Figure 4.7a might have originated from nitrogen present in the support as well. The cross-linked PI support contains both amide and imide bonds, which can explain the presence of two chemical states in the spectrum. However, the observation of only one chemical state in Figure 4.7b unexpectedly suggests that no free amine groups were present on the PA surface when applying the reversed orientation.

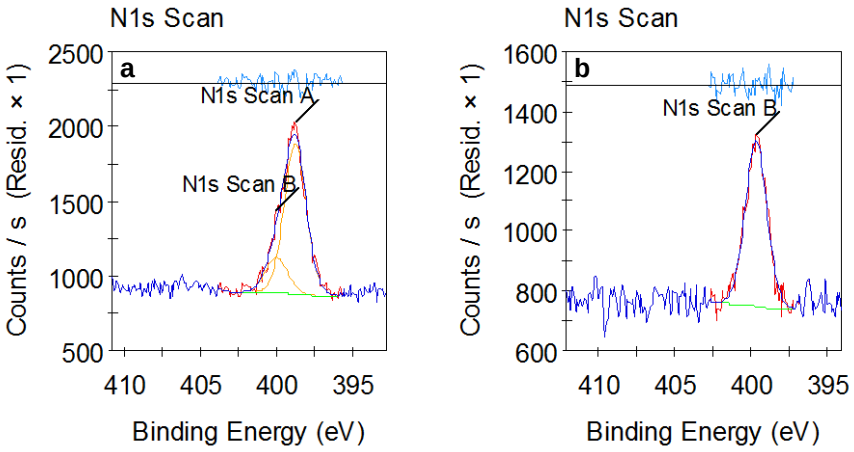

Figure 4.7: XPS spectra of the top surface of membranes made according to the heptane/IL system (a) using the normal and (b) the reversed orientation of the monomer phases.

The surprising XPS result of the membrane made via the reversed IL/heptane system was further elucidated via zeta potential analysis. Figure 4.8 shows that the membrane prepared via the reversed IL/heptane system had a significantly more negative surface charge at neutral pH compared to conventional water/hexane-prepared membranes. This also contradicts the presence of free amine instead of carboxylic acid groups at the surface. It, however, may be an indication of a lower degree of cross-linking of the top layer, resulting in more carboxylic acid end groups, being negatively charged at neutral pH. With decreasing pH, the carboxylic acid groups are starting to become protonated, explaining the diminishing difference in negative charge between the two membranes in the low pH region in Figure 4.8. The lower cross-linking degree of the top layer was supported by solvent activation tests, in which immersion in DMF normally results in an improved permeance without loss in selectivity (see Chapter 5). Solvent activation on a membrane prepared via the reversed IL/heptane system, however, resulted in a drastic decrease in NaCl retention (to only 14%), indicating a partial breakdown of the top layer structure in DMF.

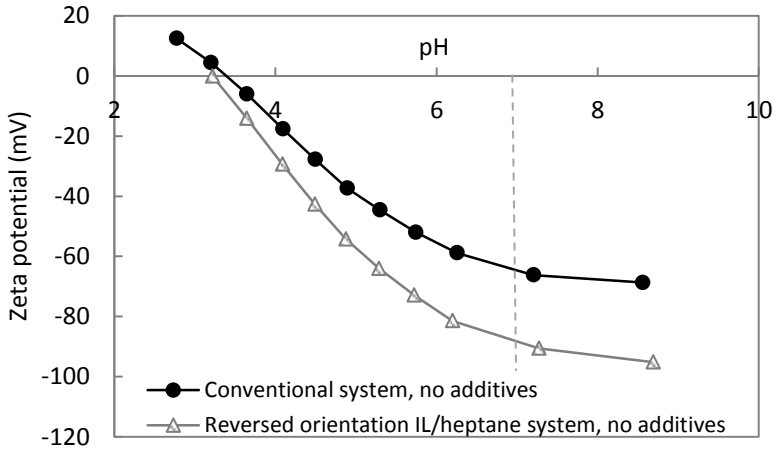

Figure 4.8: Zeta potential as function of pH of TFC membranes synthesized according to the conventional system on a PSf support, and of a TFC membrane synthesized according to the reversed IL/heptane system on a cross-linked PI support without the use of additives.

Figure 4.9 summarizes the effects of the solvent properties on top layer formation in the conventional and the reversed IL/heptane system. Since the reaction zone is shifted towards the IL, TMC instead of MPD is mainly transported across the interface in the reversed IL/heptane system. The low necessary TMC concentration in the bottom phase in this reversed IL/heptane system (0.2 % w v^{-1}) compared to the MPD concentration in the bottom phase in the conventional system (2.0 % w v^{-1}) is probably due to the faster transport of TMC from heptane to the IL than that of MPD from water to hexane. This can be derived from the MPD transport test in the conventional system (Figure 2.5 in Chapter 2) and the TMC transport test in the IL/heptane system (Figure 4.5), although they should be compared with care since different starting concentrations were used in both tests. The high necessary MPD concentration in the upper phase in the reversed IL/heptane system (2.0 % w v^{-1}) compared to the TMC concentration in the upper phase in the conventional system (0.1% w v^{-1}) results from the high IL viscosity, drastically lowering the diffusion of MPD towards the reaction zone. This high viscosity also caused the top layer to be less rough than the conventionally prepared one. The effect of the addition of SDS and TEA in the reversed IL/heptane system is discussed in 4.3.4.

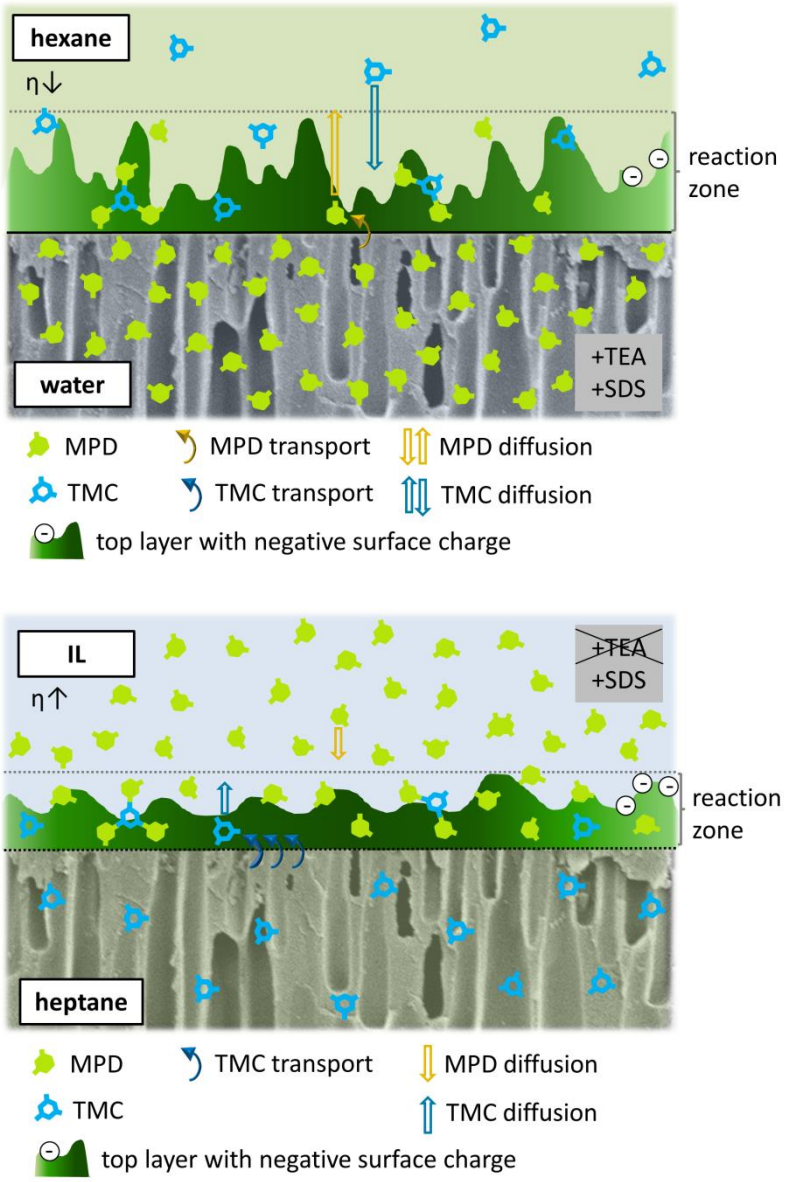

Figure 4.9: Schematic representation of the effects of the properties of the used solvents on the interfacial polymerization process in the conventional and the reversed IL/heptane system.

4.3.4 Improvement of the performance

The best performing membrane, obtained by replacing hexane by heptane, showed a NaCl retention of 90.2 ± 1.7%, which is still too low for RO applications. Since the NaCl selectivity of PA RO membranes originates from both charge and size effects, these two parameters were investigated to improve the NaCl retention by either altering the charge or the density and degree of cross-linking of the top layer. Although XPS and zeta potential measurements did not confirm the presence of surface amine groups and a resulting lower charge of the top layer surface, this could negatively affect NaCl retention if it were present. Therefore, potential free amine groups were capped with TMC to increase surface charge and NaCl retention. This was done by bringing the membrane surface into contact with a second TMC/heptane solution after interfacial polymerization. This treatment, however, did not

result in an improved NaCl retention, supporting the absence of free amine groups at the surface, as suggested by XPS (Figure 4.7). This approach was therefore not further investigated.

As the lower selectivity might also be caused by the high IL viscosity, resulting in a low-density top layer, the use of an IL with lower viscosity was investigated. Based on a screening of different ILs in an IL/heptane film formation test with varying MPD and TMC concentrations (similar to the experiment in Table 4.1), 1-ethyl-3-methylimidazolium trifluoromethanesulfonate ([C_2mim][OTf]) was selected, thanks to the formation of a well-cross-linked film. This IL has a viscosity of around 50 mPa s at 20°C,[223] which is drastically lower than that of [C_2mim][$EtSO_4$] (123.5 mPa s at 20°C [221]). By forming a top layer on a cross-linked PI support via the reversed [C_2mim][OTf]/heptane system, using the optimal monomer concentrations (2.0% (w v^{-1}) MPD and 0.2% (w v^{-1}) TMC), a membrane with a NaCl retention of 89.0 (± 1.2)% and a water permeance of 0.47 (± 0.04) L m^{-2} h^{-1} bar^{-1} was obtained. This is equal to the performance of the membrane prepared via the reversed [C_2mim][$EtSO_4$]/heptane system (Table 4.2). No improvement of the retention was thus observed by using an IL with lower viscosity. Nevertheless, it would be incorrect to conclude that the viscosity of the IL has no effect on top layer formation, since other solvent properties are also altered by changing the IL type (e.g. interfacial tension with heptane, coordination capacity of the IL anion). The observed influence on membrane performance is then the sum of the effects of all these properties on the interfacial polymerization process.

In the third attempt to improve membrane selectivity, the commonly used additives SDS and TEA were added to the [C_2mim][$EtSO_4$] phase. The addition of SDS resulted in an increase in NaCl retention, with a maximum of 97.0 ± 0.6% at 0.3% (w v^{-1}) SDS, as shown in Figure 4.10. When SDS is added to the aqueous phase in the conventional interfacial polymerization, it improves MPD transport towards the reaction zone by lowering the interfacial tension between water and hexane. This mainly results in an improved permeance of the membrane with unchanged retention. Here, the effect of SDS was significantly different. This might be due to the shift of the reaction zone to the IL phase, causing SDS to be present not only at the interface between heptane and IL, but also inside the reaction zone. Therefore, it might not only affect monomer transport across the interface, but also influence the reaction itself. It is, however, unclear how this exactly affects top layer properties. Similar to the water/IL system, adding TEA could not further improve membrane performance.

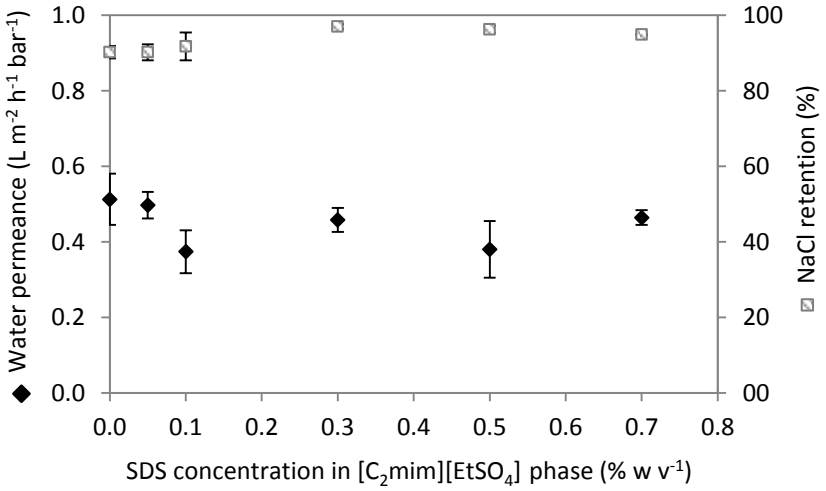

Figure 4.10: Influence of the SDS concentration in the IL phase on water permeance and NaCl retention of TFC membranes synthesized according to the reversed IL/heptane system.

Although a high NaCl retention was now obtained, the water permeance of 0.46 ± 0.03 L m^{-2} h^{-1} bar^{-1} in Figure 4.10 was still too low for potential industrial use. The positive effect on the permeance caused by using co-solvents in interfacial polymerization, either in the aqueous or the organic phase, was already described frequently. It is explained by a decrease in interfacial tension between the aqueous and the organic phase, which improves MPD transport towards the reaction zone. This would either result in a thinner dense layer, a lower density or an increased surface roughness, which increases the area for solvent transport during filtration.[63,105,112,114–116] Therefore, the influence of adding a low concentration of acetone to the heptane phase, or DMSO, acetone or ethyl acetate to the IL phase was investigated. As derived from Figure 4.11 and Figure 4.12, the use of these co-solvents generally resulted in an increased permeance. While the addition of acetone to the heptane or IL phase, or ethyl acetate to the IL phase resulted in a rather low permeance improvement, the addition of DMSO to the IL phase ensured a 2.4 times higher permeance. This trend was unexpected, since acetone and ethyl acetate are miscible with heptane, while DMSO is immiscible. As literature states that the improved permeance is caused by an increase in miscibility between the two phases, the largest improvement should be obtained with acetone or ethyl acetate as co-solvent in the IL. However, the gain in permeance was always accompanied by a decrease in NaCl retention, thus still providing membranes which are not useful for RO applications. Therefore, their potential lower fouling tendency was not tested yet.

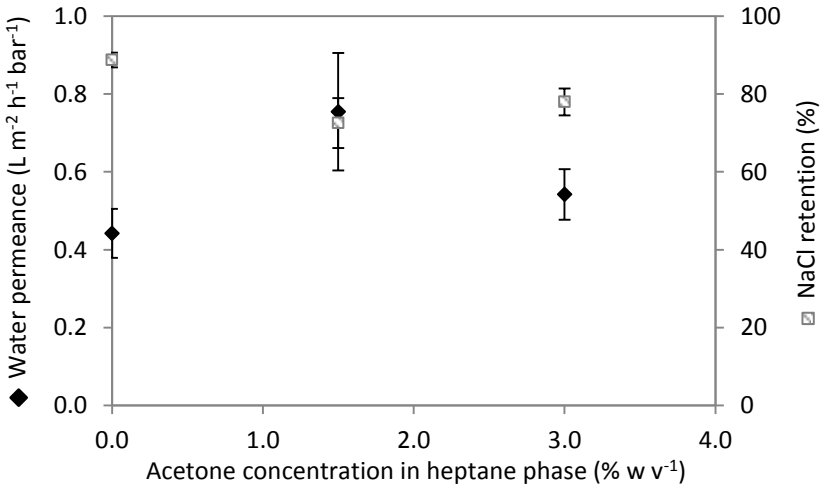

Figure 4.11: Influence of the concentration of acetone added to the heptane phase on water permeance and NaCl retention of TFC membranes synthesized according to the reversed IL/heptane system.

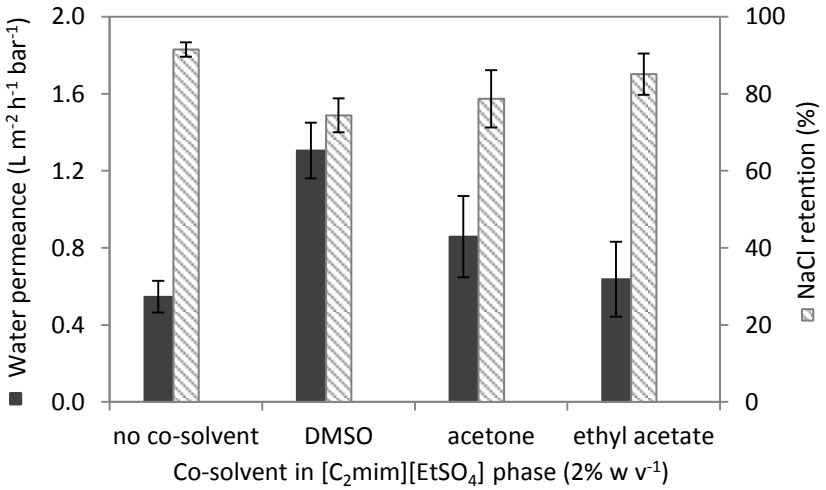

Figure 4.12: Influence of the addition of different co-solvents to the IL phase on water permeance and NaCl retention of TFC membranes synthesized according to the reversed heptane/IL system.

4.4 Conclusions

A modified interfacial polymerization system was developed, in which the aqueous phase was replaced by an IL, [C_2mim][$EtSO_4$]. Due to the higher solubility of TMC in the IL phase compared to the conventional aqueous phase, the reaction zone was shifted and top layer formation occurred inside the IL. Therefore, the orientation of the monomer phases was reversed to assure the formation of a homogeneous top layer on top of the support. As hexane was too volatile to keep the support impregnated in this reversed orientation, it was replaced by less volatile and less toxic heptane.

Top layer morphology was influenced largely by applying the IL as reaction phase. A less rough top layer with a nodular surface morphology was formed. Due to the supply of MPD from the top phase in the reversed orientation, the surface was expected to contain free amine groups instead of carboxylic acid groups, rendering it more neutral. This was however

countered by the XPS and zeta potential data, which suggested the absence of amine groups and a higher negative charge at neutral pH. The latter might be caused by a lower cross-linking degree of the top layer. This would, together with a potential lower density of the top layer, explain the lower membrane selectivity compared to conventional PA RO membranes.

Several adaptations were made to the synthesis process in an attempt to improve the RO performance of the IL/heptane-based membranes. Although the addition of SDS resulted in an increase in NaCl retention from 90.2 ± 1.7 to 97.0 ± 0.6%, the water permeance remained low (0.46 ± 0.03 L m^{-2} h^{-1} bar^{-1}). The permeance was improved by adding a co-solvent to the heptane or IL phase, which was, however, always accompanied by a decrease in NaCl retention. Therefore, none of the membranes made via the reversed IL/heptane system was useful yet for RO applications. Using this system, membrane fouling tendency was believed to be reduced, based on the expected low roughness and low surface charge of the top layer. However, since the membrane surface charge appeared to be even higher than for conventional PA membranes, and the RO performance was not optimal yet, the potential lower fouling tendency was not tested in this work.

4.5 Acknowledgements

We are grateful for the financial support from KU Leuven (OT (11/061) funding), from the Dutch and Flemish Governments (STW-SBO project Nanomexico) and the Belgian Federal Government (I.A.P. – P.A.I. grant (IAP 7/05 FS2)). We also wish to thank A. Volodin from the Laboratory of Solid-State Physics and Magnetism of KU Leuven for the AFM measurements, A. Szymczyk from the Institut des Sciences Chimiques of the university of Rennes for performing the zeta potential measurements and R. Bernstein from the Zuckerberg Institute for Water Research of the Ben-Gurion University of the Negev Sede Boqer Campus for XPS analysis.

CHAPTER 5

Solvent activation on interfacially polymerized SRNF membranes: elucidation of the mechanism

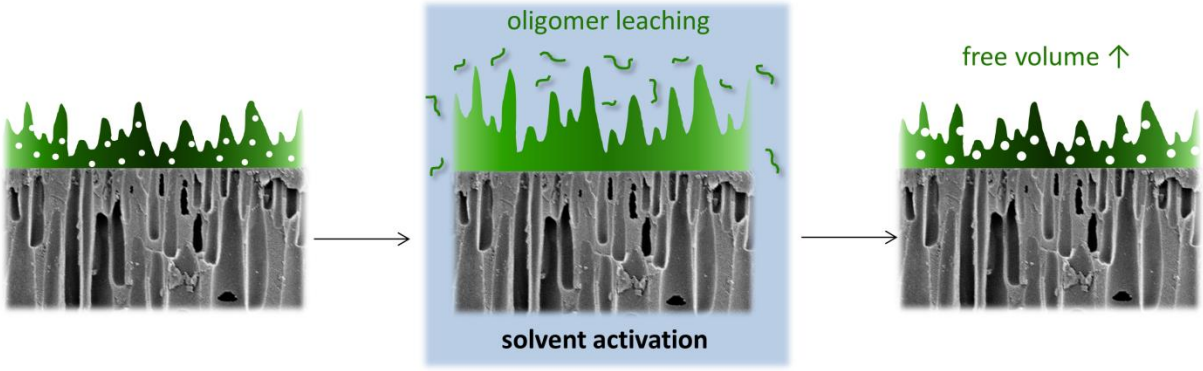

Abstract

Solvent activation is an interesting technique to improve the performance of thin film composite reverse osmosis and (solvent-resistant) nanofiltration membranes. The mechanism behind the changing performance is, however, still unclear. In this work, the hypothesis of polyamide oligomer leaching out of the top layer during DMF activation, resulting in an increase in free volume, was proven. The oligomers were identified via H-NMR analysis, while their molecular weight was estimated via comparison with polystyrene standards in a GPC analysis. An attempt was made to further improve the permeance after solvent activation, by creating a top layer containing more low molecular weight, leachable polyamide fragments. Therefore, trimesoyl chloride (TMC), the trifunctional acyl chloride used in the interfacial polymerization process, was partly replaced by a bi- or monofunctional acyl chloride. However, no improved membrane performance could be obtained. This was expected to be caused by the higher reactivity of TMC compared to that of the bi- and monofunctional acyl chlorides, causing *meta*-phenylenediamine to mainly react with TMC during top layer formation.

5.1 Introduction

Thin film composite (TFC) membranes are a widely applied membrane type in reverse osmosis (RO) and aqueous nanofiltration (NF) applications.[17,74,161,224] More recently, they are also being investigated for use in solvent-resistant nanofiltration (SRNF) applications.[13,62] TFC membranes consist of a very thin top layer (< 150 nm),[74] applied on a porous support which provides the mechanical strength. The top layer is made via interfacial polymerization,[61] in which the support is first impregnated with an aqueous solution of the first monomer, and subsequently being brought into contact with a solution of the second monomer in an apolar (mostly hexane) solvent. At the surface of the support, where the two immiscible solvents come into contact, the two monomers react to from a thin film on top of the support. A bifunctional amine (mostly *meta*-phenylenediamine (MPD) or piperazine) and a trifunctional acyl chloride (mostly trimesoyl chloride) are commonly used monomers in the aqueous and organic phase, respectively, which polymerize into a dense, highly cross-linked and thus highly selective polyamide (PA) top layer.[109,161] The extremely low thickness of this layer, together with its ability to form hydrogen bonds, causes the water permeance of these membranes to be high. To obtain a high permeance for more apolar solvents in SRNF applications, the PA top layer can be modified.[121]

A general method to improve the performance of TFC PA membranes is solvent activation. It was first reported by Kulkarni *et al*., who observed an improvement in the water permeance of commercial TFC RO membranes without compromising selectivity, after immersion in ethanol or isopropanol for different times.[119,120] The method was further developed by Solomon *et al*., who replaced the general poly(ether)sulfone support of RO membranes by a solvent-stable, cross-linked polyimide (PI) support. This allowed the use of other, more harsh activating solvents. A 10 min filtration with dimethylformamide (DMF) as activating solvent caused the methanol, DMF and acetone permeance to increase with a factor of 3, 5 and 2, respectively, while a flux was initiated for toluene, ethyl acetate and tetrahydrofuran. Moreover, in many cases, the retention even increased.[57] The effect of the immersion time was shown by Hermans *et al*., who observed an increase in ethanol permeance with a factor 5.5 or 16 after a 12 or 24 h immersion in DMF, respectively. A similar trend was observed after immersion in dimethylsulfoxide (DMSO), with a respective rise in ethanol permeance by a factor of 3.5 or 5.5.[73] The cross-linked PI support was also used further on in the preparation of TFC membranes for aqueous applications to enable the use of these harsh activating solvents, which showed a generally stronger effect on membrane permeance compared to mild organic solvents.[225]

Although the mechanism of solvent activation is still unclear, it is hypothesized that the activating solvent acts as a swelling agent for the PA top layer. During swelling, low molecular weight PA fragments would dissolve and leach out of the top layer. This would create additional free volume, which was first blocked by the PA oligomers.[57,119] The activating power of a solvent can thus be linked to the Hansen solubility parameter distance

between the PA top layer and the solvent (Δ_{s-p}). Table 5.1 shows that the harsh activating solvents tested in literature (DMF and DMSO) have a lower Δ_{s-p} value than the mild ones (ethanol and isopropanol), and thus a better interaction with the PA top layer, confirming their stronger effect on membrane performance. The increase in retention which is often observed, is explained by the occurrence of annealing during the activation process, which leads to removal of imperfections and defects in the top layer.[57,119] Until now, the only indication of the removal of PA oligomers is the observation in gel permeation chromatography (GPC) of unidentified, 1700 – 11700 Da components in the activation solution after bringing a TFC membrane into contact with DMF.[57] In this work, the mechanism of solvent activation is further elucidated via identification of the PA oligomers and determination of the change in top layer free volume. Moreover, an attempt is made to enhance the positive effect of solvent activation on membrane performance.

Table 5.1: Hansen solubility parameter distance between aromatic PA and the different activating solvents used in literature.

solvent	δ_D $(MPa)^{1/2}$	δ_P $(MPa)^{1/2}$	δ_H $(MPa)^{1/2}$	Δ_{s-p} $(MPa)^{1/2}$
DMF [226]	17.4	13.7	11.3	4.0
DMSO [226]	18.4	16.4	10.2	5.1
Ethanol [226]	15.8	8.8	19.4	12.7
Isopropanol [226]	15.8	6.1	16.4	11.2
Aromatic PA [227]	18	11.9	7.9	

5.2 Experimental

5.2.1 Materials

Polyimide (PI, Matrimid® 9725) was purchased from Huntsman (Switzerland). The non-woven polypropylene/polyethylene fabric Novatexx 2471 was kindly provided by Freudenberg (Germany). Hexanediamine (HDA, 99.5%, Acros), *meta*-phenylenediamine (MPD, 99+%, Acros), trimesoyl chloride (TMC, 98%, Acros), isophthaloylchloride (IPC, 99+%, Sigma-Aldrich) and benzoylchloride (BC, 99%, Sigma-Aldrich) were used for membrane synthesis. N-methylpyrrolidone (NMP, 99%, Acros), tetrahydrofuran (THF, 99.9+%, Sigma-Aldrich), hexane (99+%, Chem-Lab), dimethylformamide (DMF, 99+%, Acros) and ethanol (EtOH, 99.99%, Fisher) were used as received. Methyl orange (MO, 327 Da, Fluka) was applied as test solute. Polystyrene (PS) standards (Polymer Laboratries) were applied for GPC.

5.2.2 Membrane synthesis

Supports were synthesized via phase inversion.[19] PI powder was first dried overnight in an oven at 100 °C. A homogeneous polymer solution was prepared by stirring a mixture of PI (14% (w w^{-1})) in NMP/THF (3/1). It was left untouched overnight to remove air bubbles created during the stirring. The polymer solution was cast at a constant speed (4.4 x 10^{-2} m

s^{-1}) and with a wet thickness of 200 µm using an automatic casting device (Braive Instruments, Belgium) on a non-woven impregnated with NMP. The film was then immersed in a coagulation bath. 30 s evaporation was inserted between the casting and the immersion to allow THF evaporation from the film surface. The coagulation bath consisted of HDA (0.5% w v^{-1}) and MPD (2.0% (w v^{-1}) in Milli-Q water to simultaneously perform phase inversion, cross-linking and impregnation of the support with MPD.[73] After 5 min, the support was removed from the bath to perform the interfacial polymerization.

First, excess aqueous solution was removed from the impregnated support surface using a rubbery wiper. A solution of TMC (0.1% (w v^{-1}), TMC/IPC or TMC/BC (using different ratios, see Table 5.2) in hexane was subsequently poured gently on the support. The total acyl chloride group concentration in the hexane solution was kept constant at 1.13 x 10^{-2} M. After 60 s, the solution was drained off and the membrane was rinsed with hexane to remove unreacted TMC. Afterwards, the membrane was placed in a water bath to remove unreacted MPD. To apply solvent activation, some TFC membranes were immersed in DMF for 24 h and washed with water afterwards. Finally, the TFC membrane was stored in distilled water until further use.

Support-free PA films were formed in a petri dish by placing a solution of TMC, TMC/IPC or TMC/BC in hexane on top of a solution of MPD in Milli-Q water, using the same monomer concentrations as in TFC membrane synthesis. After 60 s, the solutions were drained off, while the formed PA film was retained in the petri dish. The formed films were rinsed with hexane and subsequently washed in a water bath. To apply solvent activation, they were immersed in DMF for 24 h.

5.2.3 Membrane performance

See 2.2.3.

For the MO feed solution, a concentration of 35 µM in EtOH was used. The absorbance of these feed and permeate samples was determined at 416 nm.

5.2.4 Membrane characterization

The change in free volume in the PA top layer was analyzed using the pulsed low energy positron system (PLEPS) at the neutron induced positron source Munich (NEPOMUC). The measurements were performed at ambient temperature (30°C) with implantation energies of 0.5-2.0 keV. The pick-off lifetime of the o-positronium (o-Ps), which can be extracted from the measured spectra, was correlated to the free volume size using the Tao-Eldrup model.[179,180]

5.2.5 Characterization of PA oligomers

Proton nuclear magnetic resonance (H-NMR) spectroscopy was used to investigate the presence of PA oligomers in the solvent after solvent activation of an immersed membrane. After removing the TFC membranes or the support-free PA films from the DMF solution, the solution was filtered with a 0.2 µm filter to remove small pieces of membrane which came loose during the immersion in DMF. Subsequently, DMF was evaporated and the residue was dissolved in $CDCl_3$ or DMSO-d. The samples were measured on a Bruker Avance 300 MHz H-NMR spectrometer.

The molecular weight of the PA oligomers in the solvent activation solution was determined with GPC. An internal PS standard with a peak molecular weight (M_p) of 316 500 Da was first added to the DMF solution containing the support-free PA films. Subsequently, DMF was evaporated and the residue was dissolved in a THF/DMF (50/50 v v^{-1}) mixture. The solution was then filtered through a 0.2 µm filter to remove the PA films and the filtrate was injected in the GPC (Shimadzu 10A). A PLgel 5µm mixed-D type column was used, with a solution of 0.05M LiBr in THF/DMF (50/50 v v^{-1}) as eluent. A UV-vis spectrophotometer was used as detector. PS standards were applied to calibrate the GPC system.

5.3 Results and discussion

5.3.1 Fundamental understanding

To verify the hypothesis of PA oligomer leaching during solvent activation of TFC membranes, an attempt was made to identify the leached oligomers in the activation solution with H-NMR. After immersing PA/cross-linked PI TFC membranes in DMF for 24 h and subsequently evaporating DMF from the solution, two types of precipitates remained: a dark and a light brown one. While only the light one fully dissolved in chloroform, the dark one could be dissolved completely in DMSO. Therefore, two different H-NMR spectra were made. The spectrum of the light brown residue in $CDCl_3$ (Figure 5.1a) shows many signals in the aliphatic region (0-6 ppm) and some in the aromatic region (6-9 ppm). Since mainly aromatic protons exist in the PA oligomers (see Figure 5.2), other components must be present in this solution. As shown in Figure 6.7b in Chapter 6, cross-linked PI membranes show a 5-6% weight loss after immersion in DMF. Therefore, the signals are expected to result from this dissolved fraction of the support. In the spectrum of the dark brown residue in DMSO-d (Figure 5.1b), mainly aromatic signals were present. The peaks between 6.6 and 7.2 ppm (zoom in Figure 5.1b) originated from MPD. However, compared to the signals of pure MPD in DMSO-d (Figure 5.3, bottom spectrum), they were shifted towards a higher chemical shift, indicating that the MPD molecules were partly protonated. This is not surprising, as HCl is formed during the interfacial polymerization, and no proton acceptors were used as additives. Since the support is impregnated with MPD before interfacial polymerization, and not all of these molecules are removed again during storage of the TFC

membrane in water, the MPD signals in the spectrum are also expected to result from leaching out of the support.

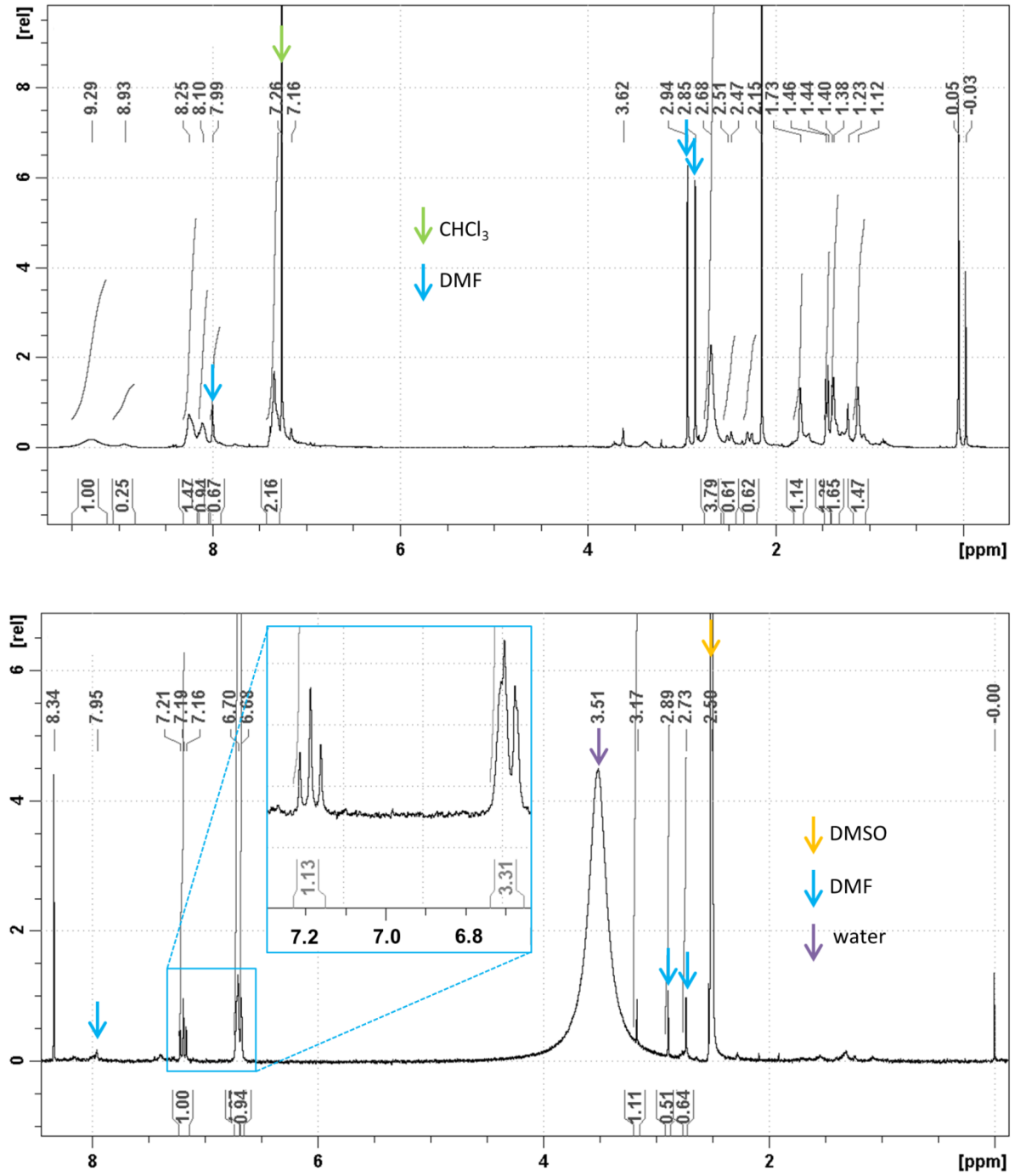

Figure 5.1: H-NMR spectrum of (a) the light brown residue in $CDCl_3$ and (b) the dark brown residue in DMSO-d, after evaporation of DMF from the solvent activation solution. Solvent activation was performed on a PA/cross-linked PI TFC membrane.

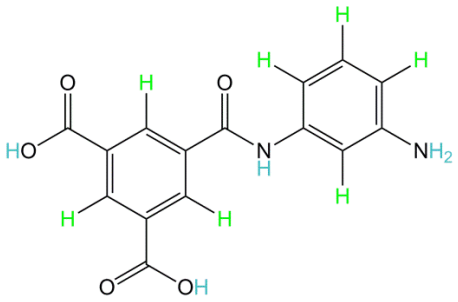

Figure 5.2: Aromatic (green) and non-aromatic protons (blue) in a dimer formed by reaction of MPD and TMC. In PA, the acyl chloride and amine groups are polymerized further.

Since the PA oligomers might be present in a very low concentration, the presence of a high concentration of other molecules in the DMF solution can cause the oligomers to be invisible in the H-NMR spectra. Therefore, an attempt was made to remove these other components. First, the signals of the dissolved fraction of the cross-linked PI support were eliminated by immersing the support in DMF for 48 h before impregnating it with MPD and applying the top layer. This caused the soluble fraction of the support to be removed already before DMF activation of the TFC membrane. Figure S5.1 in appendix D shows the H-NMR spectrum in $CDCl_3$ of this dissolved support fraction. The large similarity to the spectrum in Figure 5.1a indicates that these signals were indeed resulting from components from the support. After evaporation of DMF from the solvent activation solution, only one type of precipitate remained this time, which fully dissolved in DMSO-d. The top spectrum in Figure 5.3 shows that the number of signals reduced drastically, and that the remaining peaks were identical to those of pure MPD in the bottom spectrum in Figure 5.3. No shift of the MPD signals towards higher chemical shifts was observed in the top spectrum, indicating that they were not protonated now. Possibly, immersion of the support in DMF before interfacial polymerization caused it to densify drastically (see Chapter 6), leading to a diminished transport of MPD across the interface and a reduced top layer formation and associated HCl production.

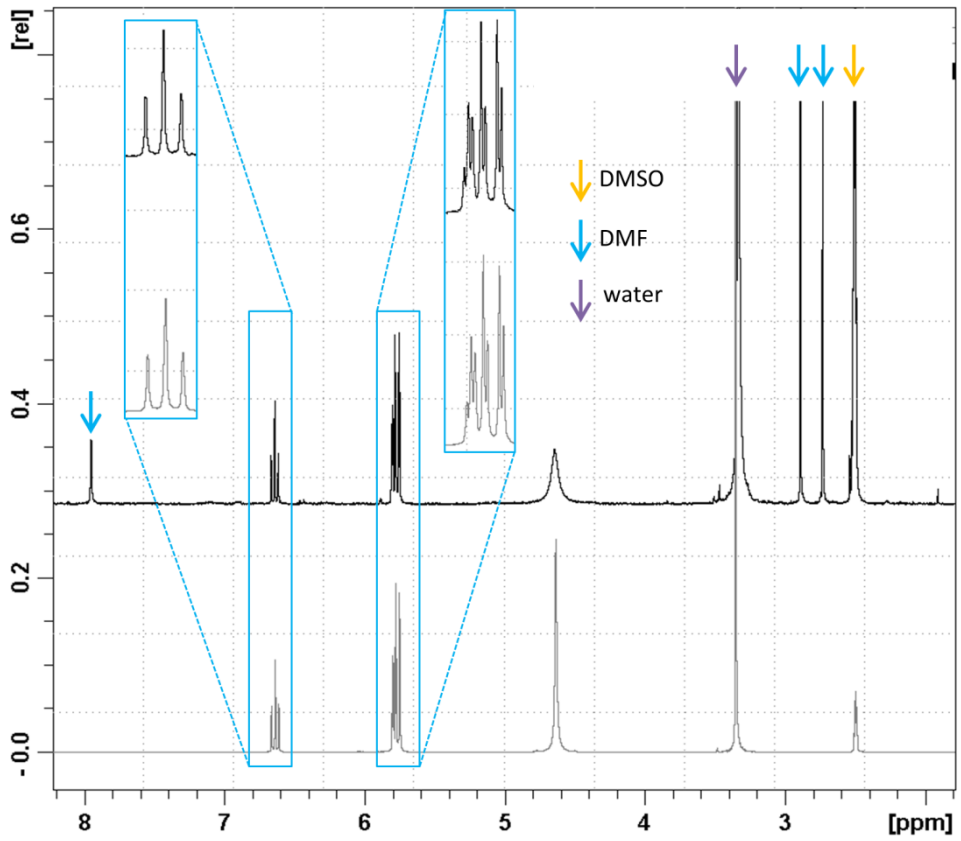

Figure 5.3: H-NMR spectrum in DMSO-d of (top) the solid residue after evaporation of DMF from the solvent activation solution and (bottom) MPD. Solvent activation was performed on a PA/cross-linked PI TFC membrane, of which the support was immersed in DMF before interfacial polymerization.

Although no support-related signals were present anymore, the presence of large MPD peaks, leached out of the support, can still mask the observation of PA oligomers. Moreover, densification of the support might inhibit proper top layer formation.[72] To overcome these two problems, PA films were formed between two liquid phases, without the use of a support. Although the absence of a support influences the rate and uniformity of interfacial MPD transport and the resulting top layer morphology,[77] analysis of these films still gives a good indication of the presence of PA oligomers in the top layer of real TFC membranes. As shown in Figure 5.4, a large amount of aromatic peaks arose from the solid residue leached out of the PA films. Since no other components than MPD, TMC, water, hexane and DMF were used during this experiment, aromatic signals can only result from MPD, TMC or PA. As no MPD, protonated MPD (see Figure 5.3 or Figure 5.1 respectively) nor TMC (one singlet around 9 ppm in $CDCl_3$) is observed in the spectrum in Figure 5.4, PA oligomers must have leached out of the PA films. It is however not possible to identify every single peak in the spectrum, since they probably result from different molecular weight oligomers with a varying fraction of reacted functional groups at each monomer unit.

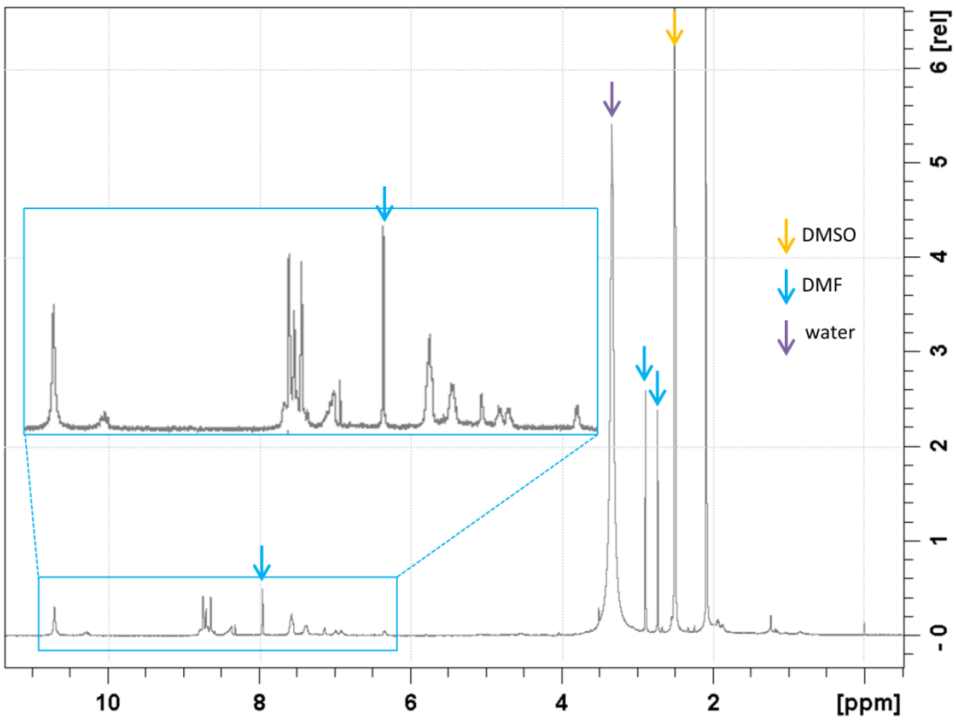

Figure 5.4: H-NMR spectrum in DMSO-d of the solid residue after evaporation of DMF from the solvent activation solution. Solvent activation was performed on PA films formed without support.

GPC was used to estimate the molecular weight of the leached PA oligomers. Figure 5.5 shows that the peak molecular weight of the leached oligomers was 3500 Da, although some shorter oligomers with a higher retention time were also present. This is in line with the results from earlier work.[57] The molecular weight determination of the PAs is based on a calibration with varying molecular weight PS standards, and is thus, due to the differences in chemical structure and linearity between PS and PA, only an estimation. The internal PS standard in Figure 5.5 was added for comparing the absorbance of different samples, as discussed further.

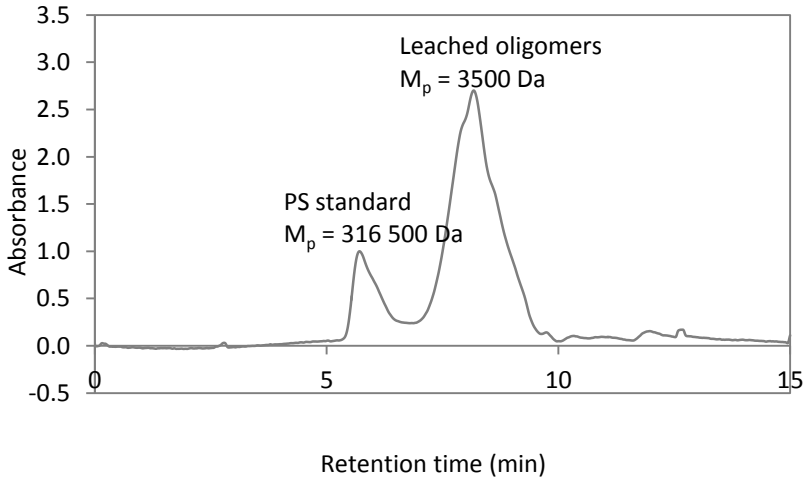

Figure 5.5: GPC spectrum in THF/DMF (50/50 v v^{-1}) of the solid residue after evaporation of DMF from the solvent activation solution. Solvent activation was performed on PA films formed without support. The signal at a retention time of 6 min originates from the addition of an internal PS standard.

As GPC confirmed the leaching of PA oligomers during solvent activation, the resulting top layer was expected to show a higher free volume. Figure 5.6 shows the result of PLEPS analysis of a TFC membrane before and after DMF activation. Due to the variation in free volume sizes in the top layer, the variance on the fit was rather high when applying only one lifetime component. Therefore, the spectrum was separated into two lifetime components (short and long). In Figure 5.6a, no difference in size of the smallest free volume elements (short lifetime) between the two samples was observed. The size of the larger free volume elements (long lifetime), however, increased somewhat after applying the DMF treatment. While the o-Ps lifetimes of the non-activated TFC membrane were situated between 3 and 4 ns, corresponding to a free volume radius of 0.364 - 0.425 nm, the activated TFC membrane showed lifetimes mainly in the range of 4 to 5 ns, corresponding to a free volume radius of 0.425 – 0.475 nm. Potentially, this very small increase in free volume size causes a significant drop in resistance for the solvent molecules to permeate, explaining the observed increase in permeance after solvent activation. Figure 5.6b shows that the intensity of both the short and the long lifetime component decreases after solvent activation. Although this might indicate the presence of a lower concentration of free volume elements, the differences might also be caused by chemical changes in the top layer during DMF activation or by the presence of residual DMF, as the intensity in PLEPS is the product of o-Ps formation probability (determined by chemistry) and free volume concentration (determined by morphology).

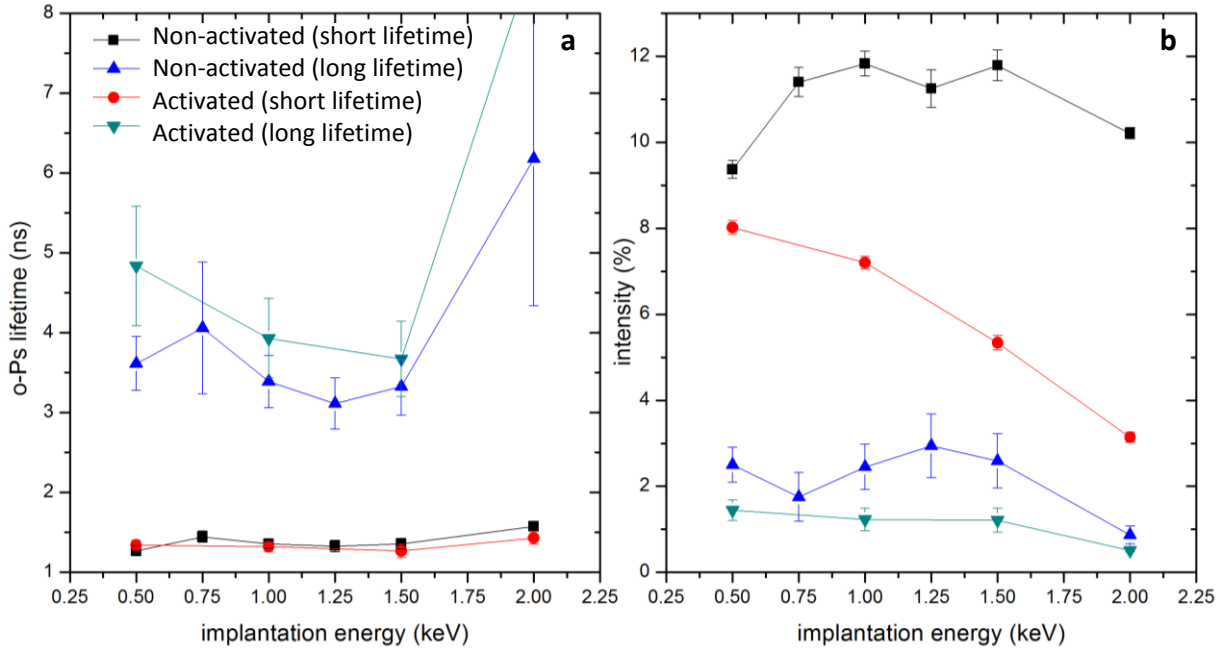

Figure 5.6: (a) O-Ps lifetime and (b) o-Ps intensity of TFC membranes before and after solvent activation. Solvent activation was performed with DMF on a PA/cross-linked PI TFC membrane.

5.3.2 Optimization of solvent activation effect

Based on the H-NMR, GPC and PLEPS data, PA oligomer leaching during DMF activation likely caused the observed increase in permeance of PA TFC membranes. It was therefore hypothesized that the effect of the solvent activation on the permeance could be enhanced by creating a top layer in which more leachable oligomers were present. To achieve this, the TMC molecules in the organic solution for interfacial polymerization were partly replaced by IPC or BC, a bifunctional or monofunctional acyl chloride respectively. This was expected to lower the cross-linking degree of the top layer, increase the concentration of oligomers and lower their molecular weight. The total concentration of acyl chloride groups in the TMC/IPC or TMC/BC mixtures was kept constant in order to maintain an optimal acyl chloride/amine ratio in the reaction zone. The applied monomer concentrations are presented in Table 5.2.

Table 5.2: Applied TMC, IPC and BC concentrations in the different TMC/IPC and TMC/BC mixtures used for interfacial polymerization.

	TMC/IPC or TMC/BC ratio					
	100/0	70/30	50/50	30/70	10/90	5/95
C_{TMC} (M)	3.77E-03	2.93E-03	2.26E-03	1.47E-03	5.40E-04	2.80E-04
Fraction of standard C_{TMC} (%)	*100*	*78*	*60*	*39*	*14*	*7*
C_{IPC} (M)	0.00E+00	1.26E-03	2.26E-03	3.44E-03	4.84E-03	5.24E-03
C_{TMC} (M)	3.77E-03	3.30E-03	2.83E-03	2.12E-03	9.40E-04	
Fraction of standard C_{TMC} (%)	*100*	*88*	*75*	*56*	*25*	
C_{BC} (M)	0.00E+00	1.41E-03	2.83E-03	4.94E-03	8.50E-03	

Figure 5.7 shows the performance of non-activated and DMF-activated TFC membranes, prepared with varying TMC/IPC or TMC/BC ratios in the organic solution. For the non-activated membranes in Figure 5.7a and c, the permeance was expected to increase with increasing IPC or BC fraction, due to the formation of a less strongly cross-linked PA network. Mainly for the BC series, the retention was also expected to decrease, since monofunctional monomers stop the growth of the polymer chains. Their presence would thus result in the formation of low molecular weight PA fragments rather than a cross-linked network. However, besides a small increase in EtOH permeance in the IPC series, none of these expectations was observed. The DMF-activated membranes in Figure 5.7b and d all show a drastically higher EtOH permeance compared to their non-activated counterparts. The hypothesized improvement of the solvent activation effect by using TMC/IPC or TMC/BC mixtures, i. e. a larger increase in permeance after DMF activation, was, however, not observed. Also the retention remained very high for all membranes, indicating that they were still highly cross-linked and thus did not dissolve in DMF. This was unexpected, certainly for the membranes made with a high fraction of BC in the organic solution.

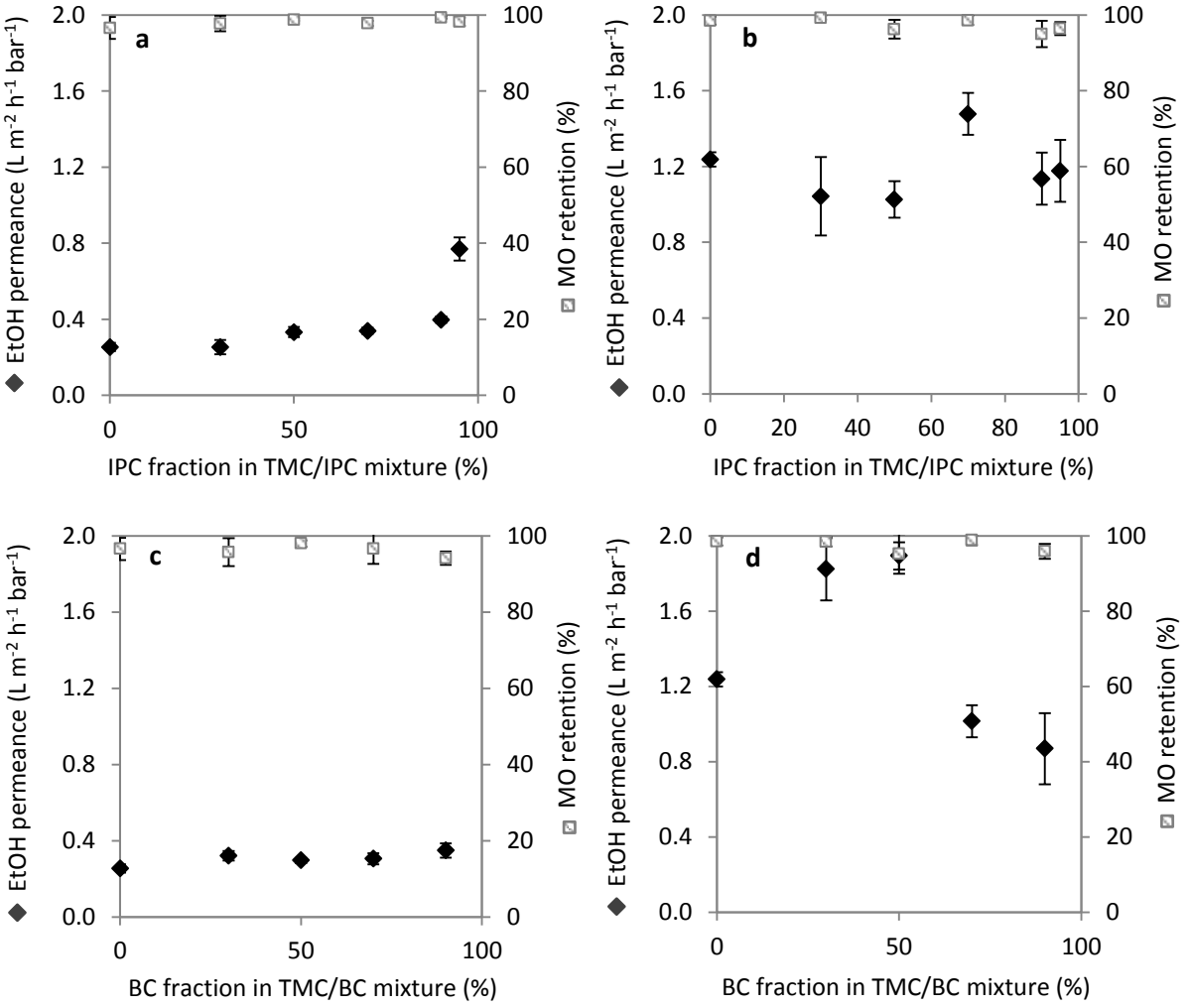

Figure 5.7: EtOH permeance and MO retention of TFC membranes prepared with varying TMC/IPC ratios, (a) without and (b) with DMF activation, and with varying TMC/BC ratios, (c) without and (d) with DMF activation.

To investigate potential differences in concentration and molecular weight of the leached PA oligomers, a GPC analysis was performed on the leached fraction of support-free PA films, prepared with pure TMC, a TMC/IPC ratio of 50/50, or a TMC/BC ratio of 70/30 in the organic phase. The same concentration of the PS standard was added to every sample to enable a quantitative interpretation of the differences in oligomer concentration. As derived from Figure 5.8, the differences in both the molecular weight and the concentration of leached oligomers were negligible. Nevertheless, it is possible that there do are differences in the presence of higher molecular weight oligomers in the top layer. These oligomers might not be soluble in DMF, and might thus not leach during DMF activation. Based on the unchanged membrane performances in Figure 5.7 and the identical GPC spectra in Figure 5.8, it is assumed that IPC and BC hardly participate in the polymerization, due to their lower reactivity compared to TMC. Therefore, the top layer of all membranes in Figure 5.7 probably consists mainly of a PA matrix formed via reaction between TMC and MPD. However, in this case, it is still surprising that the decreased TMC concentration in the

organic phase when using TMC/IPC or TMC/BC mixtures does not influence the resulting top layer properties and performance.

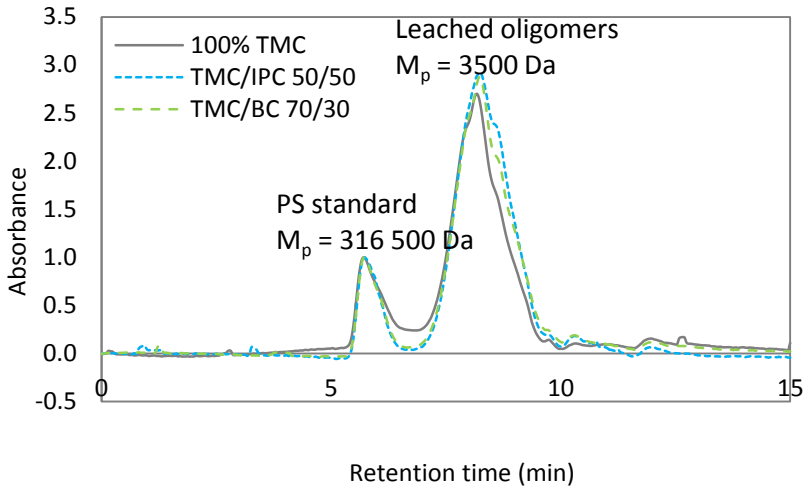

Figure 5.8: GPC spectra in THF/DMF (50/50 v v^{-1}) of the solid residues after evaporation of DMF from the solvent activation solution. Solvent activation was performed on PA films formed without support, using different acyl chloride monomers in the organic phase. The signal at a retention time of 6 min originates from the addition of an internal PS standard.

Therefore, TFC membranes were prepared with lower TMC concentrations in the organic phase, identical to the TMC concentrations used in the 90/10 TMC/BC, 90/10 TMC/IPC and 95/5 TMC/IPC solutions, which are 25, 14 and 7% of the conventional 0.1 % (w v^{-1}) TMC (see Table 5.2). As it was assumed that IPC and BC do not or hardly participate in the interfacial polymerization, the resulting TFC membranes were expected to have a similar performance to the ones prepared with the TMC/IPC and TMC/BC mixtures. Without solvent activation, a decrease in TMC concentration indeed did not significantly affect the TFC membrane performance (Figure 5.9a), similar to the observations in Figure 5.7a and c. After solvent activation, a decreasing trend in permeance with decreasing TMC concentration was observed, while the trend in retention was not clear. This was similar to the observations in Figure 5.7d, where a very low TMC concentration in the TMC/BC mixture also resulted in a lower permeance. For the lowest TMC concentrations in the TMC/IPC mixtures in Figure 5.7c, this was, however, not observed. Potentially, a low amount of IPC did react here during top layer formation. Generally, it can be concluded that the membrane performances in Figure 5.9 are comparable to the ones in Figure 5.7, indicating that it is indeed plausible that mainly TMC reacts with MPD when applying TMC/IPC and TMC/BC mixtures in the organic phase. Therefore, the use of these mixtures proved to be unsatisfactory to improve the effect of solvent activation.

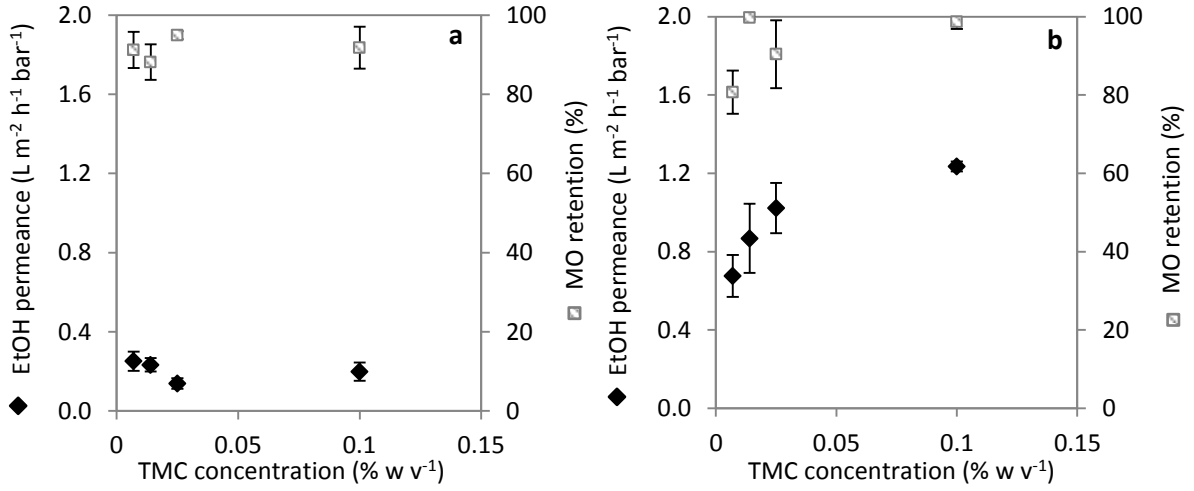

Figure 5.9: EtOH permeance and MO retention of TFC membranes prepared with varying TMC concentrations, (a) without and (b) with DMF activation.

5.4 Conclusions

Solvent activation is an interesting technique to improve the performance of TFC RO and SRNF membranes. The mechanism behind the changing performance is, however, still unclear. In this work, the hypothesis of PA oligomer leaching out of the top layer during DMF activation, resulting in an increase in free volume, was proven. The oligomers were identified via H-NMR analysis, while their molecular weight was estimated via comparison with PS standards in a GPC measurement. H-NMR also indicated that, although the PI support is cross-linked, it is not fully stable and loses some uncross-linked components during DMF activation. This, together with the presence of a large amount of MPD in the support after interfacial polymerization, complicated the observation of leached PA oligomers in the activation solution. Therefore, support-free PA films were used to prove leaching of low molecular weight PA during DMF activation.

An attempt was made to further improve the permeance after solvent activation, by creating a top layer containing more low molecular weight, leachable PA fragments. Therefore, the trifunctional acyl chloride used in the interfacial polymerization process was partly replaced by a bi- or monofunctional acyl chloride. However, no improved membrane performance could be obtained. This was expected to be caused by the higher reactivity of TMC compared to that of IPC and BC, causing MPD to mainly react with TMC during top layer formation.

5.5 Acknowledgements

We are grateful for the financial support from KU Leuven (OT (11/061) funding and Hercules AKUL/13/19 project) and the Belgian Federal Government (I.A.P. – P.A.I. grant (IAP 7/05 FS2)). We would also like to thank T. Hardeman for performing H-NMR and GPC measurements and analyzing the results, the Heinz Maier-Leibnitz Zentrum for the PLEPS measurements and T. Koschine and R. Verbeke for the evaluation of the PLEPS results.

CHAPTER 6

Transformation of cross-linked polyimide UF membranes into highly permeable SRNF membranes via solvent annealing

Based on Hanne Mariën, Ivo F.J. Vankelecom in Journal of Membrane Science, 2017, 541, 205-213.

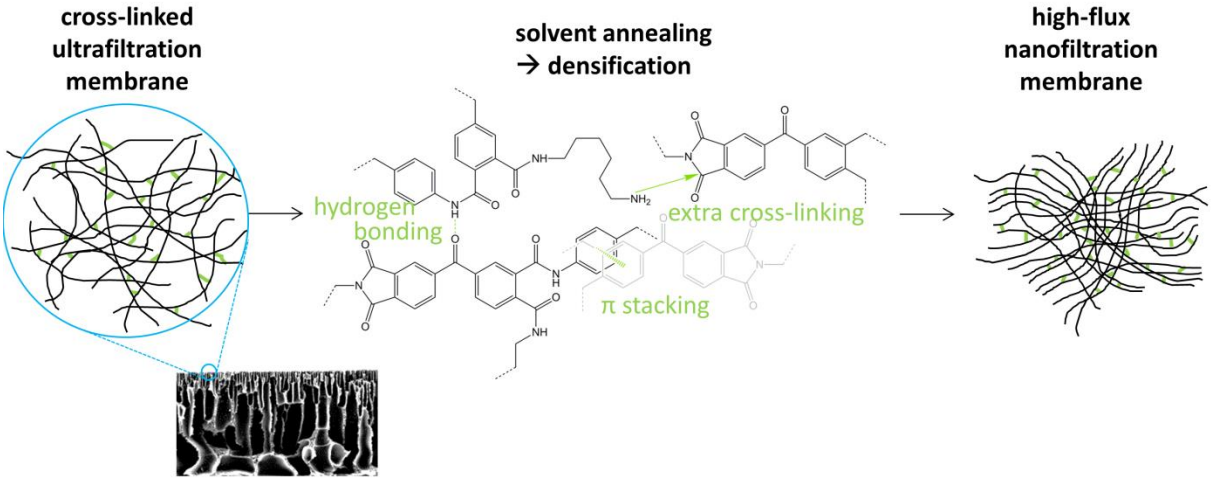

Abstract

A simple method for the preparation of highly permeable solvent-resistant nanofiltration (SRNF) membranes was developed. By applying a solvent treatment to cross-linked polyimide ultrafiltration membranes, polymer chain flexibility increased and the matrix rearranged into a more dense structure, creating highly selective SRNF membranes with exceedingly high ethanol permeance. This densification was driven by the ability of the membrane to lower its free energy while in the solvated state via the establishment of extra favorable interactions, like hydrogen bonds and π interactions. Moreover, further reaction of only partly reacted cross-linker molecules was completed during the treatment, thus enhancing the cross-linking degree. The extent of densification depended on the solvent type, the immersion time and the initial cross-linking degree of the membrane, all influencing the degree of solvation and chain rearrangement. By altering the synthesis conditions, a membrane with equal selectivity to Duramem 300 but showing a 400% higher ethanol permeance was obtained. This demonstrates the high potential of the technique to be applied as novel method for the preparation of SRNF membranes with exceptionally high solvent permeance.

6.1 Introduction

Nanofiltration (NF) is a pressure-driven membrane process in which low molecular weight components (<1000 Da) can be retained. This technique is widely applied in aqueous separation processes, e.g. for the removal of dissolved organic matter, pesticides, disinfection by-products, divalent ions, heavy metals and pharmaceuticals from surface water, groundwater and wastewater [18,21,224]. More recently, solvent-resistant nanofiltration (SRNF) has emerged as a potential energy-saving replacement for distillation and a waste-free alternative for extractions and chromatographic separations in the (petro)chemical, pharmaceutical and food industry.[13–15] Since 40-70% of the capital and operating costs in the chemical and pharmaceutical industry are related to separation processes,[3] improvements in this field can contribute significantly to the creation of a cost-efficient production process. Moreover, the ambient temperature conditions of SRNF allow the separation of mixtures containing thermolabile components, in contrast to distillation.

Since SRNF can be a valuable separation technique in several industrial processes, potential applications have been intensively investigated.[13] Nevertheless, real industrial SRNF applications are still scarce. This is largely caused by the conditions of solvent stability, high solvent permeance and high solute retention which all must be satisfied. Moreover, the wide range of organic solvents applied in industry makes the membrane performance and stability strongly depending on the application. Most SRNF membranes are integrally skinned asymmetric (ISA) membranes, which can be cross-linked to enhance their solvent stability.[50,56,228,229] Due to the rather low permeance of many organic solvents through these types of membranes, the use of thin-film composite (TFC) membranes, with a selective layer of less than 100 nm thick, is being investigated nowadays.[57,62,73,230,231] The most common type of TFC membranes are interfacially polymerized polyamide (PA) membranes, which are widely applied in aqueous NF and reverse osmosis applications.[17] Although the water permeance is high due to the hydrophilicity of the selective layer, the permeance of many (more apolar) organic solvents is still too low to be applied in industry.[121] An improvement in organic solvent permeance of either ISA or TFC membranes could therefore greatly contribute to the large-scale implementation of SRNF.

A new, easy method is presented here to prepare ISA SRNF membranes with a strikingly improved solvent permeance. In this method, polyimide-based ultrafiltration (UF) membranes, having a generally thinner skin layer than ISA NF membranes, were first prepared via phase inversion. Then, the thin skin layer of the cross-linked membrane was selectively densified by performing a solvent treatment to rearrange the polymer chains. By comparing the resulting SRNF membranes with commercial SRNF membranes with equal selectivity, a 400% improvement in ethanol permeance was proven. Moreover, a 184% improvement in ethanol permeance compared to state-of-the-art lab-prepared TFC membranes with similar selectivity,[203] generally showing a higher permeance than ISA

membranes, was observed. Different characterizations were performed to elucidate these findings.

6.2 Experimental

6.2.1 Materials

Polyimide (PI, Matrimid® 9725) was purchased from Huntsman (Switzerland). The non-woven polypropylene/polyethylene fabric Novatexx 2471 was kindly provided by Freudenberg (Germany). Hexanediamine (HDA, 99.5%, Acros) was used for membrane cross-linking. N-methylpyrrolidone (NMP, 99%, Acros), tetrahydrofuran (THF, 99.9+%, Sigma-Aldrich), n-hexane (99+%, Chem-Lab), acetonitrile (ACN, 99.99%, Fisher), dimethylformamide (DMF, 99+%, Acros), ethanol (EtOH, 99.99%, Fisher) and 1-butyl-3-methylimidazolium bis(trifluoromethylsulfonyl)imide ($[C_4mim][Tf_2N]$, 99+%, Iolitec) were used as received. Rose Bengal (RB, 1017 Da, Sigma Aldrich, Figure S6.1a in appendix E) and methyl orange (MO, 327 Da, Fluka, Figure S6.1b in appendix E) were used as test solute.

6.2.2 Membrane synthesis

UF membranes were synthesized via phase inversion. PI powder was first dried overnight in an oven at 100 °C. Homogeneous polymer solutions were prepared by stirring mixtures of PI (14% (w w^{-1})) in NMP/THF (75/25). They were left untouched overnight to remove air bubbles created during the stirring. The polymer solution was cast at a constant speed (4.4 x 10^{-2} m s^{-1}) and with a wet thickness of 200 µm using an automatic casting device (Braive Instruments, Belgium) on a non-woven impregnated with NMP. After a 30 s evaporation to allow THF evaporation from the surface, the film was immersed in a coagulation bath. The coagulation bath consisted of HDA (0.5% (w v^{-1})) in Milli-Q water to simultaneously perform phase inversion and cross-linking of the membrane.[52,58,73] After 5 min, the membrane was removed from the coagulation bath and stored in water until further use. In specified cases where a more dense membrane was desired, a polymer concentration of 16% (w w^{-1}), an NMP/THF ratio of 70/30 or 60/40 or an evaporation time of 60 s was applied. In other specified cases, a HDA concentration of 2.0% (w v^{-1}) and an immersion time in the coagulation bath of 60 min were used to form more strongly cross-linked membranes.

After synthesis and storage of the membranes in water, the cross-linked PI membranes were immersed in a solvent (hexane, EtOH, ACN, $[C_4mim][Tf_2N]$ or DMF) for specified times (1 min, 1.5 h, 30 h or 70 h). Afterwards, they were stored in water for at least 16 h until filtration.

6.2.3 Membrane performance

See 2.2.3.

For the MO feed solution, also a concentration of 35 µM in EtOH was used. The absorbance of these feed and permeate samples was determined at 416 nm.

6.2.4 Membrane characterization

See 2.2.4 for SEM, AFM and ATR-IR procedure.

To analyze top layer cross-sections at high resolution, transmission electron microscopy (TEM) was applied. Unstained membrane samples were embedded in an araldite resin (Polyscience) and cut into ultrathin (70 nm) cross-sections with a Reichert Ultracut E microtome. Images were taken with a JEOL ARM-200F at 80 kV.

The change in free volume in the membrane skin layer was analyzed using the pulsed low energy positron system (PLEPS) at the neutron induced positron source Munich (NEPOMUC). The measurements were performed at ambient temperature (30°C) with implantation energies of 0.5-4.0 keV. The pick-off lifetime of the o-positronium (o-Ps), which can be extracted from the measured spectra, was correlated to the free volume size using the Tao-Eldup model.[179,180]

To determine the weight loss of the membrane after immersion in a solvent, a dry piece of membrane (without non-woven) was weighed before and after immersion. The membrane was dried in an oven at 80°C for at least 24 h. After immersion in a non-volatile solvent, the membrane was washed with water before drying. The weight loss was calculated using Equation 6.1, with m_i and m_f (g) the initial and final dry mass of the membrane piece respectively.

$$Weight\ loss = \frac{m_i - m_f}{m_i} \times 100 \qquad (6.1)$$

To determine the degree of swelling of the membrane during immersion in a solvent, a dry piece of membrane (without non-woven) was first impregnated with water and, after drying, impregnated with the solvent. As the membrane does not swell in water, its pore volume can be derived from the wet mass after impregnation with water. The extra volume of solvent taken up in the polymer matrix is then related to the degree of swelling. It was calculated using Equation 6.2, with m_m, m_{m+s} and m_{m+w} (g) the mass of the dry membrane, and the solvent or water impregnated membrane respectively, and ρ_s and ρ_w the density of the solvent and water respectively.

$$Degree\ of\ swelling = \frac{\frac{m_{m+s} - m_m}{\rho_s} - \frac{m_{m+w} - m_m}{\rho_w}}{m_m} \qquad (6.2)$$

6.2.5 Interaction parameters

The Hansen solubility parameter distance between the uncross-linked PI membrane and the solvents used for immersion ($\Delta_{s\text{-}p}$) was calculated using Equation 6.3,[226] with δ_D, δ_P and δ_H the contribution of dispersive interactions, polar interactions and hydrogen bonding,

respectively. A low $\Delta_{s\text{-}p}$ indicates a strong interaction between the membrane and the solvent.

$$\Delta_{s-p}= \sqrt{4(\delta_{D,solvent} - \delta_{D,PI})^2 + (\delta_{P,solvent} - \delta_{P,PI})^2 + (\delta_{H,solvent} - \delta_{H,PI})^2} \quad (6.3)$$

6.3 Results and discussion

6.3.1 Principle

Membranes with a dense skin layer with selectivities in the NF range were formed by preparing cross-linked PI UF membranes via phase inversion, followed by a solvent treatment. The solvent treatment caused (the skin of) the membrane to densify, drastically improving the selectivity of the membrane. The extent of this effect depended on the type of solvent, the immersion time and the cross-linking degree of the membrane, as discussed in 6.3.2, 6.3.3 and 6.3.4. Under the optimal conditions, a UF membrane could be transformed into a highly selective NF membrane with a superior performance compared to commercial SRNF membranes (directly prepared via phase inversion), as presented in 6.3.5.

The principle of the solvent treatment is presented in Figure 6.1. After casting the PI solution into a thin film, the highly solvated, flexible polymer chains are in a disordered state to minimize their free energy. During phase inversion, the film is transformed into a solid membrane. Because this demixing process occurs instantaneously, the polymer chains are ‘frozen’ in their initial, disordered conformation, without reaching the thermodynamic equilibrium. By adding HDA to the coagulation bath, the membrane is cross-linked during phase inversion, making it resistant to dissolution in any organic solvent, and ‘fixing’ the non-equilibrium state even more effectively. When the membrane is then immersed in a good solvent for the polymer, the interaction between the solvent and the membrane causes re-solvation of the polymer chains, thus increasing their mobility. This improved flexibility is expected to enable the PI chains to reorganize and establish extra favorable interchain interactions, like π interactions between the aromatic rings and hydrogen bonds, resulting in a decrease in free energy. Moreover, partly unreacted HDA molecules can at that moment better approach imide groups in the surrounding, flexible PI chains which were not yet cross-linked before, leading to extra cross-linking. This reorganization and the resulting interactions and cross-linking between the polymer chains are expected to lower the interchain distance and create a more dense membrane. Since the membrane is asymmetric, having a more dense skin on top of a highly porous sublayer, the largest effect is assumed to be observed in the skin layer, where the polymer chains are already in close proximity before the solvent treatment. Further densification of the skin layer can then cause the membrane to be transformed from a UF to a NF membrane.

It is thus expected that the effect on chain flexibility and subsequent membrane densification in the case of solvation of the polymer chains during immersion in a good solvent, as described in this work, is similar to the effect of applying high temperature annealing, as often accomplished in e.g. gas separation, aqueous NF or SRNF.[29,232–235] During high temperature annealing, the increased temperature is also assumed to cause a thermodynamically driven reorganization of the polymer chains towards more dense structures.[236]

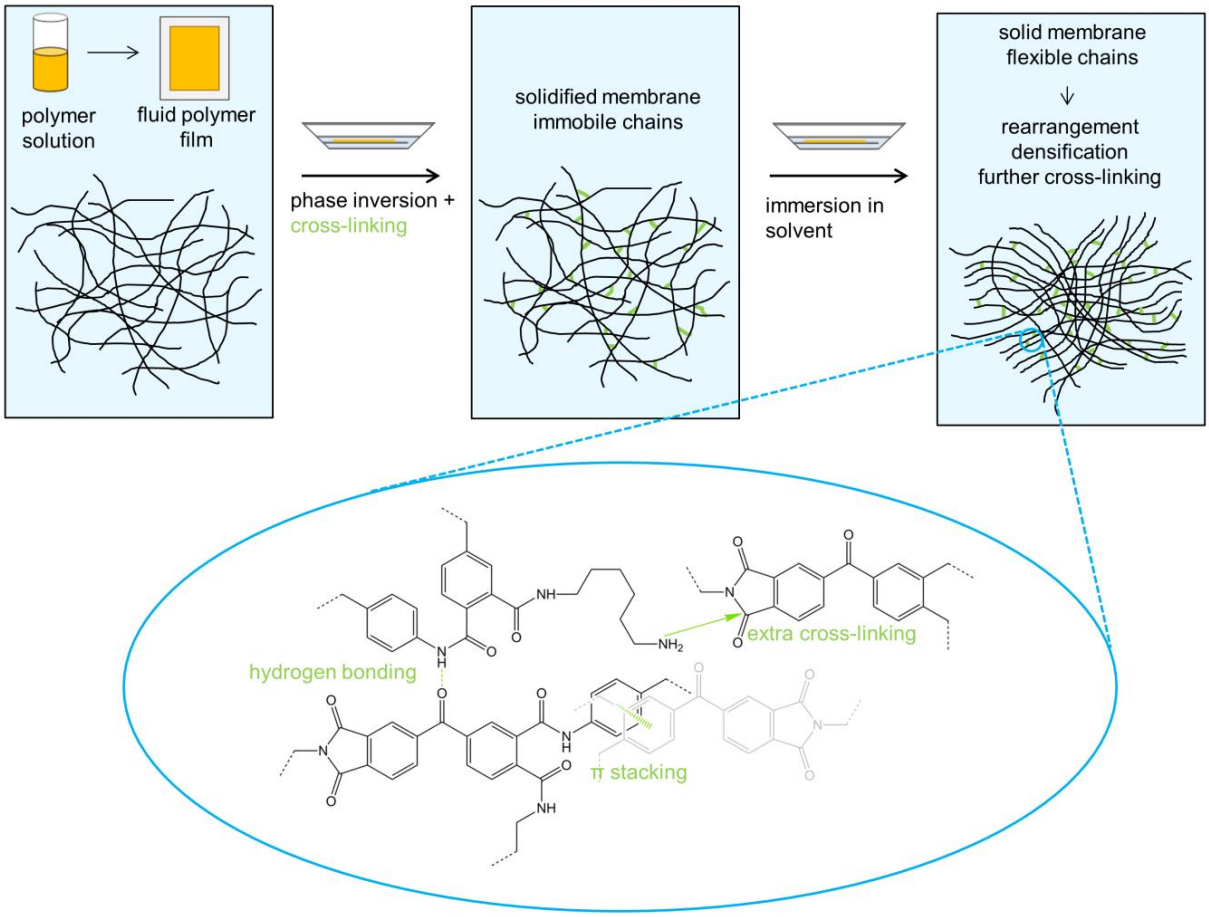

Figure 6.1: Basic principle of the post-synthesis membrane densification via solvent treatment.

6.3.2 Solvent type

First, the effect of a 30 h immersion of cross-linked PI membranes in different types of solvents was investigated. Because ionic liquids are an emerging class of solvents in polymer synthesis,[142,237] and more specifically in membrane preparation,[156,158,203] $[C_4mim][Tf_2N]$ was incorporated in the study as an example of this type of solvents. The results are shown in Figure 6.2. Without solvent treatment, the membrane showed a very low RB retention, together with a high EtOH permeance, as could be expected from a membrane prepared using a typical UF membrane recipe. All tested solvents caused the retention to increase and the permeance to decrease, but to an extremely different extent. While the effect of immersing the membrane in hexane, EtOH and ACN was low to moderate, a very strong

effect was observed after immersion in [C_4mim][Tf_2N] and DMF. Pictures of the membrane coupons after filtration (Figure 6.2) clearly prove that – in clear contrast to the four other samples - no RB was sorbed in the membranes treated with [C_4mim][Tf_2N] and DMF, indicating that the increased retention is not realized by dye adsorption on or in the membrane, but that a true densification of the skin had occurred.

A washing step with water of at least 16 h was applied between the solvent treatment and the filtration, during which EtOH, ACN and DMF were removed. Hexane and [C_4mim][Tf_2N], however, are immiscible with water, and could thus still have been present in the membrane at the start of the filtration, during which they were removed by EtOH. The observed decrease in permeance over the filtration time of the membrane treated with [C_4mim][Tf_2N] might indicate that the polymer chains were still somewhat solvated and flexible at the start of the filtration, caused by the initial presence of residual ionic liquid.

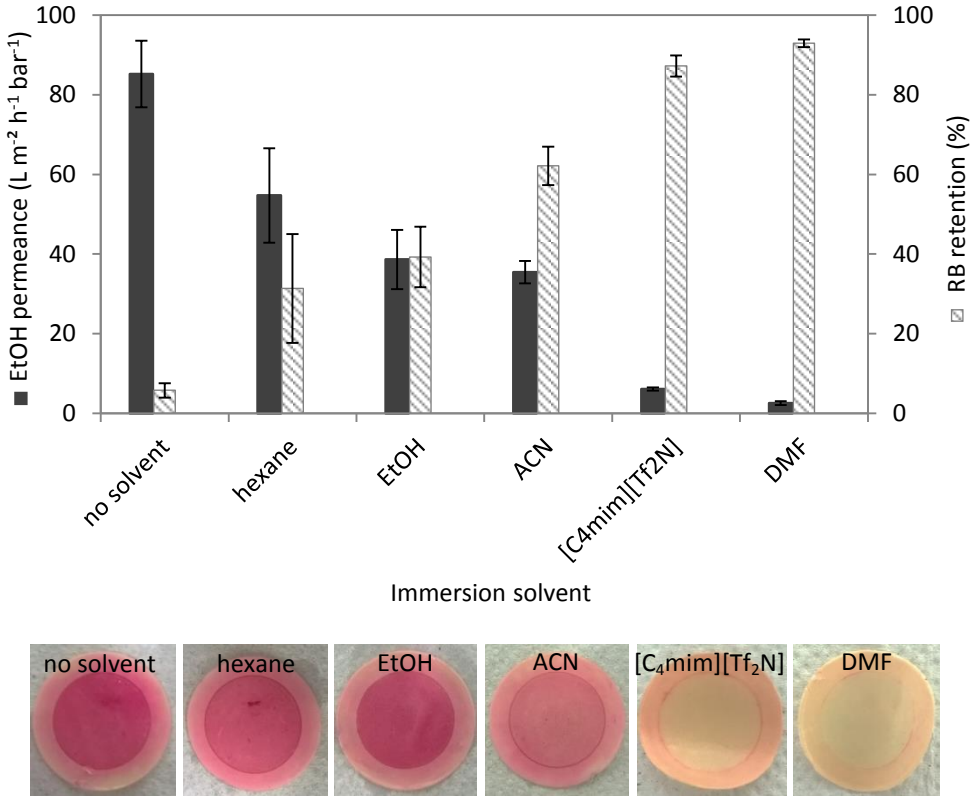

Figure 6.2: EtOH permeance and RB retention of cross-linked PI membranes after 30 h of immersion in different solvent types (top) and visual observation of possible sorption of RB in the membrane coupons during the filtration (bottom).

To link the densification effect of the different solvents to membrane-solvent interactions, which would cause solvation and reorganization of the flexible polymer chains, the difference in Hansen solubility parameters between PI and the different solvents ($\Delta_{s\text{-}p}$) was calculated (Table S6.1 in appendix E). $\Delta_{water\text{-}p}$ was also included, since the performance of the reference membrane without solvent treatment corresponds to a membrane stored in water before filtration. Only $\Delta_{[C4mim][Tf2N]\text{-}p}$ could not be calculated because the Hansen solubility parameters are not available for this solvent.

Figure 6.3 shows the decrease in permeance and increase in retention caused by the solvent treatment, as function of the difference in Hansen solubility parameters between the membrane and the solvent used for the treatment. The trend indicates that the solvents having the smallest effect on membrane performance (lowest $-\Delta_{EtOH\ permeance}$ and $\Delta_{RB\ retention}$) also had the weakest interaction with the PI membrane (highest Δ_{s-p}), while the interaction increased for solvents having a larger effect on membrane performance. This supports the hypothesis of the need for sufficient swelling to reorganize the polymer chains. The larger densification effect of EtOH compared to hexane (Figure 6.2), which contradicts their equal Δ_{s-p} values in Table S6.1 in appendix E, can be explained by the fact that these values were calculated using the Hansen solubility parameters of pristine, non-cross-linked PI. Cross-linking the PI membrane caused the polarity of the membrane to increase, improving its interaction with EtOH, while diminishing its affinity for hexane.

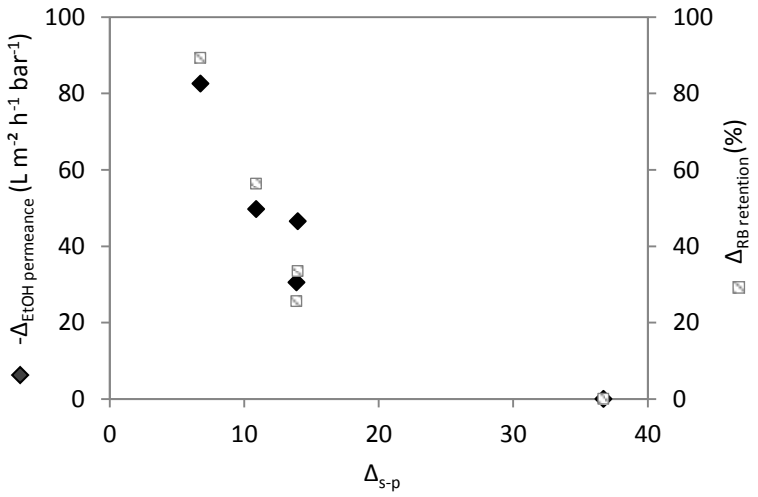

Figure 6.3: Change in EtOH permeance and RB retention of cross-linked PI membranes caused by the solvent treatment, as function of their interaction with the respective solvents used for the treatment.

As the magnitude of the membrane-solvent interaction changes with the type of solvent, a difference in swelling behavior of the membrane should also be observed. Therefore, the degrees of swelling and the weight losses of the membrane after a 30 h immersion in the different solvents were calculated. The weight loss was expected to be proportional to the degree of swelling, since a larger membrane-solvent interaction would both cause a larger swelling and a higher solubility, hence facilitating leaching of non-cross-linked polymer chains from the membrane. The degree of swelling could only be measured accurately in the case of non-volatile solvents, while the weight loss could only be determined when the solvent was able to evaporate or to be fully replaced by water, which could then be evaporated.

As shown in Figure 6.4a, hexane and EtOH, having the highest Δ_{s-p}, did not induce any significant weight loss of the membrane. However, the weight loss increased after immersing the membrane in ACN and, even more, in DMF, corresponding to the trend in Δ_{s-p}. The differences in weight loss perfectly agree with the trend in membrane performance,

as elucidated in Figure 6.4b. It should be mentioned that the weight loss remained low (< 6%) for all membranes, suggesting that the membrane integrity was maintained. A too high weight loss could result in a loss of membrane structure and performance. Also the swelling degree of the membrane increased going from $[C_4mim][Tf_2N]$ to DMF as immersion solvent (Figure 6.4a).

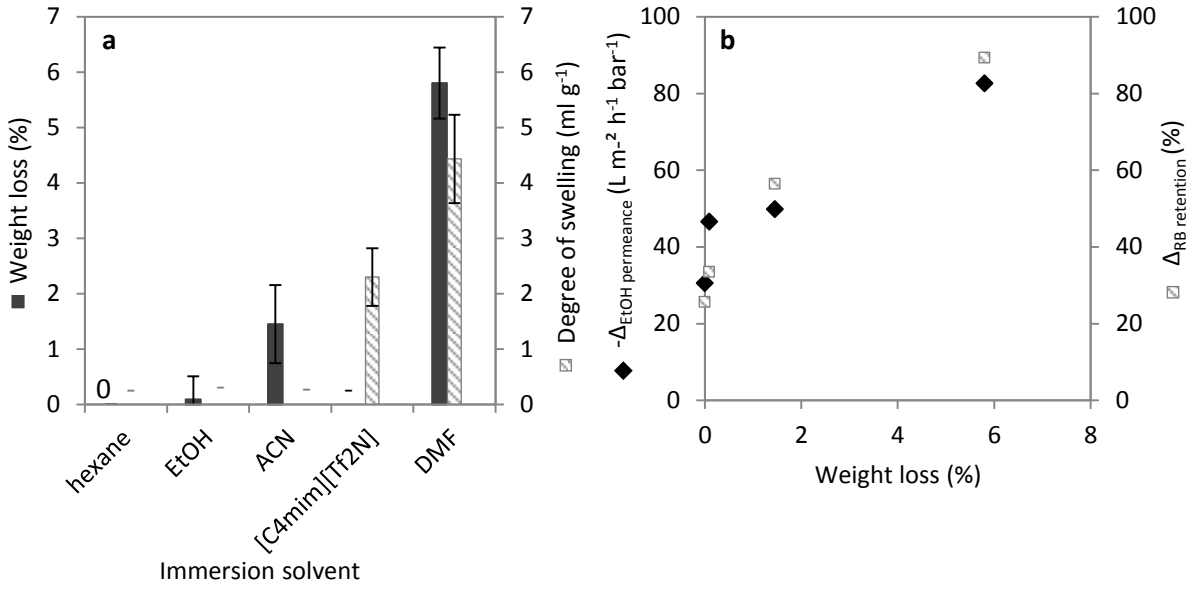

Figure 6.4: (a) Weight loss and degree of swelling of cross-linked PI membranes after 30 h of immersion in different solvent types. '0' means the value was zero, '-' means the value was not measured. (b) Change in EtOH permeance and RB retention of cross-linked PI membranes as function of their weight loss after immersion in the different solvents.

Densification was expected to be caused by both the establishment of favorable interactions between the polymer chains and by further cross-linking of the PI matrix (Figure 6.1). The effect of the solvent treatment on the degree of cross-linking of the membranes is shown in Figure 6.5. To quantify the cross-linking degree, the ratio of the amide over imide absorbance was calculated, since cross-linking causes the imide bonds of the PI membrane to be transformed into amide bonds. A higher amide/imide ratio thus indicates a stronger cross-linking. The largest imide (at 1720 cm^{-1}) and amide signals (at 1602 and 1662 cm^{-1}) in the UV-vis spectrum were used to calculate the ratio. Figure 6.5 indicates that the cross-linking degree of the membranes did not change significantly after immersion in hexane, EtOH and ACN. Immersion in $[C_4mim][Tf_2N]$ and DMF, however, caused the membranes to be further cross-linked. Especially when using DMF, the difference in cross-linking degree with the reference membrane was large. This proves that during the initial phase inversion and cross-linking step, not all HDA molecules are able to react at both sides with a PI chain, probably because the PI chains are 'frozen' instantaneously when immersing the polymer film in the coagulation bath containing the cross-linker. Subsequent immersion of the solidified membrane in a solvent which makes the polymer matrix swell significantly ($[C_4mim][Tf_2N]$ or DMF), causes the PI chains to become flexible, and enables the unreacted amine group of HDA to physically reach a second polymer chain to complete its cross-linking

reaction. This improvement of membrane cross-linking is assumed to be one of the driving forces of the densification of the membrane.

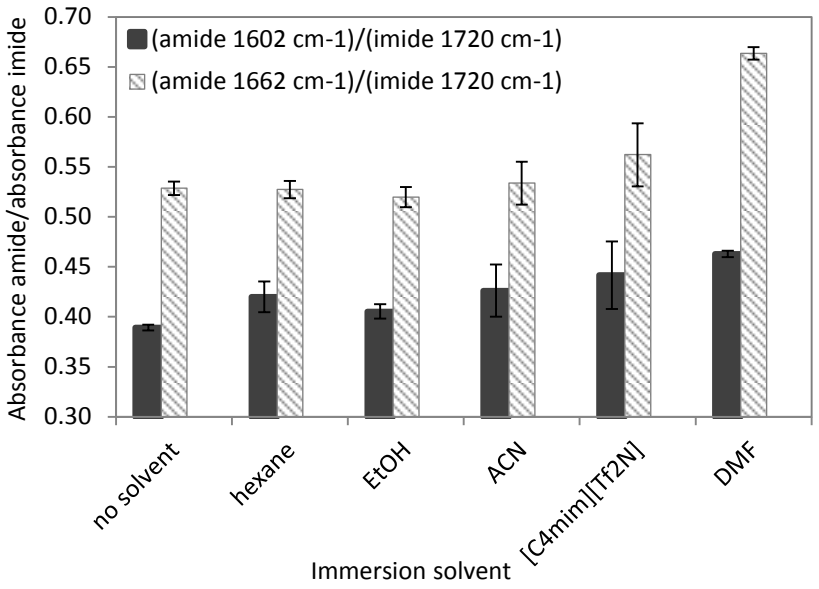

Figure 6.5: ATR-IR results of cross-linked PI membranes after 30 h of immersion in different solvent types. The amide/imide absorbance ratio indicates the cross-linking degree of the membranes.

In an attempt to visualize the changes in membrane density and pore structure caused by immersion in the different solvents, SEM and TEM cross-sectional images were made. The SEM images in Figure 6.6a, b and c indicate that the overall membrane pore structure was not altered by the solvent treatments. By focusing on the skin layer of the membrane with TEM, an increase in thickness of the denser layer was observed after treating the membrane with ACN or DMF (Figure 6.6d, e and f). However, the difference was small and difficult to quantify. It is therefore expected that the density (free volume) of the skin layer rather than its thickness is affected by the solvent treatment. An attempt was made to quantify this change in free volume with PLEPS. However, since o-Ps formation is inhibited in some materials, like polyimide,[238] extremely low intensities were measured and the results were not useful.

Also the surface morphology was assumed to be affected by the solvent treatment. Reorganization of the polymer chains into a more densely packed structure was expected to lower the surface roughness. AFM indicated that the RMS roughness indeed decreased from 5.2 ± 0.6 nm for the reference membrane to 4.2 ± 0.4 nm or 3.6 ± 0.2 nm after immersion in ACN or DMF respectively (Figure 6.6g, h and i), which corresponds to the expected extent of reorganization in polymer chains caused by these two solvents.

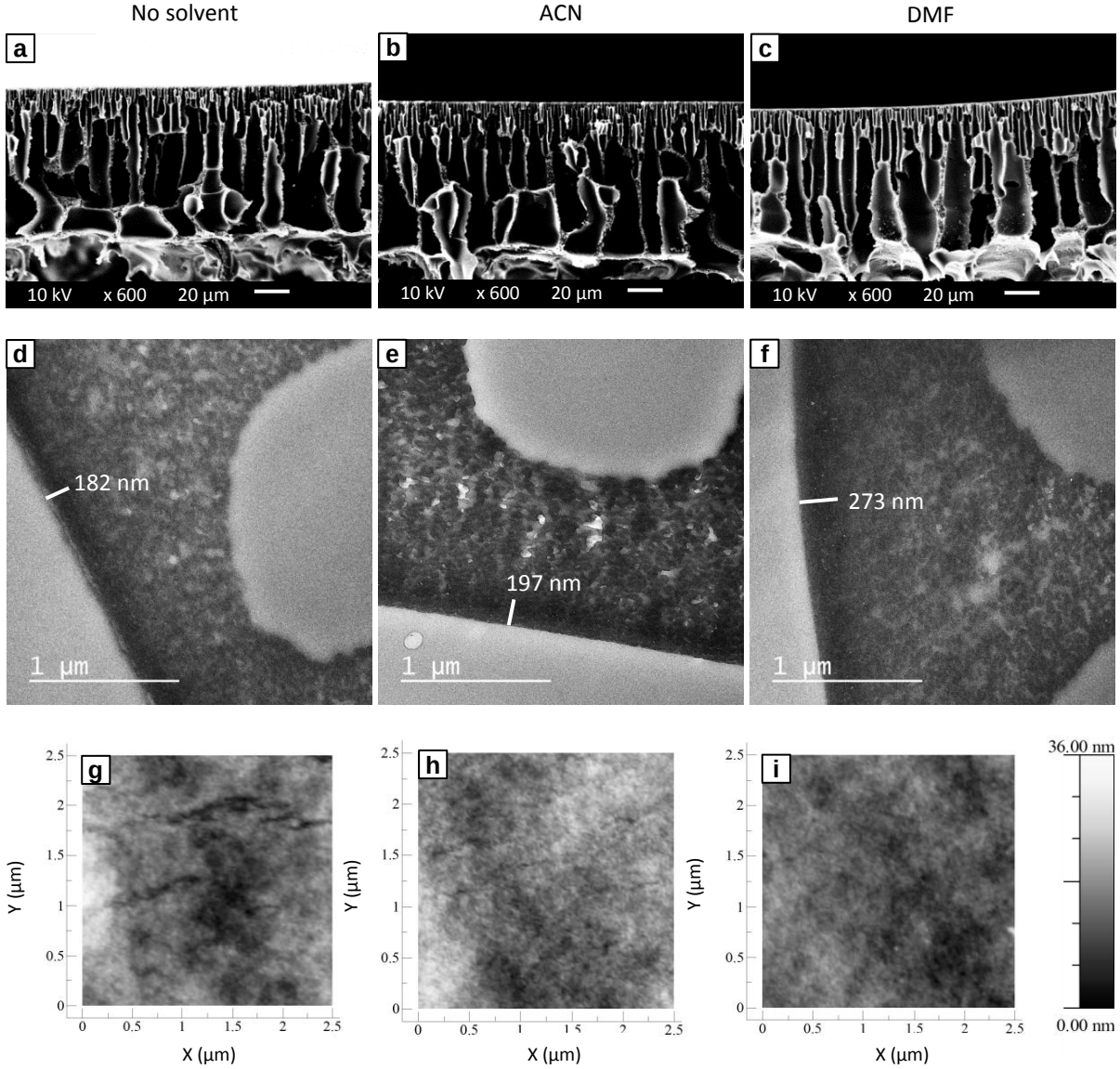

Figure 6.6: (a, b, c) Cross-section SEM images, (d, e, f) cross-section TEM images and (g, h, i) surface AFM images of cross-linked PI membranes without solvent treatment or after 30 h of immersion in ACN or DMF.

6.3.3 Immersion time

Since DMF had the largest effect on membrane performance, this solvent was chosen to investigate the influence of the immersion time. As shown in Figure 6.7a, a 1 min immersion in DMF already caused the RB retention to increase drastically towards the NF range, while the permeance dropped accordingly. By increasing the immersion time to 1.5 h, the effect on performance was intensified. However, a further increase of the immersion time resulted in a small reversal of the densification effect.

To explain this trend, the swelling degree and weight loss of the membranes after different immersion times was determined (Figure 6.7b). Although swelling occurs immediately after immersion and the swelling degree remains constant at increasing immersion times, 1 min is probably too short for the polymer chains to fully rearrange and establish interchain

interactions and cross-linking. Therefore, a further increase in RB retention and decrease in EtOH permeance takes place at longer treatment times (Figure 6.7a). The weight loss is, however still very small after 1 min of immersion due to the rather slow disentanglement and leaching of non-cross-linked PI chains. The increasing weight loss after longer DMF treatments possibly counteracts the membrane densification effect, which might explain the slightly reversing trend in performance after 30 and 70 h immersion (Figure 6.7a).

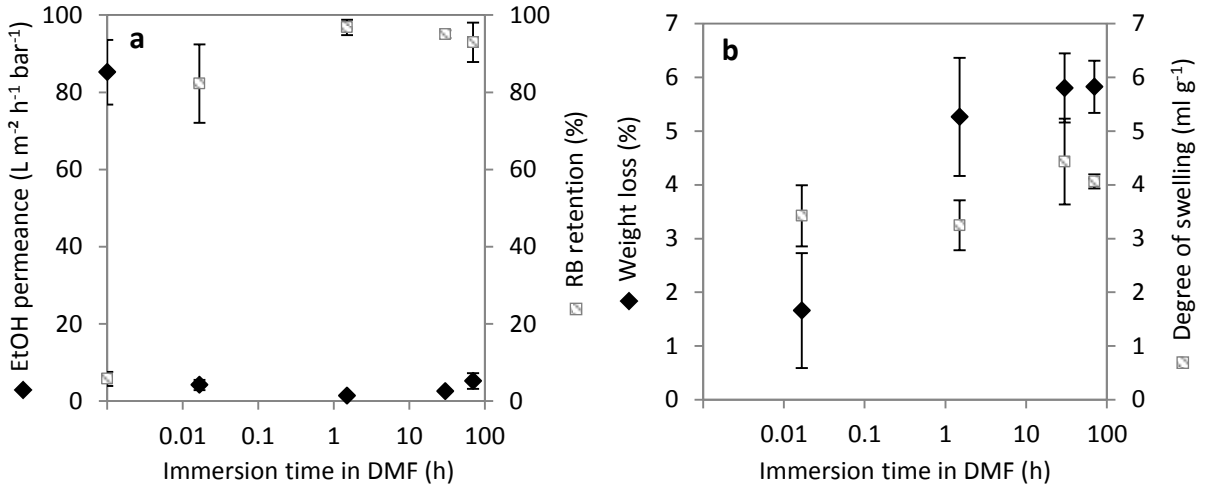

Figure 6.7: (a) EtOH permeance and RB retention of cross-linked PI membranes after immersion in DMF for different times (log scale), and (b) weight loss and degree of swelling of cross-linked PI membranes after immersion in DMF for different times (log scale).

6.3.4 Degree of cross-linking

Since cross-linking limits the PI chains to become flexible and rearrange during immersion in a solvent, membranes with a higher degree of cross-linking after the coagulation step were expected to be less affected by the solvent treatment. Therefore, more strongly cross-linked PI membranes were prepared and the effect of immersion in $[C_4mim][Tf_2N]$ and DMF on their performance was investigated. First, the significant difference in cross-linking between the two membranes, realized by altering the HDA concentration and reaction time, was demonstrated with ATR-IR (Figure 6.8). The strongly cross-linked PI membrane (high-XL) clearly shows larger amide signals (green bars) and reduced imide signals (blue bars). The spectrum of an uncross-linked PI membrane is shown for comparison.

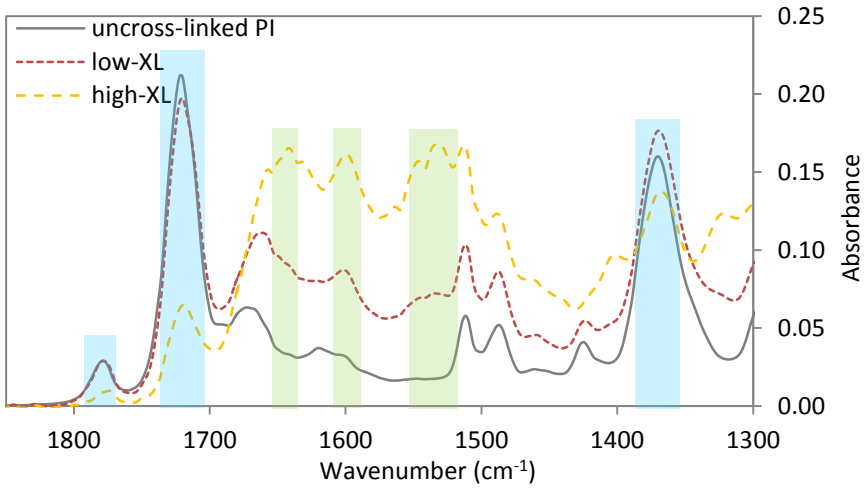

Figure 6.8: ATR-IR spectra of PI membranes with a low (low-XL) and high degree of cross-linking (high-XL), and an uncross-linked PI membrane for comparison. The blue bars represent imide and the green bars amide signals.

As shown in Figure 6.9, increasing the cross-linking degree of the membrane (without solvent treatment) caused the membrane to densify, as derived from the decreasing EtOH permeance and increasing RB retention. However, after immersion in [C_4mim][Tf_2N] or DMF, the increase in retention and decrease in permeance (relative to the value of the non-treated membranes) was lower at higher cross-linking degree. This difference was more pronounced for [C_4mim][Tf_2N] than for DMF. Increasing the cross-linking thus clearly lowered the effect of the solvent treatment. This can either be caused by the lower potential of a more highly cross-linked membrane to reorganize, or by the lower diffusion rate of the solvents inside a more dense, highly cross-linked membrane, reducing the available time for reorganization.

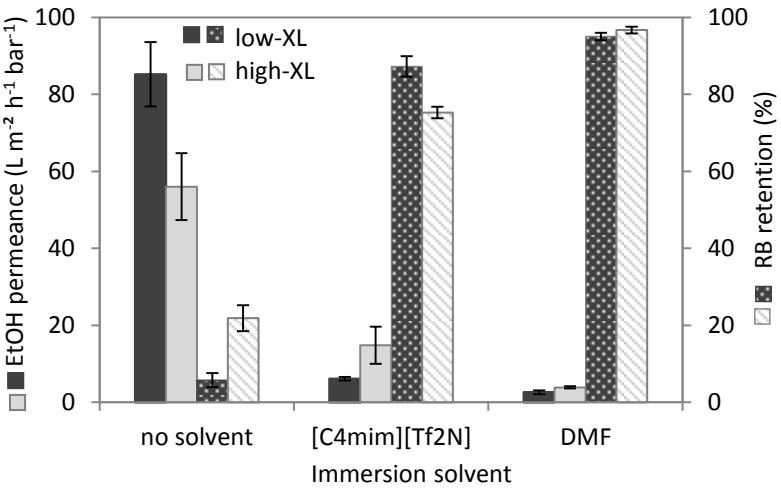

Figure 6.9: EtOH permeance and RB retention of PI membranes with low (low-XL) and high degree of cross-linking (high-XL), before and after immersion in [C_4mim][Tf_2N] and DMF for 30 h.

6.3.5 Formation of nanofiltration membranes

NF membranes are classified as membranes having a MWCO of less than 1000 Da.[160] RB has a MW of 1017 Da and therefore represents the upper limit of NF. The best performing membrane prepared by the solvent treatment, showed a RB retention of 96.8% and an EtOH permeance of 1.44 L m^{-2} h^{-1} bar^{-1} (Figure 6.7a, 1.5 h immersion in DMF) and can thus be classified as a NF membrane. It was, however, expected that even more dense membranes could be prepared by changing the synthesis conditions, which could then be transformed again into even tighter NF membranes by applying the solvent treatment.

Table 6.1 shows the synthesis conditions of cross-linked PI membranes in which either polymer concentration, NMP/THF ratio or evaporation time were adapted to obtain denser membranes. For every membrane, a 1.5 h DMF treatment was applied after phase inversion, and membrane performance was determined with a solution of MO in EtOH. This dye (MW = 327 Da) was more suitable than RB to distinguish the selectivities of these denser membranes. As derived from Figure 6.10, an increase in polymer concentration form 14 to 16% (w w^{-1}) or a decrease in NMP/THF ratio from 70/30 to 60/40 both resulted in an improved selectivity without loss in permeance. An increase in evaporation time, however, caused the permeance to decrease significantly, probably by increasing the thickness of the skin layer. [26,29,30] Combining the higher polymer concentration and lower NMP/THF ratio resulted in a highly selective NF membrane with a 95% MO retention, while the EtOH permeance remained unaffected (i.e. 1.12 L m^{-2} h^{-1} bar^{-1}).

Table 6.1: Conditions for the preparation of denser, cross-linked PI membranes (with low cross-linking degree) via phase inversion, followed by a DMF treatment.

Membrane	PI concentration (% w w^{-1})	NMP/THF ratio (w w^{-1})	Evaporation time (s)	Immersion time in DMF (h)
PI-ref	14	70/30	30	1.5
PI-16%	**16**	70/30	30	1.5
PI-60/40	14	**60/40**	30	1.5
PI-60s	14	70/30	**60**	1.5
PI-16%-60/40	**16**	**60/40**	30	1.5

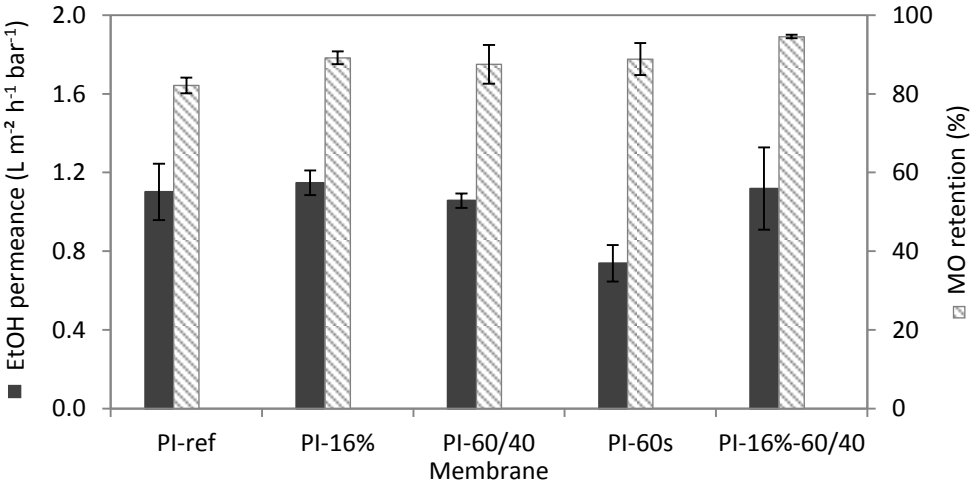

Figure 6.10: EtOH permeance and MO retention of denser, cross-linked PI membranes (with low cross-linking degree) prepared via phase inversion, followed by a 1.5 h DMF treatment.

In Figure 6.11, the performance of Duramem 500 and Duramem 300 (commercial, cross-linked PI membranes) is compared with the solvent treated membranes prepared in this work. Membranes from Figure 6.10 with a selectivity similar to the Duramem membranes were selected to compare the EtOH permeance more correctly. Since Duramem 500 has a MWCO of 500 Da, it showed a MO retention below 90%. The solvent treated PI membrane with similar selectivity had a significantly higher EtOH permeance (x 270%). The more dense Duramem 300 showed a higher MO retention and, accordingly, a lower EtOH permeance. In this case, an even larger difference in EtOH permeance could be observed (x 400%). The DMF treatment of cross-linked PI-based UF membranes thus clearly proved to result in high-performance NF membranes with a drastically higher EtOH permeance compared to commercial Duramem membranes with equal selectivity.

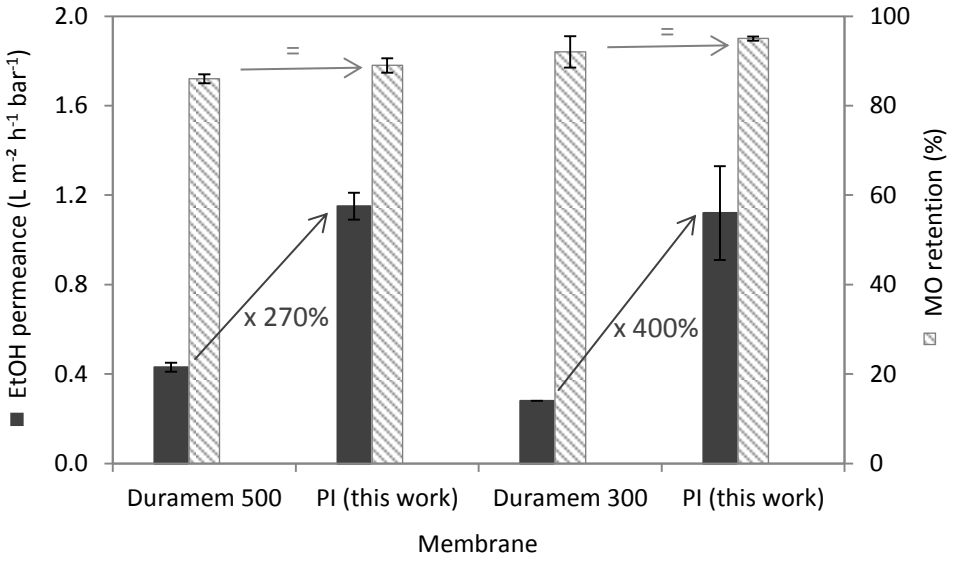

Figure 6.11: Comparison of the EtOH permeance and MO retention of commercial Duramem membranes and solvent treated cross-linked PI membranes prepared in this work.

Even compared to lab-made TFC PA membranes,[203] which generally reach higher permeances than ISA membranes, these densified crosslinked PI membranes showed a 180% higher EtOH permeance (0.61 for the TFC membrane compared to 1.12 L m^{-2} h^{-1} bar^{-1} for the ISA PI membrane) with similar selectivity (99% RB (1017 Da) and 96% Sudan Black B (457 Da) retention for the TFC membrane compared to 95% MO (327 Da) retention for the ISA PI membrane).

6.4 Conclusions

A new, simple method to form highly permeable ISA SRNF membranes was presented, in which a solvent treatment allowed cross-linked PI UF membranes, prepared via phase inversion, to be transformed into NF membranes. The link between the degree of swelling, weight loss of the membranes after immersion in different solvents, Hansen solubility parameters and the effect of the solvent treatment on membrane performance proved that membrane-solvent interactions and swelling were determining factors in the membrane densification. The increased polymer chain flexibility during immersion in a good solvent (i.e. DMF) caused densification and improved chain stacking, by establishing favorable interactions (e.g. hydrogen bonds and π interactions) and increasing the cross-linking degree. Furthermore, the immersion time in the organic solvent and the initial degree of cross-linking of the membrane also influenced the extent of densification.

By changing the PI concentration, the NMP/THF ratio in the polymer solution and the evaporation time between casting and phase inversion of the initial membranes, the performance of the solvent treated membranes could be further tuned. The best performing densified membranes from this work with selectivity equal to Duramem 500 or Duramem 300, reached a respectively 270 or 400% higher EtOH permeance compared to these commercial membranes. Compared to lab-made TFC PA membranes,[203] solvent treated membranes from this work with similar selectivity showed a 180% higher EtOH permeance. This very simple treatment of existing membranes thus shows a huge potential for SRNF applications, since it enables the formation of highly selective SRNF membranes with exceedingly high EtOH permeance compared to commercial membranes.

6.5 Acknowledgements

We are grateful for the financial support from KU Leuven (OT (11/061) funding and Hercules AKUL/13/19 project) and the Belgian Federal Government (I.A.P. – P.A.I. grant (IAP 7/05 FS2)). We also wish to thank A. Vandoren from the Laboratory for Entomology of KU Leuven for sample preparation for TEM, C. Van Goethem from the Centre of Surface Chemistry and Catalysis for performing the TEM measurements, and A. Volodin from the Laboratory of Solid-State Physics and Magnetism of KU Leuven for the AFM measurements. We would also like to thank the Heinz Maier-Leibnitz Zentrum for the PLEPS measurements and T. Koschine and R. Verbeke for the evaluation of the PLEPS results.

CHAPTER 7

General conclusions and perspectives

7.1 General conclusions

Membrane technology has grown significantly over the last decades due to its beneficial properties in terms of energy use, separation conditions and/or waste production compared to conventional separation processes, like distillation, extraction, crystallization and adsorption. NF and RO are applied for the separation of low molecular weight components (< 1000 Da) and salts. The main part of the commercial NF and RO membranes are either ISA or interfacially polymerized TFC membranes. PA TFC membranes are the standard in aqueous NF and RO applications, thanks to their very thin, dense top layer, able to form hydrogen bonds with water. However, efforts should still be made to improve their performance and to tackle certain shortcomings, like their high fouling tendency and low chlorine resistance. For SRNF applications, mainly ISA membranes are applied nowadays, which are very simple and fast to prepare. Unfortunately, they often suffer from rather low solvent permeances, associated with their thicker selective layer compared to that of TFC membranes. Therefore, the application of TFC membranes in SRNF is intensively investigated currently.

The importance of the type of solvents used in the synthesis and post-treatment of (SR)NF and RO membranes cannot be underestimated. Since they have an impact on several aspects of the membrane preparation process, like monomer and polymer solubility, monomer diffusion coefficients, solvent exchange rate and degree of swelling of the membrane, they drastically influence the final chemical and morphological properties of the membrane. In this work, the effect of the solvent type in interfacial polymerization and in post-synthesis solvent treatments was investigated.

7.1.1 ILs as solvent in interfacial polymerization

ILs were chosen as alternative solvents in interfacial polymerization, since they were assumed to largely affect PA top layer formation via interfacial polymerization due to their very different physicochemical properties compared to conventional solvents. This resulted in a top layer with beneficial properties, affecting both the general RO performance and the fouling resistance of TFC PA membranes in a positive way. Either the conventional hexane or aqueous phase was replaced by an IL.

Water/IL system

In the first part, the toxic and volatile hexane phase was replaced by an IL, $[C_4mim][Tf_2N]$. Besides the exclusion of hexane, this water/IL system showed several other advantages in the preparation process. Due to the altered interfacial tension, monomer diffusivity and solubility in the reaction zone, a 20 times lower MPD concentration could be applied, while no commonly used additives (SDS and TEA) were needed anymore. A 5 times higher TMC concentration was, however, necessary to form a well cross-linked PA top layer. Since the IL protected TMC from hydrolysis by lowering the reactivity of dissolved water molecules,

residual TMC in the IL after top layer formation could, together with the IL itself, be recycled for consecutive interfacial polymerization cycles. This was a great advantage in terms of sustainability, since TMC/IL recycling caused the mass intensity of the top layer formation process to decrease with 64%. Moreover, a more complete recycling of the organic phase in the water/IL system compared to the water/hexane system, resulted in a 52% lower mass intensity.

Besides the preparation process, also the membrane performance was influenced positively by switching from hexane to $[C_4mim][Tf_2N]$. When no additives were applied in both systems, membranes prepared according to the water/IL system showed a 350% higher water permeance, combined with a 97% NaCl retention. The addition of SDS and TEA in the conventional system caused the water permeance to increase to a similar value to that of the water/IL system. However, conventional PA membranes are very prone to fouling, which is caused by a combination of surface roughness, charge and hydrophilicity. This can drastically lower their permeance during filtration. The application of an IL as organic reaction medium resulted in a significantly more smooth PA top layer, being considerably more resistant to organic and colloidal fouling.

IL/heptane system

Secondly, the aqueous phase was replaced by an IL, $[C_2mim][EtSO_4]$. Since interfacial polymerization performed with the MPD/IL phase as top phase resulted in the best performance, the top layer is assumed to be formed in the IL, as the most homogeneous top layer is formed when the reaction zone is located in the top phase. This was further supported by a transport test, indicating a more intense TMC transport from hexane to the IL phase than to the aqueous phase. Although membrane performance could be further enhanced by replacing hexane by less volatile heptane and by adding SDS to the IL phase, a membrane with both an acceptable water permeance and a high NaCl selectivity could not be obtained. The smooth top layer surface of these membranes, comparable to that of a membrane prepared via the water/IL system, indicates their potentially higher resistance to fouling. If their RO performance could be enhanced, it might thus be useful to test the fouling tendency of these membranes.

7.1.2 Post-synthesis solvent treatments

In the second part of this thesis, the effect of post-synthesis solvent treatments on membrane performance was studied. The starting point was the frequently used solvent activation of PA TFC membranes. This treatment causes the permeance of these membranes to increase drastically, although the mechanism is still unclear. First, an attempt was made to unravel the mechanism, in order to enable a more targeted optimization of the solvent activation of TFC membranes. Subsequently, the effect of a similar solvent treatment on ISA membranes was investigated.

Solvent activation of TFC membranes

First, different characterizations were performed to confirm the currently existing hypothesis of PA oligomer leaching from the top layer during solvent activation with DMF. H-NMR indeed proved the presence of these oligomers in the activating solvent solution, while their molecular weight could be estimated with GPC. The effect on the free volume element sizes in the top layer, determined with PLEPS, was, however, very small. In the next step, the functionality of the acyl chloride monomer used in top layer formation was varied in order to form a larger amount of leachable oligomers in the top layer, which would improve the effect of solvent activation. Unfortunately, this method proved to be unsuitable. Probably, the di- and monofunctional acyl chlorides were barely incorporated in the PA matrix due to their lower reactivity compared to the common trifunctional acyl chloride. An improvement of the solvent activation effect might be obtained by further lowering the triacyl/diacyl chloride or triacyl/monoacyl chloride ratio during interfacial polymerization, which would force the di- and monoacyl chloride to be incorporated in the top layer.

Solvent annealing of ISA membranes

Due to the drastic, positive effect of solvent activation on the permeance of PA TFC membranes, the influence of a similar solvent treatment on the performance of ISA PI membranes was investigated. The membrane was cross-linked chemically to enable the use of harsh organic solvents. Since these ISA, cross-linked PI membranes are totally composed of preformed high MW polymers, no oligomeric fragments can leach here during the treatment. Therefore, instead of an increase in permeance, a drastic decrease in permeance and improvement of the retention was observed after immersion in DMF, caused by densification of the membrane skin layer. The degree of densification was related to the polymer-solvent interactions, supporting the hypothesis of solvation, chain flexibilization and rearrangement during this solvent annealing step. Besides the possibility to establish more favorable interchain interactions, densification was also driven by extra cross-linking during immersion, due to a facilitated contact between the solvated, flexible polymer chains and partly unreacted cross-linker molecules.

After the fundamental investigation, solvent annealing was applied to transform cross-linked PI UF membranes into highly permeable SRNF membranes. By altering the synthesis parameters, a retention of MO (327 Da) equal to that of commercial Duramem 500 or 300 was obtained, while the EtOH permeance was 270 or 400% higher, respectively. This significant improvement in permeance compared to commercial ISA SRNF membranes shows the huge potential of this very simple treatment for the formation of high-performance SRNF membranes.

7.2 Future prospects and challenges

This thesis contributed to the improvement of membranes for both aqueous and organic solvent applications. In both fields, specific developments are still desired to further optimize membrane performance.

7.2.1 RO applications

Industrial TFC PA membranes for RO applications show a very high NaCl retention, often higher than 99.5%. However, uncharged components present in the feed, like urea, boron and N-nitrosodimethylamine, are often not retained adequately, which induces the need for extra purification steps on the permeate. Therefore, to allow the removal of both charged and uncharged components in a single step, an **improvement in retention of uncharged solutes** is desirable. As the retention of these components is mainly related to their hydrated size, a reduction in top layer free volume size could be beneficial. In this case, the solutes need to shed more water molecules from their hydration shell to pass the membrane, which is energetically unfavorable. This is, however, a very difficult task and might negatively influence the flux.

To further **improve the water permeance of TFC membranes,** either the membrane **synthesis conditions** can be altered or the **solvent post-treatment** procedure can be optimized:

Different **conditions in membrane synthesis** via interfacial polymerization can be modified. In this research, ILs confirmed to be a very useful solvent to obtain a top layer with reduced thickness and roughness. To implement this technology industrially, attention should be paid to IL toxicity and consumption. IL consumption should be minimized to lower the cost of the top layer preparation process via an effective upscaling of the IL recycling procedure. In terms of toxicity, water-immiscible ILs have a lower chance to pollute aqueous environments. However, they often have a higher compatibility with biological cell components, mainly when large alkyl chains are present. To prevent their uptake in organisms, this affinity can be further lowered, e.g. by introducing ester groups in the alkyl chains of the IL. It would be useful to test the applicability of these less toxic types of ILs as solvent in interfacial polymerization. Moreover, other, preferably green, solvents can be introduced as well. Besides being immiscible with water and non-reactive with the used monomers, they should, based on this research, combine a high viscosity and low interfacial tension with an adequate monomer solubility to obtain a high-flux, low-fouling membrane. A potential alternative water-immiscible solvent is styrene carbonate. On top of its green character, it might possess a lower interfacial tension with water compared to conventionally used hexane, since it combines an apolar aromatic ring with a more polar carbonate group. Besides the organic solvent in interfacial polymerization, other factors, like the homogeneity of the support surface porosity, also influence top layer thickness. It would be interesting to gain clear insights in all parameters influencing the thickness of the intrinsic

selective layer in order to alter it in a well-considered way. In addition to thickness, also the top layer free volume determines the permeance. The use of contorted monomers in interfacial polymerization to form a top layer with intrinsic microporosity was presented recently, and has a high potential to largely improve the solvent flux. It might, however, negatively influence the retention of uncharged components, as discussed earlier. Therefore, it would be interesting to investigate the possibilities of this type of membranes for RO applications.

After preparing the top layer, **post-treatment with an activating solvent** further improves the permeance. In this thesis, the mechanism behind this treatment was further elucidated. However, some ambiguities still remain, e.g. the discrepancy between the observed oligomer leaching and associated increase in permeance, and the absence of a significant free volume change in PLEPS. This might be clarified by developing a technique to determine the free volume of a water-impregnated top layer, as the drying process necessary for PLEPS analysis might affect the top layer free volume. Moreover, the incorporation of fluorescent monomers in the top layer during interfacial polymerization (e.g. diaminofluoresceins and sulforhodamine B acyl chloride) might enable the application of fluorescence microscopy to visualize changes in internal top layer morphology during and after solvent activation. Once the solvent activation mechanism and its effects on top layer morphology are fully clear, the technique can be further optimized. If oligomer leaching appears to be the determining factor for the improvement in permeance, the method presented in this thesis to increase the concentration of leachable oligomers in the top layer can be further developed.

The main drawback of current RO membranes is their decreasing performance over time, caused by their rather low **fouling and chlorine resistance**. The application of an IL as organic reaction phase in interfacial polymerization proved to be a very effective method to lower the surface roughness of the top layer and improve its fouling resistance. Nevertheless, the negative surface charge of PA top layers also contributes to the attachment of foulants, either directly or via ion bridging. The negative charge can be eliminated by capping the unreacted acyl chloride groups at the surface. The effect of this treatment on salt retention should, however, be studied, as a high salt retention is governed at least partly by Donnan exclusion. The chlorine resistance of TFC membranes can be improved by altering the molecular structure of the PA chains (e.g. via the application of secondary diamines in interfacial polymerization) or by switching to totally other polymer types. Recent work by our group showed the large potential of poly(epoxy ether) top layers for this purpose. However, a profound insight in the effects of chlorine incorporation on top layer chemistry and morphology is needed first, since ambiguities on this topic still exist in literature.

7.2.2 SRNF applications

Both ISA and TFC membranes are investigated for SRNF applications. Generally, the **screening of these membranes in a broad range of organic solvents** (e.g. in methanol, NMP,

acetonitrile, methyl ethyl ketone, toluene) would be very useful. Many types of solvents are applied in industrial synthesis processes, so it would be highly valuable for these industries to have an idea about membrane performances in these specific solvents. The performance of the same membrane can vary largely in different solvents, since a high affinity between solvent and membrane can cause swelling and loss of selectivity, while a very low affinity reduces solvent flux. Interactions of the solvent with the solutes in the feed can influence the degree of solvation of the solutes, and thus their solvated size and retention by the membrane.

To **improve the solvent permeance** of TFC SRNF membranes, the solvent activation technique and the application of contorted monomers in top layer formation can be further developed, as discussed for RO applications. TFC PA membranes generally suffer from a lower permeance for apolar organic solvents. To specifically improve the **apolar solvent permeance**, the hydrophobicity of the top layer can be increased by end-capping the unreacted acyl chlorides with apolar amines. This method was already proposed earlier and shows a high potential for this purpose. To further reduce top layer hydrophilicity and diminish its hydrogen bonding capacity, hydrophobic polymers can be blended in the top layer by adding them to the organic phase before interfacial polymerization. The hydrogen bonding capacity might also be lowered by applying other monomer systems in interfacial polymerization, e.g. to form polyesters, or polyamines and polyamides made from secondary amines. Although these chemistries already exist in interfacial polymerization, they are not yet intensively investigated for solvent resistant applications. Moreover, it would be interesting to study the benefits of applying ILs as organic reaction phase in these various interfacial polymerization systems.

Special attention should be paid to the **solvent annealing of ISA membranes**, presented in this thesis, as this very simple method resulted in membranes with a significantly improved solvent permeance compared to commercial ISA SRNF membranes. It would be useful to study the effect of the treatment on other cross-linked membrane types, and to investigate the use of other annealing solvents, being more environmentally friendly than DMF. Moreover, the performance of the resulting membranes should be analyzed in other organic solvents as feed solution. It is still unclear how the membrane would perform when tested with a feed solution containing e.g. DMF. If the effect of solvent annealing would be partly reversed in this case due to swelling during filtration, it might be useful to add cross-linker to the solvent during the annealing step. While initial cross-linking of the membrane during phase inversion causes it to be solvent resistant, which enables the use of highly solvating solvents, the addition of extra cross-linker to the annealing solvent is expected to result in a very effective further cross-linking, as the cross-linker can easily reach the flexible polymer chains during solvation. This very strong cross-linking might reduce the potential loss in selectivity caused by swelling of the membrane when solvents with a large affinity for the membrane are used during filtration.

Bibliography

[1] M. Mulder, *Basic Principles of Membrane Technology*, Kluwer Academic Publishers, Dordrecht, **1996**.

[2] R. W. Baker, in *Membr. Technol. Appl.*, John Wiley & Sons, Ltd, **2012**, pp. 1–14.

[3] S. Adler, E. Beaver, P. Bryan, S. Robinson, J. Watson, *Vision 2020: 2000 Separations Roadmap*, Center For Waste Reduction Technologies Of The AIChE And Dept. Of Energy Of The United States Of America, **2000**.

[4] H. Strathmann, *Introduction to Membrane Science and Technology*, Wiley, **2011**.

[5] H. Verweij, *Curr. Opin. Chem. Eng.* **2012**, *1*, 156–162.

[6] A. Dashti, M. Asghari, *ChemBioEng Rev.* **2015**, *2*, 54–70.

[7] C.J.M. van Rijn, Ed. , in *Membr. Sci. Technol.*, Elsevier, **2004**, pp. 1–23.

[8] Koros W. J., Ma Y. H., Shimidzu T., *Pure Appl. Chem.* **2009**, *68*, 1479.

[9] R. D. Noble, S. A. Stern, *Membrane Separations Technology: Principles and Applications*, Elsevier Science, **1995**.

[10] J. Wang, D. S. Dlamini, A. K. Mishra, M. T. M. Pendergast, M. C. Y. Wong, B. B. Mamba, V. Freger, A. R. D. Verliefde, E. M. V. Hoek, *J. Membr. Sci.* **2014**, *454*, 516–537.

[11] G. Amy, N. Ghaffour, Z. Li, L. Francis, R. V. Linares, T. Missimer, S. Lattemann, *50th Anniv. Desalination* **2017**, *401*, 16–21.

[12] T. Mezher, H. Fath, Z. Abbas, A. Khaled, *Desalination* **2011**, *266*, 263–273.

[13] P. Marchetti, M. F. Jimenez Solomon, G. Szekely, A. G. Livingston, *Chem. Rev.* **2014**, *114*, 10735–10806.

[14] P. Vandezande, L. E. M. Gevers, I. F. J. Vankelecom, *Chem. Soc. Rev.* **2008**, *37*, 365–405.

[15] G. Szekely, M. F. Jimenez-Solomon, P. Marchetti, J. F. Kim, A. G. Livingston, *Green Chem.* **2014**, *16*, 4440–4473.

[16] Synder Filtration, **2017**, http://synderfiltration.com/.

[17] J. R. Werber, C. O. Osuji, M. Elimelech, *Nat. Rev. Mater.* **2016**, *1*, 16018.

[18] A. W. Mohammad, Y. H. Teow, W. L. Ang, Y. T. Chung, D. L. Oatley-Radcliffe, N. Hilal, *Desalination* **2015**, *356*, 226–254.

[19] A. K. Hołda, I. F. J. Vankelecom, *J. Appl. Polym. Sci.* **2015**, *132*, 42130.

[20] S. Loeb, S. Sourirajan, in *Saline Water Conversion—II*, American Chemical Society, **1963**, pp. 117–132.

[21] A. I. Schäfer, A. G. Fane, T. D. Waite, *Nanofiltration: Principles and Applications*, Elsevier Advanced Technology, **2005**.

[22] H. Strathmann, K. Kock, *Desalination* **1977**, *21*, 241–255.

[23] G. R. Guillen, Y. Pan, M. Li, E. M. V. Hoek, *Ind. Eng. Chem. Res.* **2011**, *50*, 3798–3817.

[24] S. P. Nunes, K.-V. Peinemann, in *Membr. Technol.*, Wiley-VCH Verlag GmbH, **2001**, pp. 6–11.

[25] C. A. Smolders, A. J. Reuvers, R. M. Boom, I. M. Wienk, *J. Membr. Sci.* **1992**, *73*, 259–275.

[26] A. K. Hołda, B. Aernouts, W. Saeys, I. F. J. Vankelecom, *J. Membr. Sci.* **2013**, *442*, 196–205.

[27] A. K. Hołda, M. De Roeck, K. Hendrix, I. F. J. Vankelecom, *J. Membr. Sci.* **2013**, *446*, 113–120.

[28] K. Boussu, C. Vandecasteele, B. Van der Bruggen, *Polymer* **2006**, *47*, 3464–3476.

[29] Y. H. See-Toh, F. C. Ferreira, A. G. Livingston, *J. Membr. Sci.* **2007**, *299*, 236–250.

[30] P. Vandezande, X. Li, L. E. M. Gevers, I. F. J. Vankelecom, *J. Membr. Sci.* **2009**, *330*, 307–318.
[31] I.-C. Kim, H.-G. Yoon, K.-H. Lee, *J. Appl. Polym. Sci.* **2002**, *84*, 1300–1307.
[32] K. Hendrix, G. Koeckelberghs, I. F. J. Vankelecom, *J. Membr. Sci.* **2014**, *452*, 241–252.
[33] J. Huang, K. Zhang, *Curr. Dev. Wastewater Treat. India* **2011**, *282*, 19–26.
[34] I. Soroko, A. Livingston, *J. Membr. Sci.* **2009**, *343*, 189–198.
[35] K. Vanherck, S. Hermans, T. Verbiest, I. Vankelecom, *J. Mater. Chem.* **2011**, *21*, 6079–6087.
[36] Y. Li, T. Verbiest, I. Vankelecom, *J. Membr. Sci.* **2013**, *428*, 63–69.
[37] A. K. Hołda, I. F. J. Vankelecom, *J. Membr. Sci.* **2014**, *450*, 499–511.
[38] A. K. Hołda, I. F. J. Vankelecom, *J. Membr. Sci.* **2014**, *450*, 512–521.
[39] I.-C. Kim, K.-H. Lee, T.-M. Tak, *J. Membr. Sci.* **2001**, *183*, 235–247.
[40] S. R. Panda, S. De, *Desalination* **2014**, *347*, 52–65.
[41] I.-C. Kim, K.-H. Lee, *J. Membr. Sci.* **2004**, *230*, 183–188.
[42] I. Soroko, M. Makowski, F. Spill, A. Livingston, *J. Membr. Sci.* **2011**, *381*, 163–171.
[43] N. A. Mohamed, A. O. H. Al-Dossary, *Eur. Polym. J.* **2003**, *39*, 1653–1667.
[44] A. P. Duarte, J. C. Bordado, M. T. Cidade, *J. Appl. Polym. Sci.* **2007**, *103*, 134–139.
[45] W. Macdonald, C. Pan, *Method for Drying Water-Wet Membranes*, **1974**, US 3842515 A.
[46] J. da Silva Burgal, L. Peeva, P. Marchetti, A. Livingston, *J. Membr. Sci.* **2015**, *493*, 524–538.
[47] L. E. M. Gevers, S. Aldea, I. F. J. Vankelecom, P. A. Jacobs, *J. Membr. Sci.* **2006**, *281*, 741–746.
[48] M. Sairam, X. X. Loh, Y. Bhole, I. Sereewatthanawut, K. Li, A. Bismarck, J. H. G. Steinke, A. G. Livingston, *J. Membr. Sci.* **2010**, *349*, 123–129.
[49] Y. H. See Toh, F. W. Lim, A. G. Livingston, *J. Membr. Sci.* **2007**, *301*, 3–10.
[50] I. Struzynska-Piron, J. Loccufier, L. Vanmaele, I. F. J. Vankelecom, *Chem. Commun.* **2013**, *49*, 11494–11496.
[51] V. Altun, M. Bielmann, I. F. J. Vankelecom, *RSC Adv.* **2016**, *6*, 55526–55533.
[52] K. Vanherck, G. Koeckelberghs, I. F. J. Vankelecom, *Prog. Polym. Sci.* **2013**, *38*, 874–896.
[53] L. Shao, L. Liu, S.-X. Cheng, Y.-D. Huang, J. Ma, *J. Membr. Sci.* **2008**, *312*, 174–185.
[54] X. Qiao, T.-S. Chung, *AIChE J.* **2006**, *52*, 3462–3472.
[55] P. S. Tin, T. S. Chung, Y. Liu, R. Wang, S. L. Liu, K. P. Pramoda, *J. Membr. Sci.* **2003**, *225*, 77–90.
[56] K. Vanherck, P. Vandezande, S. O. Aldea, I. F. J. Vankelecom, *J. Membr. Sci.* **2008**, *320*, 468–476.
[57] M. F. Jimenez Solomon, Y. Bhole, A. G. Livingston, *J. Membr. Sci.* **2012**, *423–424*, 371–382.
[58] K. Vanherck, A. Cano-Odena, G. Koeckelberghs, T. Dedroog, I. Vankelecom, *J. Membr. Sci.* **2010**, *353*, 135–143.
[59] K. Hendrix, K. Vanherck, I. F. J. Vankelecom, *J. Membr. Sci.* **2012**, *421–422*, 15–24.
[60] M. Paul, S. D. Jons, *Polymer* **2016**, *103*, 417–456.
[61] J. E. Cadotte, *Interfacially Synthesized Reverse Osmosis Membrane*, **1981**, US 4 277 344 A.
[62] S. Hermans, H. Mariën, C. Van Goethem, I. F. Vankelecom, *Curr. Opin. Chem. Eng.* **2015**, *8*, 45–54.

[63] S. Yu, M. Liu, X. Liu, C. Gao, *J. Membr. Sci.* **2009**, *342*, 313–320.
[64] L.-F. Liu, S.-C. Yu, L.-G. Wu, C.-J. Gao, *J. Membr. Sci.* **2006**, *283*, 133–146.
[65] B. Tang, Z. Huo, P. Wu, *J. Membr. Sci.* **2008**, *320*, 198–205.
[66] B. Tang, C. Zou, P. Wu, *J. Membr. Sci.* **2010**, *365*, 276–285.
[67] Y. Zhang, Y. Su, J. Peng, X. Zhao, J. Liu, J. Zhao, Z. Jiang, *J. Membr. Sci.* **2013**, *429*, 235–242.
[68] C. Zhou, Y. Shi, C. Sun, S. Yu, M. Liu, C. Gao, *J. Membr. Sci.* **2014**, *471*, 381–391.
[69] L. Pérez-Manríquez, P. Neelakanda, K.-V. Peinemann, *J. Membr. Sci.* **2017**, DOI 10.1016/j.memsci.2017.06.078.
[70] K. P. Lee, J. Zheng, G. Bargeman, A. J. B. Kemperman, N. E. Benes, *J. Membr. Sci.* **2015**, *478*, 75–84.
[71] M. Liu, G. Yao, Q. Cheng, M. Ma, S. Yu, C. Gao, *J. Membr. Sci.* **2012**, *415–416*, 122–131.
[72] S. Hermans, H. Mariën, E. Dom, R. Bernstein, I. F. J. Vankelecom, *J. Membr. Sci.* **2014**, *451*, 148–156.
[73] S. Hermans, E. Dom, H. Mariën, G. Koeckelberghs, I. F. J. Vankelecom, *J. Membr. Sci.* **2015**, *476*, 356–363.
[74] R. J. Petersen, *J. Membr. Sci.* **1993**, *83*, 81–150.
[75] J. da Silva Burgal, L. G. Peeva, S. Kumbharkar, A. Livingston, *J. Membr. Sci.* **2015**, *479*, 105–116.
[76] A. K. Ghosh, E. M. V. Hoek, *J. Membr. Sci.* **2009**, *336*, 140–148.
[77] S.-J. Park, W. Choi, S.-E. Nam, S. Hong, J. S. Lee, J.-H. Lee, *J. Membr. Sci.* **2017**, *526*, 52–59.
[78] S. Karan, Z. Jiang, A. G. Livingston, *Science* **2015**, *348*, 1347–1351.
[79] M. F. Jimenez-Solomon, P. Gorgojo, M. Munoz-Ibanez, A. G. Livingston, *J. Membr. Sci.* **2013**, *448*, 102–113.
[80] N. K. Saha, S. V. Joshi, *J. Membr. Sci.* **2009**, *342*, 60–69.
[81] Y. Song, P. Sun, L. L. Henry, B. Sun, *J. Membr. Sci.* **2005**, *251*, 67–79.
[82] I. J. Roh, S. Y. Park, J. J. Kim, C. K. Kim, *J. Polym. Sci. Part B Polym. Phys.* **1998**, *36*, 1821–1830.
[83] G. Chen, S. Li, X. Zhang, S. Zhang, *J. Membr. Sci.* **2008**, *310*, 102–109.
[84] H. Wang, L. Li, X. Zhang, S. Zhang, *J. Membr. Sci.* **2010**, *353*, 78–84.
[85] S. Yu, M. Ma, J. Liu, J. Tao, M. Liu, C. Gao, *J. Membr. Sci.* **2011**, *379*, 164–173.
[86] M. Liu, Y. Zheng, S. Shuai, Q. Zhou, S. Yu, C. Gao, *Desalination* **2012**, *288*, 98–107.
[87] Q.-F. An, W.-D. Sun, Q. Zhao, Y.-L. Ji, C.-J. Gao, *J. Membr. Sci.* **2013**, *431*, 171–179.
[88] H. Wang, Q. Zhang, S. Zhang, *Membr. Sustain. Future Sect.* **2011**, *378*, 243–249.
[89] S. Yu, M. Liu, Z. Lü, Y. Zhou, C. Gao, *J. Membr. Sci.* **2009**, *344*, 155–164.
[90] M. F. Jimenez-Solomon, Q. Song, K. E. Jelfs, M. Munoz-Ibanez, A. G. Livingston, *Nat Mater* **2016**, *15*, 760–767.
[91] Y. Li, Y. Su, X. Zhao, R. Zhang, J. Zhao, X. Fan, Z. Jiang, *J. Membr. Sci.* **2014**, *455*, 15–23.
[92] X. Li, Y. Cao, G. Kang, H. Yu, X. Jie, Q. Yuan, *J. Appl. Polym. Sci.* **2014**, *131*, 41144.
[93] B. Van der Bruggen, *Eur. Polym. J.* **2009**, *45*, 1873–1882.
[94] A. A. Abuhabib, A. W. Mohammad, N. Hilal, R. A. Rahman, A. H. Shafie, *Desalination* **2012**, *295*, 16–25.
[95] T. Ma, Y. Su, Y. Li, R. Zhang, Y. Liu, M. He, Y. Li, N. Dong, H. Wu, Z. Jiang, *J. Membr. Sci.* **2016**, *503*, 101–109.
[96] X. Li, Y. Cao, H. Yu, G. Kang, X. Jie, Z. Liu, Q. Yuan, *J. Membr. Sci.* **2014**, *466*, 82–91.

[97] J. Xu, Z. Wang, X. Wei, S. Yang, J. Wang, S. Wang, *Desalination* **2013**, *313*, 145–155.
[98] T. Shintani, H. Matsuyama, N. Kurata, *Desalination* **2009**, *247*, 370–377.
[99] T. Shintani, H. Matsuyama, N. Kurata, *Desalination* **2007**, *207*, 340–348.
[100] Y.-J. Tang, Z.-L. Xu, S.-M. Xue, Y.-M. Wei, H. Yang, *J. Membr. Sci.* **2016**, *498*, 374–384.
[101] S. Konagaya, O. Watanabe, *J. Appl. Polym. Sci.* **2000**, *76*, 201–207.
[102] F. Yuan, Z. Wang, X. Yu, Z. Wei, S. Li, J. Wang, S. Wang, *J. Phys. Chem. C* **2012**, *116*, 11496–11506.
[103] T. D. Matthews, H. Yan, D. G. Cahill, O. Coronell, B. J. Mariñas, *J. Membr. Sci.* **2013**, *429*, 71–80.
[104] A. K. Ghosh, B.-H. Jeong, X. Huang, E. M. V. Hoek, *J. Membr. Sci.* **2008**, *311*, 34–45.
[105] J. Jegal, S. G. Min, K.-H. Lee, *J. Appl. Polym. Sci.* **2002**, *86*, 2781–2787.
[106] I.-C. Kim, J. Jegal, K.-H. Lee, *J. Polym. Sci. Part B Polym. Phys.* **2002**, *40*, 2151–2163.
[107] B. Khorshidi, T. Thundat, B. A. Fleck, M. Sadrzadeh, *Sci. Rep.* **2016**, *6*, 22069.
[108] P. W. Morgan, S. L. Kwolek, *J. Polym. Sci. Part Polym. Chem.* **1996**, *34*, 531–559.
[109] W. J. Lau, A. F. Ismail, N. Misdan, M. A. Kassim, *Desalination* **2012**, *287*, 190–199.
[110] S. Hermans, R. Bernstein, A. Volodin, I. F. J. Vankelecom, *React. Funct. Polym.* **2015**, *86*, 199–208.
[111] S. Qiu, L. Wu, L. Zhang, H. Chen, C. Gao, *J. Appl. Polym. Sci.* **2009**, *112*, 2066–2072.
[112] S. H. Kim, S.-Y. Kwak, T. Suzuki, *Environ. Sci. Technol.* **2005**, *39*, 1764–1770.
[113] M. Duan, Z. Wang, J. Xu, J. Wang, S. Wang, *Sep. Purif. Technol.* **2010**, *75*, 145–155.
[114] C. Kong, M. Kanezashi, T. Yamomoto, T. Shintani, T. Tsuru, *J. Membr. Sci.* **2010**, *362*, 76–80.
[115] C. Kong, T. Shintani, T. Kamada, V. Freger, T. Tsuru, *J. Membr. Sci.* **2011**, *384*, 10–16.
[116] T. Kamada, T. Ohara, T. Shintani, T. Tsuru, *J. Membr. Sci.* **2014**, *453*, 489–497.
[117] T. Kamada, T. Ohara, T. Shintani, T. Tsuru, *J. Membr. Sci.* **2014**, *467*, 303–312.
[118] A. S. AL-Hobaib, M. S. Alsuhybani, K. M. AL-Sheetan, M. R. Shaik, *Desalination Water Treat.* **2016**, *57*, 16733–16744.
[119] A. Kulkarni, D. Mukherjee, W. N. Gill, *J. Membr. Sci.* **1996**, *114*, 39–50.
[120] D. Mukherjee, A. Kulkarni, W. N. Gill, *Desalination* **1996**, *104*, 239–249.
[121] M. F. Jimenez Solomon, Y. Bhole, A. G. Livingston, *J. Membr. Sci.* **2013**, *434*, 193–203.
[122] I.-C. Kim, K.-H. Lee, *Ind. Eng. Chem. Res.* **2002**, *41*, 5523–5528.
[123] D. M. Koenhen, A. H. A. Tinnemans, *Semi-Permeable Composite Membrane and Process for Manufacturing Same*, **1991**, US5207908 A.
[124] G. Y. Chai, W. B. Krantz, *J. Membr. Sci.* **1994**, *93*, 175–192.
[125] Y. Zhang, N. E. Benes, R. G. H. Lammertink, *Lab. Chip* **2015**, *15*, 575–580.
[126] V. Freger, *Langmuir* **2005**, *21*, 1884–1894.
[127] R. Nadler, S. Srebnik, *J. Membr. Sci.* **2008**, *315*, 100–105.
[128] R. Oizerovich-Honig, V. Raim, S. Srebnik, *Langmuir* **2010**, *26*, 299–306.
[129] V. Freger, *Langmuir* **2003**, *19*, 4791–4797.
[130] F. A. Pacheco, I. Pinnau, M. Reinhard, J. O. Leckie, *J. Membr. Sci.* **2010**, *358*, 51–59.
[131] T. Fujioka, N. Oshima, R. Suzuki, W. E. Price, L. D. Nghiem, *J. Membr. Sci.* **2015**, *486*, 106–118.
[132] M. Henmi, Y. Fusaoka, H. Tomioka, M. Kurihara, *Water Sci. Technol.* **2010**, *62*, 2134.
[133] Z. Chen, K. Ito, H. Yanagishita, N. Oshima, R. Suzuki, Y. Kobayashi, *J. Phys. Chem. C* **2011**, *115*, 18055–18060.
[134] F. Pacheco, R. Sougrat, M. Reinhard, J. O. Leckie, I. Pinnau, *J. Membr. Sci.* **2016**, *501*, 33–44.

[135] P. Walden, *Bull. Académie Impériale Sci. St-Pétersbourg VI Sér.* **1914**, *8*, 405–422.
[136] D. D. Patel, J.-M. Lee, *Chem. Rec.* **2012**, *12*, 329–355.
[137] V. Fábos, D. Lantos, A. Bodor, A.-M. Bálint, L. T. Mika, O. E. Sielcken, A. Cuiper, I. T. Horváth, *ChemSusChem* **2008**, *1*, 189–192.
[138] S. Keskin, D. Kayrak-Talay, U. Akman, Ö. Hortaçsu, *J. Supercrit. Fluids* **2007**, *43*, 150–180.
[139] B. Clare, A. Sirwardana, D. R. MacFarlane, in *Ion. Liq.* (Ed.: B. Kirchner), Springer Berlin Heidelberg, Berlin, Heidelberg, **2010**, pp. 1–40.
[140] T. Zhou, L. Chen, Y. Ye, L. Chen, Z. Qi, H. Freund, K. Sundmacher, *Ind. Eng. Chem. Res.* **2012**, *51*, 6256–6264.
[141] R. Alcalde, G. García, M. Atilhan, S. Aparicio, *Ind. Eng. Chem. Res.* **2015**, *54*, 10918–10924.
[142] P. Kubisa, *Prog. Polym. Sci.* **2009**, *34*, 1333–1347.
[143] J. Ranke, S. Stolte, R. Störmann, J. Arning, B. Jastorff, *Chem. Rev.* **2007**, *107*, 2183–2206.
[144] D. Zhao, Y. Liao, Z. Zhang, *CLEAN – Soil Air Water* **2007**, *35*, 42–48.
[145] A. Mohammad, *Green Solvents II: Properties and Applications of Ionic Liquids*, Springer Netherlands, **2012**.
[146] T. Vander Hoogerstraete, S. Jamar, S. Wellens, K. Binnemans, *Anal. Chem.* **2014**, *86*, 3931–3938.
[147] E. I. Lozinskaya, A. S. Shaplov, Y. S. Vygodskii, *Eur. Polym. J.* **2004**, *40*, 2065–2075.
[148] M. Yoneyama, Y. Matsui, *High Perform. Polym.* **2006**, *18*, 817–823.
[149] S. Harrisson, S. R. Mackenzie, D. M. Haddleton, *Macromolecules* **2003**, *36*, 5072–5075.
[150] I. Woecht, G. Schmidt-Naake, S. Beuermann, M. Buback, N. García, *J. Polym. Sci. Part Polym. Chem.* **2008**, *46*, 1460–1469.
[151] A. Jeličić, S. Beuermann, N. García, *Macromolecules* **2009**, *42*, 5062–5072.
[152] L. Zhu, Applications of Room Temperature Ionic Liquids in Interfacial Polymerization, Ph.D., New Jersey Institute of Technology, **2006**.
[153] H. Gao, T. Jiang, B. Han, Y. Wang, J. Du, Z. Liu, J. Zhang, *Polymer* **2004**, *45*, 3017–3019.
[154] D. Y. Xing, N. Peng, T.-S. Chung, *Ind. Eng. Chem. Res.* **2010**, *49*, 8761–8769.
[155] D. Y. Xing, N. Peng, T.-S. Chung, *J. Membr. Sci.* **2011**, *380*, 87–97.
[156] D. Y. Xing, S. Y. Chan, T.-S. Chung, *Green Chem.* **2014**, *16*, 1383–1392.
[157] X.-L. Li, L.-P. Zhu, B.-K. Zhu, Y.-Y. Xu, *Sep. Purif. Technol.* **2011**, *83*, 66–73.
[158] S. Livazovic, Z. Li, A. R. Behzad, K.-V. Peinemann, S. P. Nunes, *J. Membr. Sci.* **2015**, *490*, 282–293.
[159] L. Yung, H. Ma, X. Wang, K. Yoon, R. Wang, B. S. Hsiao, B. Chu, *J. Membr. Sci.* **2010**, *365*, 52–58.
[160] L. K. Wang, J. P. Chen, Y. T. Hung, N. K. Shammas, *Membrane and Desalination Technologies*, Springer, New York, **2010**.
[161] K. P. Lee, T. C. Arnot, D. Mattia, *J. Membr. Sci.* **2011**, *370*, 1–22.
[162] D. Cohen-Tanugi, R. K. McGovern, S. H. Dave, J. H. Lienhard, J. C. Grossman, *Energy Environ. Sci.* **2014**, *7*, 1134–1141.
[163] C. Hobbs, J. Taylor, S. Hong, *J. Water Supply Res. Technol. - Aqua* **2006**, *55*, 559–570.
[164] M. Elimelech, Xiaohua Zhu, A. E. Childress, Seungkwan Hong, *J. Membr. Sci.* **1997**, *127*, 101–109.
[165] E. M. Vrijenhoek, S. Hong, M. Elimelech, *J. Membr. Sci.* **2001**, *188*, 115–128.

[166] E. Garcia-Verdugo, B. Altava, M. I. Burguete, P. Lozano, S. V. Luis, *Green Chem.* **2015**, *17*, 2693–2713.
[167] P. Lozano, J. M. Bernal, S. Nieto, C. Gomez, E. Garcia-Verdugo, S. V. Luis, *Chem. Commun.* **2015**, *51*, 17361–17374.
[168] C. Yuan, J. Guo, Z. Si, F. Yan, *Polym. Chem.* **2015**, *6*, 4059–4066.
[169] L. C. Tomé, D. Mecerreyes, C. S. R. Freire, L. P. N. Rebelo, I. M. Marrucho, *J. Membr. Sci.* **2013**, *428*, 260–266.
[170] S. Raeissi, L. J. Florusse, C. J. Peters, *AIChE J.* **2013**, *59*, 3886–3891.
[171] D. R. MacFarlane, N. Tachikawa, M. Forsyth, J. M. Pringle, P. C. Howlett, G. D. Elliott, J. H. Davis, M. Watanabe, P. Simon, C. A. Angell, *Energy Environ. Sci.* **2014**, *7*, 232–250.
[172] I.-C. Kim, J. Jegal, K.-H. Lee, *J. Polym. Sci. Part B Polym. Phys.* **2002**, *40*, 2151–2163.
[173] R. L. Gardas, R. Ge, N. Ab Manan, D. W. Rooney, C. Hardacre, *Ion. Liq. Spec. Issue* **2010**, *294*, 139–147.
[174] Y. Mansourpanah, S. S. Madaeni, A. Rahimpour, *J. Membr. Sci.* **2009**, *343*, 219–228.
[175] Y. Mansourpanah, K. Alizadeh, S. S. Madaeni, A. Rahimpour, H. Soltani Afarani, *Desalination* **2011**, *271*, 169–177.
[176] C. Klaysom, S. Hermans, A. Gahlaut, S. Van Craenenbroeck, I. F. J. Vankelecom, *J. Membr. Sci.* **2013**, *445*, 25–33.
[177] P. Vandezande, L. E. M. Gevers, J. S. Paul, I. F. J. Vankelecom, P. A. Jacobs, *J. Membr. Sci.* **2005**, *250*, 305–310.
[178] I. Horcas, R. Fernández, J. M. Gómez-Rodríguez, J. Colchero, J. Gómez-Herrero, A. M. Baro, *Rev. Sci. Instrum.* **2007**, *78*.
[179] S. J. Tao, *J. Chem. Phys.* **1972**, *56*, 5499–5510.
[180] M. Eldrup, D. Lightbody, J. N. Sherwood, *Chem. Phys.* **1981**, *63*, 51–58.
[181] A. Bergmaier, G. Dollinger, C. M. Frey, *Ion Beam Anal.* **1998**, *136*, 638–643.
[182] M. G. Freire, P. J. Carvalho, R. L. Gardas, I. M. Marrucho, L. M. N. B. F. Santos, J. A. P. Coutinho, *J. Phys. Chem. B* **2008**, *112*, 1604–1610.
[183] Fisher Scientific, **MSDS hexane**.
[184] S. Zeppieri, J. Rodríguez, A. L. López de Ramos, *J. Chem. Eng. Data* **2001**, *46*, 1086–1088.
[185] M. Tariq, P. J. Carvalho, J. A. P. Coutinho, I. M. Marrucho, J. N. C. Lopes, L. P. N. Rebelo, *Fluid Phase Equilibria* **2011**, *301*, 22–32.
[186] M. Tariq, A. P. Serro, J. L. Mata, B. Saramago, J. M. S. S. Esperança, J. N. Canongia Lopes, L. P. N. Rebelo, *Ion. Liq. Spec. Issue* **2010**, *294*, 131–138.
[187] M. A. Vorotyntsev, V. A. Zinovyeva, M. Picquet, *Electrochimica Acta* **2010**, *55*, 5063–5070.
[188] S. C. Ayirala, D. N. Rao, *Fluid Phase Equilibria* **2006**, *249*, 82–91.
[189] A. Chaumont, R. Schurhammer, G. Wipff, *J. Phys. Chem. B* **2005**, *109*, 18964–18973.
[190] J. Bowers, M. C. Vergara-Gutierrez, J. R. P. Webster, *Langmuir* **2003**, *20*, 309–312.
[191] J. N. A. Canongia Lopes, A. A. H. Pádua, *J. Phys. Chem. B* **2006**, *110*, 3330–3335.
[192] C. Hansch, A. Leo, D. H. Hoekman, *Exploring QSAR.: Hydrophobic, Electronic, and Steric Constants*, American Chemical Society, **1995**.
[193] E. M. V. Hoek, S. Bhattacharjee, M. Elimelech, *Langmuir* **2003**, *19*, 4836–4847.
[194] Y. Zhao, J. Taylor, S. Hong, *Water Res.* **2005**, *39*, 1233–1244.
[195] K. Boussu, A. Belpaire, A. Volodin, C. Van Haesendonck, P. Van der Meeren, C. Vandecasteele, B. Van der Bruggen, *J. Membr. Sci.* **2007**, *289*, 220–230.

[196] H. Jin, B. O'Hare, J. Dong, S. Arzhantsev, G. A. Baker, J. F. Wishart, A. J. Benesi, M. Maroncelli, *J. Phys. Chem. B* **2008**, *112*, 81–92.
[197] R. Y. Ning, *Desalination Water Treat.* **2010**, *21*, 79–86.
[198] A. Tiraferri, Y. Kang, E. P. Giannelis, M. Elimelech, *Environ. Sci. Technol.* **2012**, *46*, 11135–11144.
[199] E.-S. Kim, Q. Yu, B. Deng, *Appl. Surf. Sci.* **2011**, *257*, 9863–9871.
[200] C. S. Ong, P. S. Goh, W. J. Lau, N. Misdan, A. F. Ismail, *Fouling Scaling Desalination* **2016**, *393*, 2–15.
[201] J. Nikkola, X. Liu, Y. Li, M. Raulio, H.-L. Alakomi, J. Wei, C. Y. Tang, *J. Membr. Sci.* **2013**, *444*, 192–200.
[202] G. Mustafa, K. Wyns, P. Vandezande, A. Buekenhoudt, V. Meynen, *J. Membr. Sci.* **2014**, *470*, 369–377.
[203] H. Mariën, L. Bellings, S. Hermans, I. F. J. Vankelecom, *ChemSusChem* **2016**, *9*, 1101–1111.
[204] C. Jimenez-Gonzalez, D. J. C. Constable, C. S. Ponder, *Chem. Soc. Rev.* **2012**, *41*, 1485–1498.
[205] J. P. Hallett, T. Welton, *Chem. Rev.* **2011**, *111*, 3508–3576.
[206] E. Amigues, C. Hardacre, G. Keane, M. Migaud, M. O'Neill, *Chem. Commun.* **2006**, 72–74.
[207] M. G. Freire, P. J. Carvalho, A. M. Fernandes, I. M. Marrucho, A. J. Queimada, J. A. P. Coutinho, *J. Colloid Interface Sci.* **2007**, *314*, 621–630.
[208] V. L. Martins, B. G. Nicolau, S. M. Urahata, M. C. C. Ribeiro, R. M. Torresi, *J. Phys. Chem. B* **2013**, *117*, 8782–8792.
[209] M. A. Kuehne, R. Q. Song, N. N. Li, R. J. Petersen, *Environ. Prog.* **2001**, *20*, 23–26.
[210] Surface tension values of some common test liquids for surface energy analysis, **2006**, http://www.surface-tension.de/.
[211] LookChem, **2008**, http://www.lookchem.com/.
[212] S. Katsuta, Y. Watanabe, Y. Araki, Y. Kudo, *ACS Sustain. Chem. Eng.* **2016**, *4*, 564–571.
[213] I. G. Wenten, Khoiruddin, *Adv. Membr. Keynotes MEMDES 2-Singap.* **2016**, *391*, 112–125.
[214] Parker, *General Comparison of Reverse Osmosis to Vapor Compression Distillers*, Parker Hannifin Corporation, **2012**.
[215] T. Uemura, M. Henmi, in *Adv. Membr. Technol. Appl.*, John Wiley & Sons, Inc., **2008**, pp. 1–19.
[216] M. Herzberg, M. Elimelech, *J. Membr. Sci.* **2007**, *295*, 11–20.
[217] Q. Li, M. Elimelech, *Environ. Sci. Technol.* **2004**, *38*, 4683–4693.
[218] S.-H. Yoon, C.-H. Lee, K.-J. Kim, A. G. Fane, *Water Res.* **1998**, *32*, 2180–2186.
[219] J. Ross, J. Xiao, *Green Chem.* **2002**, *4*, 129–133.
[220] M. C. Uzagare, Y. S. Sanghvi, M. M. Salunkhe, *Green Chem.* **2003**, *5*, 370–372.
[221] H. Schmidt, M. Stephan, J. Safarov, I. Kul, J. Nocke, I. M. Abdulagatov, E. Hassel, *J. Chem. Thermodyn.* **2012**, *47*, 68–75.
[222] S. Mallakpour, M. Dinari, *Iran. Polym. J.* **2010**, *19*.
[223] H. Rodríguez, J. F. Brennecke, *J. Chem. Eng. Data* **2006**, *51*, 2145–2155.
[224] M. M. Pendergast, E. M. V. Hoek, *Energy Environ. Sci.* **2011**, *4*, 1946–1971.
[225] P. Gorgojo, M. F. Jimenez-Solomon, A. G. Livingston, *Desalination* **2014**, *344*, 181–188.

[226] C. M. Hansen, *Hansen Solubility Parameters: A User's Handbook, Second Edition*, CRC Press, **2007**.
[227] S. M. Aharoni, *J. Appl. Polym. Sci.* **1992**, *45*, 813–817.
[228] K. Hendrix, M. Van Eynde, G. Koeckelberghs, I. F. J. Vankelecom, *J. Membr. Sci.* **2013**, *447*, 212–221.
[229] I. B. Valtcheva, S. C. Kumbharkar, J. F. Kim, Y. Bhole, A. G. Livingston, *J. Membr. Sci.* **2014**, *457*, 62–72.
[230] J. Aburabie, P. Neelakanda, M. Karunakaran, K.-V. Peinemann, *React. Funct. Polym.* **2015**, *86*, 225–232.
[231] L. Pérez-Manríquez, J. Aburabie, P. Neelakanda, K.-V. Peinemann, *React. Funct. Polym.* **2015**, *86*, 243–247.
[232] I.-C. Kim, H.-G. Yun, K.-H. Lee, *J. Membr. Sci.* **2002**, *199*, 75–84.
[233] A. Cano-Odena, M. Spilliers, T. Dedroog, K. De Grave, J. Ramon, I. F. J. Vankelecom, *J. Membr. Sci.* **2011**, *366*, 25–32.
[234] S. Basu, A. L. Khan, A. Cano-Odena, C. Liu, I. F. J. Vankelecom, *Chem. Soc. Rev.* **2010**, *39*, 750–768.
[235] J. J. Krol, M. Boerrigter, G. H. Koops, *J. Membr. Sci.* **2001**, *184*, 275–286.
[236] J. da Silva Burgal, L. Peeva, A. Livingston, *J. Membr. Sci.* **2017**, *525*, 48–56.
[237] N. Winterton, *J. Mater. Chem.* **2006**, *16*, 4281–4293.
[238] K.-S. Liao, H. Chen, S. Awad, J.-P. Yuan, W.-S. Hung, K.-R. Lee, J.-Y. Lai, C.-C. Hu, Y. C. Jean, *Macromolecules* **2011**, *44*, 6818–6826.

Appendices

Appendix A

Supporting information for Chapter 2

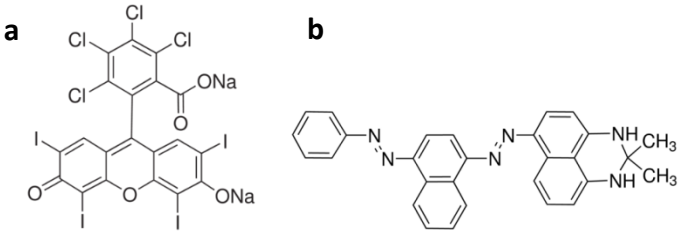

Figure S2.1: Chemical structure of (a) Rose Bengal and (b) Sudan Black B.

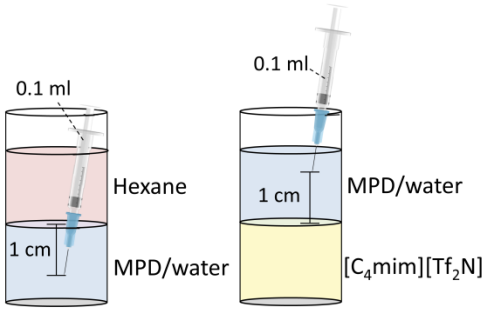

Figure S2.2: Experimental setup of the mass transfer tests.

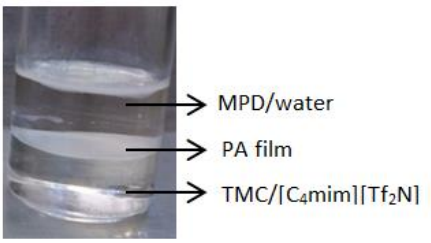

Figure S2.3: Representation of the preliminary film formation tests, in which a solution of MPD in water is brought into contact with a solution of TMC in [C_4mim][Tf_2N], followed by a visual determination of PA formation.

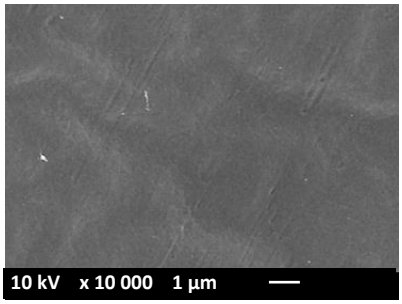

Figure S2.4: SEM image of the surface of a PSf support.

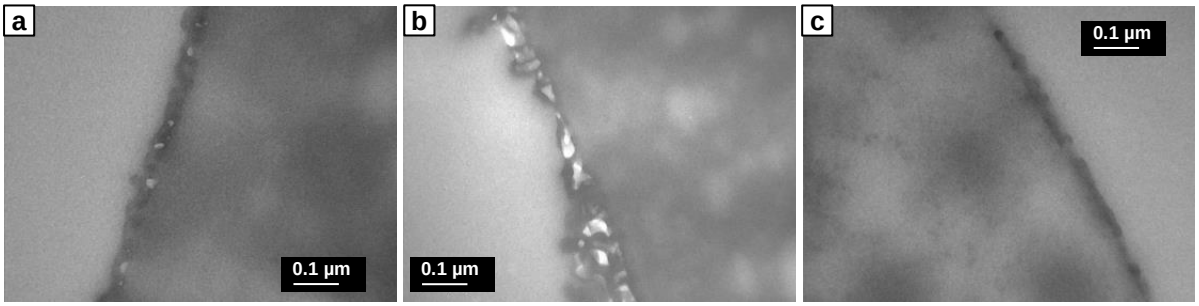

Figure S2.5: Cross-section TEM images of the top layer of TFC membranes synthesized (a) according to the conventional system on a PSf support without additives, (b) according to the conventional system on a PSf support with SDS and TEA and (c) according to the water/IL system on a PSf support without additives.

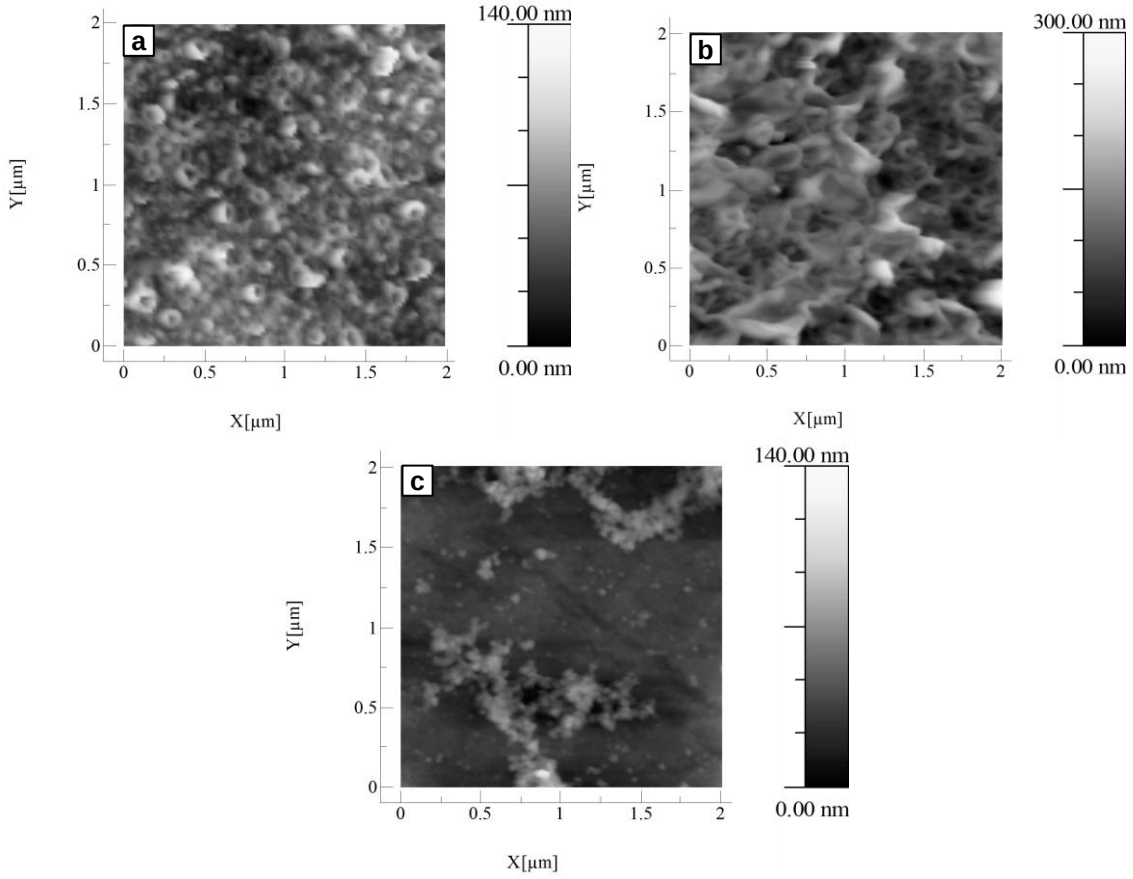

Figure S2.6: Surface AFM images of the top layer of TFC membranes synthesized (a) according to the conventional system on a PSf support without additives, (b) according to the conventional system on a PSf support with SDS and TEA and (c) according to the water/IL system on a cross-linked PI support without additives.

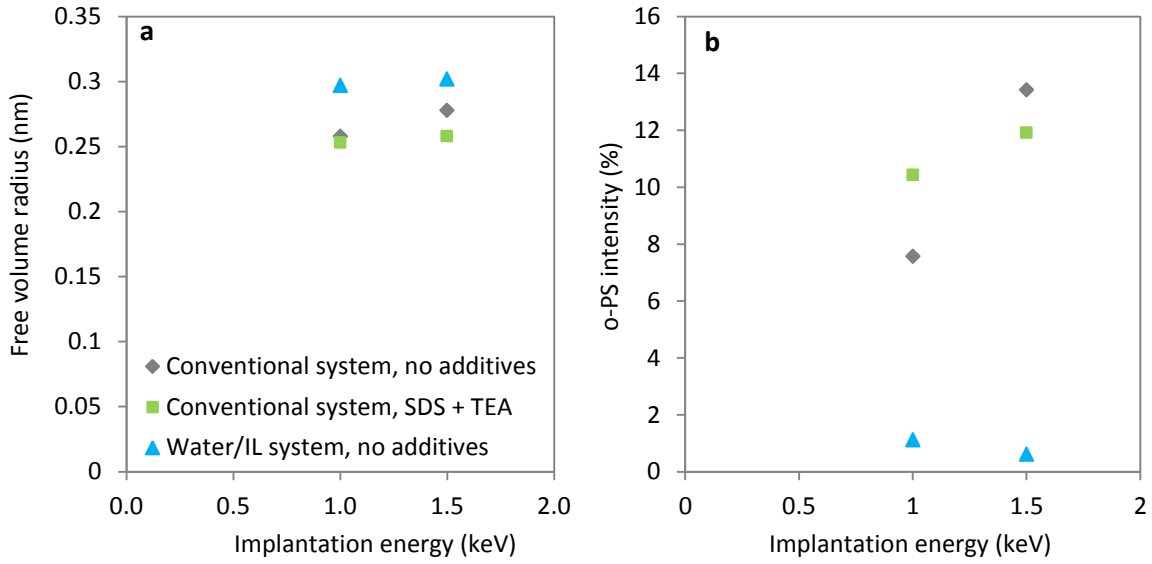

Figure S2.7: PLEPS determination of (a) free volume radius and (b) o-positronium (o-Ps) intensity of TFC membranes synthesized according to the conventional system on a PSf support, either without or with the addition of SDS and TEA, and of a TFC membrane synthesized according to the water/IL system on o cross-linked PI support without additives.

The free volume radius at an implantation energy of 1 keV was used, since interference from the support pores is expected at higher energies. The much lower o-Ps intensity of the membrane made via the water/IL system is attributed to inhibition of o-Ps formation. Either differences in chemical structure of the top layer (e.g. by a varying degree of cross-linking) or the influence of a different support chemistry (PSf in the conventional system versus cross-linked PI in the water/IL system) can cause variations in the extent of o-Ps inhibition.

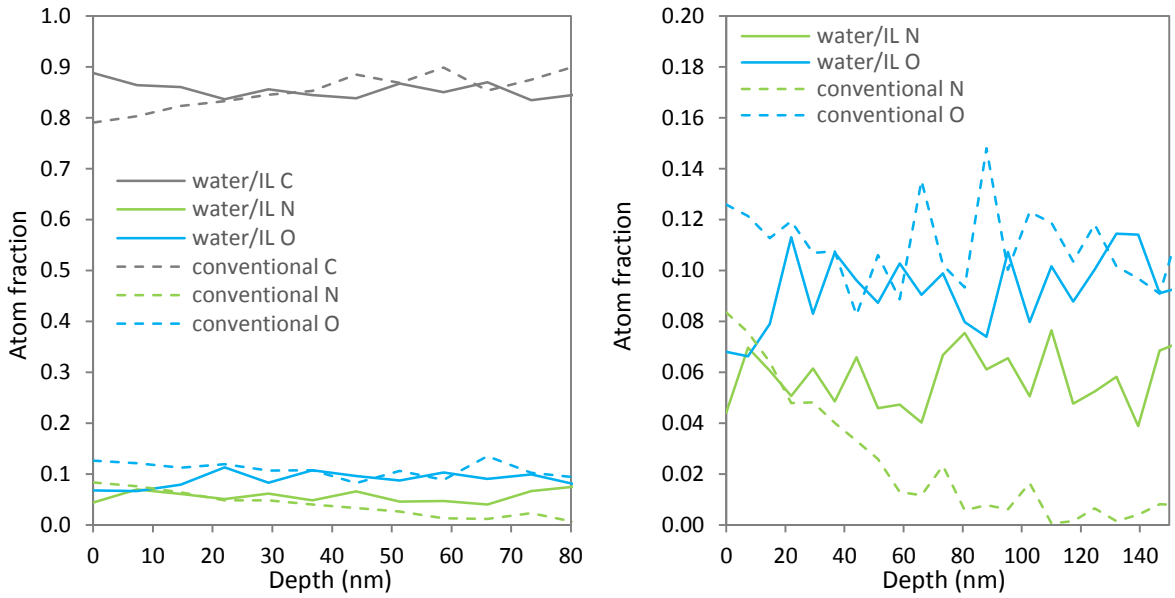

Figure S2.8: ERD determination of (a) atom fractions of C, N and O in TFC membranes synthesized according to the conventional system on a PSf support or according to the water/IL system on a cross-linked PI support, both without the use of additives, and (b) zoom of the atom fractions of N and O.

The O/N ratio was calculated to analyze differences in degree of cross-linking of the top layer. The average O/N ratio over the upper 0-22 nm region was taken, as the top layer prepared according to the water/IL system had a thickness of only 25 nm, derived from TEM analysis (Table 2.3). The top layer thickness could not be derived from the ERD measurements, as the PA top layer and the cross-linked PI support have a very similar elemental composition. For the conventionally prepared TFC membrane, the PA top layer and PSf support could be distinguished in ERD. The large decrease in N with increasing depth (Figure S2.8b) suggests the top layer to be between 40 and 60 nm in thickness, which corresponds to the values derived from TEM analysis (Table 2.3).

Although the overall O/N ratio of both membranes is very similar, the membrane prepared according to the water/IL system had a remarkably higher C content, while the O and N content were lower. No clear explanation for this observation could be found.

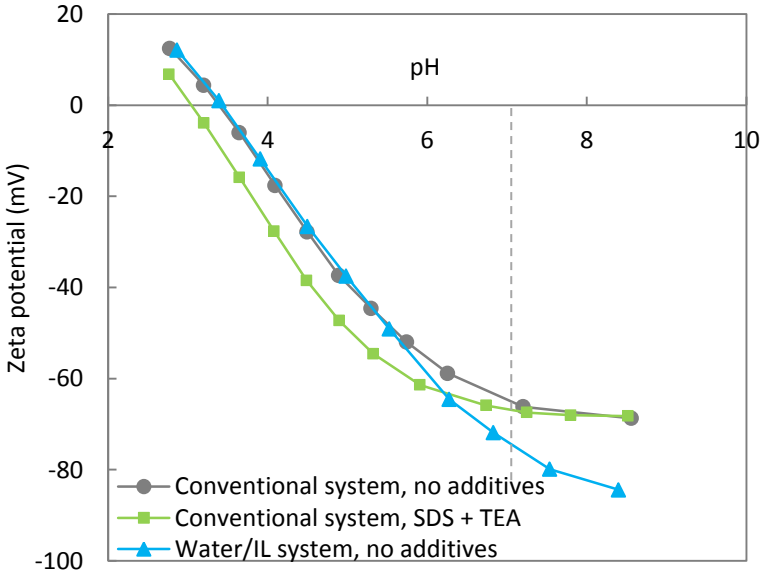

Figure S2.9: Zeta potential as function of pH of TFC membranes synthesized according to the conventional system on a PSf support, either without or with the addition of SDS and TEA, and of a TFC membrane synthesized according to the water/IL system on a cross-linked PI support without additives.

Table S2.1: Calculations of the interfacial surface coverage by TMC molecules and by the initially formed PA oligomers.

Interfacial polymerization conditions	
TMC concentration (g/L)	1
TMC concentration (molecules/L)	2.27×10^{21}
Interfacial area (nm)	2.38×10^{15}
Number of TMC molecules in 0-1.6 nm region from interface	8.62×10^{12}
TMC properties	
Molecule radius (nm)	0.45
Projected area of one molecule (circle) (nm²)	0.64
Projected area of all molecules in 0-1.6 nm region (nm²)	5.49×10^{12}
Fraction of interfacial area covered with TMC (%)	**0.23**
MPD properties	
Molecule radius (nm)	0.35
Projected area of one molecule (circle) (nm²)	0.38
Projected area of all molecules reacted with TMC in 0-1.6 nm region (nm²) [a]	9.96×10^{12}
Fraction of interfacial area covered with initial oligomers (%)	**0.65**

[a] Assuming that 3 MPD molecules react with every TMC molecule and no MPD reacts at both sides.

Appendix B

Supporting information for chapter 3

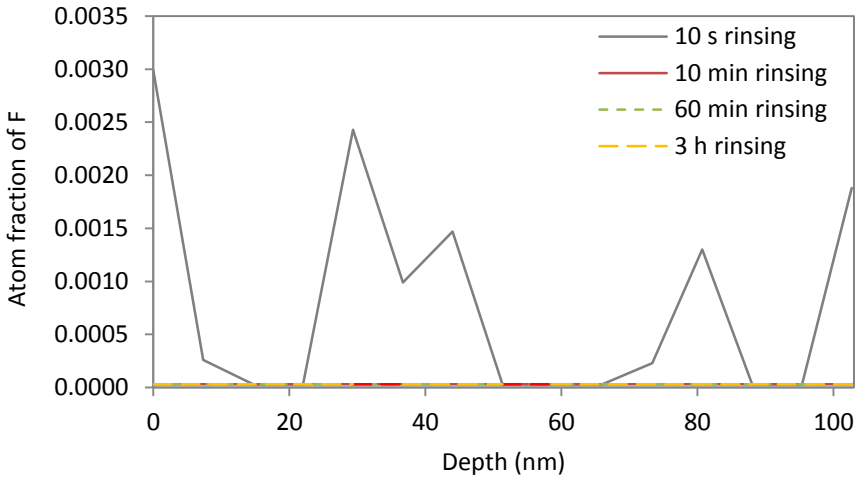

Figure S3.1: ERD determination of the atom fraction of F in TFC membranes synthesized according to the water/IL system on a cross-linked PI support, after rinsing with acetone for different times

The presence of F in the graph after 10 s rinsing indicates the presence of residual [C_4mim][Tf_2N] in the membrane. After 10 min, 60 min and 3 h rinsing, no F was detected anymore.

Table S3.1: pH measurements of the equilibrated aqueous phase after washing a non-dried and vacuum-dried TMC/[C_4mim][Tf_2N] solution with fresh water in five subsequent cycles. Calculation of the original concentration of TMC present in the IL.

Non-dried TMC/[C_4mim][Tf_2N]					
Washing cycle	pH aq. solution	C_{HCl} (M)	V_{water} (L)	m_{TMC} (mol)	C_{TMC} (M) [a]
1	1.96	1.096×10^{-2}	10.012×10^{-3}	3.659×10^{-5}	1.830×10^{-2}
2	3.13	7.413×10^{-4}	10.014×10^{-3}	2.474×10^{-6}	1.237×10^{-3}
3	3.96	1.095×10^{-4}	10.025×10^{-3}	3.661×10^{-7}	1.831×10^{-4}
4	5.63	2.244×10^{-6}	10.003×10^{-3}	7.483×10^{-9}	3.742×10^{-6}
5	6.19	5.457×10^{-7}	10.013×10^{-3}	1.821×10^{-9}	9.107×10^{-7}
				Total:	**1.972×10^{-2}**
Vacuum-dried TMC/[C_4mim][Tf_2N]					
Washing cycle	pH aq. solution	C_{HCl} (M)	V_{water} (L)	m_{TMC} (mol)	C_{TMC} (M) [b]
1	2.05	8.912×10^{-3}	10.000×10^{-3}	2.971×10^{-5}	1.485×10^{-2}
2	3.02	9.549×10^{-4}	10.025×10^{-3}	3.191×10^{-6}	1.595×10^{-3}
3	3.74	1.819×10^{-4}	10.023×10^{-3}	6.076×10^{-7}	3.037×10^{-4}
4	4.79	1.612×10^{-5}	10.028×10^{-3}	5.388×10^{-8}	2.693×10^{-5}
5	5.53	2.851×10^{-6}	10.003×10^{-3}	9.507×10^{-9}	4.752×10^{-6}
				Total:	**1.678×10^{-2}**

[a] Calculated with a volume of [C_4mim][Tf_2N] of 2.000×10^{-3} L.

[b] Calculated with a volume of [C_4mim][Tf_2N] of 2.001×10^{-3} L.

Table S3.2: Calculations of the mass and solvent intensities of the conventional and the water/IL-based interfacial polymerization, starting from a non-impregnated support.

Membrane surface (m²): 0.0024

Mass of 1 m² membrane (g): 109.75

Without recycling of the organic phase						
	Conventional system			Water/IL system		
Description	Quantity (g)	Quantity (g m^{-2})	Product	Quantity (g)	Quantity (g m^{-2})	Product
Impregnation with MPD solution	0.42	173.63	MPD	0.02	8.68	MPD
	20.04	8282.45	Water	20.98	8673.65	Water
	0.42	173.63	TEA	/	/	TEA
	0.02	8.68	SDS	/	/	SDS
Contact with TMC solution	0.0037	1.51	TMC	0.01	3.00	TMC
	2.41	995.20	Hexane	2.08	860.26	$[C_4mim][Tf_2N]$
Rinsing (removal of TMC)	0.80	330.14	Hexane	0.96	395.66	Acetone
Rinsing (removal of MPD)	21.00	8681.27	Water	21.00	8681.27	Water
Mass intensity		**15.33**			**11.55**	
Solvent intensity		**12.08**			**11.44**	

With recycling of the organic phase						
	Conventional system			Water/IL system		
Description	Quantity (g)	Quantity (g m^{-2})	Product	Quantity (g)	Quantity (g m^{-2})	Product
Impregnation with MPD solution	0.42	173.63	MPD	0.02	8.68	MPD
	20.04	8282.45	Water	20.98	8673.65	Water
	0.42	173.63	TEA	/	/	TEA
	0.02	8.68	SDS	/	/	SDS
Contact with TMC solution	0.0037	1.51	TMC	0.01	3.00	TMC
	2.41	995.20	Hexane	2.08	860.26	$[C_4mim][Tf_2N]$
Recycling TMC solution	-0.0027	-1.11	TMC	-0.01	-2.40	TMC
	-1.77	-731.47	Hexane	-1.96	-809.51	$[C_4mim][Tf_2N]$
Rinsing (removal of TMC)	0.80	330.14	Hexane	0.96	395.66	Acetone
Rinsing (removal of MPD)	21.00	8681.27	Water	21.00	8681.27	Water
Mass intensity		**8.66**			**4.15**	
Solvent intensity		**5.41**			**4.07**	

Appendix C

Supporting information for chapter 4

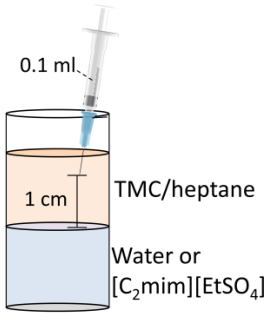

Figure S4.1: Experimental setup of the mass transfer tests.

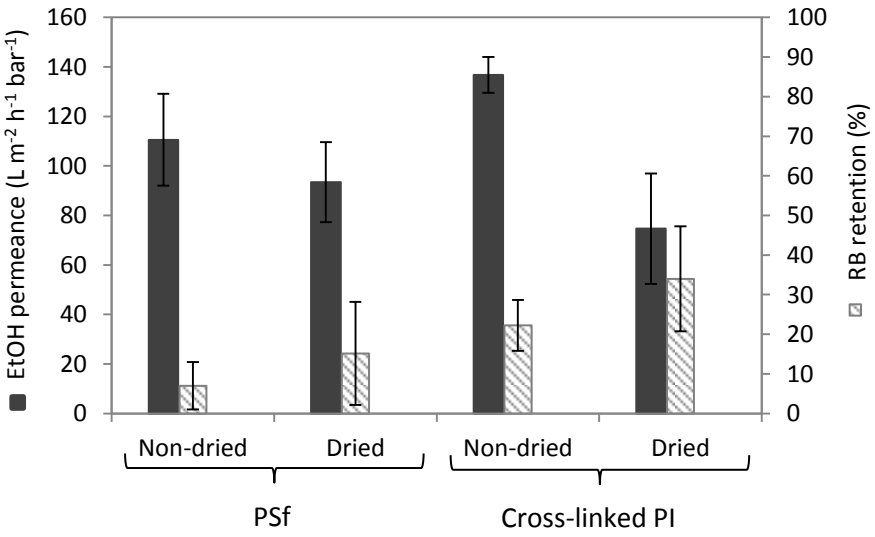

Figure S4.2: EtOH permeance and RB retention of PSf and cross-linked PI supports, either non-dried, or dried at room temperature after impregnation with a [C_2mim][$EtSO_4$]/EtOH (1/3 (v v^{-1})) mixture.

Appendix D

Supporting information for chapter 5

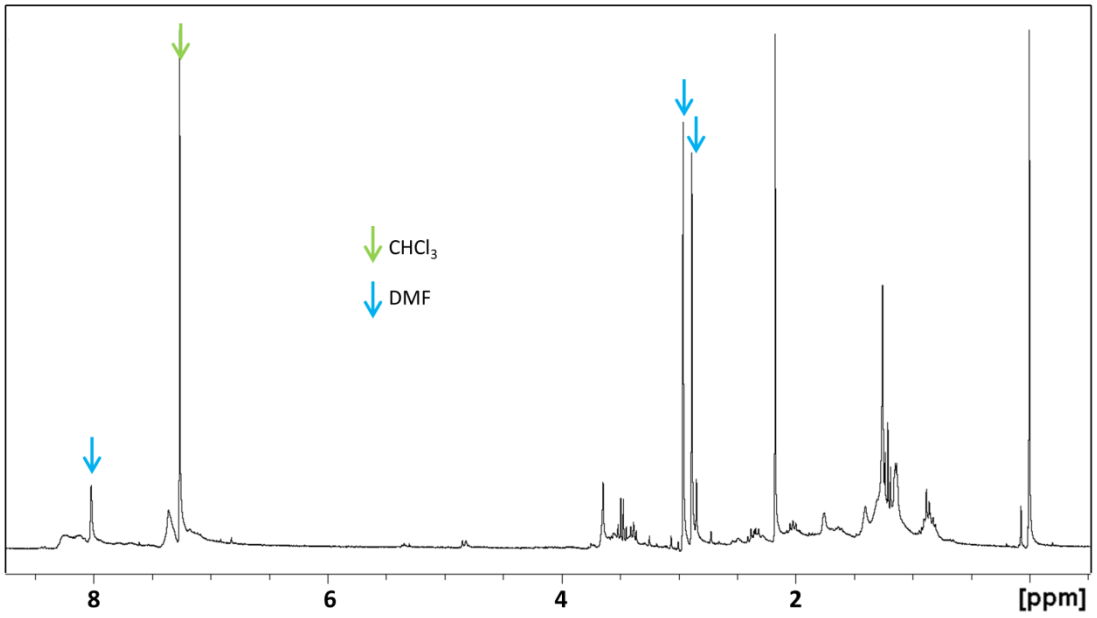

Figure S5.1: H-NMR spectrum of the solid residue in DMSO-d, after evaporation of DMF from the solution obtained by immersing a cross-linked PI support in DMF.

Appendix E

Supporting information for chapter 6

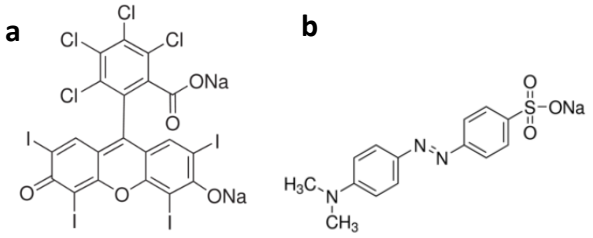

Figure S6.1: Chemical structure of (a) Rose Bengal and (b) methyl orange.

Table S6.1: Difference in Hansen solubility parameters between uncross-linked PI and the different types of solvents.

component	δ_D (MPa)$^{1/2}$	δ_P (MPa)$^{1/2}$	δ_H (MPa)$^{1/2}$	$\Delta_{s\text{-}p}$ (MPa)$^{1/2}$
Uncross-linked PI [30]	18.7	9.5	6.7	
Water [226]	15.6	16.0	42.3	**36.7**
Hexane [226]	14.9	0.0	0.0	**13.9**
EtOH [226]	15.8	8.8	19.4	**14.0**
ACN [226]	15.3	18.0	6.1	**10.9**
DMF [226]	17.4	13.7	11.3	**6.7**

List of publications

Publications related to this work

H. Mariën, L. Bellings, S. Hermans, I.F.J. Vankelecom, Sustainable process for the preparation of high-performance thin-film composite membranes using ionic liquids as the reaction medium, *ChemSusChem*, **2016**, 9, 1101-1111.

H. Mariën, I.F.J. Vankelecom, Transformation of cross-linked polyimide UF membranes into highly permeable SRNF membranes via solvent annealing, *J. Membr. Sci.*, **2017**, 541, 205-213.

H. Mariën, I.F.J. Vankelecom, Nanofiltration membrane materials and preparation, in *Nanofiltration: Principles and Applications, 2nd edition*, Elsevier, **2018**.

H. Mariën, I.F.J. Vankelecom, Optimization of the ionic liquid-based interfacial polymerization system for the preparation of high-performance, low-fouling RO membranes, *submitted*.

Patent application related to this work

H. Mariën, S. Hermans, I.F.J. Vankelecom, *Improved method for synthesis of polyamide composite membranes*, **2014**, WO2016070247 A1.

Publications not related to this work

S. Hermans, H. Mariën, E. Dom, R. Bernstein, I.F.J. Vankelecom, Simplified synthesis route for interfacially polymerized polyamide membranes*, J. Membr. Sci*., **2014**, 451, 148-156.

S. Hermans, E. Dom, H. Mariën, G. Koeckelberghs, I.F.J. Vankelecom, Efficient synthesis of interfacially polymerized membranes for solvent resistant nanofiltration, *J. Membr. Sci.*, **2015**, 476, 356-363.

S. Hermans, H. Mariën, C. Van Goethem, I.F.J. Vankelecom, Recent developments in thin film (nano)composite membranes for solvent resistant nanofiltration, *Curr. Opin. Chem. Eng*., **2015**, 8, 45-54.